



2011-12-19

Design and Synthesis of Cationic Steroid Antimicrobial Compounds, Synthesis of Glycolipids Recognized by Natural Killer T Cells and Development of TLR-1, TLR-6 Heterodimer Binders and Studies of Their Immunology Activities

Yanshu Feng

Brigham Young University - Provo

Follow this and additional works at: <https://scholarsarchive.byu.edu/etd>

 Part of the [Biochemistry Commons](#), and the [Chemistry Commons](#)

BYU ScholarsArchive Citation

Feng, Yanshu, "Design and Synthesis of Cationic Steroid Antimicrobial Compounds, Synthesis of Glycolipids Recognized by Natural Killer T Cells and Development of TLR-1, TLR-6 Heterodimer Binders and Studies of Their Immunology Activities" (2011). *All Theses and Dissertations*. 2751.

<https://scholarsarchive.byu.edu/etd/2751>

Design and Synthesis of Cationic Steroid Antimicrobial Compounds, Synthesis of
Glycolipids Recognized by Natural Killer T cells and Development
of TLR-2 and TLR-6 Heterodimer Binders
and Studies of Their Immunology
Activities

Yanshu Feng

A dissertation submitted to the faculty of
Brigham Young University
in partial fulfillment of the requirements for the degree of

Doctor of Philosophy

Paul B. Savage, chair
Merritt B. Andrus
Steven L. Castle
Matt A. Peterson
Scott R. Burt

Department of Chemistry and Biochemistry

Brigham Young University

December, 2011

Copyright © 2011 Yanshu Feng

All Rights Reserved

ABSTRACT

Design and Synthesis of Cationic Steroid Antimicrobial Compounds, Synthesis of Glycolipids Recognized by Natural Killer T cells and Development of TLR-2 and TLR-6 Heterodimer Binders and Studies of Their Immunology Activities

Yanshu Feng

Department of Chemistry and Biochemistry, BYU

Doctor of Philosophy

Cationic steroid antimicrobial agents (CSAs) are a family of bile acid derivatives. These compounds are amphiphilic and mimic endogenous antimicrobial peptides. The antimicrobial activities of CSA-13 have been investigated and due to potent bactericidal activities and low toxicity, a large amount of CSA-13 is demanded for clinic trials and other antimicrobial applications. During our studies, we optimized the synthetic route of CSA-13, so that it can be prepared at the kilogram, even in tons scale. We investigated three routes and one of them is suitable for industry, because only recrystallization is needed in the synthesis.

Natural killer T cells (NKT cells) are a kind of lymphocyte that bridge the adaptive immune system with the innate immune system. Once stimulated by glycolipids, NKT cells influence immune responses. To search for better glycolipid ligands, scientists have isolated many natural products to get inspiration. Thraustochysides A-C was isolated from a group of marine protists. These compounds have an interesting structure on their sphingosine lipid chains. We finished the total synthesis of thraustochyside B, and made substantial progress toward the synthesis of thraustochyside A.

Toll like receptors (TLRs) are integral components of the innate immune system. They recognize antigens and induce dendritic cells to give immune responses. TLR1, TLR2 and TLR6 recognize lipopeptides, and these TLRs function as heterodimers. TLR1/TLR2 dimer recognition gives inflammatory responses, and TLR2/TLR6 dimer recognition gives immunomodulatory responses. We used modeling of TLRs to find a compound, which can fill the lipid binding pockets of the TLR2 and TLR6 dimer. In our study, we found the peptide chain of the antigen Pam2CSK4 can be replaced by a water soluble polyamine, which confirmed the function of the peptide to increase the water solubility.

Keywords: Synthesis, Cationic steroid antimicrobial, glycolipids, TLR-1, TLR-6, Immunology

ACKNOWLEDGEMENTS

First I need to thank my research advisor Dr. Paul B. Savage for his serious and patient direction. Without him this dissertation would not exist. During the last six years Paul took every opportunity to help me develop the proper attitude and vision toward science, which I think is extremely important for a Ph.D. student. In addition to helping with experiments Paul trained me a lot on how to read, think, write, and present my work. For me the experience of working for him is really invaluable education experiences which have benefited and will continue benefit my whole professional life.

Next I would like to thank the faculty members Dr. Merritt B. Andrus, Dr. Steven L. Castle, Dr. Matt A. Peterson. Each gave me nice suggestions on my research plan and research proposals. Also I thank Dr. Scott R. Burt for being willing to be my committee member one month before my dissertation defense.

I thank the lab mates of the Savage group. They all have contributed very important data for this dissertation. Yang, Xiangtian, Shenglou, Brian, Vinod, Fang, Liming also provided all kinds of help and care. Working with you is always a pleasant and encouraging experience.

Finally I would like to thank my parents and my wife's support. During the course of my graduate study I endured some really difficult times, but because of you my efforts and insistence are especially meaningful.

Table of Contents

CHAPTER ONE: Design and Synthesis of Cationic Steroid Antimicrobial Compounds.....	1
1.1 Introduction.....	1
1.1.1 Diseases caused by bacteria.....	1
1.1.2 Bacteria differentiation by membrane structure.....	1
1.1.3 Drug resistance of bacteria.....	2
1.1.4 Bactericidal mechanisms AMPs.....	4
1.1.5 Selectivity of antimicrobial peptide between prokaryotic and eukaryotic cells.....	5
1.1.6 Development of CSAs.....	5
1.2 Mechanism of CSA-13 as a antimicrobial agent.....	8
1.2.1 Membrane depolarization and antimicrobial activities of CSAs.....	8
1.2.1.1 Permeabilization of CSAs into E. coli ML-35p outer membrane and inner membrane.....	8
1.2.1.2 Membrane depolarization.....	12
1.2.2 Resistance of Gram-negative and Gram-positive bacteria to CSA-13.....	14
1.2.2.1 Resistance of Gram-negative and Gram-positive bacteria to AMPs.....	14
1.2.2.2 Resistance of Gram-positive bacteria to CSA-13.....	15
1.2.2.3 Resistance of Gram-negative bacteria to CSA-13.....	16
1.2.3 Results and discussion.....	19
1.3. Process Development of CSA-13.....	20
1.3.1 Route 1.....	21
1.3.2 Route 2.....	23
1.4 Development of ceragenins derivatives and the applications.....	31
1.4.1 ^{99m} Tc binded CSA derivatives in cell imaging.....	31
1.4.1.1 Medical imaging.....	31
1.4.1.2 ^{99m} Tc.....	32
1.4.1.3 CSA derivative used in medical imaging as ^{99m} Tc binder.....	32
1.5 Experiment section.....	35
1.6 References.....	47
CHAPTER TWO: Natural Killer T cells Recognize Glycolipids as Antigens.....	51
2.1 INTRODUCTION.....	51
2.1.1 Immune systems.....	51
2.1.2 NKT cells.....	52
2.1.3 Cytokine release by NKT cells.....	52
2.1.4 Glycolipids as antigens.....	53
2.2 Thraustochytrins A and B.....	58
2.2.1 Background.....	58
2.2.2 Synthesis of Thraustochytrin B and the analog 2-36.....	59

2.2.3 Approach Synthesis of Thraustochytrioside A.....	63
2.3 Asperamides A and B	71
2.3.1 Background.....	71
2.3.2 Synthesis of Asperamide A.....	72
2.4 Experimental section.....	76
2.5 References.....	100
CHAPTER THREE: Development of TLR-2 and TLR-6 heterodimer binders and studies of their immunology activities	105
3.1 INTRODUCTION.....	105
3.1.1 Immune systems.....	105
3.1.2 Toll like receptors	106
3.1.3 TLR2 / TLR6 induce TH2 response	107
3.2 Result and disscussion	109
3.2.1 Design of TLR-1 / TLR-6 heterodimer binders	110
3.2.2 Synthesis of 3-10	112
3.2.3 Synthesis of 3-12	114
3.2.4 Synthesis of LMP-1 and LMP-2	115
3.2.5 Results and discussion	117
3.3 Experimental section	119
3.4 References	127
Appendix: Spectra.....	131

Chapter 1. Design and Synthesis of Cationic Steroid Antimicrobial Compounds

1.1 Introduction

1.1.1 Diseases caused by bacteria

With the first observation of bacteria by Antonie van Leeuwenhoek in 1676,¹ people started to find that many diseases are caused by bacteria. Diphtheria, granulomatous lymphadenitis, pneumonitis, pharyngitis, skin infections, and endocarditis are caused by strains of *Corynebacterium*.² As a result, the war against the diseases caused by various types of bacteria became significant.

Pseudomonas aeruginosa is found almost everywhere throughout the world, in places such as soil, water, and skin. It uses a wide range of organic material for food, even diesel. It infects the pulmonary tract, urinary tract, burns, wounds, and causes diffuse bronchopneumonia, urinary tract catheterization, hemorrhage and necrosis.³

Staphylococcus aureus was found in 1880.⁴ Many diseases are caused by *S. aureus*, such as pneumonia, meningitis, osteomyelitis, endocarditis, and sepsis. At this point, it is one of the five most common causes of nosocomial infections.⁵

1.1.2 Bacteria differentiation by membrane structure

Bacteria are divided into two domains by their cell wall structure and compositions: Gram-positive bacteria and Gram-negative bacteria.⁶ To characterize a bacteria sample, the Gram-staining method technique is used first.⁷ A certain dye, called crystal violet is used to treat the bacteria. Then, iodine is added to react with crystal violet to generate a larger crystal. For Gram-positive bacteria, the dye will enter the bacteria cell through the membrane, and the formed larger crystal is not allowed to traverse in the bacteria cell membrane, which keeps the dye in the cell. That will cause the bacteria to become purple.⁸ For Gram-negative bacteria, the outer membrane prevents the dye entering the bacteria cell, thus, after staining, they remain colorless or pink.

1.1.3 Drug resistance of bacteria

Since the discovery of penicillin, many antimicrobial drugs have been developed, and people benefited from them.⁹ However, the extensive use of antibiotics, within medicine and veterinary medicine, has resulted in increased resistance in bacterial isolates due to the ability of bacteria to evolve and adapt to selective pressures.¹⁰ The longer the duration of exposure to an antibiotic, the greater the risk of the development of resistance. As resistance becomes more common, there becomes a greater need for alternative treatments. *P. aeruginosa* is naturally resistant to a large range of antibiotics and may demonstrate additional resistance after unsuccessful treatment.¹¹ One of the super bacteria, methicillin resistant *S. aureus* (MRSA), have become resistant to most antibiotics.^{12, 13, 14} Statistically, to bring a new drug to market, ten years is needed; however, bacteria can usually engender antibiotic resistance in only two years.

Due to increased microbial resistance, cationic antimicrobial peptides (AMPs) isolated from nature, such as magainins¹⁵ and cecropins,¹⁶ are attracting attention in the antibiotic development community.^{17, 18, 19} They are important components of natural defenses in living organisms. These compounds consist of amino acids with both polar (lysine and arginine) and non-polar residue. In their active conformations, these compounds are typically amphiphilic, with a hydrophobic face and a cationic polar face,²⁰ and generally target the bacterial membrane, disrupt the barrier, and kill the bacteria. These features produce greater affinity for prokaryotic membrane surfaces (comprised of lipids such as lipid A, **Figure 1-1**), which are typically negatively charged, unlike eukaryotic membranes.²¹

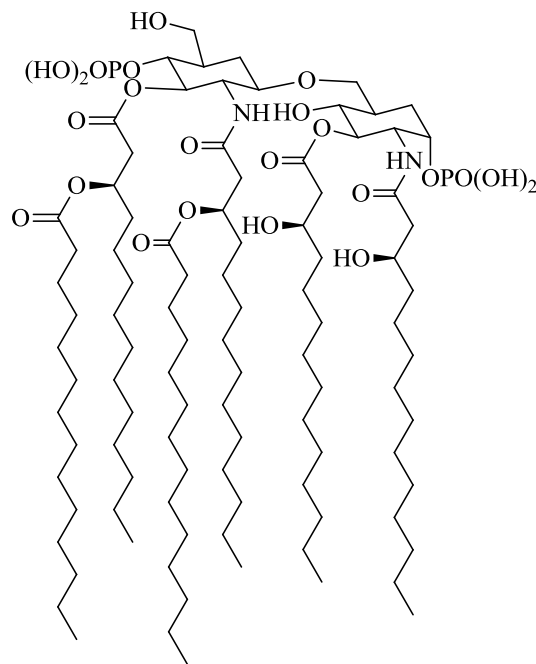


Figure 1-1: Structure of Lipid A

The human body also produces antimicrobial peptides, including defensins,²² cathelicidins²³ and histatins. As a key component of cathelicidins, LL-37 is found throughout the body, such as in tears, gastrointestinal extract, semen, and et al.

1.1.4 Bactericidal mechanisms of AMPs

The microbial killing mechanism of AMPs is still not fully understood. There are several permeabilization mechanisms have been proposed to explain the bactericidal activity.²⁴ In the “barrel-stave model”, the peptides aggregate and insert into the membrane. The hydrophobic surfaces of the peptides face the membrane lipid chains, whereas the hydrophilic surfaces form the lumen. Another bactericidal mechanism of antimicrobial peptides is the “carpet model”, shown in **Figure 1-2**

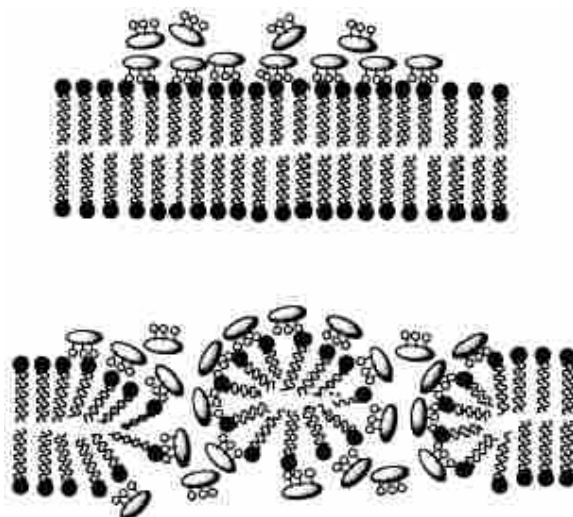


Figure 1-2. Carpet model of bactericidal activity of antimicrobial peptides

The cationic residues bind to the membrane surface via ionic interactions. Some of the antimicrobial peptide molecules re-orient back to back to separate the hydrophobic residues with the hydrophobic core of the membrane, and disrupt the membrane. The cytotoxicity caused by the aggregation of this kind of detergent like compound has also been reported in the studies of amitriptyline.²⁵

Unlike the “barrel-stave” model, the “torroidal-pore model” is more like the “carpet model”. Peptides associate with the polar surface and induce the membrane to bend through the membrane bilayer to form transmembrane pores. On the channel walls, the hydrophobic surface face inside, which allow larger molecules to traverse through the cell membrane and cause bacteria to die.

1.1.5 Selectivity of antimicrobial peptide between prokaryotic and eukaryotic cells

For clinical use, antimicrobial peptides, especially LL-37, have good selectivity between prokaryotic and eukaryotic cells.²⁶ Both prokaryotic and eukaryotic membrane surfaces are polar. In prokaryotic cytoplasmic membranes, anionic PG (phosphatidylglycerol) and CL (cardiolipin) are the major components (**Table 1-1**), whereas the eukaryotic membrane is composed principally of neutral PC (phosphatidylcholine) and sphingomyelin. There are four cationic residues on LL-37, and it has a higher affinity to the bacteria membranes than human cell membranes.

1.1.6 Development of CSAs

Generally, it is necessary for antibiotics to enter bacterial cells first to inhibit bacterial duplication, such as quinolones and sulfonamides. To gain resistance, bacteria developed their defense system by building biofilm to prevent drugs entering their cells,²⁷ pumping out those toxic compounds²⁸ or releasing enzymes to degrade them.²⁹ Unlike other antibiotic agents, AMPs target bacteria cell membranes, which avoid those limitations.

However, there are still drawbacks that make the clinical use of antimicrobial peptides challenging. AMPs are generally large in size, which makes them difficult and expensive in producing on a large scale. Also, AMPs are relatively unstable due to proteolytic degradation in the presence of proteases released by both human bodies and bacteria.³⁰ Hence, use of smaller molecules to mimic their behaviors may be more efficient. The design and synthesis of small and stable molecules to mimic these peptides is being pursued in four groups.^{31, 32, 33, 34}

During the studies of AMPs bactericidal activities, the enantiomer of LL-37 was found to be equally effective,³⁵ which leads our attention to the facially amphiphilic morphology. Cholic acid is commercially available and inexpensive. By simple modification of the core structure, facially amphiphilic molecules could be obtained. Cationic steroid antimicrobial (CSA) compounds are families of cholic acid-derived antimicrobial agents that mimic the activity of natural antimicrobial peptides. We have prepared more than one hundred CSAs consisting of different chain lengths on the side chains at position 3, 7 and 12, with free amino groups on the terminals. Due to the stereochemistry of the oxygen atoms on the steroid scaffold, the amino groups are predisposed to be on one face of the molecules, which induces the facial amphiphilicity. Instead of oxygen, nitrogen was also tried in those side chain linkages. At

position 24, linkages of different chain lengths have also been made. *E. Coli* was used to test their basic antimicrobial activities. Of all the CSAs, CSA-13 (**Figure 1-3**) has been characterized and studied in greatest depth due to its excellent activities (the range of minimum bacteria inhibitory concentration (MIC) is from 35 µg/mL to 0.03 µg/mL against a broad range of organisms).³⁶

	% Total membrane phospholipid			
	PE	PG	CL	PC
<i>Proteus mirabilis</i>	80	10	5	–
<i>E. coli</i>	80	15	–	–
<i>Pseudomonas aeruginosa</i>	60	21	11	–
<i>B. anthracis</i>	43	40	17	–
<i>B. Subtilis</i>	12	70	4	–
<i>S. aureus</i>	–	58	42	–
<i>Mammalian liver plasma membrane</i>	23	–	1	39

Table 1-1. Major phospholipid components¹⁵. PE, phosphatidylethanolamine

CSA-8 is another well studied compound, because it helps to drop other antimicrobial agents' MICs dramatically. The value to estimate this property is called in the fractional inhibitory concentration (FIC).

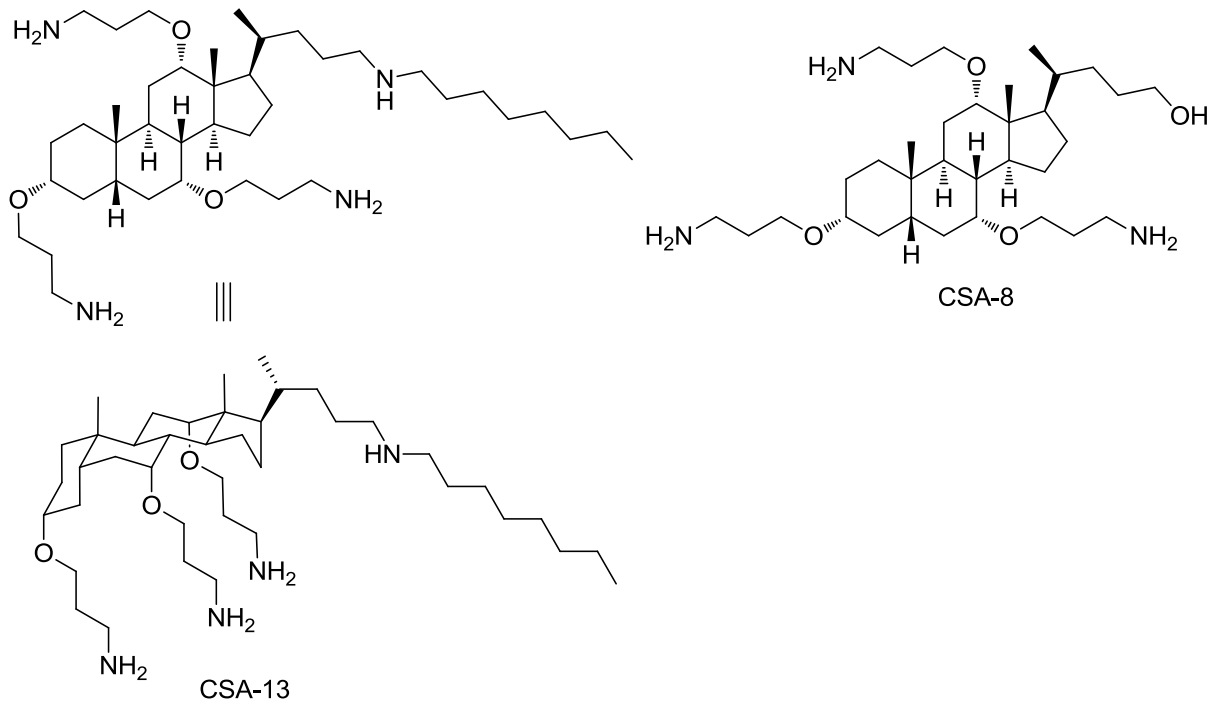


Figure 1-3: Structure of CSA-13 and CSA-8

1.2 Mechanism of CSA-13 as an antimicrobial agent

1.2.1 Membrane depolarization and antimicrobial activities of CSAs

1.2.1.1 Permeabilization of CSAs into *E. coli* outer membrane and inner membrane

E. coli strain ML-35p lacks lac permease, but is constitutive for plasmid-encoded periplasmic β -lactamase, and expresses cytoplasmic β -galactosidase.

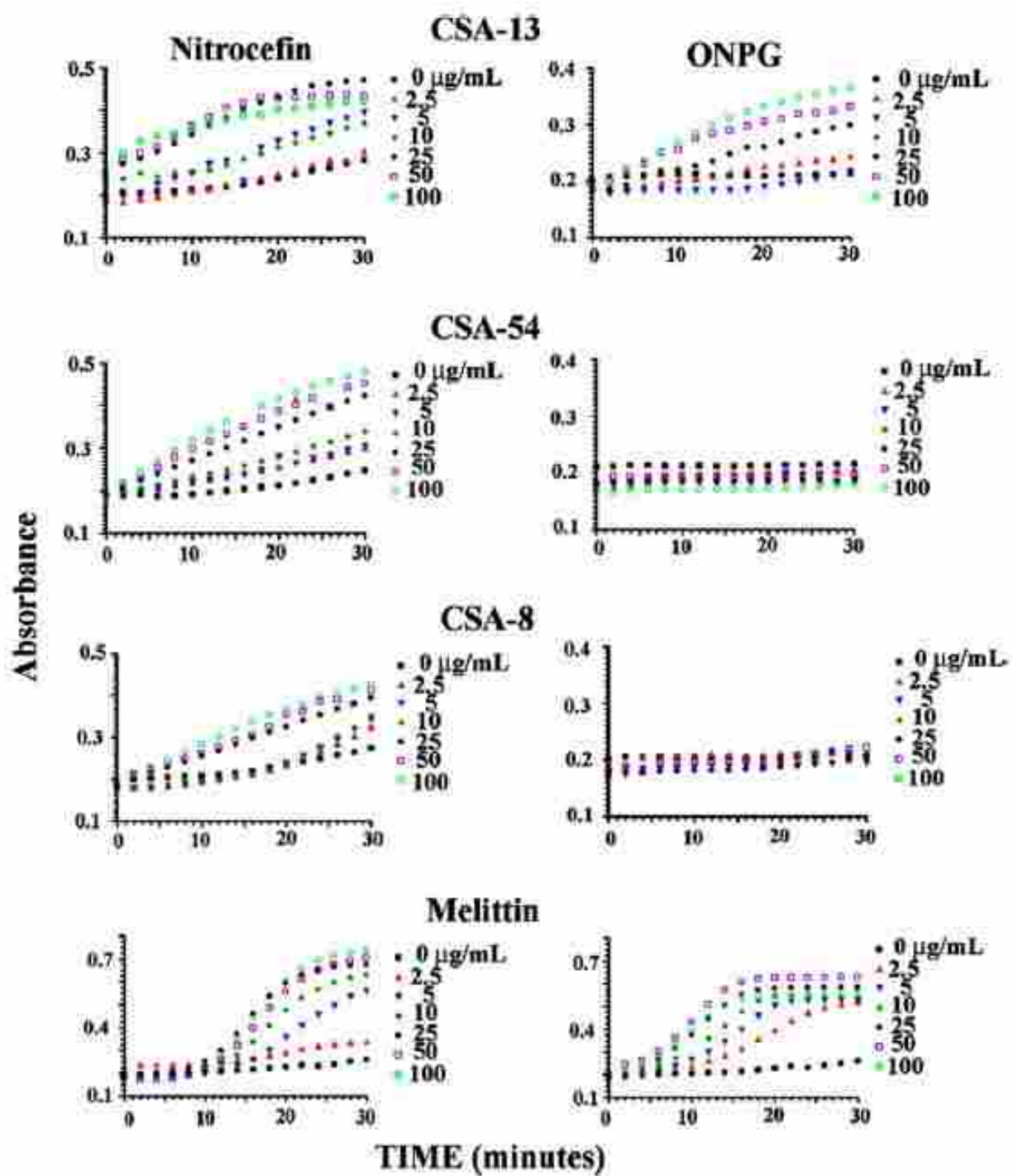


Figure 1-4: Permeabilization of CSAs into *E. coli* ML-35p outer membrane and inner membrane

Nitrocefin was used to monitor the permeabilization of the outer membranes of *E. coli* strain ML-35p. This molecule is not able to cross the outer membrane to access the periplasmic space, unless there is permeabilization of the outer membrane. Once nitrocefin enters the periplasm, the 4-membered lactam is cleaved by β -lactamase. The amino group generated donates electrons to the conjugated π -system and causes color change that can be observed at 486 nm (**Figure 1-4**).

o-Nitrophenyl-3-D-galactoside (ONPG) was used to monitor the permeabilization of the inner membranes of *E. coli* strain ML-35p. ONPG is not able to traverse the inner cytoplasmic membrane without the help of permease. If it does traverse the cytoplasmic membrane, *o*-nitrophenol is produced by cytoplasmic β -galactosidase cleaving the glycosidic bond to cause color change, monitored under 420 nm.

CSA-8, CSA-13 and CSA-54 were used in the permeabilization tests, and an antimicrobial peptide, melittin, acted as control due to the strong effect of membrane permeabilization. From Figure 1-4 we can see, the nitrocefin fluorescence increasing could be detected right after any of all three CSAs were added, rather than melittin. This means the CSAs caused permeation of the *E. coli* strain ML-35p outer membrane is more rapid than melittin. For ONPG, adding CSA-13 and melittin helped the observation of the fluorescence increases. No permeabilization was observed for CSA-8 and CSA-54 even at concentrations well above the minimum bactericidal concentration (MBC). That argues that for CSA-8 and CSA-54, the bactericidal activity does not involve cytoplasmic membrane disruptions.

1.2.1.2 Membrane depolarization

To test the depolarization of CSAs, 3, 3'-diethylthiadicarbocyanine iodide (DiS-C₂ (5)) was used. This molecule is a type of lipophilic fluorescent stain for labeling membranes and other hydrophobic structures. It has a high extinction coefficient: polarity-dependent fluorescence and short excited-state lifetime. Once applied to cells, this dye diffuses laterally within the cellular membranes. The fluorescence of this environment-sensitive dye is greatly enhanced in polarized membranes. An excitation wavelength of 600 nm and an emission wavelength of 660 nm were used to monitor depolarization (**Table 1-2**).

The dye was put into the cuvettes along with the bacteria cell suspension in buffer (PH=7.0) at 37 °C. The baselines were determined after 7 mins. Measurements were taken every 30s before and after the addition of CSAs in different concentrations.

Bacterial species		Lipid composition %			CSA-13		CSA-54		CSA-8	
		PE	PG	CL	MBC	Depolarization at MBC %	MBC	Depolarization at MBC %	MBC	Depolarization at MBC %
Gram-Positive bacteria	<i>B. polymyxa</i>	60	3	8	2.5	88.4	2.5	39.6	15	96.6
	<i>B. cereus</i>	43	40	17	1	86.7	7	79.7	7	84.7
	<i>E. faecalis</i>	0	27	19	5.5	74	280	77.2	50	80.6
	<i>S. epidermis</i>	0	90	1	1	25	2.5	26.3	12	60.1
	<i>S. aureus</i>	0	57	19	2.5	41.5	49	39.8	35	82.8
	<i>MRSA</i>	0	57	19	2	45.8	28	15.3	19	39
Gram-Negative bacteria	<i>E. coli</i>	85	15	5	1.5				10	
	<i>K. pneumoniae</i>	82	5	6	2.5				12.5	
	<i>P. aeruginosa</i>	60	21	11	3.5				12	

Table 1-2: Membrane depolarization ratios

Of the Gram-positive bacteria that were tested, *E. faecalis* was the most resistant to the CSAs, which could be the result of the lack of PE and PG in the cell membranes. In the membrane depolarization test, all the CSAs gave positive results by increasing the polarity of the cell membrane, which was observed by the elevating fluorescent. 4*MBC was the highest concentration of CSAs that were used as a control. The level of depolarization reached a maximum from 1 min to 5 mins. For Gram-positive bacteria, cyanine dye was used straightforward because it entered the cytoplasmic membrane directly. Results showed that at

the concentration of the MBCs, membrane depolarization reached 50% to 90%. For Gram-negative bacteria, EDTA was used to allow the dye to traverse the outer membrane, and was compared to CSA-8. In the experiment, the fluorescent dye accesses the cytoplasmic membrane through the help of CSAs or EDTA to permeabilize the OM barrier. The phenomenon could be observed by the loss of fluorescence after the addition of the agents under relatively low concentration caused by incorporation of the dye in the cytoplasmic membrane. At the MBC and above the CSAs, the fluorescence of the probe increased. This supported the idea that the incorporation was competitive with the membrane depolarization. By understanding the relationship between the MBC and concentration depolarization required for, we were able to correlate membrane depolarization with the bactericidal activity of the CSAs (**Figure 1-5**).

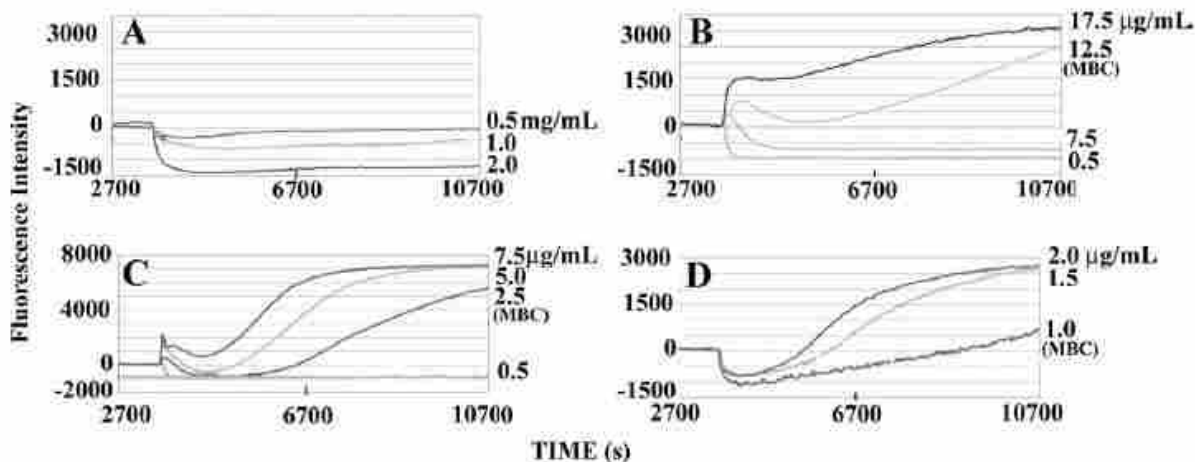


Figure 1-5: DiS-C₂ (5) levels in the process of membrane depolarization

1.2.2 Resistance of Gram-negative and Gram-positive bacteria to CSA-13

1.2.2.1 Resistance of Gram-negative and Gram-positive bacteria to AMPs

Over 1,600 antimicrobial peptides (AMPs) have been isolated in nature, and bacteria have been exposed to them for eons.³⁸ As a result, it is not surprising that bacteria evolved means to resist AMPs. To avoid being killed by AMPs, some bacteria alter the structure of their membrane components. For Gram-negative bacteria, modification of the lipid A containing outer membrane by addition of cationic groups is the most common way to generate resistance.³⁹ However, this resistance does not come from the mutation of genes, thus, outside the presence of AMPs, bacteria return to susceptible forms. Adding aminoarabinose on the lipid A has been shown to be a means to obtain resistance. The modified lipid A has been detected in the lipopolysaccharide (LPS) extraction. The procedures for analysis of this modification have been well developed.⁴⁰

1.2.2.2 Resistance of Gram-positive bacteria to CSA-13

Since CSAs mimic the actions of AMPs, we wanted to test the bacterial resistance to CSAs and study the mechanism of action. Evaluation of the propensity of bacteria to generate resistance to antibacterial agents can be performed using the following multiple challenge procedures. First, bacteria are exposed to incrementally varied concentrations of an antimicrobial agent. The organisms that grow at the highest concentration of the antimicrobial are cultured and re-exposed to the same reagents. The procedure is repeated, and the MIC and MBC to the reagents are monitored. In multiple studies, 15 to 20 passages are performed and bacterial resistance is observed with some antibacterial agents after only a few passages.

For Gram-positive bacteria, *Staphylococcus aureus* was used in the test (Figure 1-6). After 10 serial passages, the MIC of ciprofloxacin increased to over 10 µg/ml. By 18 passages, the MIC had increased to over 100 µg/ml. The MIC of vancomycin increased from 1 to 5-7 µg/ml over 20 passages, while variations in the MIC of CSA-13 were minor. Compared to AMPs, similar results were obtained. Because the cytoplasmic membrane is exposed to the agents directly, there is not a large resistance to CSA-13 after 30 passages, as compared to other antimicrobial agents. The highest MIC values measured were 1.2 µg/ml.

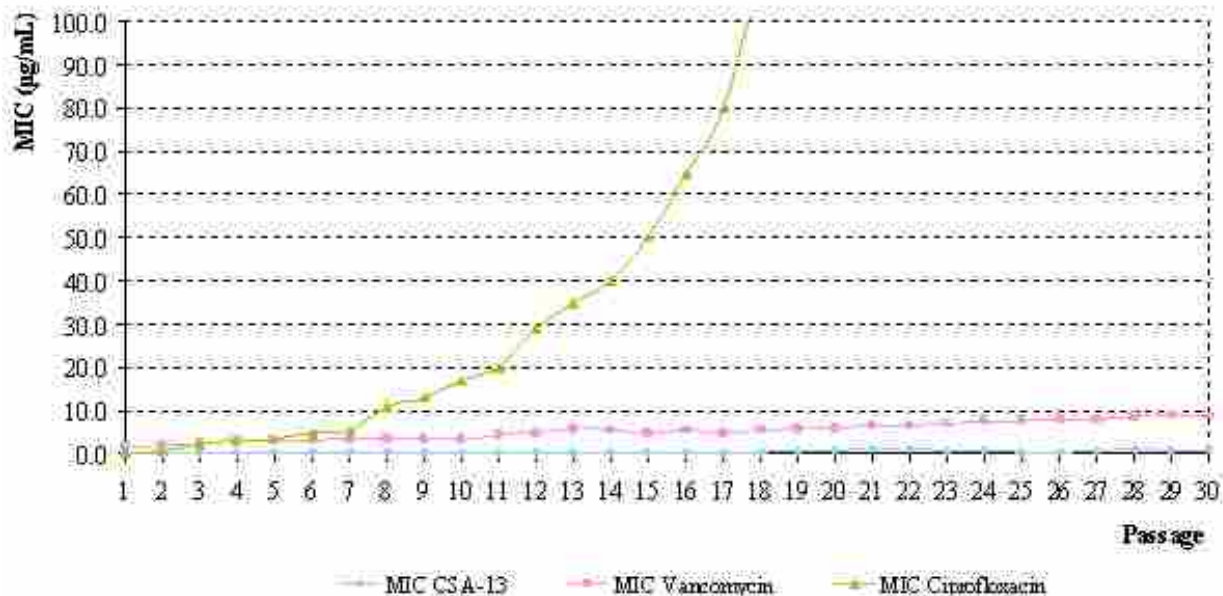


Figure 1-6: Serial Passage *S. aureus*

1.2.2.3 Resistance of Gram-negative bacteria to CSA-13

For Gram-negative bacteria, high resistance was observed against ciprofloxacin and colistin. The MIC values against CSA-13 increased, but the slope was much lower than those of

colistin and ciprofloxacin (**Figure 1-7** and **Figure 1-8**). Strains with high resistance to the comparator antibiotics were not cross-resistant to CSA-13, suggesting that mechanisms of action and of resistance are distinct. The increase in MIC values against CSA-13 appears to be due to lipid A modifications. To confirm this hypothesis, lipid A modification in the LPS extraction from the strain with resistance was tested.

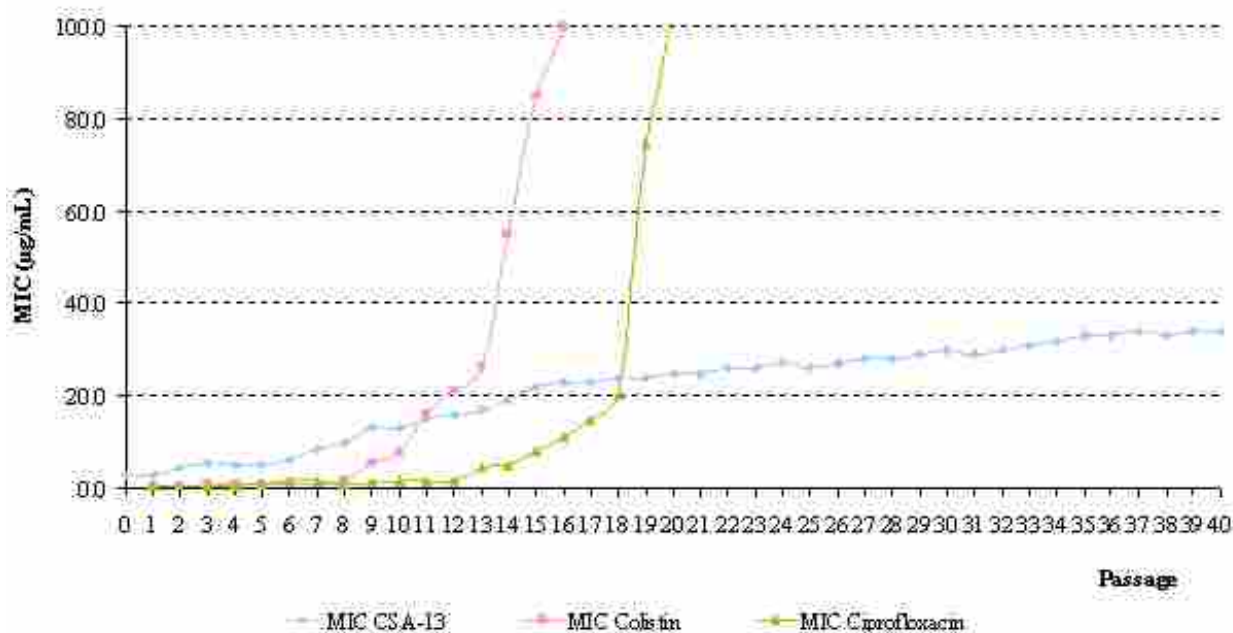


Figure 1-7: Serial Passage *A. baumannii*

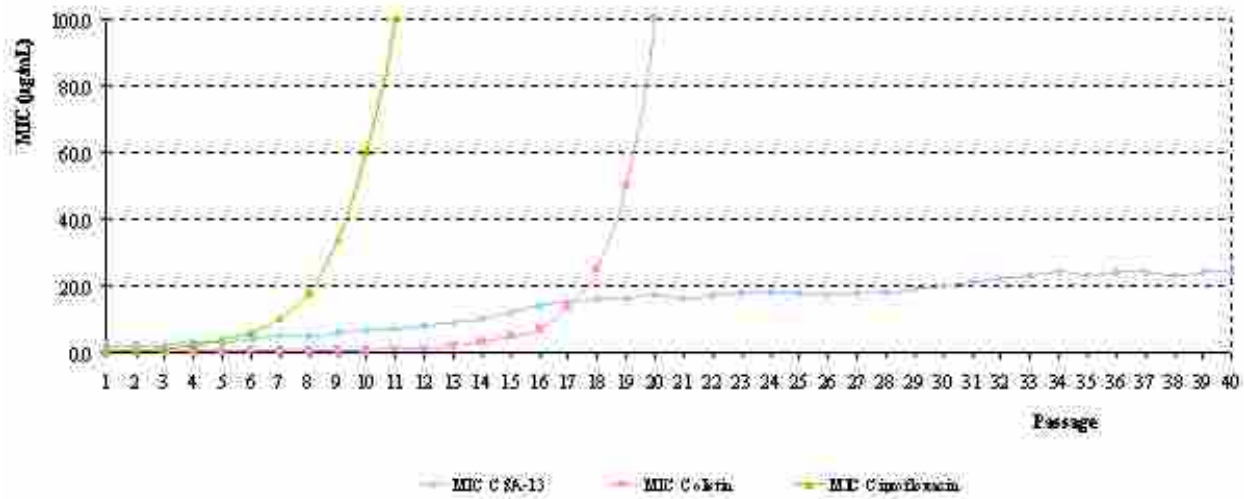


Figure 1-8: Serial Passage *P. aeruginosa*

Lyophilized bacterial cells were vigorously vortexed in chloroform. Then, cells were centrifuged to separate solids. The aqueous phase was lyophilized. LPS was further purified by adding $MgCl_2$ solution. The resulting mixture was centrifuged. The solid was washed with a mixture of chloroform and methanol. Lipid A was obtained as a precipitate after being centrifuged. Then, detergent was added to hydrolysis LPS. After lyophilization, the detergent was removed using diluted HCl in ethanol. After being dried, the residue was considered to be pure lipid A. MALDI-TOF was used to characterize the lipid A. For the wild type of lipid A, the mass was found to be 1617.90. As for the mutation, a mass of 1748.94 was observed together with 1617.90 (**Figure 1-9**). The difference of 131 in Mass is aminoarabinose, which is also found in bacteria resistant to AMPs.

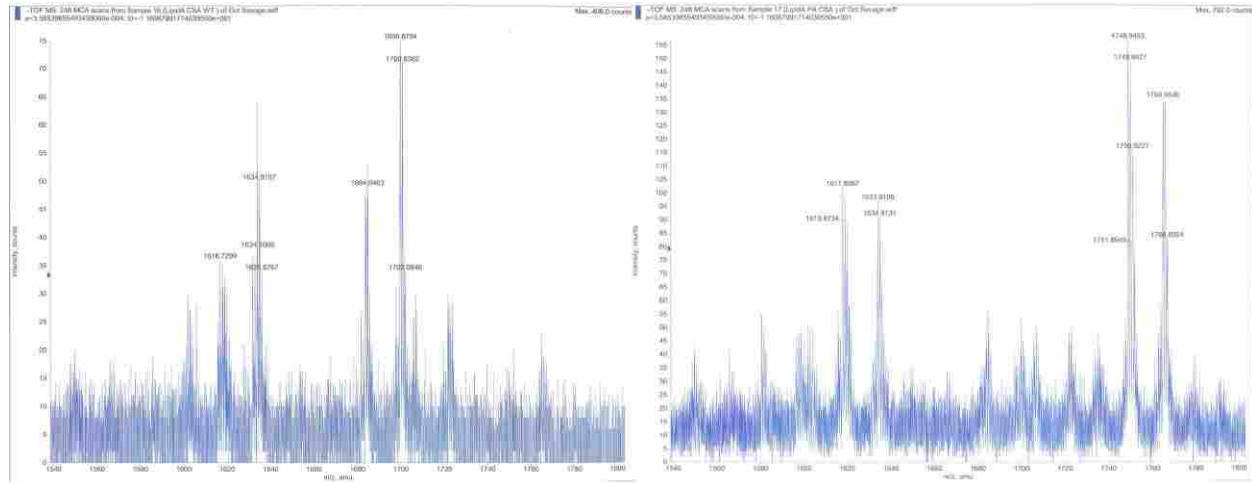


Figure 1-9: The mass spectra of the wild type lipid A and the mutation

1.2.3 Results and discussion

For the bactericidal activity of CSA-13, there is a large electric potential across the cytoplasmic membrane of bacteria. This electrical barrier can be dissolved through a perturbation of the membrane, which would allow the flow of charge without necessarily allowing the passage of small organic molecules such as ONPG. Due to the fact that results from the assays with *E. coli* ML-35p indicated that not all the CSAs achieved bactericidal activity by increases in the rate of transport of molecules across the cytoplasmic membrane, we investigated that there was a smaller breach of the permeability barrier of the cytoplasmic membrane that would allow passage of electrical current, perhaps as a result of proton flux, causing membrane depolarization without allowing passage of larger molecules. DiS-C₂(5), a kind of fluorescent cyanine dye was used to monitor membrane depolarization. In the experiment, CSA-13 can

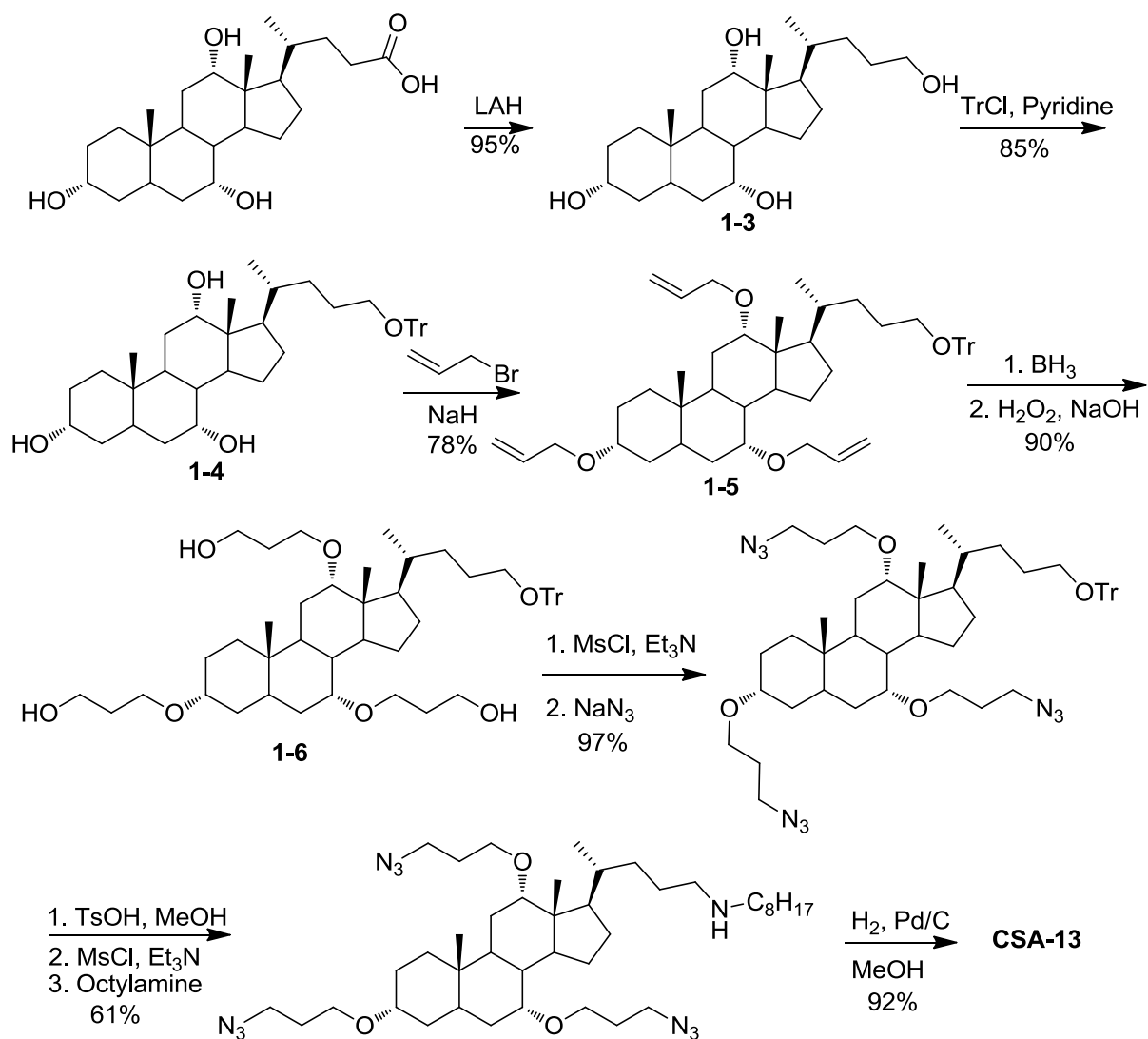
efficiently depolarize the cytoplasmic membrane of Gram-negative bacteria and induce solute leakage, causing a bactericidal effect.

For the bacterial resistance against CSA-13, the MICs of Gram-positive bacteria grew slightly. The resistance of Gram-negative bacteria against CSA-13 increased obviously, but not as significantly as that of other antimicrobial agents. Besides, the resistance is not mutated to the bacteria genes, and fades away without the presence of CSA-13. In Mass spectrum, structural changes of lipid A in the mutation of the cell membrane were observed. Aminoarabinose was found being added on the membrane surface.

1.3. Process Development of CSA-13

Due to the excellent antimicrobial activities of CSA families, many applications of CSA are possible. Hence, to synthesize CSAs in large scale will be necessary. Two routes have been developed from cholic acid or methyl cholate to CSA-13 in large scales.

In the original route (**Scheme 1-1**), sodium azide was used to replace the terminal hydroxyl groups on the side chains. But for the industry synthesis, azide is not recommended due to the explosion potency and the high toxicity. Hence, other routes or reagents to avoid azide are necessary. Fewer steps and recrystallization instead of column purification are highly desired. Two new routes have been investigated to fulfill those demands.

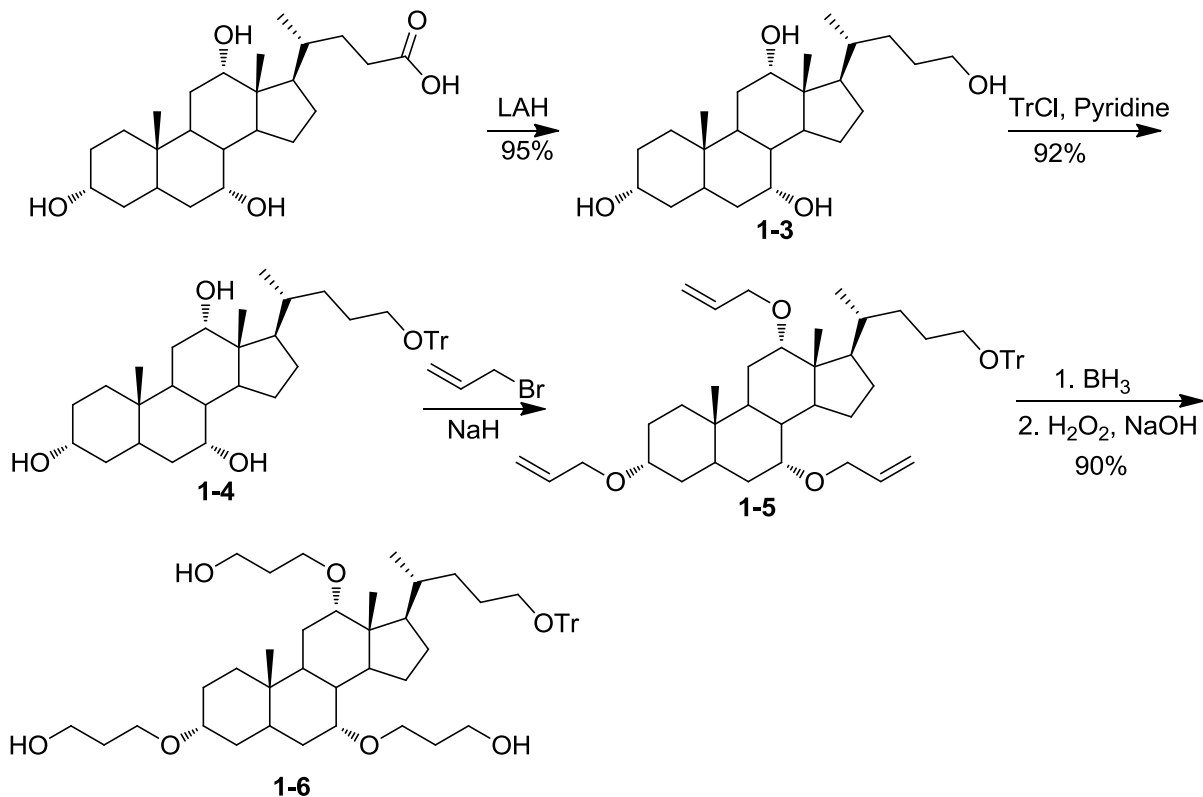


Scheme 1-1: The original route to synthesize CSA-13

1.3.1 Route 1

From cholic acid, LiAlH₄ reduction gave the tetraol 1-3, in which the unreacted acid can be washed off with MeOH. Additionally, after getting rid of water by heating, the product was obtained as a powder. Trityl group was used to selectively protect the primary hydroxyl group in

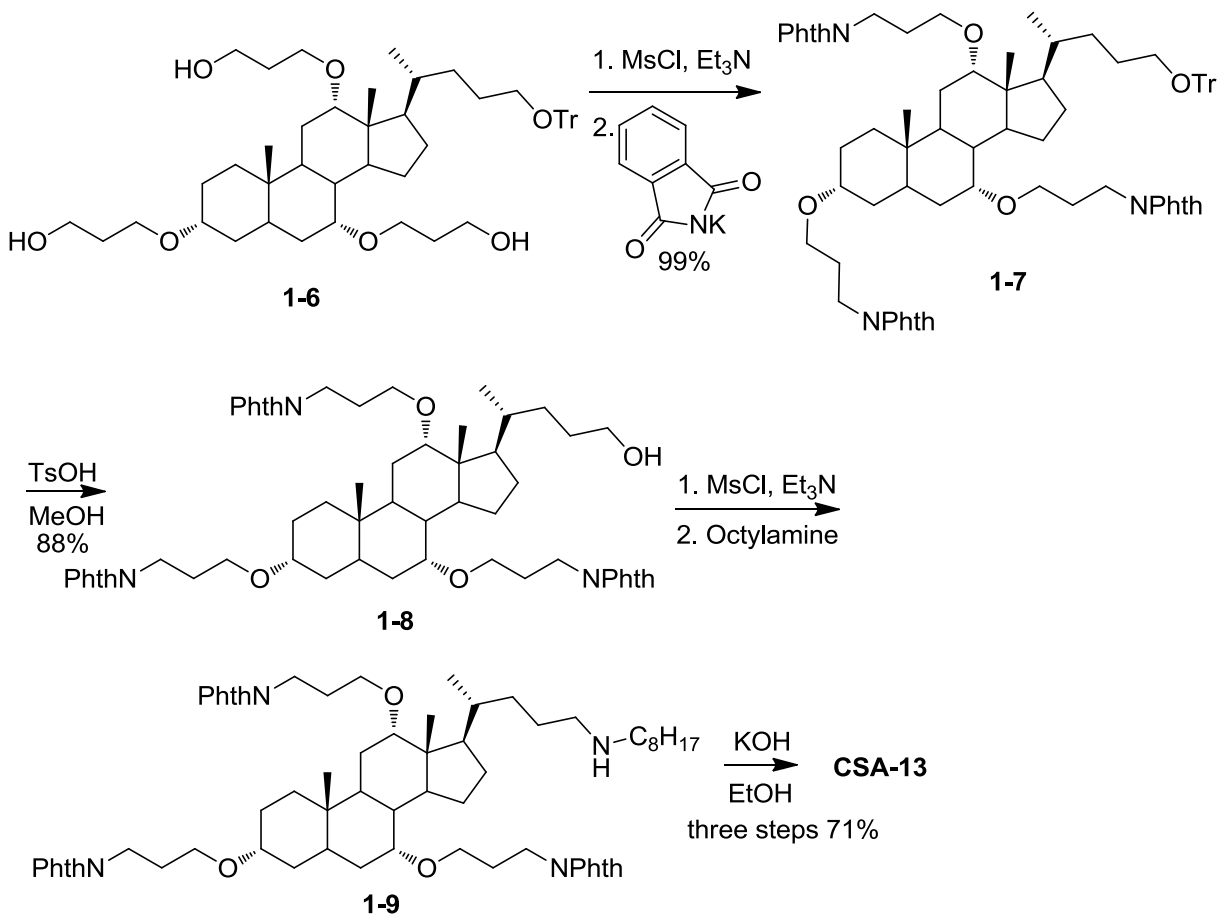
acetonitrile with pyridine at 80 °C for 12 hrs. Filtration afforded pure 1-4, and the by-product remained in the solvent. Heating of the product powder was used to remove the trace amount of the solvent. The yield was 92%. Allylation, followed by hydroboration, produced 1-6 in up to 90% yield after recrystallization (**Scheme 1-2**).



Scheme 1-2: The optimized synthesis of intermediate 1-6

1-6 was then dissolved in methyl ethyl ketone. After mesylation, followed by substitution by potassium phthalimide, 1-7 can be obtained in nearly quantitative yield. Removing the trityl protecting group and recrystallization gave 1-8 in 88% yield. Mesylation, followed by

octylamine substitution at room temperature afforded crude 1-9. Hydroxylation using KOH in EtOH produced crude CSA-13 (Scheme 1-3).



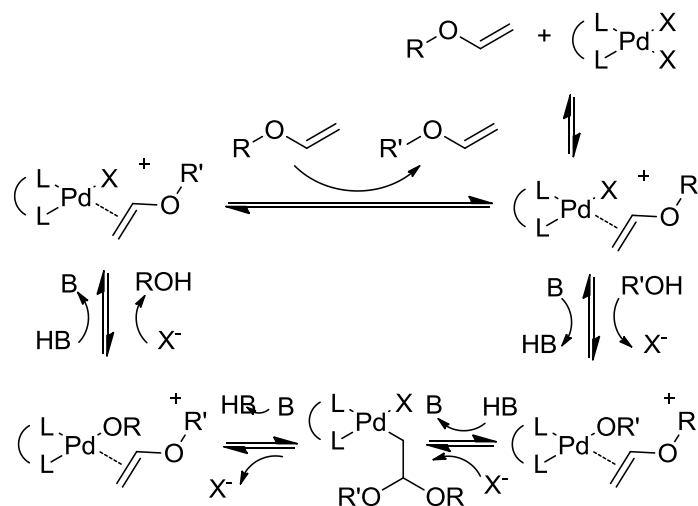
Scheme 1-3: The optimized synthesis of CSA-13 from 1-6

With a large amount of CSA-13 and the derivatives in hand, we are able to investigate their activities and behaviors in vivo.

1.3.2 Route 2

The key step in CSAs synthesis is to install the three carbon side chains on cholic acid and derivatives. Previously, only allyl halides were found to react with three hydroxyl groups in the steroid nucleus. Other electrophiles, such as acrylate, acrylamide and acrylonitrile, failed to sufficiently react with the oxygens at 3, 7 and 12 position due to the high hindrance at those positions and polymerization of the agents under basic conditions.

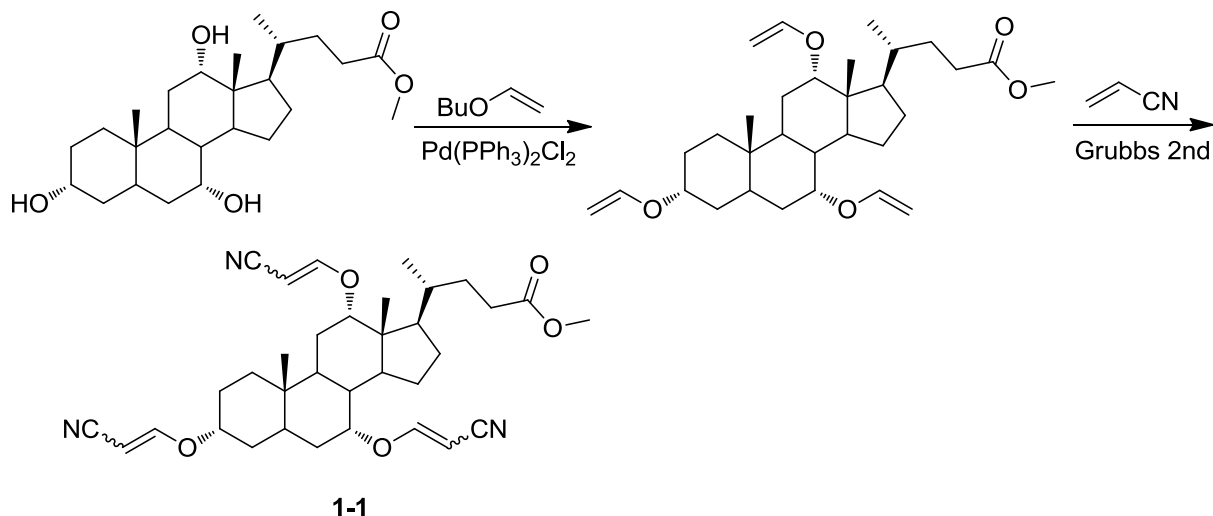
An ether transformation method has been reported by Marcel Schläpfer.⁴¹ Butyl vinyl ether was used to install a vinyl group on an alcohol and release butanol as a by-product (Scheme 1-4). This reaction was carried out using palladium acetate as catalyst under basic condition. If we can build vinyl groups on the hydroxyl groups, then, metathesis can be used to grow up the side chain.



Scheme 1-4: The mechanism of the ether transformation

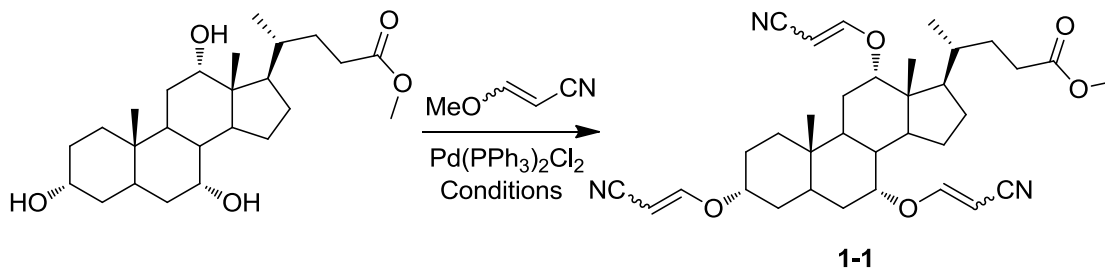
Three equivalents of palladium catalyst and butyl vinyl ether were then tried to transfer vinyl group on methyl cholate, followed by metathesis to install three carbon side chains with

terminal nitrogen on the scaffold. The hindrance on the 12 position caused the low yield of the intermediate (**Scheme 1-5**), so that the strategy was abandoned.



Scheme 1-5: Applied transvinylation on installing three-carbon side chain.

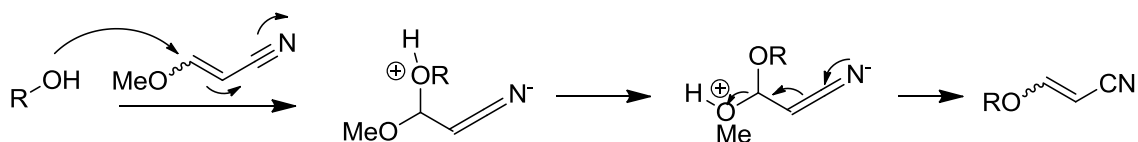
Then, we tried to synthesize 1-1 using 3-methoxy acrylonitrile to do transvinylation directly with methyl cholate. The yield surprisingly reached 80%, but unfortunately, it's not reproducible. We think the reaction system must be contaminated and the unknown compound promotes the desired result. So, a series of reactions conditions were investigated (**Scheme 1-6**).



Scheme 1-6: Synthesis of 1-1

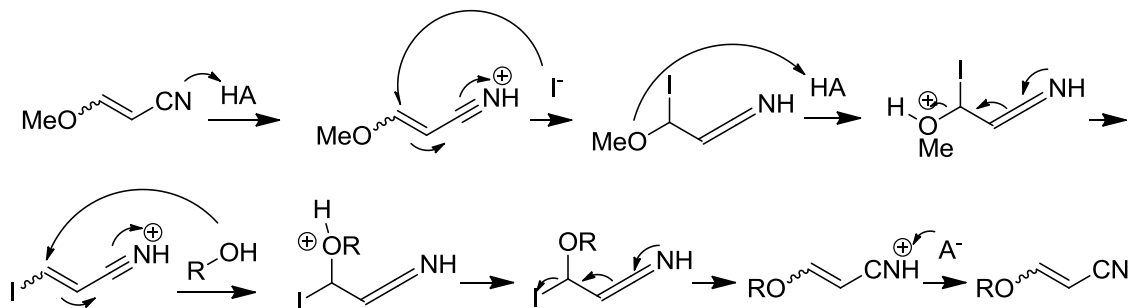
To get a consistent high yield, we tried different amounts of palladium catalyst and base. We found that the yield is not related to the amount of catalyst, nor that of base. Raising the reaction temperature and pumping methanol out of the reaction system helped increase the yield.

The following mechanism was proposed (**Scheme 1-7**). The hydroxyl group attacks the unsaturated nitrile to do 1, 4-addition. Then, the lone pair electrons on the nitrogen push back to reform the conjugated nitrile, and an equivalent of methanol is generated. Pulling off the methanol from system by connecting the reaction system with lab vacuum helps in improving the yield.



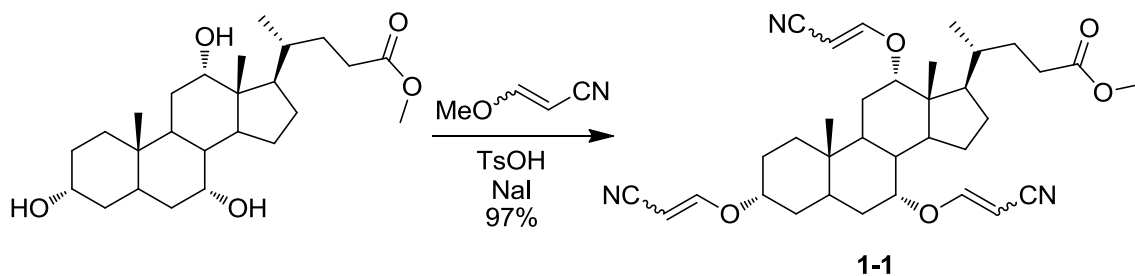
Scheme 1-7: Proposed mechanism of ether transfer on 3-methoxy-acrylonitrile under basic condition

Based on the hypothesis, the reaction should work better under acidic conditions. It is possible that iodide could also help. As a result, different amounts of NaI and acids were then added, instead of base and palladium catalyst (**Scheme 1-8**). Under acidic condition, iodide undergoes a 1, 4-addition, followed by the removal of methanol, generates the vinyl iodide. Then, the hydroxyl group on the substrate replaces the iodide by the same route to produce the product.



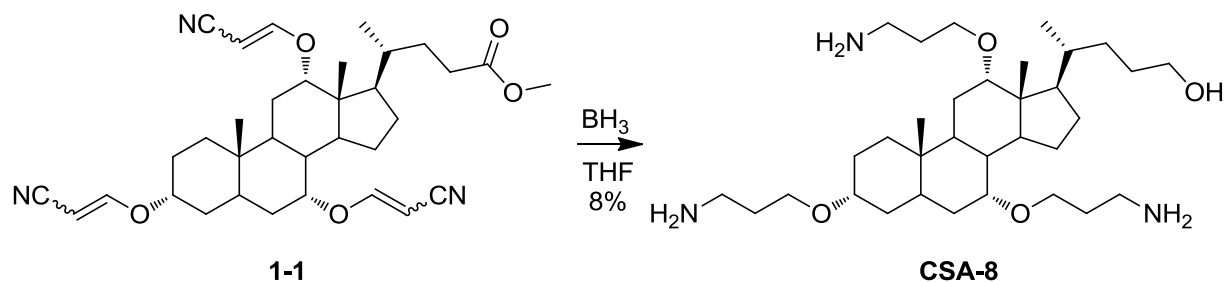
Scheme 1-8: Proposed mechanism of ether transfer on 3-methoxy-acrylonitrile under acidic condition

These series of experiments showed that 0.25 equivalent of TsOH and 0.1 equivalent of NaI gave the best yield (**Scheme 1-9**). PPTS was also tried, but it produced a significant amount of unknown by-product. With the optimized method, the reaction was applied in a large scale, with a 97% yield. A 100g scale of methyl cholate was tried and the conditions worked well.



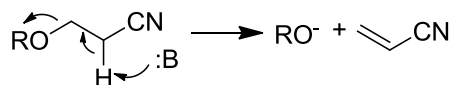
Scheme 1-9: Optimized method to install the side chains on methyl cholate

From compound 1-1 to CSA-8, there were three double bonds, three nitriles and one ester that needed to be reduced (**Scheme 1-10**). For the global reduction, seven equivalents of BH_3 were used in the next step to drive the reaction to completion, but the yield was disappointing. Less than 10% of the product was isolated. LAH reduction was also tried, but no product was observed. A strong mass peak of 1-3 showed up in the spectrum.



Scheme 1-10: Preparation of CSA-8 from 1-1

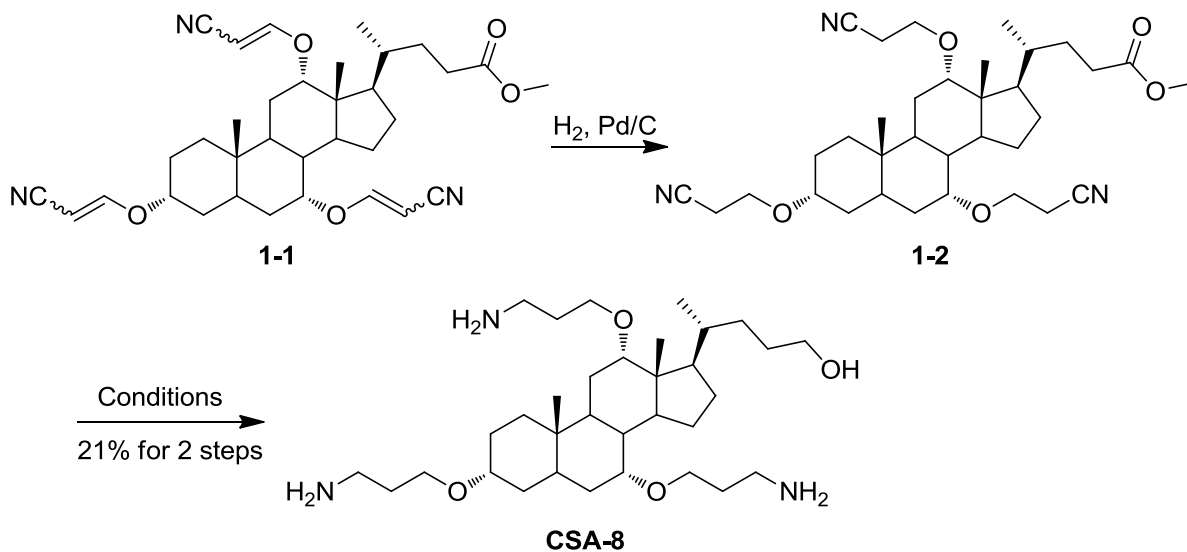
β -elimination is considered to be the main issue (**Scheme 1-11**). By monitoring the reaction using mass spectrometry, reduction of the double bonds was first observed. Since the α -proton on the saturated nitrile, formed in the hydride 1, 4-addition, is acidic, it could be pulled off by the base in the system, and the lone pair electrons should be able to eliminate the β -oxygen to generate alkoxides.



Scheme 1-11: β -elimination of the saturated nitrile intermediate

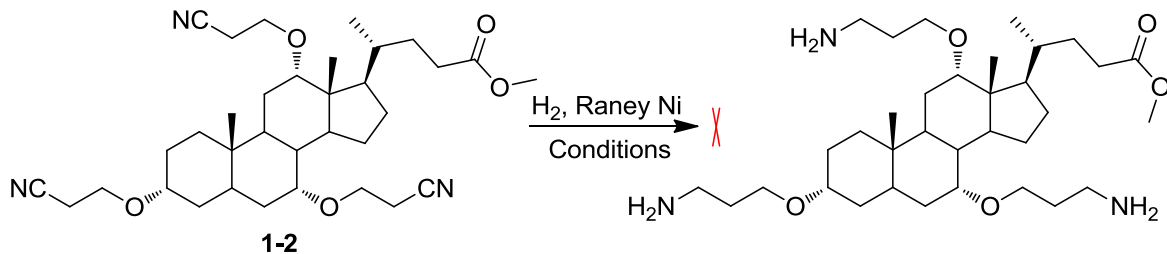
As a result, to get a better yield, the smallest amount BH_3 was used (**Scheme 1-12**). Hydrogenation was performed to reduce the three double bonds; consequently we could use 3 less equivalent of BH_3 to get all the functional groups reduced. However, the hydrogenation proceeded slowly, even after 20% palladium on carbon was used in MeOH at 100 psi of the hydrogen. Acetic acid was not helpful, due to β -elimination. The reaction would not complete in two weeks. In order to reduce the nitrile and ester, four equivalent of BH_3 was used. After refluxing for five hours, the nitrile groups were converted to free amines, and the yield rose to

20%, from 1-1 to CSA-8. NaBH₄ reduction catalyzed by NiCl₂ or CoCl₂ was also performed, but no product could be detected.



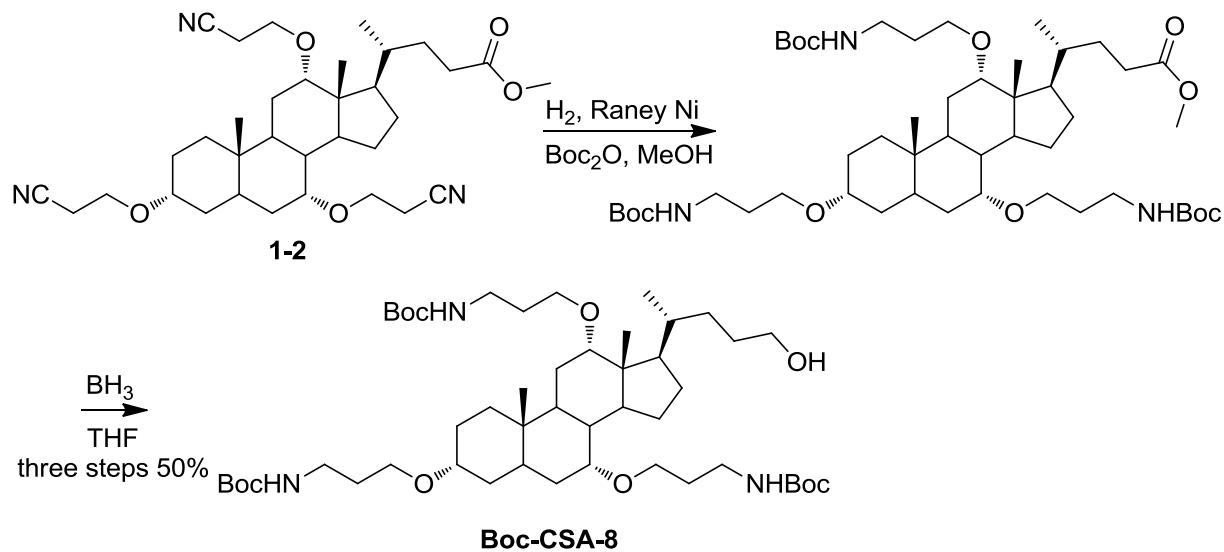
Scheme 1-12: Optimized synthesis of CSA-8 from 1-1

Further hydrogenation catalyzed by Raney Ni was pursued under acidic conditions to prevent amine ester exchange. There was almost no product detected. β -Elimination seemed to be the major issue by mass spectrometry. Considering the components in Raney Ni, we removed the NaOH by washing the catalyst using H₂O and MeOH, sequentially. However, the reaction did not proceed under this condition (**Scheme 1-13**).



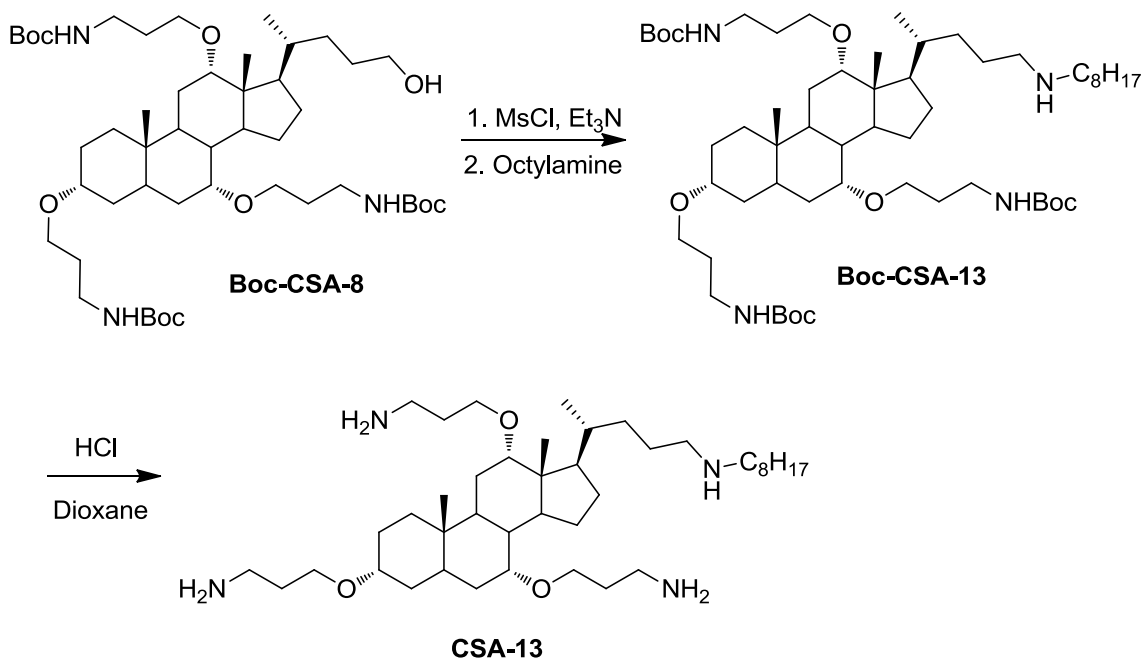
Scheme 1-13: Failed hydrogenation using Raney Ni

Considering that free amine will react with Boc_2O and release CO_2 and iso-butene, three equivalent of Boc_2O was added in the reaction system. The hydrogenation completed in one day and the formed amine was protected with Boc in situ. The intermediate was used in the next step without purification. Borane reduction afforded Boc-CSA-8 in 50% yield for 3 steps (**Scheme 1-14**).



Scheme 1-14: Optimized preparation of Boc-CSA-8 from 1-2.

Mesylation, followed by octylamine substitution, produced Boc-CSA-13. After purification, Boc-CSA-13 was deprotected under acidic conditions, and pure CSA-13, HCl salt, was obtained without purification. The synthesis was finished in 6 steps, and the yield is 43.65% (Scheme 1-15).



Scheme 1-15: Synthesis of CSA-13 from Boc-CSA-8

1.4 Development of ceragenins derivatives and the applications

1.4.1 ^{99m}Tc binded CSA derivatives in cell imaging

1.4.1.1 Medical imaging

Medical imaging is a technique using radionuclides to create image of the body for clinical purposes. It relies on the process of radioactive decay in the diagnosis and treatment of

disease.⁴² Radionuclides are combined with existing pharmaceutical compounds, to form radiopharmaceuticals. These radiopharmaceuticals can localize to specific organs or cellular receptors, once applied to the patient. This property of radiopharmaceuticals allows nuclear medicine to image the extent of a disease-process in the body, based on the cellular function and physiology, rather than relying on physical change by the tissue surgery. In some cases, nuclear medicinal studies can identify medical problems on an earlier stage than other diagnostications.

1.4.1.2 ^{99m}Tc

^{99m}Tc is a metastable nuclear isomer of ^{99}Tc . It has a 6 hour half-life which is much shorter than most of nuclear isomers that undergo γ -decay. In 24 hours, 93.7% of it decays to ground state ^{99}Tc , and the wavelength of the emitted γ -ray is about the same as conventional X-ray diagnostic equipment. The short half life of the isotope allows for rapid data collection and keeps patient radiation exposure low. Hence, ^{99m}Tc is widely used in medical imaging.⁴³

1.4.1.3 CSA derivative used in medical imaging as ^{99m}Tc binder.

Since CSAs have a high binding affinity with prokaryotic membranes over eukaryotic membrane, due to anionic PG and CL in cell membrane components, CSAs should be able to bring the radioactive elements, bound to them, to the bacteria infected organs or parts of the human body.

In our research, we designed CSA-107 to achieve that purpose (**Figure 1-10**). Literatures reports indicate that using aminothiols to chelate ^{99m}Tc produced a relatively stable complex.ⁿ In CSA-107, we added similar functional groups on the 24 position of the CSA scaffold.

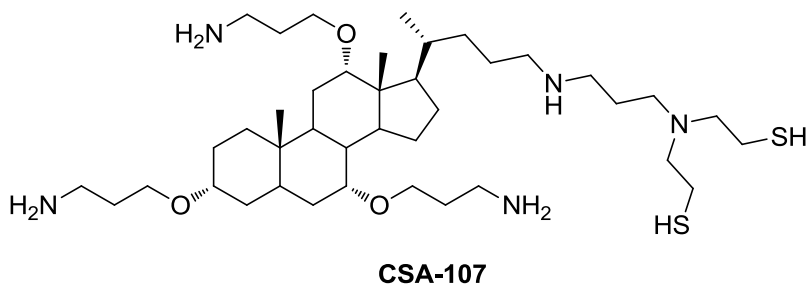
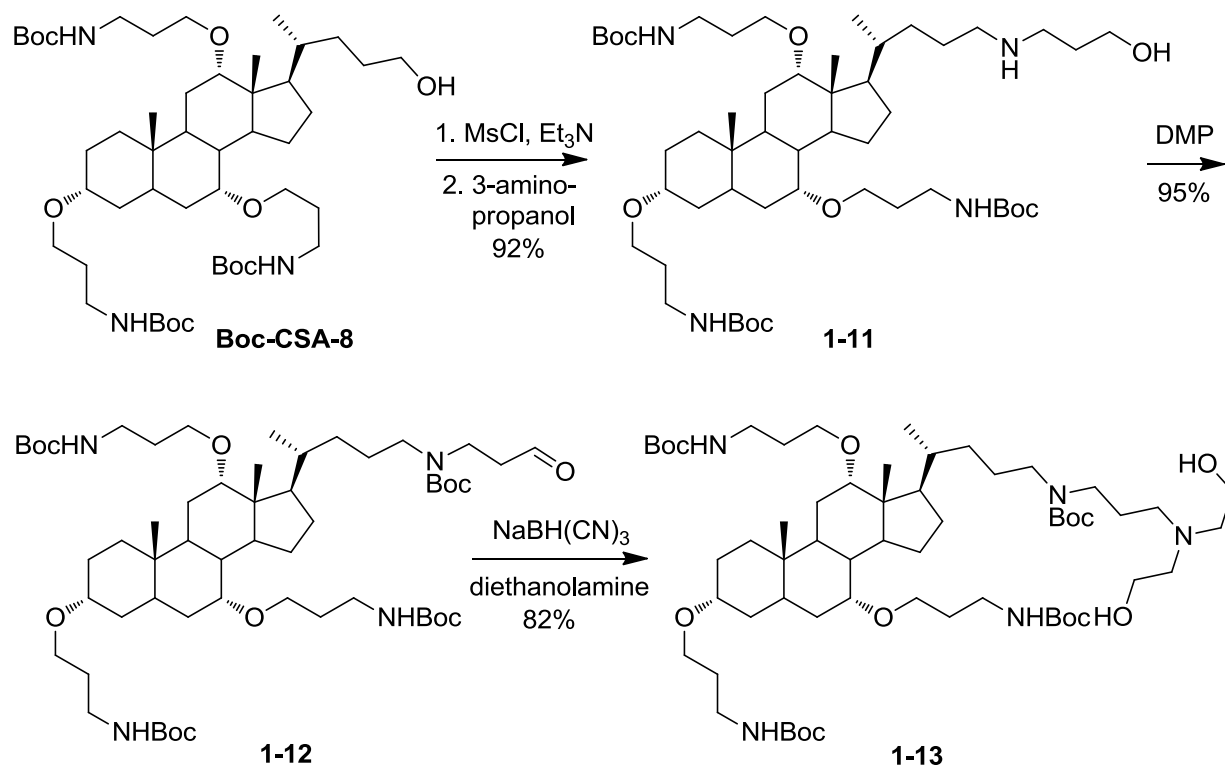


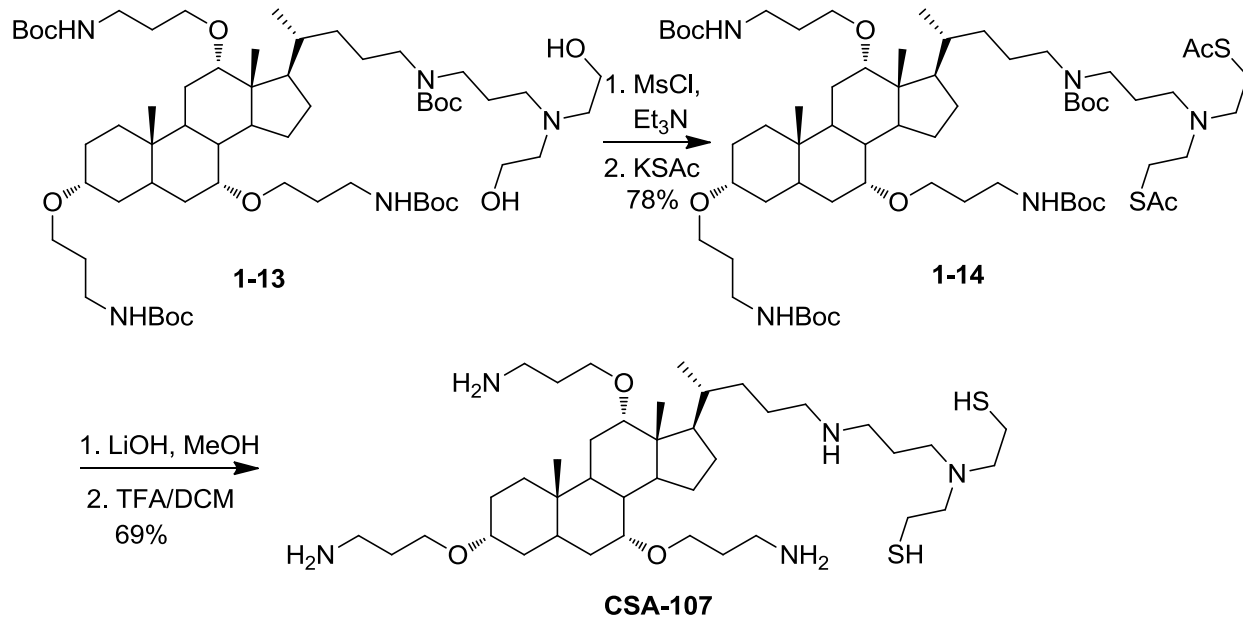
Figure 1-10: Structure of CSA-107

First, Boc-protected-CSA-8 was used as starting material. Mesylation followed by 3-aminopropanol substitution produced 1-11. Boc-protection followed by Dess-Martin oxidation gave the corresponding aldehyde 1-12. Reductive amination with diethanolamine produced 1-13 (**Scheme 1-16**).



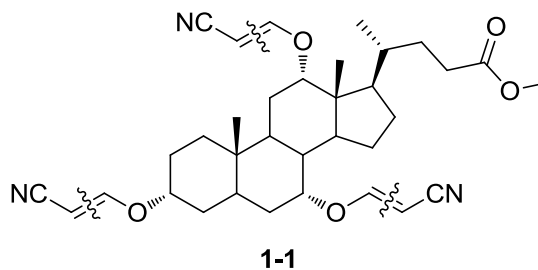
Scheme 1-16: Synthesis of intermediate 1-13

Mesylation followed by potassium thioacetate substitution generated 1-14. Boc-deprotection under acidic condition followed by LiOH hydroxylation failed to produce CSA-107. The amino groups was freed by LiOH would attack the thioacetate to form the corresponding amide. Removing acetyl group from the thioacetate, followed by deprotecting the Boc groups afforded target CSA-107 (**Scheme 1-17**).



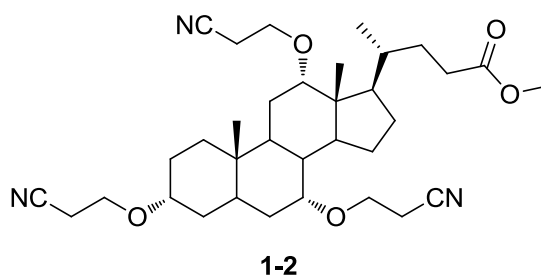
Scheme 1-17: Synthesis of CSA-107

1.5 Experiment Section

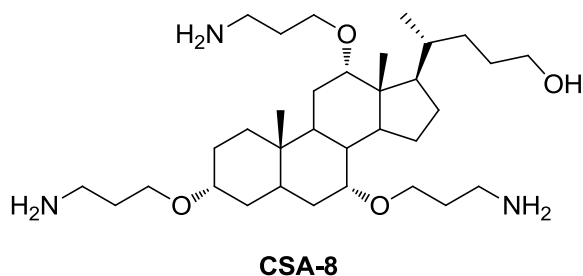


To a solution of methyl cholate (50 g, 118 mol) in 800 mL of 3-methoxy-acrylonitrile, PTS (3.5 g, 19.2 mmol) and NaI (700 mg, 4.7 mmol) were added. The mixture was heated to 80 °C under lab vacuum 1 day. The solvent was removed by distillation under vacuum. 66 g of

the product was isolated, as a foam, through a column chromatography (SiO₂). The yield was 97%.

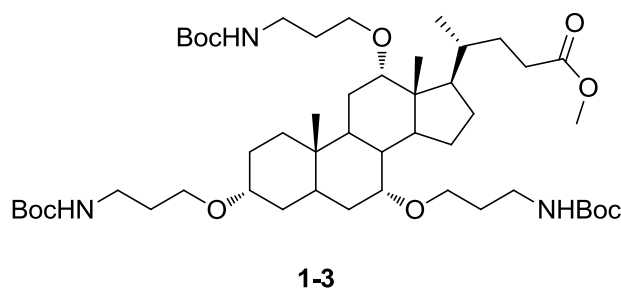


To a solution of the **1-1** (65 g, 123 mmol) in 300 mL of MeOH, 15 g of Pd(OH)₂ was added. The mixture was stirred 3 days under 1000 psi of H₂. After filtration, the solvent was removed and the residue was used in the next step without further purification. ¹H NMR (CDCl₃, 500 MHz) δ 3.724-3.797 (m, 4 H), 3.656-3.686 (m, 4 H), 3.359-3.404 (m, 3 H), 3.179 (br, 1 H), 2.569-2.706 (m, 7 H), 1.996 (q, *J* = 7.5 Hz, 2 H), 1.651 (s, 3 H), 1.388-1.416 (m, 2 H), 1.268-1.313 (m, 10 H), 0.881 (t, *J* = 7.5 Hz, 3 H); ¹³C NMR (CDCl₃, 125 MHz) δ 136.58, 40.10, 27.77; HRMS (ESI) calcd for C₁₂H₂₄O [M+H]⁺: 184.1827, found: 184.1836.

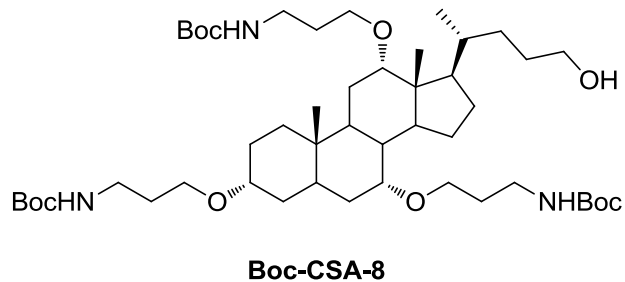


To a solution of 65 g of crude **1-2** in 600 mL of THF, 400 mL of 1 M BH₃ in THF was added. The solution was reflux for 6 hrs. After the solvent was removed, 14 g of **CSA-8** was

isolated through a column chromatography (SiO₂). The yield was 21%. ¹H NMR (CDCl₃/ 30% CD₃OD, 300 MHz) δ 4.43 (bs, 7 H), 3.74-3.68 (m, 1 H), 3.66-3.60 (m, 1 H), 3.50-3.57 (m, 5 H), 3.25-3.34 (m, 2 H), 3.06-3.17 (m, 2 H), 2.74-2.84 (m, 6 H), 2.01-2.19 (m, 3 H), 0.96-1.97 (m, 27 H), 0.94 (d, *J* = 7.2 Hz, 3 H), 0.92 (s, 3 H), 0.69 (s, 3 H); ¹³C NMR (CDCl₃, 75 MHz) δ 80.44, 79.27, 75.77, 66.59, 66.53, 65.86, 62.51, 46.21, 45.84, 42.55, 41.53, 40.09, 39.43, 39.31, 39.02, 35.16, 34.93, 34.86, 34.57, 32.93, 32.71, 31.57, 28.66, 28.33, 27.64, 27.22, 23.04, 22.40, 22.29, 17.06, 11.98; HRMS (ESI) calcd for C₁₀H₁₇Si [M+H]⁺: 566.4889, found: 566.4898.

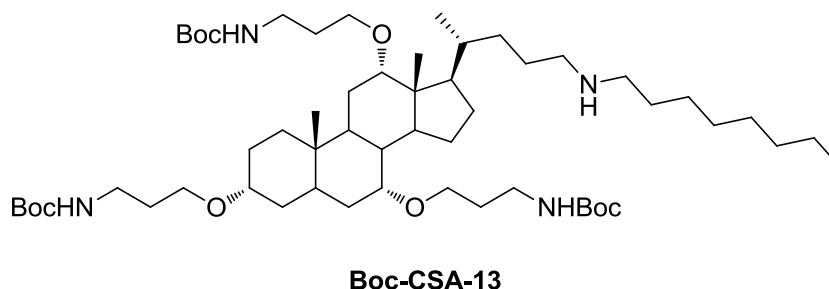


To a solution of the **1-2** (65 g, 123 mmol) and Boc₂O (88.7 g, 406 mmol) in 500 mL of MeOH, 15 g of Raney Ni was added. The mixture was stirred 3 days under 1000 psi of H₂. After filtration, MeOH was removed and toluene was used to help remove the water. The residue was used in the next step without further purification. ¹H NMR (CDCl₃, 500 MHz) δ 3.724-3.797 (m, 4 H), 3.656-3.686 (m, 4 H), 3.359-3.404 (m, 3 H), 3.179 (br, 1 H), 2.569-2.706 (m, 7 H), 1.996 (q, *J* = 7.5 Hz, 2 H), 1.651 (s, 3 H), 1.388-1.416 (m, 2 H), 1.268-1.313 (m, 10 H), 0.881 (t, *J* = 7.5 Hz, 3 H); ¹³C NMR (CDCl₃, 125 MHz) δ 136.58, 40.10, 27.77; HRMS (ESI) calcd for C₁₂H₂₄O [M+H]⁺: 184.1827, found: 184.1836.



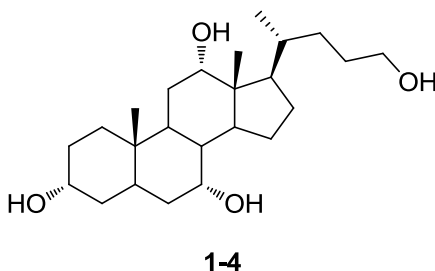
From **CSA-8**: To a solution of **CSA-8** (14 g, 24.8 mmol) in 200 mL of THF, Boc₂O (18 g, 81.6 mmol) was added in portion. The solution was stirred overnight. 20.5 g of the product was isolated through a column chromatography (SiO₂)

From **1-3**: To a solution of 54 g of crude **1-3** in 500 mL of THF, 200 mL of 1 M BH₃ in THF was added. The solution was stirred at room temperature for 24 hrs. After the solvent was removed, 24 g of **CSA-8** was isolated through a column chromatography (SiO₂). The overall yield was 50%.

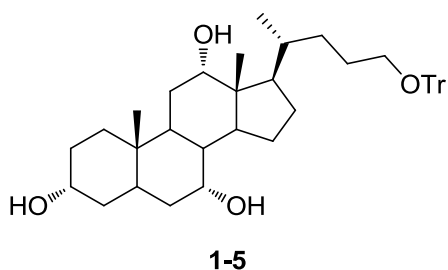


To a solution of **Boc-CSA-8** (20.5 g, 23.7 mmol) in 200 mL of THF, MsCl (2.98 g, 26.1 mmol) and Et₃N (2.64 g, 26.1 mmol) were added at 0 °C. The temperature was allowed to rise up to room temperature. The solution was stirred for 30 mins. Then, 100 mL of water was used to wash the solution. The aqueous layer was extracted with DCM three times. The combined

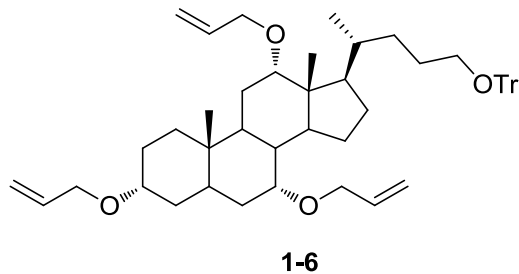
organic layer was dried over Na_2SO_4 . After the solvent was removed, 50 mL of octylamine was added to dissolve the residue. The mixture was stirred at 80 °C overnight. The temperature was cooled to room temperature then, 200 mL of water and 200 mL of DCM were added. The aqueous layer was extract with DCM three times and the combined organic phase was dried over Na_2SO_4 . After removing the solvent, 19.32 g of the product was isolated through a column chromatography (SiO_2). The yield was 85%.



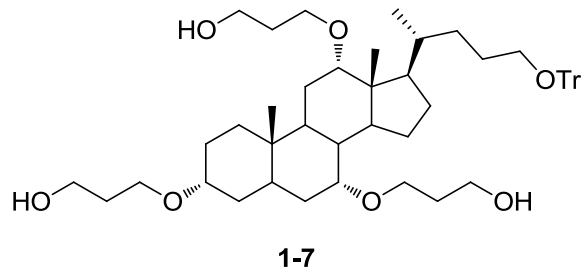
To a suspension of LiAlH_4 (9 g, 236.8 mmol) in 1 L of THF, cholic acid (50 g, 122.5 mmol) was added at 0 °C. The mixture was refluxed 24 hrs. 120 mL of saturated Na_2SO_4 was added to quench the reaction at 0 °C. The filter cake was washed with 100 mL of cold MeOH. 42 g of **1-3** was obtained as a white powder, after the trace amount of water was removed under 120 °C. The yield was 95%. ^1H NMR (CDCl_3 / 30% CD_3OD , 200 MHz) δ 3.98 (br, 1 H), 3.83 (br, 1 H), 3.60-3.46 (m, 2 H), 3.38 (br, 5 H), 2.30-2.10 (m, 2 H), 2.05-1.05 (m, 22 H), 1.03 (br, 2 H), 0.92 (s, 3 H), 0.71 (s, 3 H); ^{13}C NMR (CDCl_3 , 50 MHz) δ 73.89, 72.44, 68.99, 63.51, 48.05, 47.12, 42.49, 40.37, 39.99, 36.62, 36.12, 35.58, 35.40, 32.77, 30.69, 30.04, 29.02, 28.43, 27.27, 23.96, 23.08, 18.00, 13.02; HRMS (ESI) calcd for $\text{C}_{24}\text{H}_{42}\text{O}_4$ $[\text{M}+\text{H}]^+$: 566.4889, found: 566.4898.



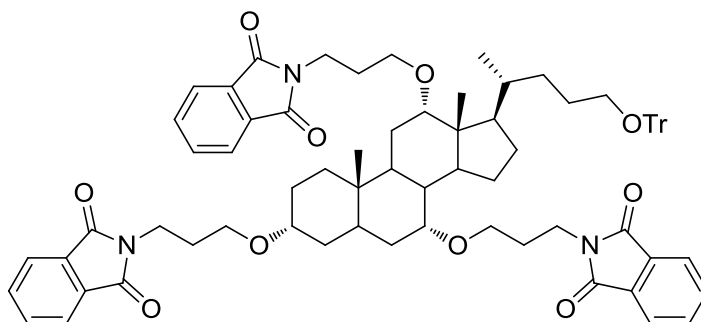
To a suspension of **1-4** (42 g, 106.5 mmol) in 400 mL of MeCN, TrCl (41.5 g, 149 mmol) and dry pyridine (12.6 g, 159.75 mmol) was added. The suspension was heated at 65 °C for 16 hrs. After the temperature was cooled down to room temperature, 240 mL of MeCN was added. The mixture was stirred for 2 hrs. The solid was washed with 100 mL of MeCN. 61 g of **1-4** was obtained as a white powder, after the trace amount of the solvent was removed under 120 °C. The yield was 92%. ¹H NMR (CDCl₃, 200 MHz) δ 7.46-7.42 (m, 6 H), 7.32-7.17 (m, 9H), 3.97 (br, 1 H), 3.83 (br, 1 H), 3.50-3.38 (m, 1 H), 3.01 (br, 1 H), 2.94 (dd, *J* = 14.2, 12.2 Hz, 2 H), 2.64 (br, 1 H), 2.51 (br, 1 H), 2.36-2.10 (m, 2 H), 2.00-1.05 (m, 22 H), 0.96 (d, *J* = 5.8 Hz, 3 H), 0.87 (s, 3 H), 0.64 (s, 3 H); ¹³C NMR (CDCl₃, 50 MHz) δ 144.77, 128.93, 127.91, 127.01, 86.43, 73.35, 72.06, 68.66, 664.28, 47.47, 46.53, 41.74, 41.62, 39.64, 35.57, 35.46, 34.91, 34.82, 32.40, 30.55, 28.21, 27.69, 26.80, 26.45, 23.36, 22.59, 17.83, 12.61; HRMS (ESI) calcd for C₄₃H₅₆O₄ [M+H]⁺: 637.4179, found: 637.4183.



To a solution of **1-5** (41.5 g, 65.2 mmol) in 400 mL of dry THF, NaH (8 g, 326 mmol), tetrabutylammonium iodide (802.4 mg, 2.17 mmol), and allyl bromide (39.4 g, 326 mmol) were added. The mixture was refluxed overnight. 20 mL of MeOH was added to quench the reaction at 0 °C. After the solvent was removed, 100 mL of water was added. Hexanes were used to extract the mixture. The combined organic layer was dried over Na₂SO₄. After the solvent was removed, 44.4 g of the crude product was obtained and used in the next step directly. ¹H NMR (CDCl₃, 200 MHz) δ 7.48-7.30 (m, 6 H), 7.32-7.14 (m, 9H), 6.04-5.80 (m, 3 H), 5.36-5.04 (m, 6 H), 4.14-3.94 (m 4 H), 3.74 (dt, *J* = 13.8, 5.8 Hz, 2 H), 3.53 (br, 1 H), 3.20-2.94 (m 3 H), 3.31 (br, 1 H), 2.38-1.90 (m, 4 H), 1.90-0.96 (m, 20 H), 0.90 (d, *J* = 5.4 Hz, 3 H), 0.89 (s, 3 H), 0.64 (s, 3 H); ¹³C NMR (CDCl₃, 50 MHz) δ 144.83, 136.27, 136.08, 128.94, 127.90, 126.98, 116.46, 115.40, 86.42, 80.94, 79.29, 74.98, 69.52, 69.39, 68.86, 64.39, 46.51, 46.42, 42.67, 42.14, 39.92, 35.63, 35.51, 35.13, 32.45, 28.98, 28.09, 27.66, 27.57, 26.72, 23.32, 23.11, 17.92, 12.69; HRMS (ESI) calcd for C₅₂H₆₈O₄ [M+H]⁺: 757.5118, found: 757.5123.

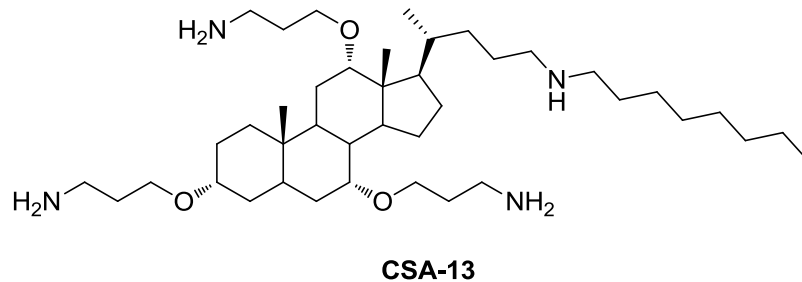


To a 100 mL of 1 M BH_3 in THF, cyclohexene (16 g, 200 mmol) in 50 mL of THF was added 0 °C. The mixture was stirred 30 mins. **1-6** (22 g, 30 mmol) in 200 mL of THF was added, and the solution was refluxed for 6 hrs. After the temperature was cooled down to 0 °C, 70 mL of 20% NaOH and 70 mL of H_2O_2 was added dropwise carefully. The reaction mixture was refluxed overnight. Before the THF was removed, KI / starch test paper was used to make sure that no peroxide remained. EtOAc was used to extract the mixture and after dried over Na_2SO_4 , the solvent and the cyclohexanol were removed under vacuum. The resulting sticky oil was used in the next step without purification. The crude yield was 90%. ^1H NMR (CDCl_3 , 200 MHz) δ 7.50-7.42 (m, 6 H), 7.32-7.14 (m, 9H), 3.90-3.65 (m, 13 H), 3.50 (br, 6 H), 3.40-2.96 (m, 6 H), 2.30-0.94 (m, 30 H), 0.90 (s, 3 H), 0.88 (d, $J = 5.4$ Hz, 3 H), 0.64 (s, 3 H); ^{13}C NMR (CDCl_3 , 50 MHz) δ 144.73, 128.88, 127.85, 126.94, 86.36, 80.52, 78.90, 76.36, 66.82, 66.18, 65.77, 64.22, 61.53, 61.41, 61.34, 46.89, 46.04, 42.60, 41.59, 39.60, 35.37, 35.27, 34.88, 32.75, 32.44, 32.31, 28.82, 27.65, 27.48, 27.13, 26.77, 23.35, 22.74, 22.38, 18.08, 12.48; HRMS (ESI) calcd for $\text{C}_{52}\text{H}_{74}\text{O}_7$ $[\text{M}+\text{H}]^+$: 811.5435, found: 811.5440.



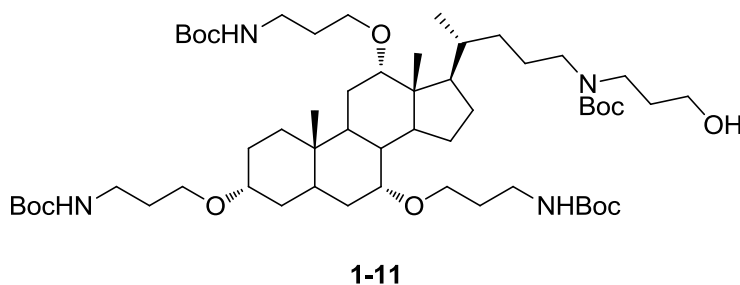
1-8

To a solution of crude **1-7** in 100 mL of THF, MsCl (3.8 g, 33 mmol) and Et₃N (3.4 g, 33.5 mmol) were added at 0 °C. The solution was stirred for 30 mins. After removing the solvent, 50 mL of water was added. The mixture was extracted with EtOAc. The combined organic phase was dried over Na₂SO₄. After the solvent was removed, 100 mL of 2-butanone was used to dissolve the residue. Potassium phthalimide (18.6 g, 100 mmol) was added, and the mixture was stirred at 80 °C for 24 hrs. The product was obtained by recrystallization in 99% yield. ¹H NMR (CDCl₃, 200 MHz) δ 7.50-7.42 (m, 6 H), 7.32-7.14 (m, 9H), 3.90-3.65 (m, 13 H), 3.50 (br, 6 H), 3.40-2.96 (m 6 H), 2.30-0.94 (m, 30 H), 0.90 (s, 3 H), 0.88 (d, *J* = 5.4 Hz, 3 H), 0.64 (s, 3 H); ¹³C NMR (CDCl₃, 50 MHz) δ 144.73, 128.88, 127.85, 126.94, 86.36, 80.52, 78.90, 76.36, 66.82, 66.18, 65.77, 64.22, 61.53, 61.41, 61.34, 46.89, 46.04, 42.60, 41.59, 39.60, 35.37, 35.27, 34.88, 32.75, 32.44, 32.31, 28.82, 27.65, 27.48, 27.13, 26.77, 23.35, 22.74, 22.38, 18.08, 12.48; HRMS (ESI) calcd for C₅₂H₇₄O₇ [M+H]⁺: 811.5435, found: 811.5440.



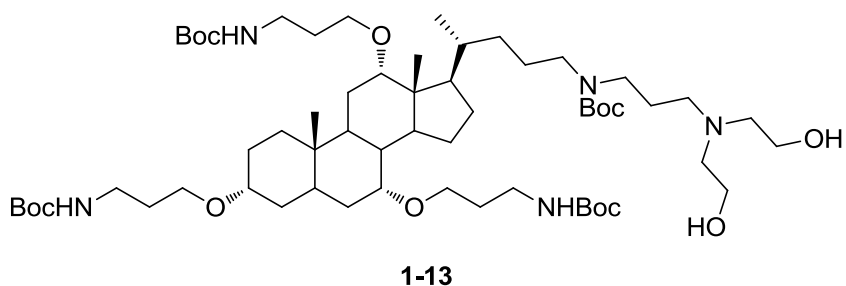
Route 1: **Boc-CSA-13** (19.32 mg, 20 mmol) was dissolved into 50 mL of 4 M HCl/Dioxane solution. The solution was stirred overnight. After removing the solvent, 200 mL of toluene was poured into the residue. 13.5 g of **CSA-13** was obtained by azeotropic removing the solvent in 92% yield.

Route 2: To a solution of **1-9** in mL of DMF, 10 g of hydrozine was added. The mixture was stirred at 80 °C 24 hrs. The mixture was poured into 100 mL of water and extracted with hexanes 10 times. The yield was 77%.

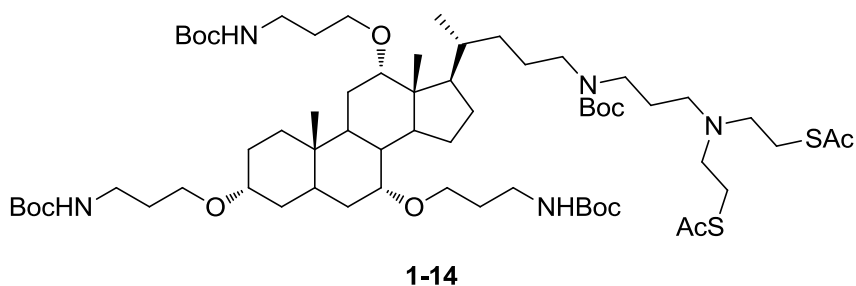


To a solution of **Boc-CSA-8** (500 mg, 0.58 mmol) in 5 mL of DCM, MsCl (73 mg, 0.64 mmol) and Et₃N (64.5 mg, 0.64 mmol) were added at 0 °C. The temperature was allowed to rise up to room temperature. The solution was stirred for 30 mins. Then, 2 mL of water was used to wash the solution. The aqueous layer was extracted with DCM three times. The combined

organic layer was dried over Na_2SO_4 . After the solvent was removed, 3-amino-1-propanol (368 mg, 5 mmol) was added to dissolve the residue. The solution was stirred at 80 °C for 2 hrs. 3-amino-1-propanol was removed under vacuum. 5 mL of water was used to wash the solution. The aqueous layer was extracted with DCM three times. The combined organic layer was dried over Na_2SO_4 . After removing the solvent, the residue was dissolved into 5 mL of DCM. Then, Boc_2O (127 mg, 0.58 mmol) was added. The solution was stirred overnight. 480 mg of the product **1-10** was isolated through a column chromatography (SiO_2) in 92% yield%.



To a solution of **1-11** (650 mg, 0.67 mmol) in 2 mL of MeOH, amine (85 mg, 1 mmol), $\text{NaBH}(\text{OAc})_3$ (120 mg, 1.38 mmol) and a drop of AcOH were added. The mixture was stirred at 50 °C overnight. After removing the solvent, the product was obtained through a column chromatography (SiO_2), in 82% yield.



1.6 References

1. Porter J. R. *Bacteriological Reviews* **1976**, 40 (2), 260–9.
2. Collins, M. D.; Hoyles, L.; Foster, G.; Falsen, E. *Int. J. Syst. Evol. Microbiol.* **2004**, 54, 925–8.
3. Balcht, A.; Smith, R. *Pseudomonas Aeruginosa: Infections and Treatment. Informa Health Care.* **1994**, 83–84.
4. Kluytmans J.; Belkum, A.; Verbrugh, H. *Clin. Microbiol. Rev.* **1997**, 10 (3), 505–20
5. Bowersox, J. *Experimental Staph Vaccine Broadly Protective in Animal Studies.* **1999**
6. Bergey, A.; David H.; John G. H.; Noel, R. K.; Snegth H. A. *Bergey's Manual of Determinative Bacteriology* (9th ed.). **1994**. Lippincott, W.; Wilkins; Madigan, M. T.; Martinko, J.; Parker, J. *Brock Biology of Microorganisms* **2004**
7. Ryan, K. J.; Ray, C. G. *Sherris Medical Microbiology* **2004**, 232–3
8. Beveridge, T. J.; Davies, J. A. *Journal of bacteriology* **1983**, 156(2): 846–58
9. Garrod, L. P. *British Medical Journal*, **1960**, 5172, 527–29
10. Goossens, H.; Ferech, M.; Vander S., R.; Elseviers, M. *Lancet*, **2005**, 365 (9459), 579–87
11. Cornelis P. *Pseudomonas: Genomics and Molecular Biology*, **2008**
12. Klein E.; Smith, D. L.; Laxminarayan, R. *Emerg Infect Dis*, **2003**, 13 (12), 1840–6
13. Klevens et al. *JAMA.*, **2007**
14. Centers for Disease Control and Prevention, **2007**
15. Boman, H. G.; Hultmark, D., *Annu. Rev. Microbiol.*, **1987**, 41, 103–126
16. Bowman, H. G.; Agerberth, B.; Bowman, A. *Infect. Immun.* **1993**, 61, 2978

17. Papagianni, M. *Biotechnol Adv* **2003**, *21* (6), 465–499
18. Yeaman, M. R.; Yount, N. Y. *Pharmacological reviews*, **2003**, *55* (1), 27–55
19. Dürr, U. H. N.; Sudheendra, U. S.; Ramamoorthy, A. *Biochimica et Biophysica Acta – Biomembranes* **2006**, *1758* (9), 1408–1425
20. Vaara, *Microbiol. Rev.* **1992**, *56*, 395
21. Zasloff, M. *Proc. Natl. Acad. Sci. USA* **1987**, *84*, 5449
22. Tran D.; Tran P.; Roberts K.; Osapay G.; Schaal J.; Ouellette A.; Selsted, M. E. *Antimicrob. Agents Chemother.*, **2006**, *52* (3), 944–53
23. Nizet, V.; Ohtake, T.; Lauth, X.; Trowbridge, J.; Rudisill, J.; Dorschner, R. A.; Pestonjamas V.; Piraino J.; Huttner K.; Gallo R. L. *Nature* **2001**, *414* (6862), 454–7
24. Porter, E. A.; Weisblum, B.; Gellman, S. H. J. *Am. Chem. Soc.* **2002**, *124*, 7324
25. Liu, D.; Degrado, W. F. J. *Am. Chem. Soc.* **2001**, *123*, 7553
26. Nizet, V.; Ohtake, T.; Lauth, X.; Trowbridge, J.; Rudisill, J.; Dorschner, R. A.; Pestonjamas V.; Piraino J.; Huttner K.; Gallo R. L. *Nature* **2001**, *414* (6862), 454–7
27. Karatan, E.; Watnick, P. *Microbiology and Molecular Biology Reviews* **2009**, *73* (2), 310–47
28. Li, X.; Nikadio, H. *Drug* **2009**, *69* (12), 1555–623
29. Bush, K.; Jacoby, G. A.; Medeiros, A. A. *Antimicrob Agents Chemother.*, **1995**, *39*, 1211-33
30. Joanne, E.; Thwaite, S.; Hibbs, R.; Titball, W.; Timothy P. A. *Antimicrob Agents Chemother.* **2006**; *50*(7), 2316–2322

31. Haukland, H; Ulvatne, H; Sandvik, K; Vorland, L. H. *FEMS Microbiology Lett.* **2001**, 508, 389
32. Barrett, D. G.; Gellman, S. H. *J. Am. Chem. Soc.* **1993**, 115, 9343
33. Matsuzaki, K.; Sugushita, K.; Fujii, N.; Miyajima, K. *Biochemistry*, **1995**, 34, 3423
34. Li, C; Peters, A. S.; Meredith, E. L.; Allman, G. W.; Savage, P. B. *J. Am. Chem. Soc.* **1998**, 120, 2961
35. Scott, N.; Dean, B.; Bishop, M.; Monique, L. *Hoek Front Microbiol.* **2011**, 2, 128
36. Savage, P. B.; Li, C.; Taotafa, U.; Ding, B.; Guan, Q. Y. *FEMS Microbiology Lett.* **2002**, 217, 1
37. Beckloff, N.; Laube, D; Castro, T.; Furgang, D. Park, S.; Perlin, D.; Clements, D.; Tang, H.; Scott, R. W.; Tew, G. N.; Diamond, G. *Antimicrobial Agents and Chemotherapy* **2007**, Vol. 51, No. 11, 4125
38. William C. Wimley[✉] and Kalina Hristova *J Membr Biol.* **2011**, 239(1-2), 27–34
39. Lee, H.; Hsu, F. F.; Truk, J.; Groisman, E. A. *J. Bio. Chem.*, **2004**, 279, 20044
40. Kiyoshi, K. *Journal of Microbiological Methods* **2009**, 76, 313
41. Bosch, M.; Schlaf, M. *J. Org. Chem.*, **2004**, 68, 5225
42. Roobottom CA, Mitchell G, Morgan-Hughes G (November 2010). "Radiation-reduction strategies in cardiac computed tomographic angiography". *Clin Radiol* **65** (11): 859–67
43. Raloff, J. *Science News* **2009**, 176 (7), 16–20.
44. Kitagawa, N.; Oda, M.; Nobutaka, I.; Satoh, H.; Totoki, T.; Morimoto, M. *Toxicology and Applied Pharmacology* **2006**, 217, 100

45. Li, C. H.; Budge, L. P.; Driscoll, C. D.; Willardson, B. M.; Allman, G. W.; Savage, P. B. *J. Am. Chem. Soc.* **1999**, *121*, 931
46. Savage, P. B. *Curr. Med. Chem.-Anti-Infective Agents*, **2002**, *1*(3), 1
47. Epand, R. F.; Savage, P. B.; Epand, R. M. *Biochimica et Biophysica Acta* **2007**, *1678*, 2500

Chapter 2. Natural Killer T cells Recognize Glycolipids as Antigens

2.1 Introduction

2.1.1 Immune systems

An immune system within an organism is a system of biological structures and processes that protects against disease by detection and killing of pathogens. The immune system protects organisms from infection with layered defenses of increasing specificity. In nearly all forms of life, the innate immune system can respond first to the evasion of pathogens. The innate immune system's response is non-specific and immediate, but no immunological memory is produced.¹ If pathogens evade the innate immune system, vertebrates adopt the second layer of protection, the adaptive immune system. The responses of adaptive immune system toward pathogens are specific and can be retained in the form of immunological memory even after the pathogens have been eliminated.²

The cells of the adaptive immune system are special types of leukocytes, called lymphocytes. The two major types of lymphocytes are B cells and T cells, both are derived from hematopoietic stem cells in the bone marrow.³ B cells and T cells both carry receptor molecules that make them able to respond to specific targets. T cells recognize a “non-self” target, such as a pathogen. The recognition requires antigens (small fragments of the pathogen) to be processed and presented in combination with a “self” receptor called a major histocompatibility complex (MHC) molecule.

2.1.2 NKT cells

Natural killer T cells (NKT cells) are a special kind of lymphocyte that bridge the adaptive immune system with the innate immune system. Studies have shown that diminished numbers of NKT cells in human have been potentially relevant to various disease states.⁴ An increased incidence of autoimmune diseases including type 1 diabetes and rheumatoid arthritis have been correlated with diminished numbers of NKT cells. Stimulation of NKT cells can influence forms of lupus and generates positive outcomes in viral, bacterial and parasitic infections. Even some human cancers have been correlated with a loss of NKT cells, and stimulation of NKT cells leads to decrease in tumor size and growth. Due to the critically important impact of NKT cells on human health, people have put great efforts trying to understand the function of NKT cells in regulating immune responses.

NKT cells have been subdivided into at least three subsets.⁵ Among these the most populous and well studied are referred to as invariant NKT cells (iNKT cells). This type of NKT cells present a T cell receptor (TCR) made up of $V\alpha 14$ subunit in mice and the $V\alpha 24$ subunit in humans. Through work by multiple research groups, it has been established that NKT cell stimulation is mediated by presentation of glycolipids by CD1d to NKT cells.⁶ CD1d is one of a family of glycolipid presentation proteins that are evolutionarily related to antigen-presentation proteins major histocompatibility complexes (MHC) which are known to present peptides.

2.1.3 Cytokine release by NKT cells

Upon stimulation, NKT cells can rapidly release a variety of cytokines, which are small cell-signaling protein molecules. These cytokines can promote two different types of immune responses. One type of cytokine including interferon- γ (IFN- γ) and interleukin-2 (IL-2), considered T helper 1 (Th1) cytokines, cause an inflammatory response. The other type of cytokines includes IL-4 and IL-10, and they result in an immunomodulatory or Th2 response. Inflammatory Th1 responses are effective in controlling bacterial, parasitic, and viral infections and can even result in immune responses to tumors. However, Th1 responses also cause autoimmune diseases including multiple sclerosis, lupus, rheumatoid arthritis and type I diabetes.⁶ Th2 cytokines play a contrary role to the immunostimulatory properties of Th1 cytokines and their production can ameliorate autoimmune diseases. Since both Th1 and Th2 cytokines can be produced when the NKT cells are stimulated, optimum control of the types of response generated are necessary for potential medicinal use. In order to treat infection and tumors, a Th1 response is desirable. On the contrary, for prevention or inhibition of autoimmune diseases, Th2 responses are targeted work by multiple groups has established that different cytokine release profiles can be mediated by presentation of specific classes of glycolipids by CD1d to NKT cells.⁷ Even relatively minor changes in glycolipid structure can result in large affinity differences among the binding of CD1d loaded with glycolipid to NKT cell receptor, and this affinity appears to impact the types of cytokines released by the cells.

2.1.4 Glycolipids as antigens

The advances in the research on stimulation of NKT cells have resulted from the discovery that α -galactosylceramides possess distinct iNKT cell activating properties. During the screening natural products for anti-tumor activities, six marine natural products, termed agelasphins, were isolated from a sponge, *Agelas mauritanus*, by Koezuka et al. in 1993. These compounds were found to prolong the life span of B16 mouse melanoma cells inoculated mice and stimulated the proliferation of lymphocytes.^{8, 9} Among the agelasphins, agelasphin 9b showed potent antitumor activities. In general, only glycosylceramides that have β -glycosidic linkage are found in higher organisms. *Agelas mauritanus* contains an α -glycosidic bond between the sugar and ceramide, which is rare. The Kirin group first did structure-activity study of various of agelasphin 9b.¹⁰ They synthesized a series of analogues of agelasphin 9b and found the hydroxyl group at C2' of ceramide (see Figure 2-1 for ceramide numbering) does not significantly influence anti-tumor activity, and the C4 hydroxyl group plays a minor role, but the hydroxyl group at C3 is necessary to maximize activity. Their result also demonstrated that the branched phytosphingosine chain could be simplified into a straight-chain lipid and a longer acyl chain tended to be more biologically active. Taking these findings into consideration; a more potent compound KRN7000 was generated.

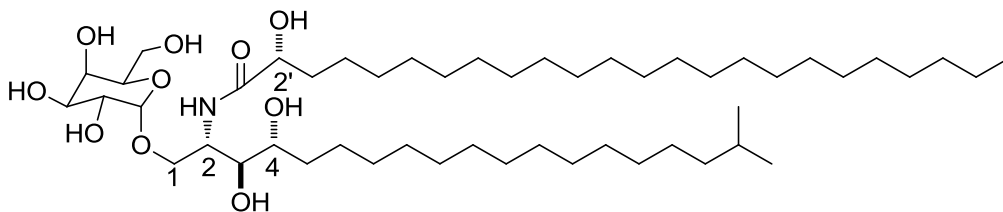


Figure 2-1. Structure of agelasphin 9b.

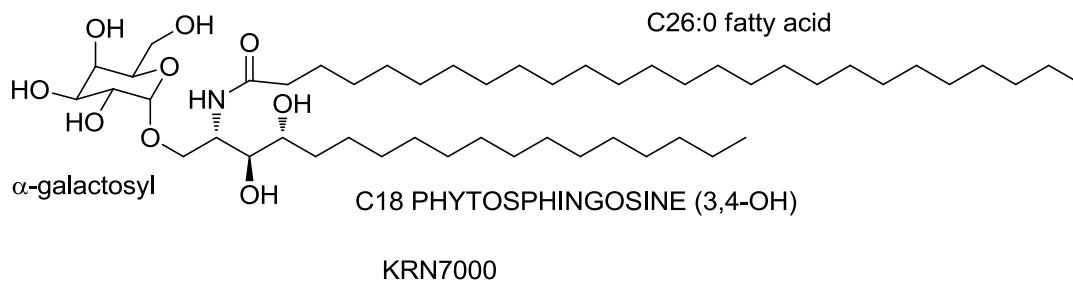


Figure 2-2. Structure of KRN 7000.

The Taniguchi group attempted to develop a ligand which can specifically activate V α 14 NKT cells, and with this compound study the mechanisms of activation of iNKT cells.¹¹ In their study, 10 synthetic glycolipids were used as candidate V α 14 T cell receptor (TCR) ligands and the proliferative responses of V α 14 NKT cells were measured as readout. The stimulation ability of monoglycosylated ceramides were compared as following (Figure 2-3).

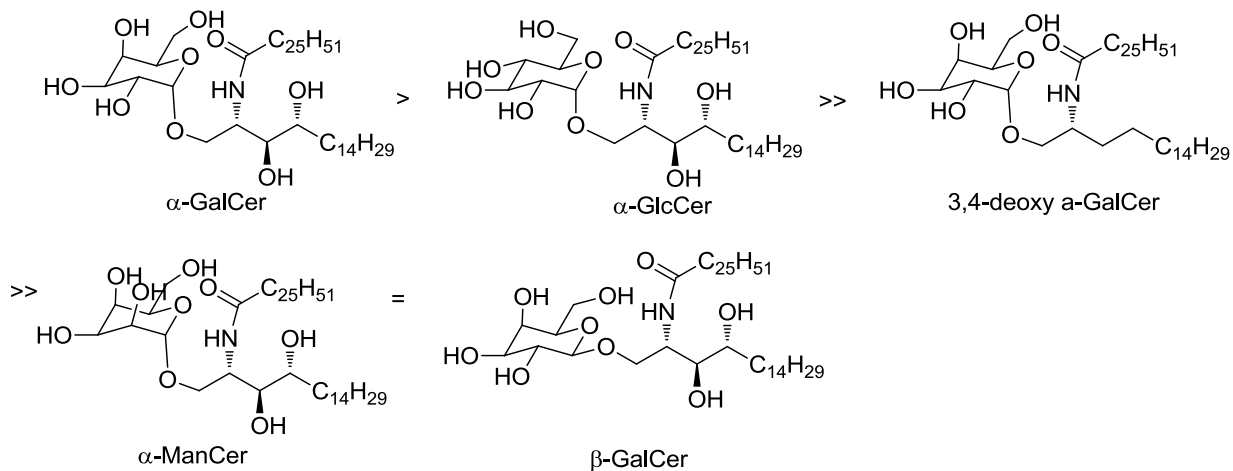


Figure 2-3. Structure of monoglycosylceramides and comparison of their propensity to stimulate proliferation of NKT cells.

In recognition that KRN7000 has relatively poor solubility in either organic or aqueous solvents, our group has synthesized a series of modified α -GalCer in order to determine which site on the sugar head can be modified without negatively influencing the interactions of glycolipid-loaded CD1d with NKT cell receptors. We found that replacing the 6 hydroxyl group of galactose in α -GalCer with an amide linked to a variety of small molecules yields the compounds which retain the ability to stimulate NKT cells comparable to KRN7000.¹² Further studies optimized the structures and generated a new glycolipid PBS-57. PBS-57 has a small acetamide group at C6 position of galactose and a cis-double bond in the acyl chain of the ceramide portion. Especially, the cis-double bond in the acyl chain results in an increase of the solubility over the fully saturated compounds and also facilitates the loading into CD1d tetramers. In vitro and in vivo studies indicated that PBS-57 can stimulate NKT cells more effectively than KRN7000.¹³

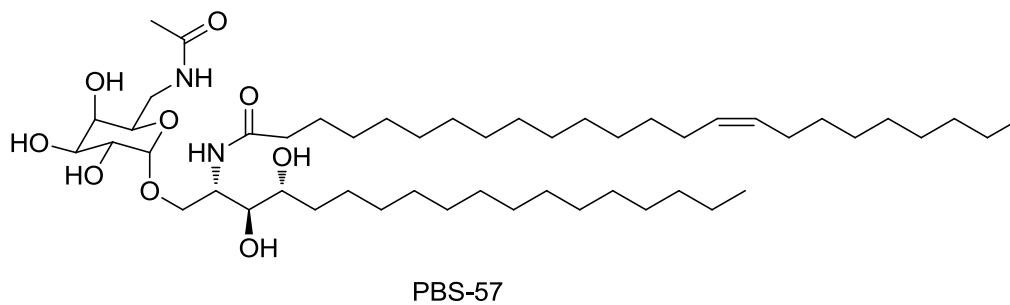


Figure 2-4. Structure of PBS 57.

A research aiming to investigate the recognition mode of $V\alpha 14i$ NKT toward the glycosphingolipid antigens was conducted by Kronenberg group recently.¹⁴ The equilibrium dissociation constant characteristic of the affinity of the $V\alpha 14i$ NKT TCR for the

glycolipid/CD1d complex was measured. The affinity was found to correlate with the ranking of the antigenic potencies of the α -GalCer related glycolipids(α -GalCer>4-deoxy α -GalCer> α -GlcGer> α ManCer). Binding was not detectable for β -GalCer and 3,4-deoxy α -GalCer analogues. The above results demonstrate that the changes in the sugar part and modifications in the ceramide part both have big impacts on the interactions among the three partners. The recognition of NKT cells comes from glycolipid interactions with CD1d and or the TCR. The excellent glycolipid structure should be bound well by CD1d first and then the proper positioned complex may be effectively recognized by the TCR.

As described above, the optimum control of the nature of the stimulation of NKT cells is needed for different potential medicinal use. In 2001 Miyamoto and coworkers' studied how the altered structure of α -GalCer can cause the NKT cells to respond with a Th2 bias.¹⁵ They synthesized three analogues of α -GalCer by changing the sugar moiety and /or truncating the aliphatic chains (Figure 2-5). Through measuring the serum cytokine levels after injection of these compounds, it was found that compound OCH could induce predominant production of IL-4 by NKT cells while α -GalCer causes NKT cells to produce both interferon (IFN)- γ and IL-4. Although compared with α -GalCer OCH was less active in inducing cell proliferation, it could be useful as a therapeutic agent to prevent against TH1 mediated diseases such as experimental autoimmune encephalomyelitis.

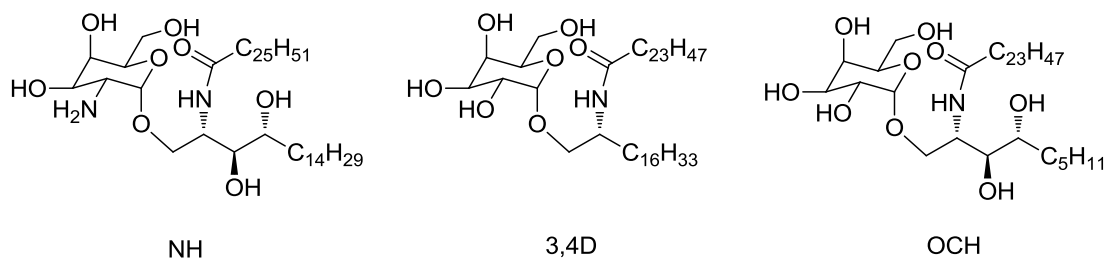


Figure 2-5. The structures of analogues of α -GalCer

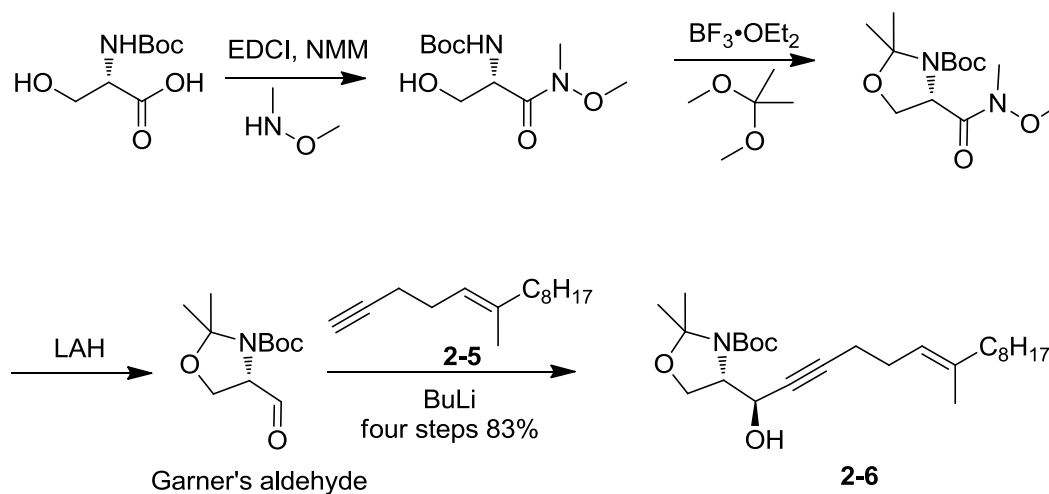
Our group also investigated the impact of truncation of lipid chains on the response of NKT cells.¹⁶ The results suggest that there is a correlation between lipid chain length and cytokine release profiles, the chain-shortened glycolipids increase the amount of IL-4 relative to INF- γ released by NKT cells. The results were consistent with the studies of Oki et al.¹⁷ They explained that truncation of the phytosphingosine chain of α -GalCer leads to a less stable complex with CD1d and INF- γ release by NKT cells requires longer stimulation by CD1d-glycolipid complexes than IL-4.

2.2 Thraustochytroside A and B

2.2.1 Background

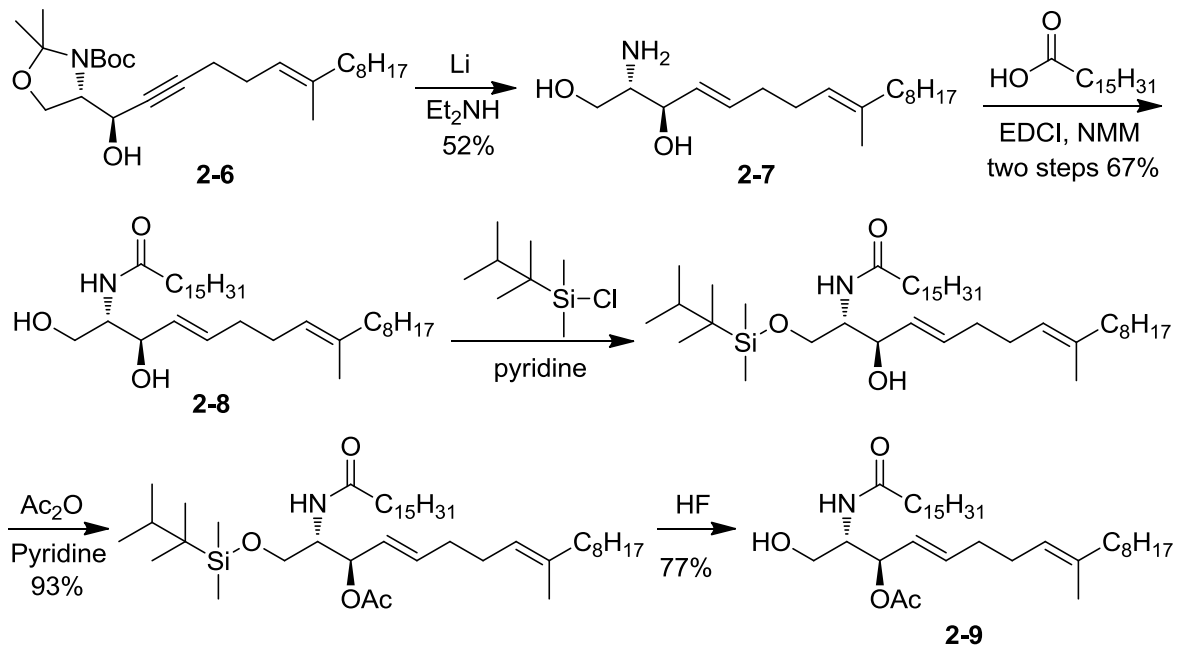
Marine microorganisms have been well known as a new source of novel nature products.¹⁸ The Fenical group examined a group of marine protists, the thraustochytrids which were isolated from the surface of the tropical seagrass, *Thalassia testudinum*, collected in the Bahamas Islands.¹⁹ They isolated one strain that produced a series of new glycosphingolipids. Through HRMS, ¹H NMR, ¹³C NMR and 2D NMR, the new glycosphingolipids were

Boc protected serine was used as the other starting material (Scheme 2-2). The corresponding Weinreb amide was prepared and the intermediate was protected with isopropylidene. LAH reduction gave Garner's aldehyde. Reacting compound 2-5 with the aldehyde produced 2-6.



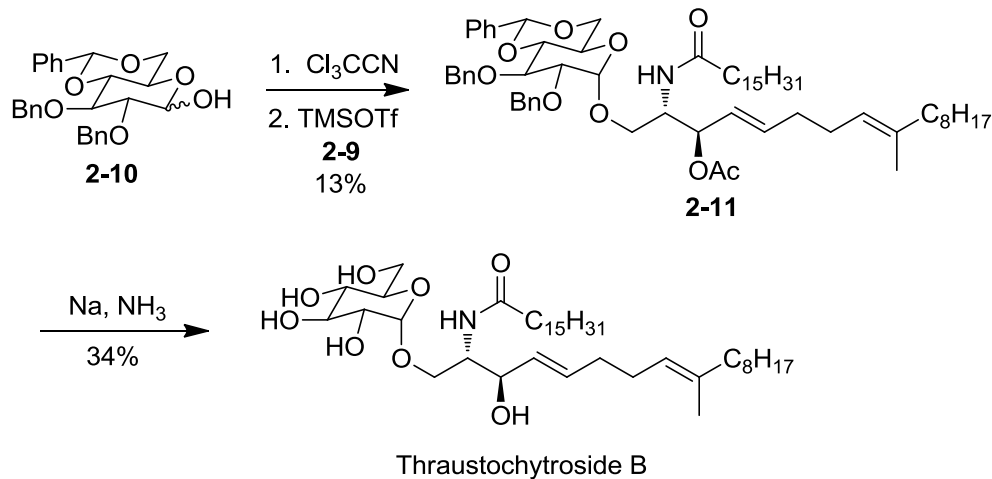
Scheme 2-2: Synthesis of 2-6

Birch reduction conditions were used to convert the triple bond to a trans-double bond, meanwhile, all the protecting groups were removed to afford 2-7 (Scheme 2-3). Reacting the intermediate 2-7 with one equivalent of palmitic acid and EDCI produced compound 2-8. Selective protecting the primary alcohol with TDS, followed by reacting the second hydroxyl group with acetic anhydride, then removing the TDS afforded 2-9.



Scheme 2-3: Synthesis of 2-9

Coupling ceramide 2-9 with 2-10 in the presence of TMSOTf gave 2-11 (Scheme 2-4). Birch reduction conditions were used to remove all the protecting groups generating Thraustochytroside B in 0.4% total yield for 12 steps.

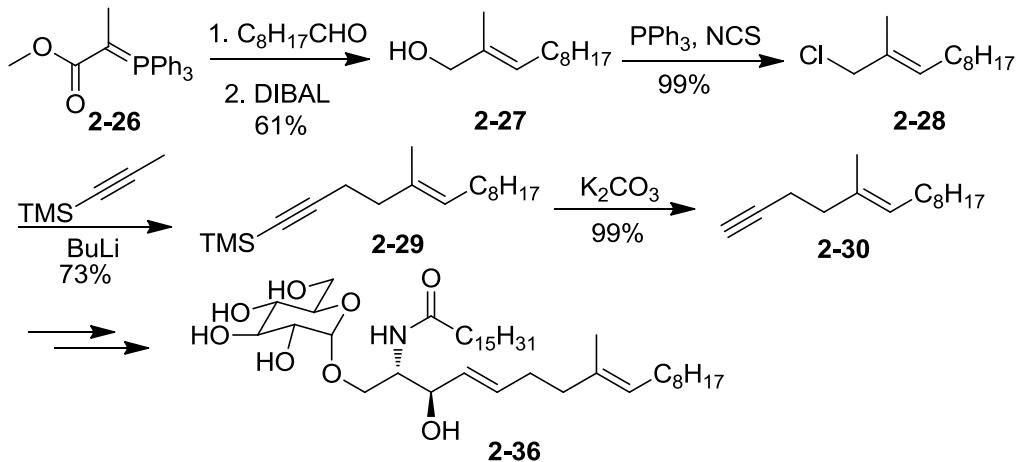


Scheme 2-4: Synthesis of Thraustochytroside B

After comparing the ^1H NMR of the synthesized thraustochytroside-B with what was reported by William Fenical, who did the isolation from the marine protist and characterization, we found that the chemical shift of the proton on the 8th carbon did not match, but the ^{13}C NMRs were identical. The chemical shift in the literature was 5.10 ppm, and we measured 5.35 ppm.

We assumed that the author had obtained another compound from the isolation. We suggested that the 19th methyl group connected with the 8th carbon. This meant that the sp² proton was on the 9th carbon, instead of 8th carbon, which might change the environment of the proton and make change the chemical shift. Hence, that led us to make 2-36.

(1-Ethoxycarbonylethyliden)-triphenylphosphoran was used as the starting material (Scheme 2-5). Wittig reaction, followed by DIBAL reduction provided 2-27. Then, similar procedures were used to prepare thraustochytroside-B.

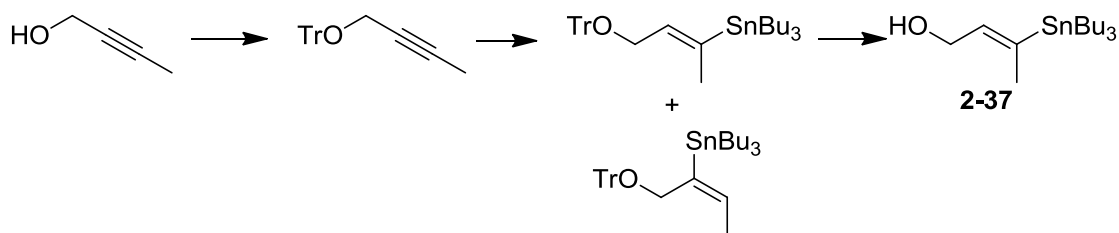


Scheme 2-5: Synthesis of 2-36

Unfortunately, the chemical shift on the 9th carbon was still around 5.35 ppm, which meant that our assumption was not true. Interestingly, the corresponding chemical shift of thraustochytroside-C located at 5.35, and the difference between the two compounds was only a hydro-carbon on one of the lipid chain terminals, which was non-significant in the ¹H NMR spectrum. We thought 5.10 might be a typo. So we bought some thraustochytrides. From the isolation, we found the compound whose ¹H NMR was identical with what we synthesized, but we didn't find the compound as reported. In summary, we think we did synthesize the thraustochytroside-B with the right structure.

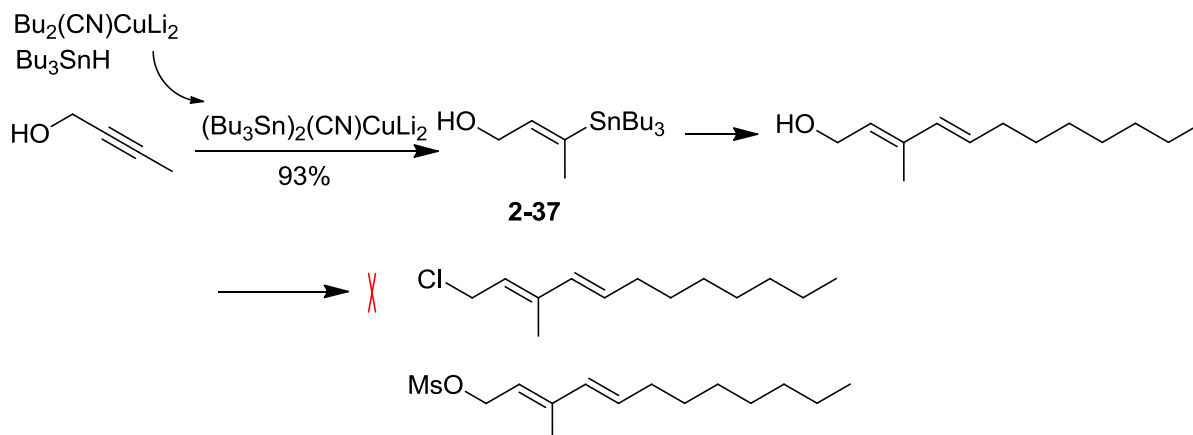
2.2.3 Approach Synthesis of Thraustochytroside A

The approach to the synthesis of thraustochytoside-A started from 1-hydroxy-2-butyne. Hydrostannation was designed to install a functional group on the C3 position and make the oxygen cis to the methyl group (Scheme 2-6). Trityl group was first tried to protect the hydroxyl group. In our hypothesis, the protecting group was big enough to drive the tin reagent approaching from the far terminal and get better ratio of 2-37. However, the ratio was not as high as we expected. Only 60% yield of the desired region-isomer was isolated after several columns, because the polarity of the other isomer was very similar to the product.



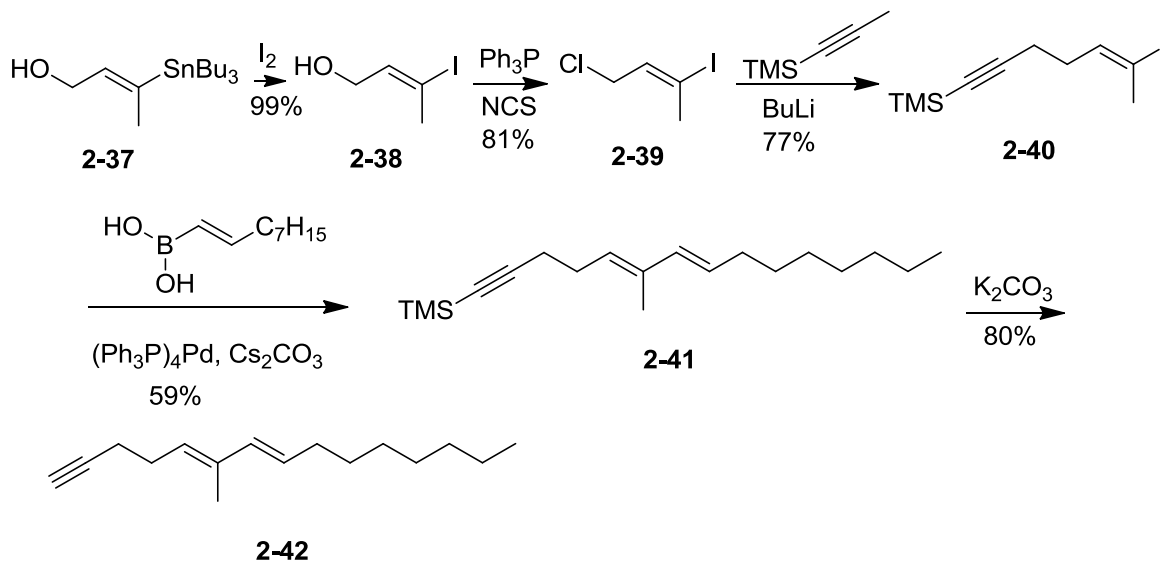
Scheme 2-6: Original route to 2-37

Hydroxyl group directed hydrostannation had been reported for successfully generation trans-double bonds.²⁸ This method also worked well with our substrate, and we were able to get 2-37 in 93% yield (Scheme 2-7). Stille coupling was used to generate the diene. Efforts to functionalize the hydroxyl group on the hydroxyl diene failed, because the new generated functional group easily went elimination and cyclization.



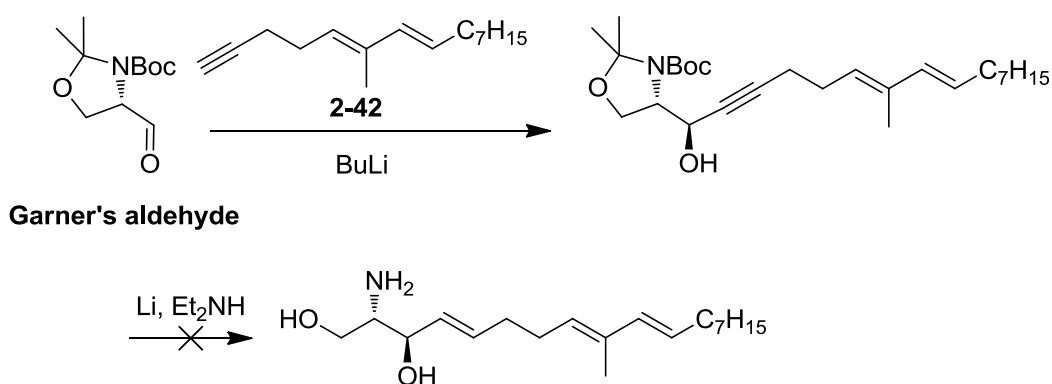
Scheme 2-7: Failed efforts to generate 2-42

To prepare 2-42, 2-37 was converted to the corresponding iodide 2-38 (Scheme 2-8). 2-39 was obtained by adding Ph_3P and NCS in THF. Substitution gave 2-40. For the Suzuki coupling, $(\text{Ph}_3\text{P})_4\text{Pd}$ gave better yield than $\text{Pd}_2(\text{dba})_3$ to generate 2-41. K_2CO_3 in methanol removing TMS group afforded 2-42.



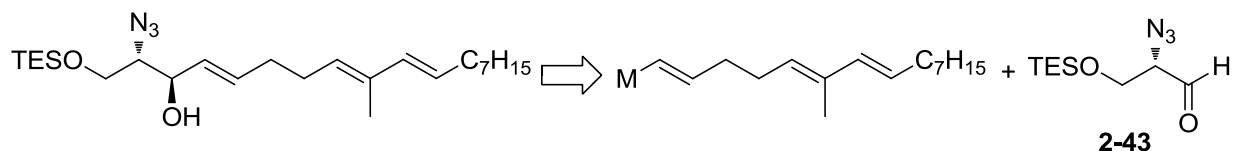
Scheme 2-8: Synthesis of 2-42.

The reaction between 2-42 and Garner's aldehyde worked well (Scheme 2-9). However, simultaneously reducing and deprotecting the adduct failed due to the reduction of the diene under Birch condition. One of the double bonds disappeared in NMR. Hence, we tried to deprotect the Boc and isopropylidene first, but the deprotection using acidic condition led to the hydrolysis of the conjugated double bond.



Scheme 2-9: Failed route to get the sphingocin derivative

Since the deprotection failed, another synthetic strategy was needed. Instead of using Garner's aldehyde, other protecting groups to protect the amino group and the primary hydroxyl group were necessary (Scheme 2-10).



Scheme 2-10: Strategy change

Considering the required reduction of the triple bond after the aldehyde addition, use of a vinyl anion to react with an aldehyde would be more convergent. To get higher yields in the sugar coupling, azide was used to protect the sphingosine amine. To get the desired configuration in the product, we had used Garner's aldehyde because the addition followed the Felkin-Ahn model due to the large size of the Boc-protecting group. Once small azide was used to replace Boc, we had to consider chelation control. However, TBS protecting group is too big for chelating the metal atom. Thus, tritethyl silyl group was chosen in the addition to protect the primary alcohol (Figure 2-6).

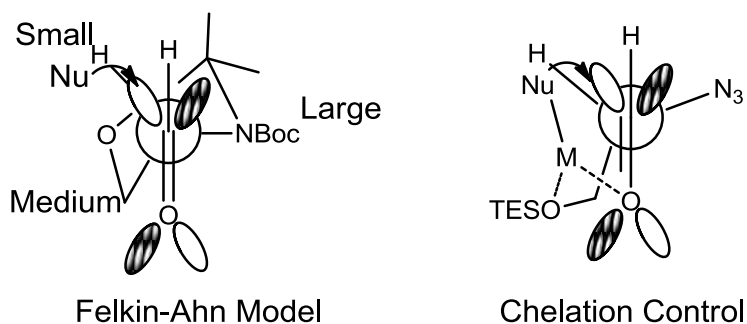
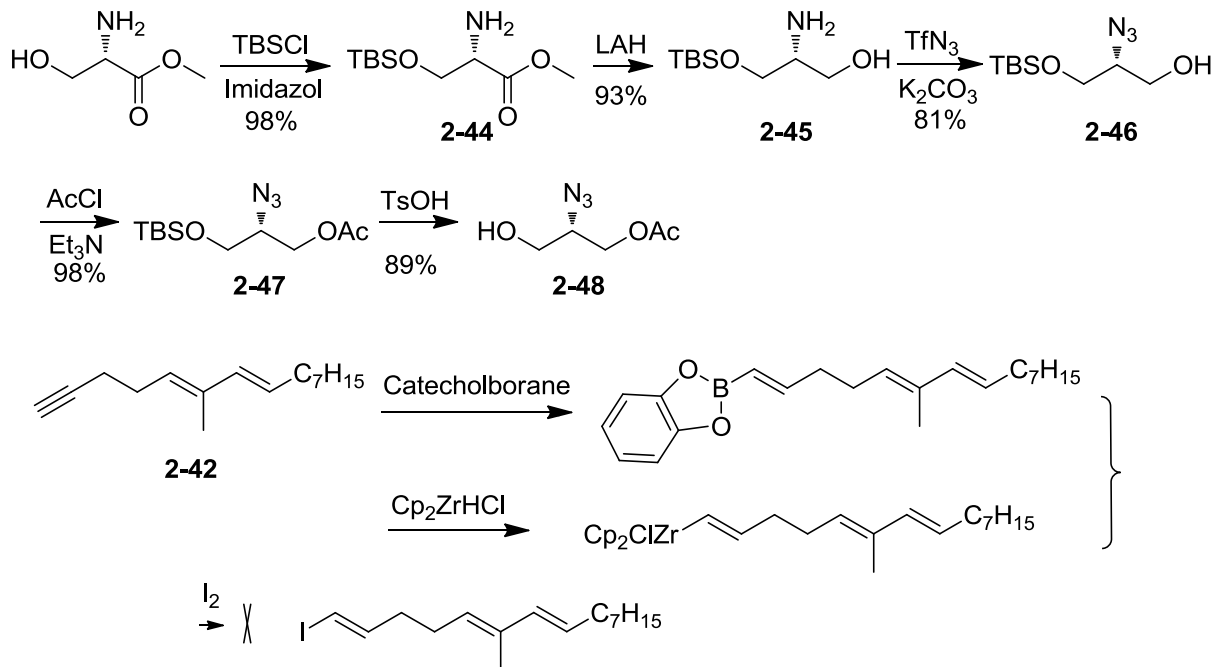


Figure 2-6: Two types of Reaction Models

Methyl serine was used as the starting material (Scheme 2-11). Selective protecting the primary alcohol using TBSCl generated 2-44 in nearly quantitative yield. LAH reduction gave 2-45. Azide transfer provided 2-46. The hydroxyl group was protected with Ac group. The TBS was removed under slightly basic condition to give 2-48.

With 2-42 in hand, hydrozirconation or hydroboration, followed by iodination provided a mixture, which was hard to characterize (Scheme 2-11).

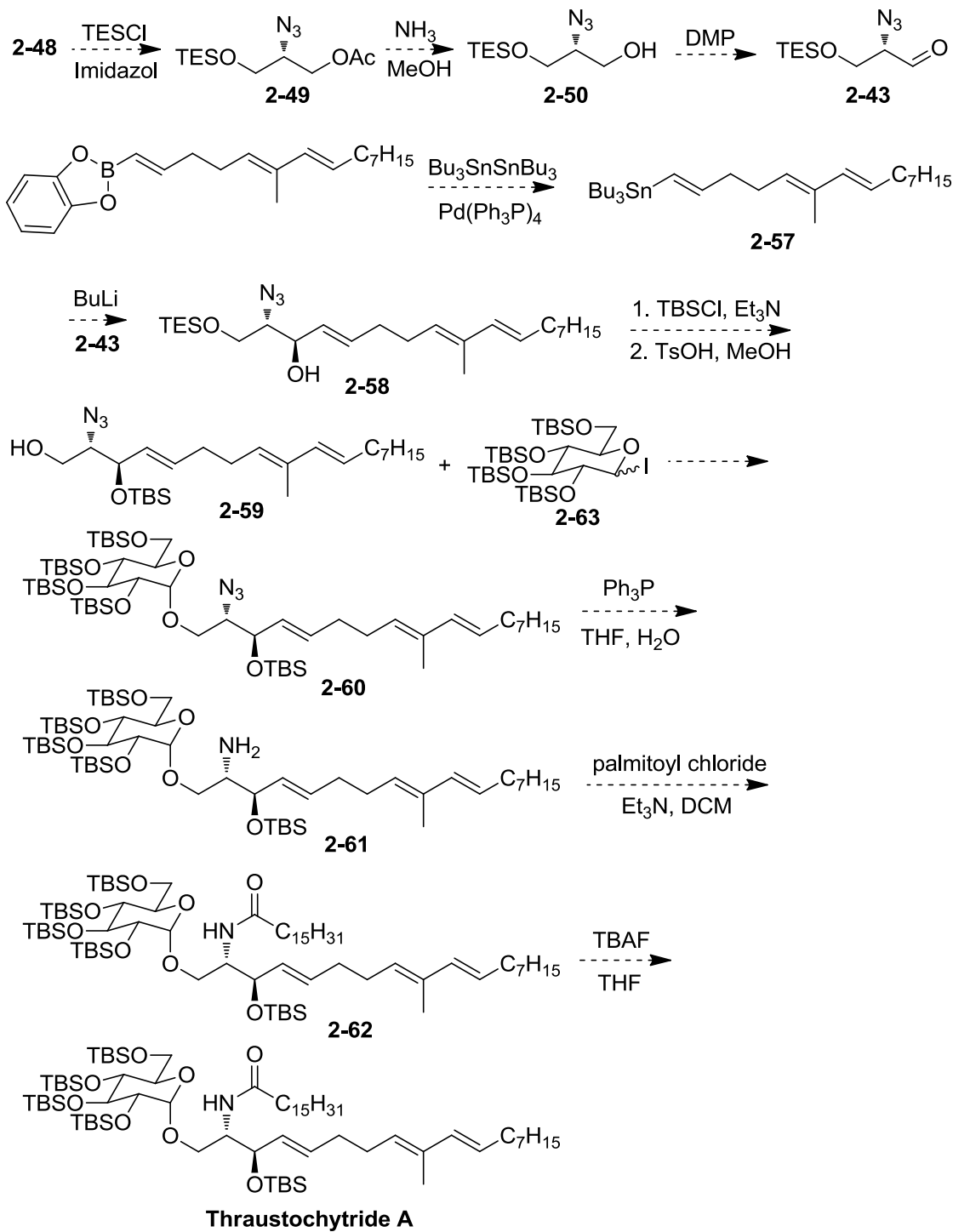


Scheme 2-11: Synthesis of 2-48 and Failed route to the iodide intermediate

The future plan is shown in Scheme 2-12. TES will be used to protect the alcohol instead of TBS group. Then, acetyl group can be removed under ammonia in MeOH. Dess Martin oxidation should give the desired aldehyde intermediate 2-43.

For the other part, with the boron intermediate, Suzuki coupling should generate the corresponding tin intermediate 2-57 without any problem. After transmetalation, the lithium agent will react with 2-43 to produce 2-58, and the stereoselectivity follows chelation control rule, as we discussed above. After masking the secondary alcohol with TBS, TES will be removed under slightly acidic condition to get 2-59. Coupling with 2-63, which is a known compound, would give 2-60, and the α -stereoselectivity is preferred with TBS protection at sugar C2 position. Staudinger reduction can convert the azide to amine group and amidation should

produce 2-62 in high yield. The final step would be TBAF deprotection, and all the TBS group would be removed to yield thraustochytroside A.

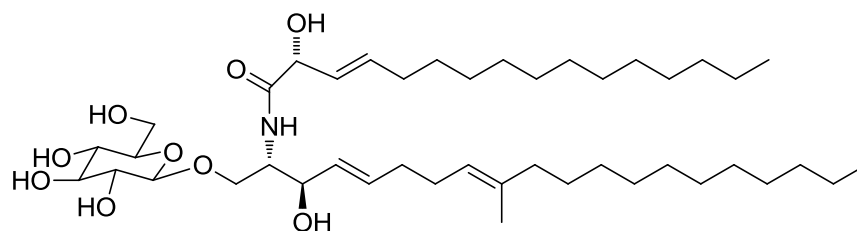


Scheme 2-12: The future plan to synthesis thraustochytride A

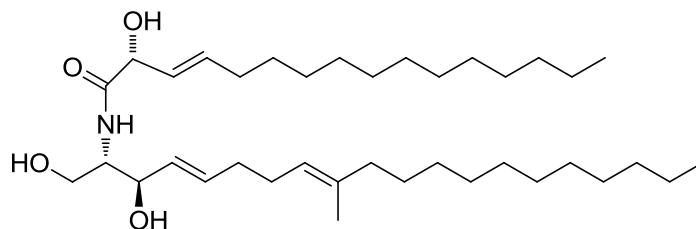
2.3 Asperamides A and B

2.3.1 Background

Since the 1990s, a large amount of novel bioactive metabolites have been discovered from marine derived fungi.²² Recently Wang group isolated an endophytic fungus from marine brown alga *Colpomenia sinuosa* and two new sphingolipids namely asperamides A and B were characterized by spectroscopic and chemical methods.²³ It is the first time that sphingolipids isolated from marine algal-derived fungi containing 9-methyl-C₂₀-sphingosine moiety were isolated. In antifungal assays, the asperamides exhibited moderate activity against *Candida albicans*.



Asperamides A



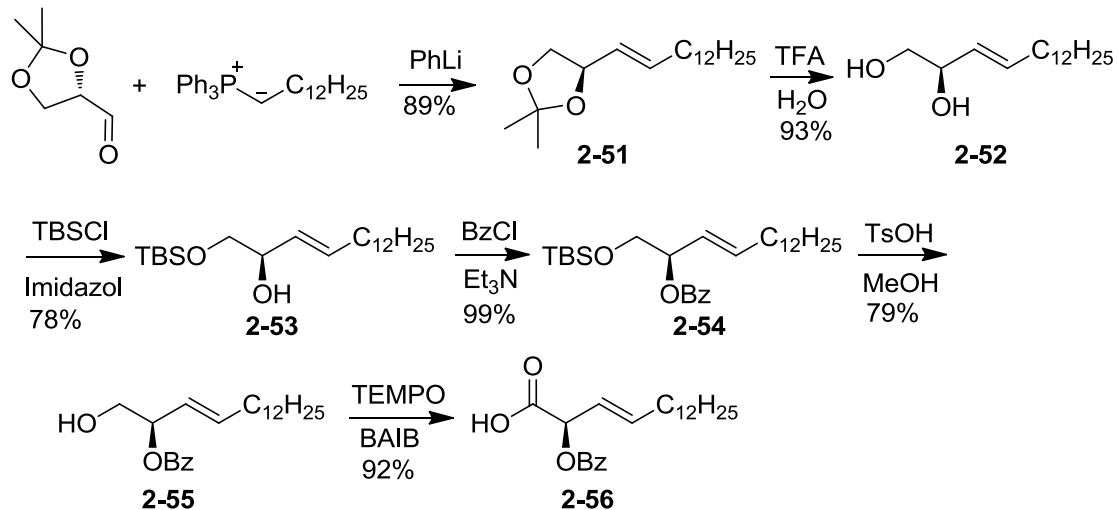
Asperamides B

Figure 2-7: Structure of Asperamides A and B

Sphingolipids are widely distributed in the bacteria and almost all eukaryotic organisms and they have a variety of functions such as signal transduction, cell differentiation and recognition of pathogens. Many sphingolipids have been proved to be potent medicinal agents, including antitumor, antifungal, antiviral, neuritogenic and immunoregulatory compounds.²⁴⁻²⁷ My research is aimed to explore novel medicinal important glycolipids mainly sphingolipids by synthetic methods. In recognition that the thraustochytriosides and asperamides compounds all share the interesting and novel sphingosine lipid chain with a methyl branch at 9th position and unsaturated double bond at 8th position, we planned to synthesize the compounds and then test and compare their bioactivity. We expected that the structurally interesting sphingosine lipids would exhibit activities including stimulating NKT cells.

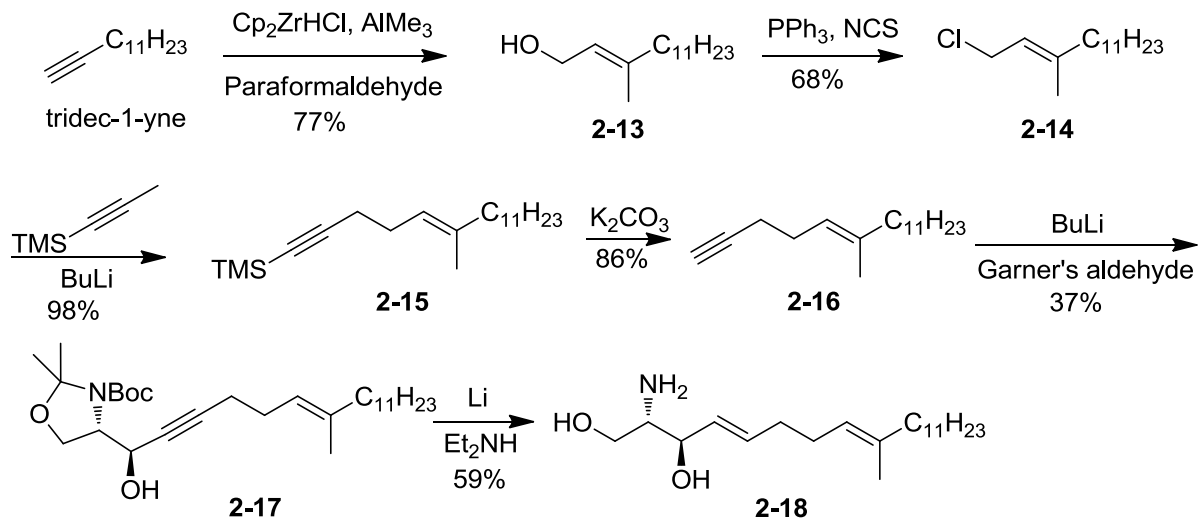
2.3.2 Synthesis of Asperamide A

The synthesis of the acyl chain on the ceramide started from the commercial available (R)-2,2-dimethyl-1,3-dioxolane-4-carbaldehyde (Scheme 2-13). Schlosser-Wittig reaction gave the trans-product 2-51. The isopropylidene was removed under acidic condition to yield 2-52. The primary alcohol was selectively protected and the secondary hydroxyl group was masked with benzoyl group to form 2-54. TBS was removed and the resulting alcohol was oxidized to generate the corresponding acid 2-56.



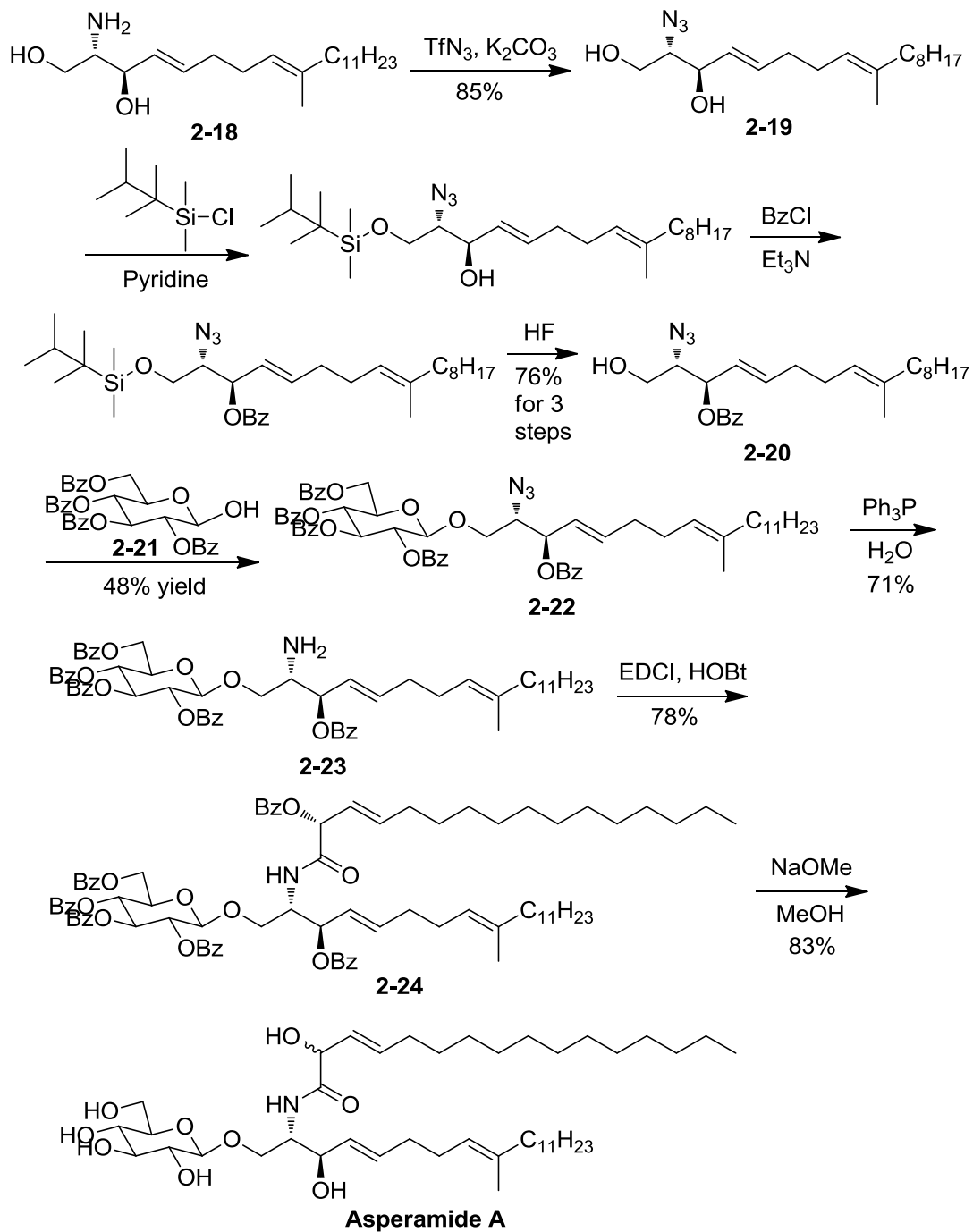
Scheme 2-13: Synthesis of the acyl chain on the ceramide

The synthesis of 2-25 started from tridec-1-yne. The difference between the key intermediate 2-18 and the amino diol 2-7 was the chain length of the hydrophobic end of the compound. Thus, the same procedure to prepare 2-7 was used to synthesize the sphingosine 2-18 (Scheme 2-14).



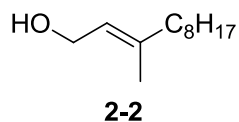
Scheme 2-14: Synthesis of the sphingosine

Azide transfer generated 2-19 (Scheme 2-15). After TDS selective protection, protecting the secondary alcohol, followed by removing TDS with HF in THF produced 2-20. Coupling 2-20 with 2-21 gave 2-22. Triphenyl phosphine mediated reduction of the azide yielded the amine 2-23. Amidation gave intermediate 2-24. Global deprotection generated asperamides A, as a mixture of diastereomers. Apparently, epimerization occurred at the C2' position during the last deprotection step. Sodium methoxide was acting as not only a nucleophile, but also a strong base. So, for the new batch, we will use ammonia in methanol to do the global deprotection.

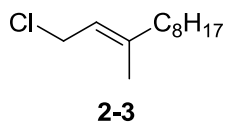


Scheme 2-15: Synthesis of asperamide A

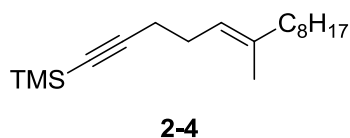
2.4 Experimental section



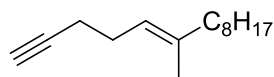
To a stirred suspension of Cp_2ZrCl_2 (3g, 10 mmol) in 50 mL of dry THF, methyl aluminium (20 mL, 2 M) in hexane was added dropwise at 0 °C. The temperature was allowed to rise up to room temperature, then, the solvent was removed under vacuum. The residue was dissolved into 40 mL of DCM and the solution was cooled to 0 °C. 1-decyne (3.6 mL, 20 mmol) was then added dropwise under 0 °C. The solution was stirred 1 hr at room temperature. The reaction temperature was cooled back down to 0 °C. Paraformaldehyde (1.25 g, 40 mmol) was added in four portions over 10 minutes. The solution was stirred for half an hour. Then, 10 mL of MeOH was added dropwise carefully. After quenching the reaction, the solvent was removed and the residue was extracted using ethyl acetate. 2.32 g of the product was isolated through a column chromatography (SiO_2) in 63% yield. ^1H NMR (CDCl_3 , 500 MHz) δ 5.386 (t, $J = 8.5$ Hz, 1 H), 4.125 (d, $J = 8.5$ Hz, 2 H), 2.251 (br, 1 H), 1.996 (q, $J = 7.5$ Hz, 2 H), 1.651 (s, 3 H), 1.388-1.416 (m, 2 H), 1.268-1.313 (m, 10 H), 0.881 (t, $J = 7.5$ Hz, 3 H); ^{13}C NMR (CDCl_3 , 125 MHz) δ 136.58, 40.10, 27.77; HRMS (ESI) calcd for $\text{C}_{12}\text{H}_{24}\text{O}$ $[\text{M}+\text{H}]^+$: 184.1827, found: 184.1836.



To a solution of triphenyl phosphine (4.62 g, 17.6 mmol) in 50 mL of dry THF, NCS (2.35 g, 17.6 mmol) was added at 0 °C. The resulting suspension was poured into 2.32 g of **2-2** at 0 °C. The temperature was allowed to rise up to room temperature. The suspension was stirred for 5 hrs. Then, the solvent was removed and the brown residue was cracked and washed with hexanes. The filtrate was collected and the solvent was removed. Then hexanes was used to extract it, and after removing the solvent, the crude product was used in the next step without any further purification.

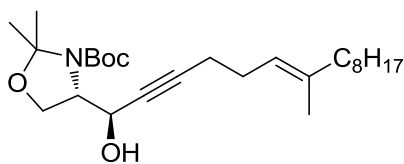


To a solution of **1-TMS-1-propyne** (3.76 mL, 25 mmol) in 50 mL of THF, *n*-BuLi (10 mL, 2.5 M) was added dropwise at -78 °C. The solution was stirred at -40 °C for 30 mins then, cooled to -78 °C. **2-3**, from the last step, was added dropwise, and the temperature was allowed to rise up to room temperature. The solution was stirred overnight. Saturated NH₄Cl was added to quench the reaction. The mixture was extracted with hexanes and dried over Na₂SO₄. 2.8 g of the product was isolated through a column chromatography (SiO₂), in 79% yield. ¹H NMR (CDCl₃, 500 MHz) δ 5.146 (br 1 H), 2.205-2.236 (m, 4 H), 1.969 (t, *J* = 7.5 Hz, 2 H), 1.607 (s, 3 H), 1.268-1.396 (m, 14 H), 0.883 (t, *J* = 7.5 Hz, 3 H), 0.143 (s, 9 H); ¹³C NMR (CDCl₃, 125 MHz) δ 137.133, 122.524, 107.660, 84.378, 39.908, 32.169, 29.778, 29.572, 29.523, 28.152, 27.563, 22.932, 20.601, 16.243, 14.344, 0.348; HRMS (ESI) calcd for C₁₈H₃₄Si [M+H]⁺: 278.2430, found: 278.2438.



2-5

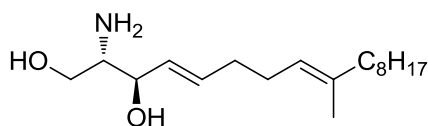
To a calpis of **2-4** (2.8 g, 10 mmol) in 10 mL of MeOH, K_2CO_3 (1.38 g, 10 mmol) was added. The mixture was stirred at room temperature overnight. The solvent was removed, and the residue was extracted with hexanes. After removing the solvent, 2.1 g of the product was isolated through a column chromatography (SiO_2), in 99% yield. 1H NMR ($CDCl_3$, 500 MHz) δ 5.171 (t, $J = 7$ Hz, 1 H), 2.190-2.245 (m, 4 H), 1.980 (t, $J = 8$ Hz, 2 H), 1.904 (t, $J = 1$ Hz, 1 H), 1.612 (s, 3 H), 1.267-1.397 (m, 12 H), 0.888 (t, $J = 6.5$ Hz, 3 H); ^{13}C NMR ($CDCl_3$, 125 MHz) δ 137.212, 122.421, 84.597, 68.288, 39.878, 32.176, 29.790, 29.602, 29.523, 28.127, 27.393, 22.938, 19.169, 16.171, 14.325; HRMS (ESI) calcd for $C_{15}H_{26}$ $[M+H]^+$: 207.2035, found: 207.2041.



2-6

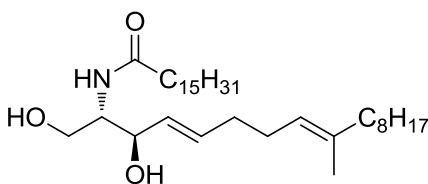
To a solution of **2-5** (1.9 g, 9.2 mmol) in 20 mL of dry THF, *n*-BuLi (10 mL, 2.5 M) was added dropwise at -78 °C. The solution was stirred at -40 °C for 30 mins then, cooled to -78 °C. Garner's aldehyde (2.5 g, 11.4 mmol) was added. The solution was stirred overnight. Saturated NH_4Cl was added to quench the reaction. The mixture was extracted with DCM and dried over Na_2SO_4 . 2.6 g of the product was isolated through a column chromatography (SiO_2), in 83%

yield. $^1\text{H NMR}$ (CDCl_3 , 500 MHz) δ 5.160 (t, $J = 6.5$ Hz, 1 H), 4.568 (d, $J = 8.0$ Hz, 1 H), 4.512 (d, $J = 8.0$ Hz, 1 H), 3.907-4.131 (m, 3 H), 2.288 (t, $J = 7.5$ Hz, 2 H), 1.959 (t, $J = 6.5$ Hz, 2 H), 1.587 (s, 3 H), 1.506-1.514 (m, 15 H), 1.263-1.327 (m, 12 H), 0.881 (t, $J = 7.0$ Hz, 3 H); HRMS (ESI) calcd for $\text{C}_{26}\text{H}_{45}\text{NO}_4$ $[\text{M}+\text{H}]^+$: 436.3421, found: 436.3409.



2-7

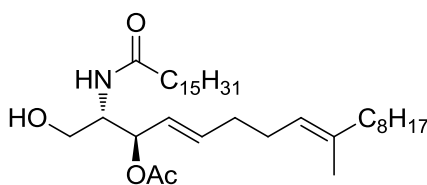
To a blue solution of Li (230 mg, 32 mmol) in 10 mL of EtNH_2 , **2-6** (2.6 g, 6 mmol) in 5 mL of dry THF was added at -78 $^\circ\text{C}$. The solution was stirred for 2 hrs. 2 g of NH_4Cl was added to quench the reaction. After the solvent was removed, the residue was extracted with Et_2O . The solution was dried over Na_2SO_4 . The crude product was obtained as a clear glass, and was used in the next step directly. The crude yield was 52%.



2-8

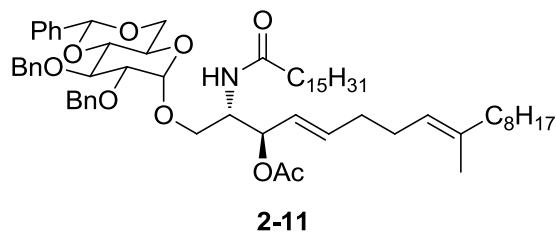
To a solution of palmitic acid (237 mg, 0.92 mmol) in 5 mL of THF, EDCI (191 mg, 0.93 mmol) and HOBT (125 mg, 0.93 mmol) were added. The solution was stirred for 30 mins, then,

250 mg of compound **2-7** was added. The solution was stirred overnight at room temperature. After removing the solvent, the product was used in the next step directly.



2-9

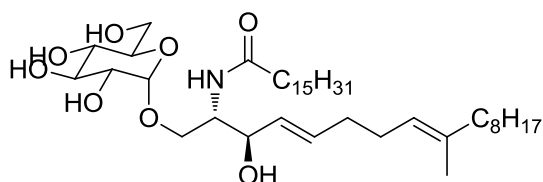
To a solution of **2-8** (310 mg, 0.58 mmol) in 2 mL of dry pyridine, TDSCl (155 mg, 0.87 mmol) was added. The solution was heated to 70 °C for half an hour. AcCl (54.6 mg, 0.7 mmol) and DMAP (8.5 mg, 0.07 mmol) were added to the solution. After stirring for 1 hrs, the solvent was removed. The residue was dissolved into 2 mL of THF. 5 mL of aqueous HF was added and the solution was stirred for 1 hrs. The mixture was poured into 20 mL of saturated NaHCO₃. The mixture was extract with Et₂O. 260 mg of the product was isolated through a column chromatography (SiO₂), in 77% yield. ¹H NMR (CDCl₃, 500 MHz) δ 5.743-5.989 (m, 1 H), 5.635 (d, *J* = 8.5 Hz, 1 H), 5.426 (dd, *J* = 15.5, 7.0 Hz, 1 H), 5.246 (t, *J* = 5.5 Hz, 1 H), 5.082 (br, 1 H), 4.205 (br, 1 H), 3.761 (d, *J* = 8.5 Hz, 1 H), 3.568 (dd, *J* = 8.5, 1 Hz, 1 H), 2.137 (t, *J* = 7.0 Hz, 4 H), 2.065 (s, 3H), 1.951 (t, *J* = 7.0 Hz, 4 H), 1.587-1.062 (m, 2 H), 1.576 (s, 3 H), 1.254-1.315 (m, 18 H), 0.882 (t, *J* = 6.5 Hz, 3 H); ¹³C NMR (CDCl₃, 125 MHz) δ 166.027, 138.797, 136.921, 133.892, 130.360, 130.292, 129.044, 124.094, 123.407, 75.119, 66.762, 62.517, 40.215, 33.151, 32.480, 30.211, 30.119, 29.902, 28.521, 27.686, 23.246, 16.544, 14.679; HRMS (ESI) calcd for C₃₆H₆₇NO₄ [M+H]⁺: 578.5070, found: 578.5074.



To a solution of **2-10** (200 mg, 1 mmol) in 4 mL of CCl_3CN , 160 mg of K_2CO_3 was added. The solution was stirred overnight. After filtration, the solvent was removed. The residue and **2-9** (160 mg, 0.27 mmol) were dissolved into 5 mL of dry DCM. 70 mg of active 4A molecular sieve was added. The mixture was stirred for half an hour. Two drops of TMSOTf was added at 0 °C. The reaction was stopped by adding 100 μL of Et_3N after 2 hrs. After filtration, the solvent was removed. 130 mg of the product was isolated through a column chromatography (SiO_2), in 13% yield. ^1H NMR (CDCl_3 , 500 MHz) δ 7.293-7.501 (m, 15 H), 6.110 (d, $J = 9.0$ Hz, 1 H), 5.792 (dt, $J = 15.5, 7.5$ Hz, 1 H), 5.543 (s, 1 H), 5.408 (dd, $J = 15.5, 7.5$ Hz, 1 H), 5.332 (t, $J = 7.5$ Hz, 1 H), 5.108 (t, $J = 5.5$ Hz, 1 H), 4.624-4.968 (m, 4 H), 4.185 (br, 1 H), 4.026 (t, $J = 7.5$ Hz, 1 H), 3.968 (dd, $J = 7.5, 1.5$ Hz, 1 H), 3.788-3.809 (m, 1 H), 3.654 (t, $J = 7.5$ Hz, 1 H), 3.587-3.605 (m, 2 H), 3.338 (dd, $J = 7.5, 1$ Hz, 1 H), 1.833-2.165 (m, 11 H), 1.587 (s, 3 H), 1.254-1.315 (m, 18 H), 0.882 (t, $J = 6.5$ Hz, 6 H); ^{13}C NMR (CDCl_3 , 125 MHz) δ 172.973, 170.059, 138.778, 138.371, 137.594, 136.763, 134.208, 129.200, 128.782, 128.569, 128.472, 128.260, 128.199, 127.883, 127.750, 126.348, 125.425, 125.316, 101.718, 99.491, 82.533, 79.553, 78.794, 75.414, 74.188, 74.115, 69.235, 67.687, 63.008, 50.517, 39.204, 36.812,

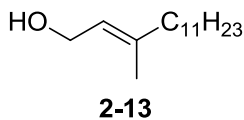
32.169, 31.320, 30.094, 29.954, 29.808, 29.693, 29.614, 29.493, 28.176, 25.918, 22.938, 14.374;

HRMS (ESI) calcd for $C_{63}H_{93}NO_9$ $[M+H]^+$: 1008.6850, found: 1008.6947.

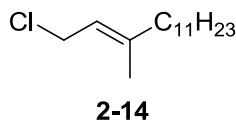


Thraustochytrioside B

To a blue solution of Na (23 mg, 1 mmol) in 5 mL of liquid NH_3 , **2-11** (50 mg, 0.05 mmol) in 1 mL of dry THF was added at $-78\text{ }^\circ\text{C}$. The solution was stirred for 2 hrs. 2 g of NH_4Cl was added to quench the reaction. After the solvent was removed, the residue was extracted with Et_2O . 12 mg of the product was obtained through a column chromatography (SiO_2) in 34% yield. 1H NMR ($CDCl_3$, 500 MHz) δ 5.798 (dt, $J = 15.5, 7.5$ Hz, 1 H), 5.479 (t, $J = 10.0$ Hz, 1 H), 5.341-5.434 (m, 2 H), 5.280 (t, $J = 7.5$ Hz, 1 H), 4.971-5.010 (m, 2 H), 4.886 (dd, $J = 10.0, 4.0$ Hz, 1 H), 4.347-4.381 (m, 1 H), 4.222 (dd, $J = 7.5, 3.5$ Hz, 1 H), 4.095 (dd, $J = 7.5, 2.0$ Hz, 1 H), 3.952-3.977 (m, 1 H), 3.720 (dd, $J = 11.0, 7.5$ Hz, 1 H), 3.540 (dd, $J = 11.0, 3$ Hz, 1 H), 1.833-2.165 (m, 6 H), 1.587 (s, 3 H), 1.254-1.315 (m, 18 H), 0.882 (t, $J = 6.5$ Hz, 3 H); ^{13}C NMR ($CDCl_3$, 125 MHz) δ 172.991, 170.490, 137.388, 131.531, 129.085, 1125.316, 96.748, 73.156, 70.722, 70.267, 69.035, 67.700, 62.025, 50.736, 37.080, 32.837, 32.606, 32.151, 29.469, 26.015, 22.914, 21.305, 20.923, 20.862, 14.338; HRMS (ESI) calcd for $C_{40}H_{75}NO_8$ $[M+H]^+$: 698.5493, found: 698.5500.

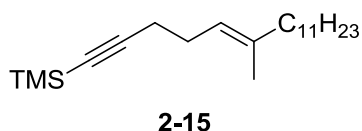


To a stirred suspension of Cp_2ZrCl_2 (4. g, 13.85 mmol) in 50 mL of dry THF, methyl aluminium (27 mL, 2 M) in hexane was added dropwise at 0 °C. The temperature was allowed to rise up to room temperature, then, the solvent was removed under vacuum. The residue was dissolved into 40 mL of DCM and the solution was cooled to 0 °C. 1-decyne (5 g, 27.7 mmol) was then added dropwise under 0 °C. The solution was stirred 1 hr at room temperature. The reaction temperature was cooled back down to 0 °C. Paraformaldehyde (1.6 g, 54 mmol) was added in four portions over 10 minutes. The solution was stirred for half an hour. Then, 10 mL of MeOH was added dropwise carefully. After quenching the reaction, the solvent was removed and the residue was extracted using ethyl acetate. 4.8 g of the product was isolated through a column chromatography (SiO_2) in 77% yield.

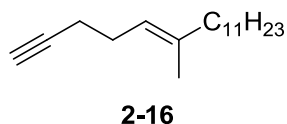


To a solution of triphenylphosine (7.8 g, 29.7 mmol) in 50 mL of dry THF, NCS (3.96 g, 29.7 mmol) was added at 0 °C. The resulting suspension was poured into 4.8 g of **2-13** at 0 °C. The temperature was allowed to rise up to room temperature. The suspension was stirred for 5 hrs. Then, the solvent was removed and the brown residue was cracked and washed with hexanes. The filtrate was collected and the solvent was removed. Then hexanes was used to

extract it, and after removing the solvent, the crude product was used in the next step without any further purification.

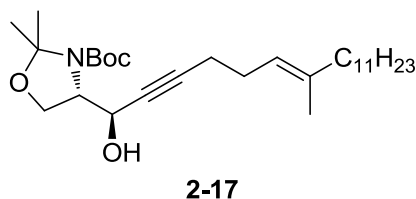


To a solution of **1-TMS-1-propyne** (3.5 g, 31.5 mmol) in 50 mL of THF, *n*-BuLi (12.6 mL, 2.5 M) was added dropwise at -78 °C. The solution was stirred at -40 °C for 30 mins then, cooled to -78 °C. 7 g of **2-14** was added dropwise, and the temperature was allowed to rise up to room temperature. The solution was stirred overnight. Saturated NH₄Cl was added to quench the reaction. The mixture was extracted with hexanes and dried over Na₂SO₄. 6.8 g of the product was isolated through a column chromatography (SiO₂) in 65% yield for two steps. ¹H NMR (CDCl₃, 500 MHz) δ 5.171 (br, 1 H), 2.190 (br, 4 H), 1.980 (t, *J* = 8 Hz, 2 H), 1.612 (s, 3 H), 1.267-1.397 (m, 18 H), 0.888 (t, *J* = 6.5 Hz, 3 H), 0.143 (s, 9 H); ¹³C NMR (CDCl₃, 125 MHz) δ 132.419, 117.372, 79.837, 63.283, 34.879, 27.171, 24.894, 24.806, 24.600, 24.508, 23.143, 22.407, 17.933, 14.191, 0.348; HRMS (ESI) calcd for C₁₈H₃₂ [M+H]⁺: 321.2899, found: 321.2910.

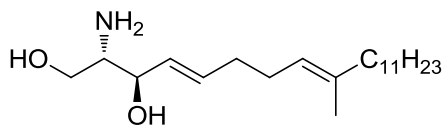


To a calpis of **2-15** (4.5 g, 14 mmol) in 10 mL of MeOH, K₂CO₃ (1.9 g, 14 mmol) was added. The mixture was stirred at room temperature overnight. The solvent was removed, and

the residue was extracted with hexanes. After removing the solvent, 3 g of the product was isolated through a column chromatography (SiO₂) in 86% yield. ¹H NMR (CDCl₃, 500 MHz) δ 5.171 (t, *J* = 7 Hz, 1 H), 2.190-2.245 (m, 4 H), 1.980 (t, *J* = 8 Hz, 2 H), 1.941 (t, *J* = 1 Hz, 1 H), 1.612 (s, 3 H), 1.267-1.397 (m, 18 H), 0.888 (t, *J* = 6.5 Hz, 3 H); ¹³C NMR (CDCl₃, 125 MHz) δ 132.419, 117.372, 79.837, 63.283, 34.879, 27.171, 24.894, 24.806, 24.600, 24.508, 23.143, 22.407, 17.933, 14.191; HRMS (ESI) calcd for C₁₈H₃₂ [M+H]⁺: 249.2504, found: 249.2503.

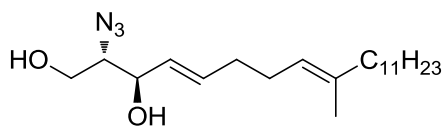


To a solution of **2-16** (3 g, 12.3 mmol) in 20 mL of dry THF, *n*-BuLi (4.92 mL, 2.5 M) was added dropwise at -78 °C. The solution was stirred at -40 °C for 30 mins then, cooled to -78 °C. Garner's aldehyde (2.8 g, 12.3 mmol) was added. The solution was stirred overnight. Saturated NH₄Cl was added to quench the reaction. The mixture was extracted with DCM and dried over Na₂SO₄. 2.2 g of the product was isolated through a column chromatography (SiO₂) in 37 % yield. ¹H NMR (CDCl₃, 500 MHz) δ 5.130 (br, 1 H), 4.663 (br, 1 H), 4.568 (br, 1 H), 3.920-4.141 (m, 3 H), 2.594 (s, 1 H), 2.210 (br, 4 H), 1.959 (t, *J* = 7.5 Hz, 2 H), 1.593 (s, 3 H), 1.357-1.400 (m, 18 H), 0.886 (t, *J* = 7.0 Hz, 3 H); HRMS (ESI) calcd for C₁₀H₁₇ISi [M+H]⁺: 448.3818, found: 448.3824.



2-18

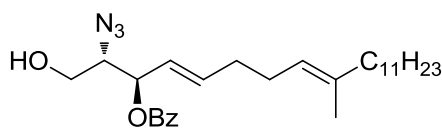
To a blue solution of Li (230 mg, 32 mmol) in 10 mL of EtNH₂, **2-17** (2.6 g, 6 mmol) in 5 mL of dry THF was added at -78 °C. The solution was stirred for 2 hrs. 2 g of NH₄Cl was added to quench the reaction. After the solvent was removed, the residue was extracted with Et₂O. 1.2 g of the product was obtained through a column chromatography (SiO₂) in 59% yield. ¹H NMR (CDCl₃, 500 MHz) δ 5.755 (dt, *J* = 15.5, 6.5 Hz, 1 H), 5.486 (dd, *J* = 15.5, 7.0 Hz, 1 H), 5.090 (br, 1 H), 4.041 (t, *J* = 6 Hz, 1 H), 3.619-3.660 (m, 2 H), 2.845 (br, 1 H), 2.315 (br, 1 H), 2.300 (br, 1 H), 2.095 (br, 4 H), 1.952 (t, *J* = 7.5 Hz, 2 H), 1.580 (s, 3 H), 1.300-1.393 (m, 18 H), 0.882 (t, *J* = 7.0 Hz, 3 H); ¹³C NMR (CDCl₃, 125 MHz) δ 136.204, 134.232, 129.601, 123.159, 73.807, 66.724, 62.578, 39.700, 32.560, 31.915, 29.688, 29.657, 29.642, 29.566, 29.352, 29.326, 27.994, 27.308, 22.685, 15.987, 14.111; HRMS (ESI) calcd for C₂₁H₄₁NO₂ [M+H]⁺: 340.3137, found: 340.3145.



2-19

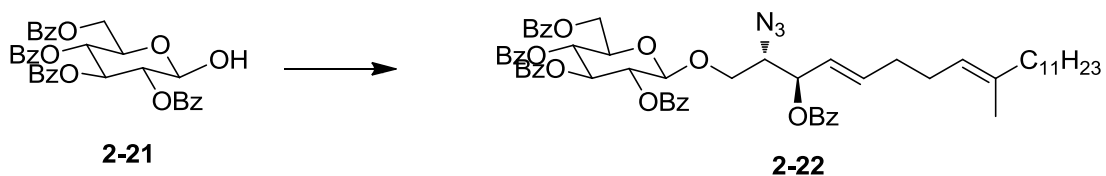
To a solution of NaN₃ (1.3 g, 20 mmol) in 10 mL of water, 10 mL of DCM was added. Tf₂O (1.13 g, 4 mmol) was added to the solution at 0 °C, and the mixture was stirred for 2 hrs. The organic layer was used to dissolve 720 mg of compound **2-18**. Then, K₂CO₃ (272 mg, 2

mmol) and $\text{CuSO}_4 \cdot 5\text{H}_2\text{O}$ (5 mg, 0.02 mmol) were added to the solution. The mixture was stirred overnight at room temperature. 620 mg of the product was isolated through a column chromatography (SiO_2) in 85% yield. ^1H NMR (CDCl_3 , 500 MHz) δ 5.600 (dt, $J = 15.5, 6.5$ Hz, 1 H), 5.488 (dd, $J = 15.5, 7.0$ Hz, 1 H), 5.026 (t, $J = 6.5$ Hz, 1 H), 4.181 (t, $J = 6$ Hz, 1 H), 3.715 (br, 2 H), 3.439 (dd, $J = 10.5, 5.5$ Hz, 1 H), 1.996-2.056 (m, 4 H), 1.886 (t, $J = 7.5$ Hz, 2 H), 1.512 (s, 3 H), 1.190-1.326 (m, 18 H), 0.811 (t, $J = 7.0$ Hz, 3 H); ^{13}C NMR (CDCl_3 , 125 MHz) δ 136.326, 135.567, 128.251, 122.987, 73.807, 66.724, 62.578, 39.681, 32.530, 31.915, 29.688, 29.657, 29.642, 29.566, 29.352, 29.326, 27.994, 27.308, 22.685, 15.987, 14.111; HRMS (ESI) calcd for $\text{C}_{21}\text{H}_{39}\text{N}_3\text{O}_2$ $[\text{M}+\text{H}]^+$: 366.3042, found: 366.3050.

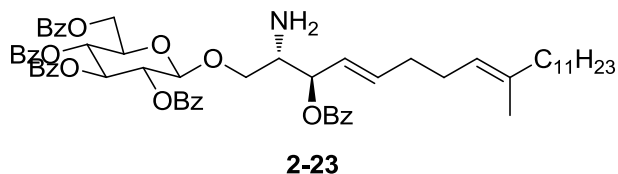


To a solution of **2-19** (140 mg, 0.38 mmol) in 0.5 mL of dry pyridine, TDSCl (107 mg, 0.6 mmol) was added. The solution was heated to 70 °C for half an hour. BzCl (84.42 mg, 0.6 mmol) and DMAP (8.5 mg, 0.07 mmol) were added to the solution. After stirring for 1 hrs, the solvent was removed. The residue was dissolved into 2 mL of THF. 5 mL of aqueous HF was added and the solution was stirred for 1 hrs. The mixture was poured into 20 mL of saturated NaHCO_3 . The mixture was extract with Et_2O . 120 mg of the product was isolated through a column chromatography (SiO_2) in 76% yield for three steps. ^1H NMR (CDCl_3 , 500 MHz) δ 8.068 (d, $J = 7$ Hz, 2 H), 7.589 (t, $J = 7.5$ Hz, 1 H), 7.464 (d, $J = 7.5$ Hz, 2 H), 5.943-5.989 (m, 1

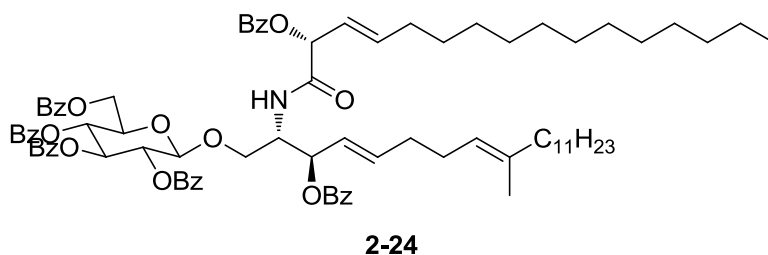
H), 5.605-5.652 (m, 2 H), 5.082 (t, $J = 5.5$ Hz, 1 H), 3.819 (dd, $J = 11.5, 4$ Hz, 1 H), 3.761 (dd, $J = 8.5, 4$ Hz, 1 H), 3.638 (dd, $J = 11.5, 8.5$ Hz, 1 H), 2.120 (m, 4 H), 1.930 (t, $J = 7$ Hz, 2 H), 1.567 (s, 3 H), 1.262-1.373 (m, 18 H), 0.888 (t, $J = 6.5$ Hz, 3 H); ^{13}C NMR (CDCl_3 , 125 MHz) δ 166.027, 138.797, 136.921, 133.892, 130.360, 130.292, 129.044, 124.094, 123.407, 75.119, 66.762, 62.517, 40.215, 33.151, 32.480, 30.211, 30.119, 29.902, 28.521, 27.686, 23.246, 16.544, 14.679; HRMS (ESI) calcd for $\text{C}_{28}\text{H}_{43}\text{N}_3\text{O}_2$ $[\text{M}+\text{H}]^+$: 487.3304, found: 487.3308.



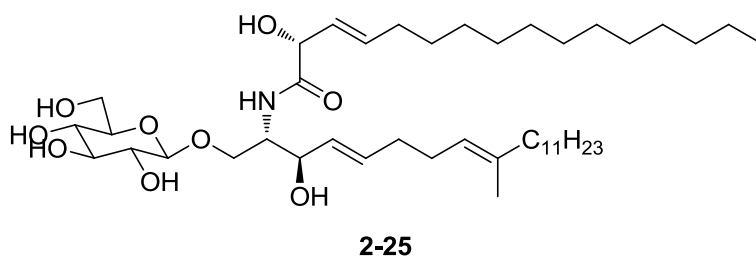
To a solution of **21** (120 mg, 0.2 mmol) in 1 mL of CCl_3CN , 54.4 mg of K_2CO_3 was added. The solution was stirred overnight. After filtration, the solvent was removed. The residue and **2-20** (50 mg, 0.1 mmol) were dissolved into 2 mL of dry DCM. 20 mg of active 4A molecular sieve was added. The mixture was stirred for half an hour. Two drops of TMSOTf was added at 0 °C. The reaction was stopped by adding 50 μL of Et_3N after 2 hrs. After filtration, the solvent was removed. 130 mg of the product was isolated through a column chromatography (SiO_2) in 48% yield.



To a solution of **2-22** (130 mg, 0.124 mmol) in 5 mL of acetic acid, Zinc (80 mg, 1.24 mmol) was added. The mixture was stirred overnight. After filtration, the solvent was removed, and then, 112 mg of the product was obtained through a column chromatography (SiO₂) in 78% yield.

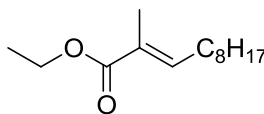


To a solution of palmitic acid (237 mg, 0.92 mmol) in 5 mL of THF, EDCI (191 mg, 0.93 mmol) and HOBT (125 mg, 0.93 mmol) were added. The solution was stirred for 30 mins, and then, 250 mg of compound **2-23** was added. The solution was stirred overnight at room temperature. After removing the solvent, 310 mg of the product was isolated through a column chromatography (SiO₂) in 73% yield.



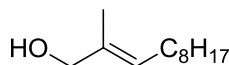
To a solution of **2-24** (310 mg, 0.225 mmol) in 1 mL of MeOH, fresh prepared 1 mol / L NaOMe in MeOH was added. The solution was stirred 2 hrs. After the solvent was removed,

the mixture was added 20 mL of DCM. After washed with 5 mL of brine and dried over Na₂SO₄, the solvent was removed to yield 92 mg of the product. The yield was 83%.



2-26

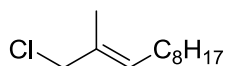
To a solution of nonyl aldehyde (5.8 mL, 32 mmol) in 150 mL of DCM, (carbethoxyethylidene)triphenylphosphorane (9.6 g, 32 mmol) was added. The mixture was refluxed overnight. After removing the solvent, 6 g of the product was isolated through a column chromatography (SiO₂). The yield was 83%. ¹H NMR (CDCl₃, 500 MHz) δ 6.702 (t, *J* = 7 Hz, 1 H), 4.096-4.142 (m, 2 H), 2.101 (q, *J* = 7.5 Hz, 2 H), 1.757 (s, 3 H), 1.374 (t, *J* = 6.5 Hz, 2 H), 1.192-1.266 (m, 12 H), 0.818 (t, *J* = 7.5 Hz, 3 H); ¹³C NMR (CDCl₃, 125 MHz) δ 168.311, 142.480, 127.798, 60.416, 32.036, 29.602, 29.572, 29.408, 28.831, 28.771, 22.823, 14.404, 14.198, 12.408; HRMS (ESI) calcd for C₁₄H₂₆O₂ [M+H]⁺: 227.1933, found: 227.1939.



2-27

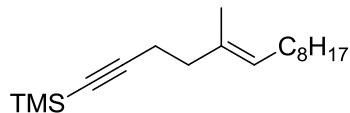
To a solution of **2-26** (3.76 mL, 25 mmol) in 50 mL of THF, *n*-BuLi (10 mL, 2.5 M) was added dropwise at -78 °C. The solution was stirred at -40 °C for 30 mins then, cooled to -78 °C. The starting material was added dropwise, and the temperature was allowed to rise up to room temperature. The solution was stirred overnight. Saturated NH₄Cl was added to quench the

reaction. The mixture was extracted with hexanes and dried over Na₂SO₄. 2.8 g of the product was isolated through a column chromatography (SiO₂). The yield was 61 for two steps. ¹H NMR (CDCl₃, 500 MHz) δ 5.377 (t, *J* = 8.5 Hz, 1 H), 3.951 (s, 2 H), 2.227 (br, 1 H), 1.996 (q, *J* = 6.5 Hz, 2 H), 1.628 (s, 3 H), 1.250-1.322 (m, 12 H), 0.861 (t, *J* = 7.5 Hz, 3 H); ¹³C NMR (CDCl₃, 125 MHz) δ 136.58, 40.10, 27.77; HRMS (ESI) calcd for C₁₂H₂₄O [M+H]⁺: 184.1827, found: 184.1836.



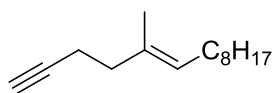
2-28

To a solution of triphenylphosine (2.8 g, 29.7 mmol) in 50 mL of dry THF, NCS (3.96 g, 29.7 mmol) was added at 0 °C. The resulting suspension was poured into 4.8 g of **2-27** at 0 °C. The temperature was allowed to rise up to room temperature. The suspension was stirred for 5 hrs. Then, the solvent was removed and the brown residue was cracked and washed with hexanes. The filtrate was collected and the solvent was removed. Then hexanes was used to extract it, and after removing the solvent, 2.1 g of the crude product was used in the next step without any further purification). ¹H NMR (CDCl₃, 500 MHz) δ 5.527 (t, *J* = 8.5 Hz, 1 H), 3.894 (s, 2 H), 1.996 (q, *J* = 6.5 Hz, 2 H), 1.621 (s, 3 H), 1.250-1.322 (m, 12 H), 0.881 (t, *J* = 7.5 Hz, 3 H); ¹³C NMR (CDCl₃, 125 MHz) δ 136.58, 40.10, 27.77; HRMS (ESI) calcd for C₁₂H₂₃Cl [M+H]⁺: 203.1488, found: 203.1494.



2-29

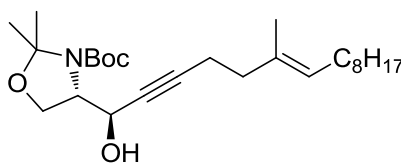
To a solution of **1-TMS-1-propyne** (3.76 mL, 25 mmol) in 50 mL of THF, *n*-BuLi (10 mL, 2.5 M) was added dropwise at -78 °C. The solution was stirred at -40 °C for 30 mins then, cooled to -78 °C. The starting material from the last step was added dropwise, and the temperature was allowed to rise up to room temperature. The solution was stirred overnight. Saturated NH₄Cl was added to quench the reaction. The mixture was extracted with hexanes and dried over Na₂SO₄. 2.8 g of the product was isolated through a column chromatography (SiO₂). ¹H NMR (CDCl₃, 500 MHz) δ 5.146 (br 1 H), 2.205-2.236 (m, 4 H), 1.969 (t, *J* = 7.5 Hz, 2 H), 1.607 (s, 3 H), 1.268-1.396 (m, 14 H), 0.883 (t, *J* = 7.5 Hz, 3 H), 0.143 (s, 9 H); ¹³C NMR (CDCl₃, 125 MHz) δ 137.133, 122.524, 107.660, 84.378, 39.908, 32.169, 29.778, 29.572, 29.523, 28.152, 27.563, 22.932, 20.601, 16.243, 14.344, 0.348; HRMS (ESI) calcd for C₁₈H₃₄Si [M+H]⁺: 278.2430, found: 278.2438.



2-30

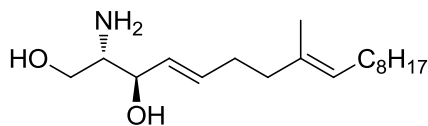
To a solution of **2-29** (2.8 g, 10 mmol) in 10 mL of MeOH, K₂CO₃ (1.38 g, 10 mmol) was added. The mixture was stirred at room temperature overnight. The solvent was removed, and the residue was extracted with hexanes. After removing the solvent, 2.1 g of the product was isolated through a column chromatography (SiO₂). ¹H NMR (CDCl₃, 500 MHz) δ 5.200 (t, *J* = 7

Hz, 1 H), 2.196-2.301 (m, 4 H), 1.947-1.995 (m, 2 H), 1.947 (t, $J = 1$ Hz, 1 H), 1.611 (s, 3 H), 1.269-1.328 (m, 18 H), 0.885 (t, $J = 6.5$ Hz, 3 H); ^{13}C NMR (CDCl_3 , 125 MHz) δ 133.139, 126.433, 84.688, 68.507, 38.694, 32.145, 29.978, 29.784, 29.572, 29.529, 29.359, 29.007, 28.740, 28.127, 22.926, 18.635, 17.840, 15.964, 14.350; HRMS (ESI) calcd for $\text{C}_{15}\text{H}_{26}$ $[\text{M}+\text{H}]^+$: 207.2035, found: 207.2042.



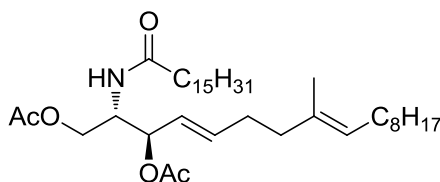
2-31

To a solution of **2-30** (1.9 g, 9.2 mmol) in 20 mL of dry THF, *n*-BuLi (10 mL, 2.5 M) was added dropwise at -78 °C. The solution was stirred at -40 °C for 30 mins then, cooled to -78 °C. Garner's aldehyde (2.5 g, 11.4 mmol) was added. The solution was stirred overnight. Saturated NH_4Cl was added to quench the reaction. The mixture was extracted with DCM and dried over Na_2SO_4 . 2.6 g of the product was isolated through a column chromatography (SiO_2). ^1H NMR (CDCl_3 , 500 MHz) δ 5.160 (t, $J = 6.5$ Hz, 1 H), 4.568 (d, $J = 8.0$ Hz, 1 H), 4.512 (d, $J = 8.0$ Hz, 1 H), 3.907-4.131 (m, 3 H), 2.288 (t, $J = 7.5$ Hz, 2 H), 1.959 (t, $J = 6.5$ Hz, 2 H), 1.587 (s, 3 H), 1.506-1.514 (m, 15 H), 1.263-1.327 (m, 12 H), 0.881 (t, $J = 7.0$ Hz, 3 H); HRMS (ESI) calcd for $\text{C}_{26}\text{H}_{45}\text{NO}_4$ $[\text{M}+\text{H}]^+$: 436.3421, found: 436.3409.



2-32

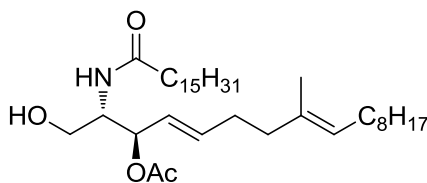
To a blue solution of Li (230 mg, 32 mmol) in 10 mL of EtNH₂, **2-31** (2.6 g, 6 mmol) in 5 mL of dry THF was added at -78 °C. The solution was stirred for 2 hrs. 2 g of NH₄Cl was added to quench the reaction. After the solvent was removed, the residue was extracted with Et₂O. The solution was dried over Na₂SO₄. The crude was obtained as a clear glass, and was used in the next step directly.



2-33

To a solution of palmitic acid (237 mg, 0.92 mmol) in 5 mL of THF, EDCI (191 mg, 0.93 mmol) and HOBT (125 mg, 0.93 mmol) were added. The solution was stirred for 30 mins, and then, 250 mg of compound **2-32** was added. The solution was stirred overnight at room temperature. Then, the product was peracetylate. After removing the solvent, 360 mg of the product was isolated through a column chromatography (SiO₂). ¹H NMR (CDCl₃, 500 MHz) δ 5.780 (dt, *J* = 15.5, 7.0 Hz, 1 H), 5.595 (d, *J* = 9.0 Hz, 1 H), 5.407 (dd, *J* = 15.5, 7.5 Hz), 5.285 (dd, *J* = 7.5, 7.0 Hz, 1 H), 5.118 (t, *J* = 5.5 Hz, 1 H), 4.437-4.467 (m, 1 H), 4.290 (dd, *J* = 11.5, 6.0 Hz, 1 H), 4.029 (dd, *J* = 11.5, 4.5 Hz, 1 H), 2.123-2.175 (m, 4 H), 2.104-2.077 (m, 8 H),

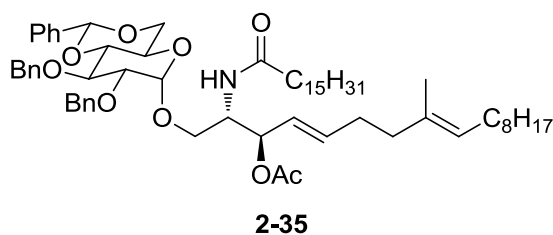
1.937-1.978 (m, 2 H), 1.587-1.602 (m, 2 H), 1.576 (s, 3 H), 1.254-1.315 (m, 40 H), 0.882 (t, $J = 6.5$ Hz, 3 H); ^{13}C NMR (CDCl_3 , 125 MHz) δ 173.009, 166.027, 136.976, 134.103, 125.680, 124.478, 73.890, 62.844, 50.639, 39.137, 37.098, 32.139, 31.101, 30.069, 29.918, 29.881, 29.742, 29.614, 29.450, 28.152, 25.924, 22.908, 21.317, 21.026, 16.165, 14.325; HRMS (ESI) calcd for $\text{C}_{38}\text{H}_{69}\text{NO}_5$ $[\text{M}+\text{H}]^+$: 620.5176, found: 620.5181.



2-34

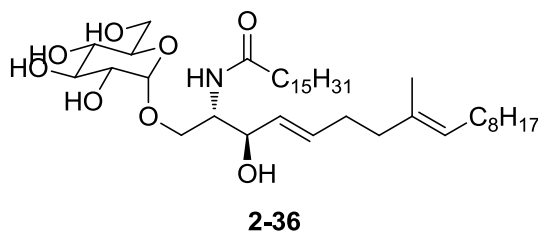
To a solution of **2-33** (360 mg, 0.58 mmol) in 2 mL of MeOH, 2 mg of Na was added. The solution was stirred for 5 hrs, and then the solvent was removed. The residue was dissolved into 2 mL of dry pyridine, TDSCl (155 mg, 0.87 mmol) was added. The solution was heated to 70 °C for half an hour. AcCl (54.6 mg, 0.7 mmol) and DMAP (8.5 mg, 0.07 mmol) were added to the solution. After stirring for 1 hrs, the solvent was removed. The residue was dissolved into 2 mL of THF. 5 mL of aqueous HF was added and the solution was stirred for 1 hrs. The mixture was poured into 20 mL of saturated NaHCO_3 . The mixture was extract with Et_2O . 260 mg of the product was isolated through a column chromatography (SiO_2). ^1H NMR (CDCl_3 , 500 MHz) δ 5.965 (d, $J = 9.0$ Hz, 1 H), 5.783 (dt, $J = 15.5, 7.5$ Hz, 1 H), 5.485 (dd, $J = 15.5, 7.5$ Hz, 1 H), 5.246 (t, $J = 5.5$ Hz, 1 H), 5.108 (t, $J = 5.5$ Hz, 1 H), 4.125 (br, 1 H), 4.106-4.139 (m, 2 H), 2.103-2.195 (m, 4 H), 2.057 (s, 3H), 2.014-2.044 (m, 2 H), 1.951-1.978 (m, 2 H), 1.587-1.062 (m,

2 H), 1.576 (s, 3 H), 1.254-1.315 (m, 18 H), 0.882 (t, $J = 6.5$ Hz, 3 H); ^{13}C NMR (CDCl_3 , 125 MHz) δ 173.628, 171.231, 136.957, 134.645, 133.995, 125.692, 125.522, 125.456, 125.031, 74.497, 66.158, 62.182, 53.540, 39.780, 39.143, 37.092, 34.682, 32.145, 31.047, 30.076, 29.918, 29.881, 29.772, 29.730, 29.590, 29.493, 28.152, 26.003, 25.936, 22.908, 21.396, 16.152, 14.325; HRMS (ESI) calcd for $\text{C}_{36}\text{H}_{67}\text{NO}_4$ $[\text{M}+\text{H}]^+$: 578.5070, found: 578.5074.



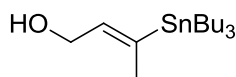
To a solution of **2-10** (200 mg, 1 mmol) in 4 mL of CCl_3CN , 160 mg of K_2CO_3 was added. The solution was stirred overnight. After filtration, the solvent was removed. The residue and **2-34** (160 mg, 0.27 mmol) were dissolved into 5 mL of dry DCM. 70 mg of active 4A molecular sieve was added. The mixture was stirred for half an hour. Two drops of TMSOTf was added at 0 °C. The reaction was stopped by adding 100 μL of Et_3N after 2 hrs. After filtration, the solvent was removed. 130 mg of the product was isolated through a column chromatography (SiO_2). ^1H NMR (CDCl_3 , 500 MHz) δ 7.293-7.501 (m, 15 H), 6.110 (d, $J = 9.0$ Hz, 1 H), 5.792 (dt, $J = 15.5, 7.5$ Hz, 1 H), 5.543 (s, 1 H), 5.408 (dd, $J = 15.5, 7.5$ Hz, 1 H), 5.332 (t, $J = 7.5$ Hz, 1 H), 5.108 (t, $J = 5.5$ Hz, 1 H), 4.624-4.968 (m, 4 H), 4.185 (br, 1 H), 4.026 (t, $J = 7.5$ Hz, 1 H), 3.968 (dd, $J = 7.5, 1.5$ Hz, 1 H), 3.788-3.809 (m, 1 H), 3.654 (t, $J = 7.5$ Hz, 1 H), 3.587-3.605 (m, 2 H), 3.338 (dd, $J = 7.5, 1$ Hz, 1 H), 1.833-2.165 (m, 11 H), 1.587 (s, 3 H),

1.254-1.315 (m, 18 H), 0.882 (t, $J = 6.5$ Hz, 6 H); ^{13}C NMR (CDCl_3 , 125 MHz) δ 172.973, 170.059, 138.778, 138.371, 137.594, 136.763, 134.208, 129.200, 128.782, 128.569, 128.472, 128.260, 128.199, 127.883, 127.750, 126.348, 125.425, 125.316, 101.718, 99.491, 82.533, 79.553, 78.794, 75.414, 74.188, 74.115, 69.235, 67.687, 63.008, 50.517, 39.204, 36.812, 32.169, 31.320, 30.094, 29.954, 29.808, 29.693, 29.614, 29.493, 28.176, 25.918, 22.938, 14.374; HRMS (ESI) calcd for $\text{C}_{63}\text{H}_{93}\text{NO}_9$ $[\text{M}+\text{H}]^+$: 1008.6850, found: 1008.6854.



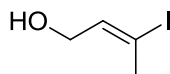
To a blue solution of Na (23 mg, 1 mmol) in 5 mL of liquid NH_3 , **10** (50 mg, 0.05 mmol) in 1 mL of dry THF was added at -78 °C. The solution was stirred for 2 hrs. 2 g of NH_4Cl was added to quench the reaction. After the solvent was removed, the residue was extracted with Et_2O . 12 mg of the product was obtained through a column chromatography (SiO_2). ^1H NMR (CDCl_3 , 500 MHz) δ 5.798 (dt, $J = 15.5, 7.5$ Hz, 1 H), 5.479 (t, $J = 10.0$ Hz, 1 H), 5.341-5.434 (m, 2 H), 5.280 (t, $J = 7.5$ Hz, 1 H), 4.971-5.010 (m, 2 H), 4.886 (dd, $J = 10.0, 4.0$ Hz, 1 H), 4.347-4.381 (m, 1 H), 4.222 (dd, $J = 7.5, 3.5$ Hz, 1 H), 4.095 (dd, $J = 7.5, 2.0$ Hz, 1 H), 3.952-3.977 (m, 1 H), 3.720 (dd, $J = 11.0, 7.5$ Hz, 1 H), 3.540 (dd, $J = 11.0, 3$ Hz, 1 H), 1.833-2.165 (m, 6 H), 1.587 (s, 3 H), 1.254-1.315 (m, 18 H), 0.882 (t, $J = 6.5$ Hz, 3 H); ^{13}C NMR (CDCl_3 , 125 MHz) δ 172.991, 170.490, 137.388, 131.531, 129.085, 1125.316, 96.748, 73.156, 70.722, 70.267, 69.035,

67.700, 62.025, 50.736, 37.080, 32.837, 32.606, 32.151, 29.469, 26.015, 22.914, 21.305, 20.923, 20.862, 14.338; HRMS (ESI) calcd for C₄₀H₇₅NO₈ [M+H]⁺: 698.5493, found: 698.5500.



2-37

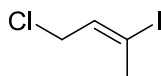
To a suspension of CuCN (9.02 g, 100.8 mmol) in 200 mL THF, 84.8 mL of 2 M BuLi was added dropwise under -78 °C. The temperature was stirred at -40 °C for 10 mins, and then recooled down to -78 °C. Bu₃SnH (60 mL, 212 mmol) was added over 1 hr, and then 1-hydroxyl-2-butyne (7.1 g, 100.8 mmol) was added. The mixture was stirred overnight and the temperature was allowed to rise up to room temperature. Saturated NH₄Cl was added to quench the reaction. After filtration, the solvent was removed. 25 g of the product was obtained through a column chromatography (SiO₂) in 93% yield. ¹H NMR (CDCl₃, 500 MHz) δ 6.409 (t, *J* = 2.0 Hz, 1 H), 4.260 (d, *J* = 2.0 Hz, 2 H), 1.89 (s, 3 H), 1.46-1.52 (m, 6 H), 1.27-1.35 (m, 6 H), 0.88-0.92 (m, 15 H); ¹³C NMR (CDCl₃, 125 MHz) δ 136.58, 40.10, 27.77; HRMS (ESI) calcd for C₁₆H₃₄OSn [M+H]⁺: 326.1632, found: 326.1638.



2-38

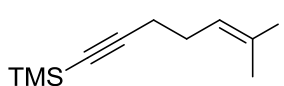
To a solution of the starting material (25 g, 60 mmol), I₂ (15.4 g, 60 mmol) was added at 0 °C. The reaction mixture was stirred 0.5 hrs. After removing the solvent, 12 g of the product

was isolated through a column chromatography (SiO₂) in 99% yield. ¹H NMR (CDCl₃, 500 MHz) δ 6.409 (t, *J* = 7.8 Hz, 1 H), 4.096 (d, *J* = 7.8 Hz, 2 H), 2.459 (s, 3 H); ¹³C NMR (CDCl₃, 125 MHz) δ 136.58, 40.10, 27.77; HRMS (ESI) calcd for C₄H₇IO [M+H]⁺: 198.9542, found: 198.9545.



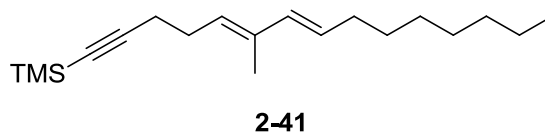
2-39

To a solution of triphenylphosine (19 g, 75 mmol) in 50 mL of dry THF, NCS (10 g, 75 mmol) was added at 0 °C. The resulting suspension was poured into 10 g of **1** at 0 °C. The temperature was allowed to rise up to room temperature. The suspension was stirred for 5 hrs. Then, the solvent was removed, and the brown residue was cracked and washed with hexanes. The filtrate was collected and the solvent was removed. Then hexanes was used to extract it, and after removing the solvent, the crude product was used in the next step without any further purification. The crude yield was 81%. ¹H NMR (CDCl₃, 500 MHz) δ 6.422 (t, *J* = 7.8 Hz, 1 H), 3.962 (d, *J* = 7.8 Hz, 2 H), 2.495 (s, 3 H); ¹³C NMR (CDCl₃, 125 MHz) δ 136.58, 40.10, 27.77; HRMS (ESI) calcd for C₄H₆ClI [M+H]⁺: 216.9203, found: 216.9209.



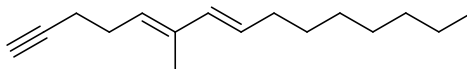
2-40

To a solution of **1-TMS-1-propyne** (6.74 g, 60 mmol) in 100 mL of THF, *n*-BuLi (24 mL, 2.5 M) was added dropwise at -78 °C. The solution was stirred at -40 °C for 30 mins then, cooled to -78 °C. 11 g of the starting material was added dropwise, and the temperature was allowed to rise up to room temperature. The solution was stirred overnight. Saturated NH₄Cl was added to quench the reaction. The mixture was extracted with hexanes and dried over Na₂SO₄. 11.5 g of the product was isolated through a column chromatography (SiO₂) in 77% yield. ¹H NMR (CDCl₃, 500 MHz) δ 6.192 (t, *J* = 1 Hz, 1 H), 2.403 (s, 3 H), 2.237-2.289 (m, 4 H), 0.159 (s, 9 H); ¹³C NMR (CDCl₃, 125 MHz) δ 139.057, 105.843, 95.209, 85.444, 29.734, 27.697, 19.435, 0.082; HRMS (ESI) calcd for C₁₀H₁₇ISi [M+H]⁺: 293.01, found: 293.01.



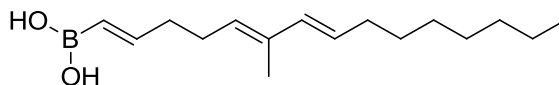
A mixture of the *trans*-1-Nonenylboronic acid (6.7 g, 39.4 mmol), palladium(0)-trisk-(triphenyl phosphine) (4.6 g, 4 mmol), cesium carbonate (12.8 g, 39.4 mmol) and the starting material (11.5 g, 39.4 mmol) in 200 mL of THF was refluxed overnight. After cooling down and filtration, the solvent was removed. 6.7 g of the product was isolated through a column chromatography (SiO₂) in 59% yield. ¹H NMR (CDCl₃, 500 MHz) δ 6.057 (d, *J* = 15.5, 1 H), 5.600 (dt, *J* = 15.5, 7.0 Hz, 1 H), 5.389 (t, *J* = 7.5 Hz, 1 H), 2.261-2.376 (m, 4 H), 2.053-2.111 (m, 2 H), 1.749 (s, 3 H), 1.253-1.404 (m, 10 H), 0.887 (t, *J* = 7 Hz, 3 H), 0.116-0.179 (m, 9 H); δ 134.987, 134.266, 128.686, 127.675, 84.212, 68.337, 32.865, 31.828, 29.650, 29.223, 29.196,

27.342, 22.662, 18.764, 14.092, 12.562, 0.082; HRMS (ESI) calcd for C₁₉H₃₄Si [M+H]⁺: 291.2403, found: 291.2452.



2-42

To a solution of **4** (6.7 g, 23 mmol) in 50 mL of MeOH, K₂CO₃ (3.1 g, 23 mmol) was added. The mixture was stirred at room temperature overnight. The solvent was removed, and the residue was extracted with hexanes. After removing the solvent, 4 g of the product was isolated through a column chromatography (SiO₂) in 80% yield. ¹H NMR (CDCl₃, 500 MHz) δ 6.066 (d, *J* = 15.5 Hz, 1 H), 5.609 (dt, *J* = 15.5, 7.0 Hz, 1 H), 5.394 (t, *J* = 7.5 Hz, 1 H), 2.348-2.390 (m, 2 H), 2.235-2.268 (m, 2 H), 2.068-2.110 (m, 2 H), 1.960 (t, *J* = 2.5 Hz, 1 H), 1.752 (s, 3 H), 1.284-1.405 (m, 10 H), 0.888 (t, *J* = 7 Hz, 3 H); ¹³C NMR (CDCl₃, 125 MHz) δ 134.987, 134.266, 128.686, 127.675, 84.212, 68.337, 32.865, 31.828, 29.650, 29.223, 29.196, 27.342, 22.662, 18.764, 14.092, 12.562; HRMS (ESI) calcd for C₁₆H₂₆ [M+H]⁺: 219.2035, found: 219.2048.



2-43

To a solution of the alkyne (4 g, 18 mmol) in mL of THF, catecholborane (18 mL, 18 mmol) was added. The solution was reflux overnight. The solvent was removed and the mL of

water was poured into the residue. After filtration, 3.2 g of the product was obtained. The yield was 68%.

2.5 References

1. Litman, G. W.; Cannon, J.P.; Dishaw, L. *J. Nature Reviews. Immunology*, **2005**, *5*, 866–879.
2. Mayer, Gene (2006). "Immunology - Chapter One: Innate (non-specific) Immunity". *Microbiology and Immunology On-Line Textbook*. USC School of Medicine. <http://pathmicro.med.sc.edu/ghaffar/innate.htm>. Retrieved 1 January 2007
3. Janeway, C.A., Jr. et al. (2005). *Immunobiology*. (6th ed.). Garland Science.
4. Yu, K.O. A.; Porcelli, S. A. *Immunol. Lett.*, **2005**, *100*, 42-55.
5. Godfrey, D. I; MacDonald, H. R; Kronenberg, M.; Smyth M. J.; Van Kaer, L. *Nat Rev Immunol.*, **2004**, *4*, 231-237.
6. Savage, P. B.; Teytonc, L.; Bendelac, A. *Chem. Soc. Rev.*, **2006**, *35*, 771–779.
7. Venkataswamy, M. M.; Porcelli, S. A. *Seminars in immunology*, **2010**, *22*, 68-78.
8. Natori, T.; Morita, M.; Akimoto, K.; Koezuka, Y. *Tetrahedron* **1994**, *50*, 2771-2784.
9. Natori, T.; Koezuka, Y.; Higa, T. *Tetrahedron Lett.* **1993**, *34*, 5591-5592.
10. Morita, M.; Motoki, K.; Akimoto, K.; Natori, T.; Sakai, T.; Sawa, E.; Yamaji, K.; Koezuka, Y.; Kobayashi, E.; Fukushima, H. *J. Med. Chem.*, **1995**, *38*, 2176-2187.
11. Kawano, T.; Cui, J.; Koezuka, Y.; Toura, I.; Kaneko, Y.; Motoki, K. ; Ueno, H.; Nakagawa, R.; Sato, H.; Kondo, E.; Koseki, H.; Taniguchi, M. *Science*, **1997**, *278*, 1626-1629.

12. Zhou, X.; Forestier, C.; Goff, R. D.; Li, C.; Teyton, L.; Bendelac, A.; Savage, P. B. *Org. Lett.*, **2002**, *4*, 1267-1270.
13. Liu, Y.; Goff, R. D.; Zhou, D.; Mattner, J.; Sullivan, B. A.; Khurana, A.; Cantu, C.; Ravkov, E. V.; Ibegbu, C. C.; Altman, J. D.; Teyton, L.; Bendelac, A.; Savage, P. B. *J. Immun. Methods*, **2006**, *312*, 34-39.
14. Sidobre, S.; Hammond, K.J. L.; Be ´nazet-Sidobre, L.; Maltsev, S. D.; Richardson, S. K., Ndonge, R. M.; Howell, A. R.; Sakai, T., Besra, G. S.; Porcelli, S. A.; Kronenberg, M. *PNAS*, **2004**, *101*, 12254-12259.
15. Miyamoto, K.; Miyake, S.; Yamamura, T. *Nature*, **2001**, *413*, 531-534.
16. Goff, R. D.; Gao, Y.; Mattner, J.; Zhou, D.; Yin, N.; Cantu, C.; Teyton, L.; Bendelac, A.; Savage, P. B. *J. Am. Chem. Soc.*, **2004**, *126*, 13602-13603.
17. Oki, S.; Chiba, A.; Yamamura, Y.; Miyake, S. *J. Clin. Invest.*, **2004**, *113*, 1631-1640.
18. Pietra, F. *Nat. Prod. Rep.*, **1997**, *14*, 453-464.
19. Jenkins, K. M.; Jensen, P. R.; Fenical, W. *Tetrahedron letter*, **1999**, *40*, 7637-7640.
20. Jin, W.; Rinehart, K.L.; Jares-Erijman, E. A. *J. Org. Chem.*, **1994**, *59*, 144-147.
21. Natori, T.; Morita, M.; Akimoto, K.; Koezuka, Y. *Tetrahedron*, **1994**, *50*, 2771-2784.
22. Bugni, T. S.; Ireland, C. M. *Nat. Prod. Rep.*, **2004**, *21*, 143-163.
23. Zhang, Y.; Wang, S.; Li, X.; Cui, C.; Feng, C.; Wang, B. *Lipids*, **2007**, *42*, 759-764.
24. Chen, J. H.; Cui, G. Y.; Liu, J. Y.; Tan, R. X. *Photochemistry*, **2003**, *64*, 903-906.
25. Mukhtar, N.; Iqbal, K.; Anis, I.; Malik, A. *Photochemistry*, **2002**, *61*, 1005-1008.
26. Brodesser, S.; Sawatzi, P.; Kolter, T. *Eur. J. Org. Chem.*, **2003**, *2003*, 2021-2034.

27. Tan, R. X.; Chen, J. H. *Nat. Prod. Rep.*, **2003**, *20*, 509-534.

Chapter 3. Development of TLR-2 and TLR-6 heterodimer binders and studies of their immunology activities

3.1 Introduction

3.1.1 Immune systems

Immune systems are found in all plants and animals.¹ They protect organisms against diseases by recognizing and killing pathogens and tumor cells. To function properly, they need to identify the agents from those intruders or tumor cells and discriminate them from the healthy cells owned by the organisms.

Physical barriers are the first layers to protect organisms from pathogens, such as bacteria and viruses. Once the first barrier is broken through by a pathogen, the mammalian immune system begins to eliminate the intruder through two broad categories of the immune system: innate immunity and acquired immunity. T cells, B cells, dendritic cells and macrophages are the major immune cells in mammalian immune system.

Pattern recognition receptors (PRRs) identify microbial components, which are difficult for the microorganism to change because usually they are important for the survival of the microorganisms. These microbial structures are termed pathogen associated molecular patterns (PAMPs). Different PRRs interact with specific PAMPs, and activate unique signaling pathways, thus, responding to pathogens distinctively.

Innate immune responses target a large range of conserved microbial and pathogenic components or antigens, including proteins, nucleic acids and carbohydrates, and constantly

screen for these conserved components via unique PRRs. In contrast, adaptive immune responses are specific to a foreign antigen and remain at rest until they encounter a component expressing that specific antigen.²

3.1.2 Toll like receptors

Substantial research has focused on toll like receptors (TLRs) due to their ability to discriminate between large assortments of microbial stimuli.³ TLRs are integral components of the innate immune system. To date, eleven TLRs have been identified and characterized. They are PRRs that are expressed on the surface of macrophages, dendritic cells, B cells, some T cells, and some non-immunological cells.^{1,4}

Depending on the PAMP, including lipopeptides, lipopolysaccharide, bacterial lipoprotein, and lipoteichoic acid, certain TLRs will bind and signal an immune response.⁵ Multiple studies have shown a proinflammatory immune response to the binding of TLRs with the targeted antigen.

TLRs are type 1 membrane glycoproteins consisting of extracellular, transmembrane, and intracellular signaling domains.⁹ The extracellular domain consists of leucine-rich repeating motifs (Lxx) and the intracellular domain comprises a homologous Toll/1L-1R domain (TIR).¹ The extracellular domain's conserved Lxx motifs number 20~30 amino acids in length. These motifs form a β sheet and an α helix connected by a loop to help form a horseshoe-like 3-d conformation (see figure 3-1).^{1,6} The TIR domains have a five-stranded β sheet, encompassed

about by five α helices. The second β sheet and second α helix play a key role in TIR dimerization. So, TLRs are likely to function as dimers, and most TLRs appear as homodimers.

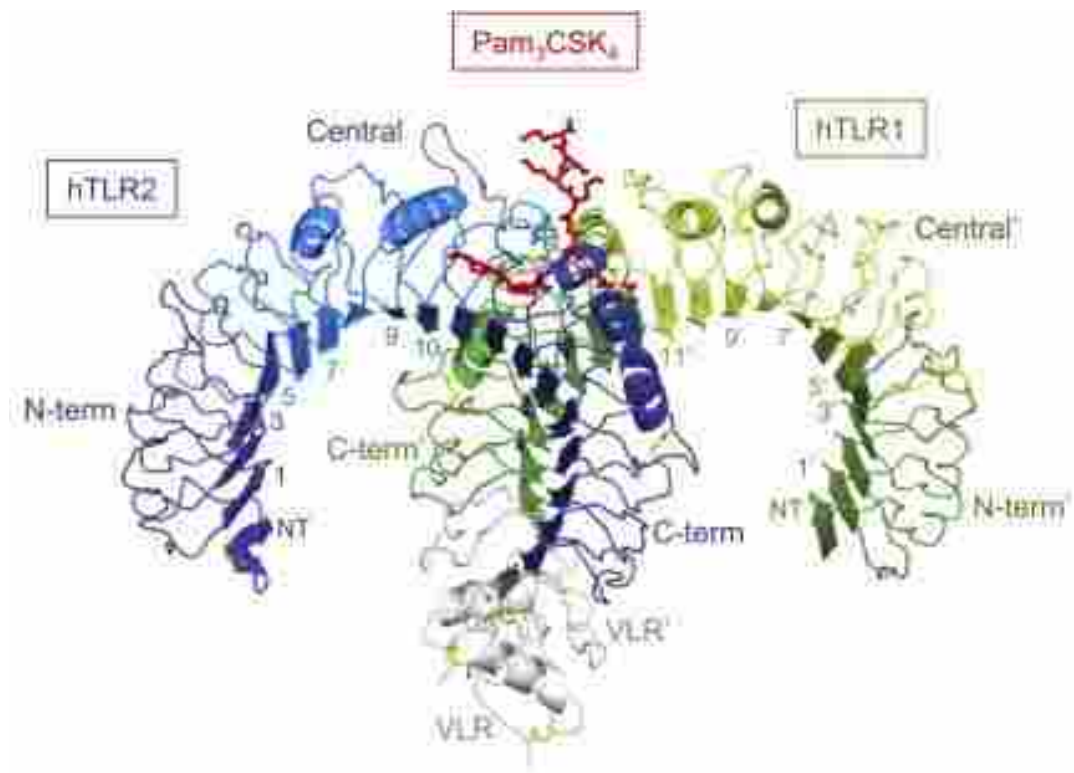


Figure 3-1: Crystal structure of TLR2-TLR1 hetero-dimer complexed with the synthesized triacylated lipopeptide Pam₃CSK₄.

3.1.3 TLR2 / TLR6 induce TH2 response

Different stimulators educate dendritic cells to secrete different cytokines. IL-10 blocks host protective inflammatory responses and promote anti-inflammatory T regulatory TH2 immune responses. However, high level of IL-10 is not sufficient to induce T regulatory type

cells. The ratio of IL-12 to IL-10 produced by dendritic cells plays the key roll. TLR1, TLR2 and TLR6 recognize lipopeptides, and TLR2 plays the major roll in detecting and recognizing lipid components of pathogens. Different from other TLRs, TLR2 forms heterodimers with TLR1 or TLR6. Each dimer has different ligand specificity and provides different immune responses.

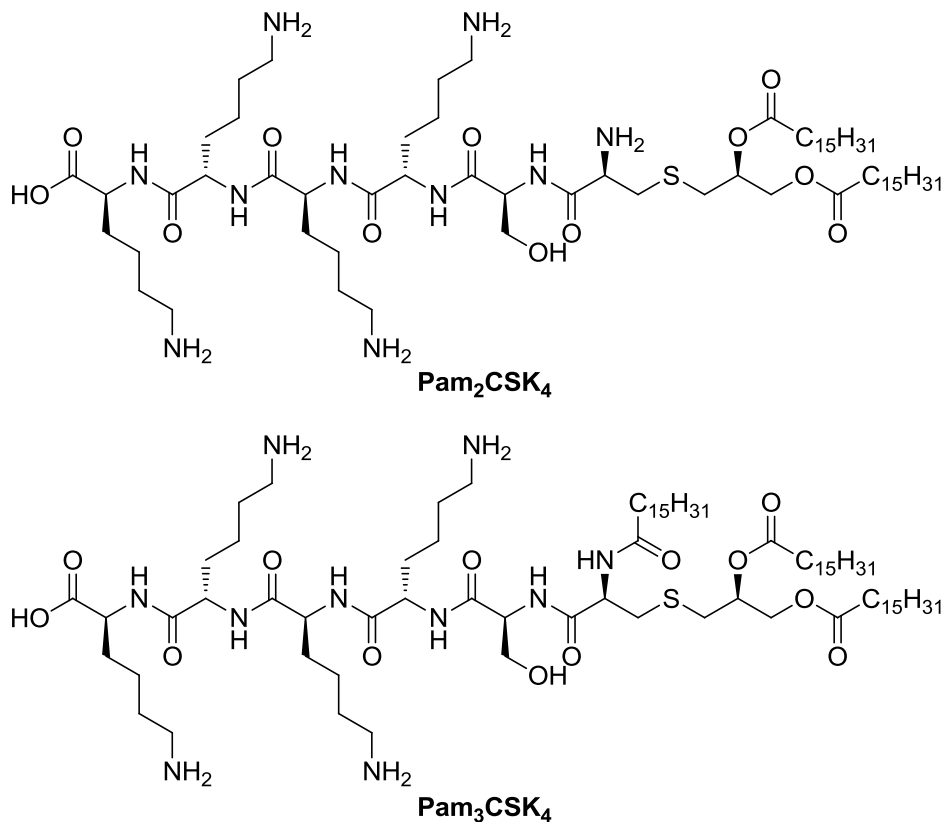


Figure 3-2: Structures of Pam₂CSK₄ and Pam₃CSK₄

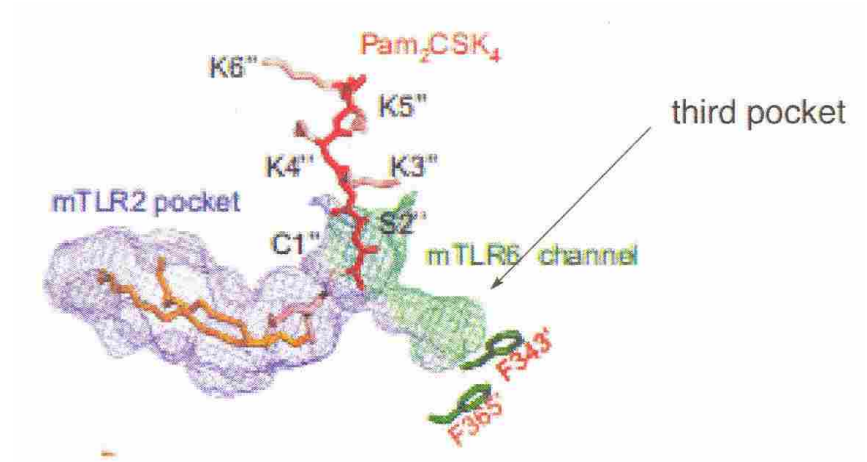


Figure 3-3: Computational crystal structures of Pam₂CSK₄ bound TLR2 and TLR6 heterodimer

Studies show that TLR1 / TLR2 heterodimer binds a triacylated lipopeptide, Pam₃CSK₄ (Figure 3-2) and induce TH1 responses. For TLR2 / TLR6 heterodimer (Figure 3-3), there is no hydrophobic pocket for the third acyl chain, and the lipopeptide's amine interacts with TLR6 via hydrogen bond stabilization,⁵ so it binds a diacylated lipopeptide, Pam₂CSK₄, to generate a regulatory anti-inflammatory TH2 immune response by promoting dendritic cell to secret relative high level of interleukin-10 to IL-12.⁷

3.2 Result and discussion

3.2.1 Design of TLR-1 / TLR-6 heterodimer binders

Based on the studies described above, we designed and synthesized two modified structures of lipopeptides, lipopeptide mimic (LPM) -1 and LPM-2 (Figure 3-4).

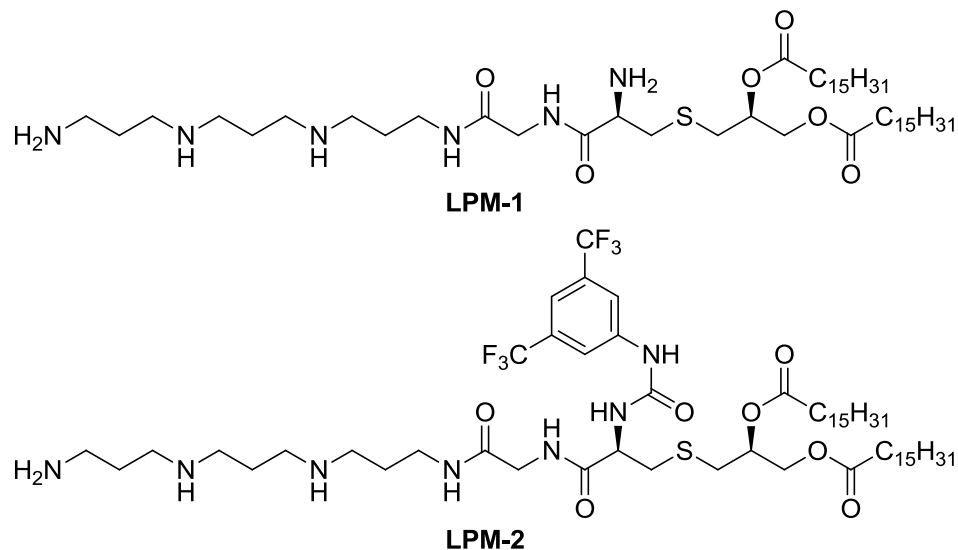


Figure 3-4: Structures of LPM-1 and LPM-2

The differences between Pam₂CSK₄ and LPM-1 are: (1) the amino acid, next to cysteine, is glycine in LPM-1, rather than serine. We used glycine because it is simpler, and in the literature it is reported that there is little difference between compounds with the two different amino acids. (2) We replaced the lysines with a polyamine. There is evidence that the only role of these lysines is to provide solubility to the lipid, and this can be achieved with a polyamine, which is much simpler. In addition, there would be no proteolytic degradation of the peptide portion if a polyamine is used to replace a sequence of lysines.

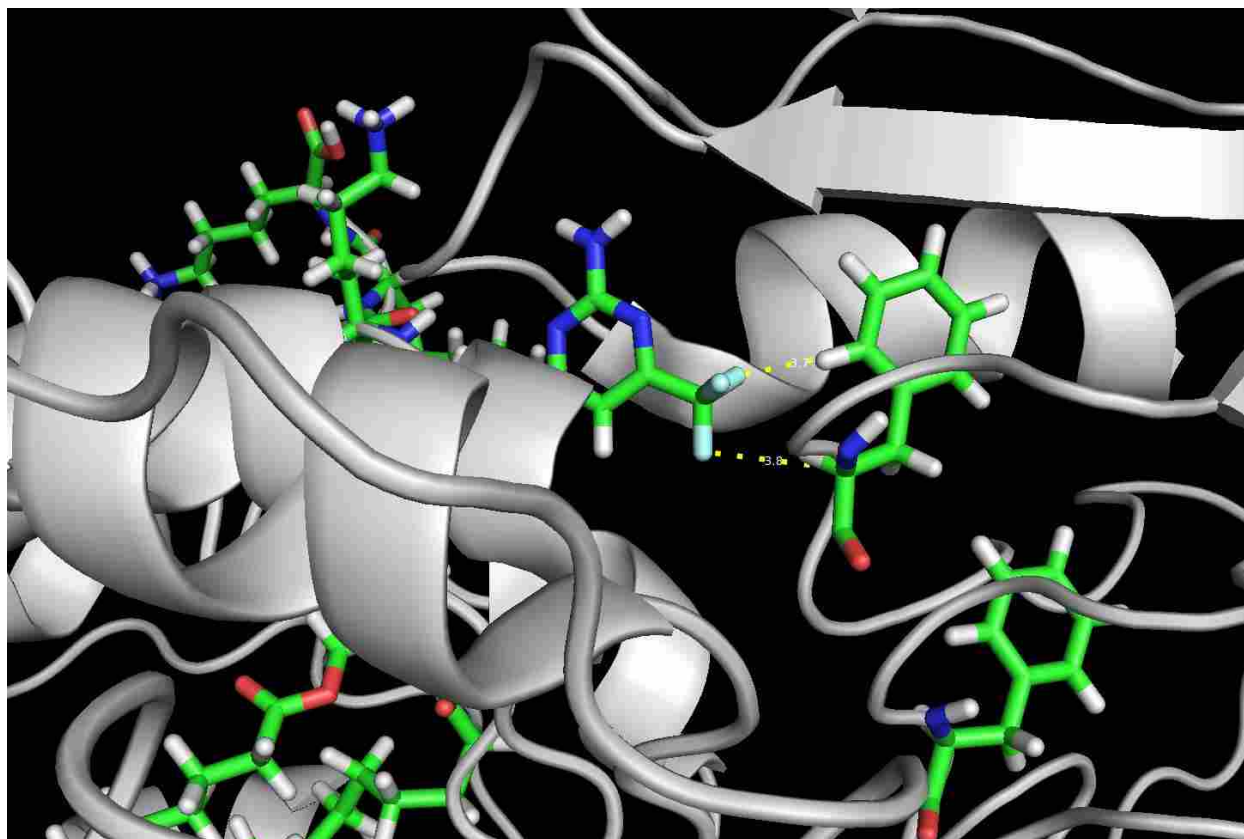
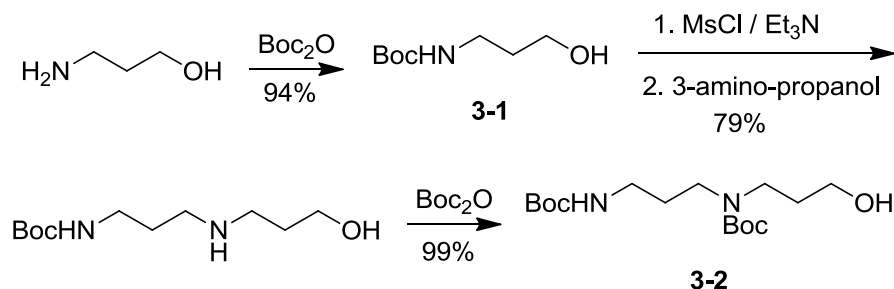


Figure 3-5: Computational crystal structures of LPM-2 binded TLR2 and TLR6 heterodimer

For LMP-2, we put a 3, 5-bistrifluoro phenyl urea on the cysteine amine. Due to modeling of the Pam₂CSK₄ and TLR2 / TLR6 heterodimer complex shown in Figure 3-3 indicated that there is an unoccupied pocket right above the Pam₂CSK₄ cysteine amine. To find a proper functional group covalently attached to the stimulator may promote TLR2 / TLR6 heterodimer formation over TLR1 / TLR2 dimer formation. There are two phenylalanines, F343' and F365', located at the terminal of the unoccupied pocket. We hope the two trifluoromethyl group can be fixed by those two phenyl group by π -stack interaction (Figure 3-5), so that we can obtain stronger stimulation and more TH2 respond in the end.

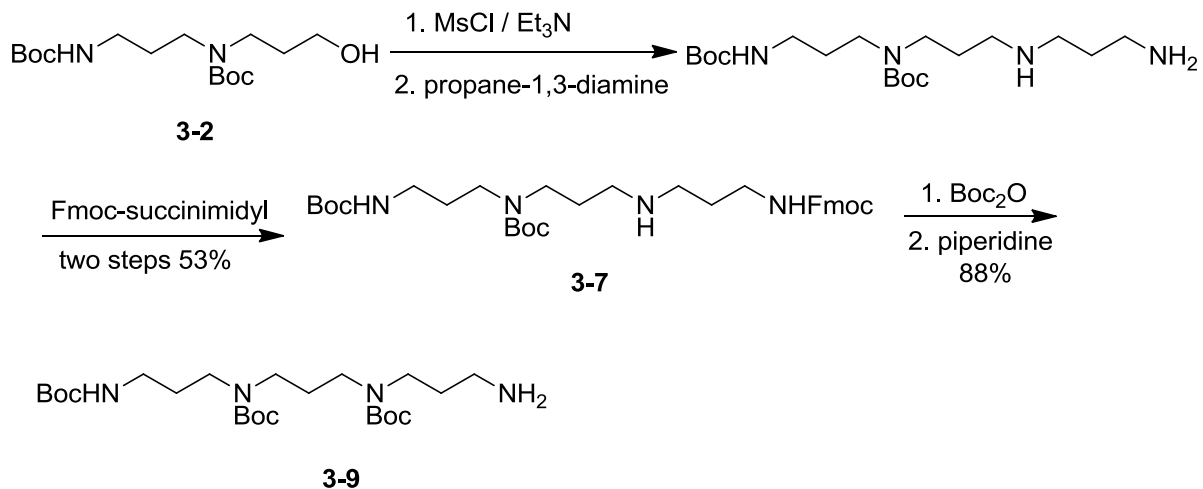
3.2.2 Synthesis of 3-10

The synthesis of polyamine part of LMP-1 starts from 3-amino-propanol. Protecting the amino group with Boc, **3-1** was produced. After mesylation of the hydroxyl group, and substitution with 3-amino-propanol, Boc₂O was used to selectively protect the secondary amine to give **3-2** (Scheme 3-1).



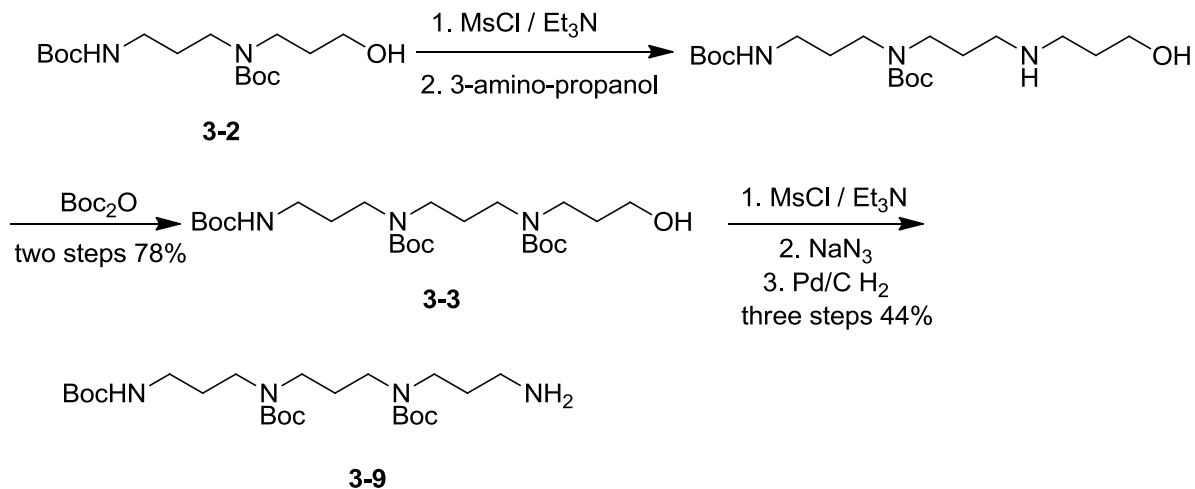
Scheme 3-1: Synthesis of 3-1

Mesylation followed by propane-1,3-diamine substitution, one equivalent of Fmoc-succinimidyl carbonate was used to selectively protect the primary amino group at 0 °C afforded **3-7**. Then Boc₂O was used to protect the secondary amine. Piperidine de-Fmoc generated **3-9** (Scheme 3-2). This route to make 3-9 is not quite satisfied, due to relatively low yield. The bottle neck is the step to make **3-7**. The selectivity is only about 7:3. The other route was performed to do the comparison.



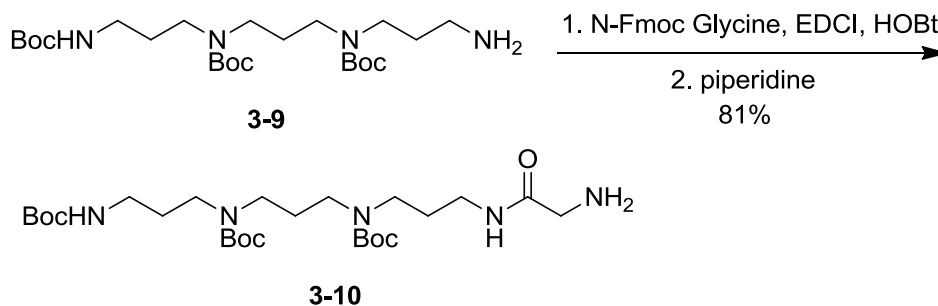
Scheme 3-2: Synthesis of 3-9

Instead of using propane-1, 3-diamine, 3-amino-propanol was used to do the substitution. Then, the free secondary amine was selectively protected by Boc to generate **3-3**. After mesylation, azide was used to replace the mesylate. Hydrogenation catalyzed by palladium on carbon afforded intermediate **3-9** in quantitative yield (Scheme 3-3).



Scheme 3-3: Alternative synthesis of 3-9

Coupling with Fmoc protected glycine, followed by removing Fmoc, gave **3-10**, the solubility improvement chain (Scheme 3-4).

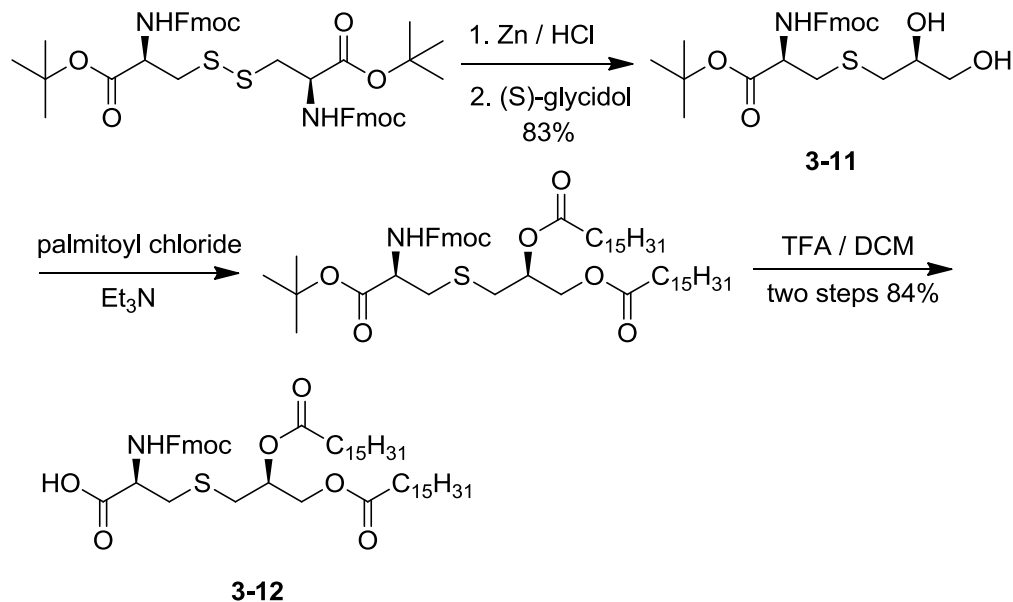


Scheme 3-4: Synthesis of 3-10

3.2.3 Synthesis of 3-12

The synthesis of the LMP binding part starts from (Fmoc-Cys-*Ot*-Bu)₂. After zinc reduction under acidic conditions, the disulfide bond was cleaved. The thiol was used as

nucleophile to attack (S)-glycidol to afford **3-11**. Acylation of the diol generated the diester. Mono esterification was observed as major in 1 hour. Prolonging the reaction time to 6 hours gave the desired intermediate. Using trifluoroacetic acid to remove *tert*-butyl ester generated **3-12** (Scheme 3-5).

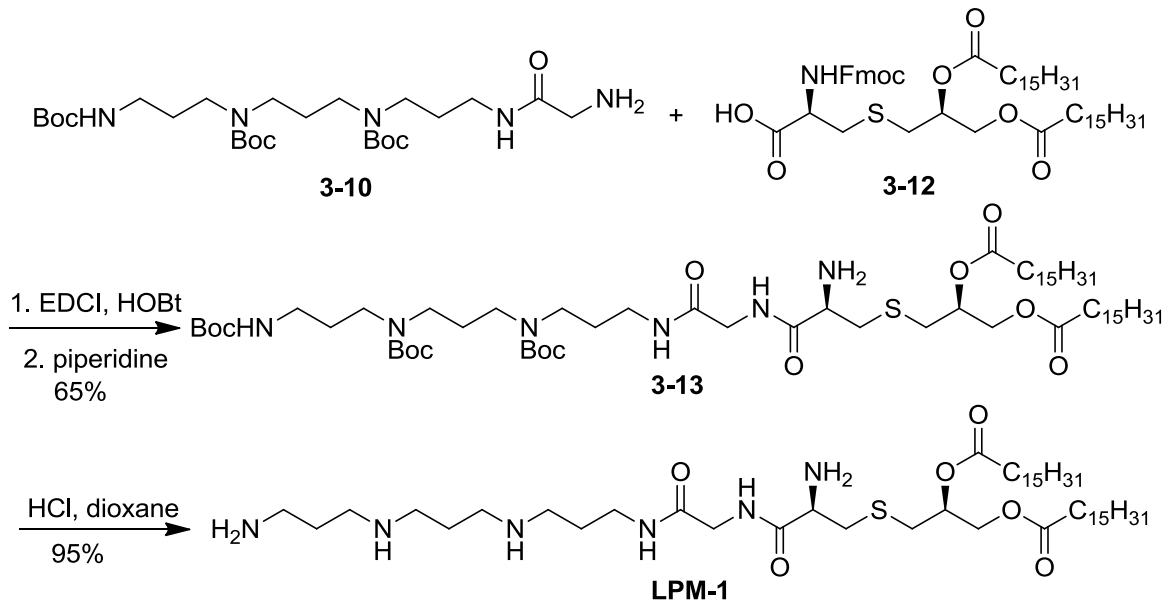


Scheme 3-5: Synthesis of 3-12

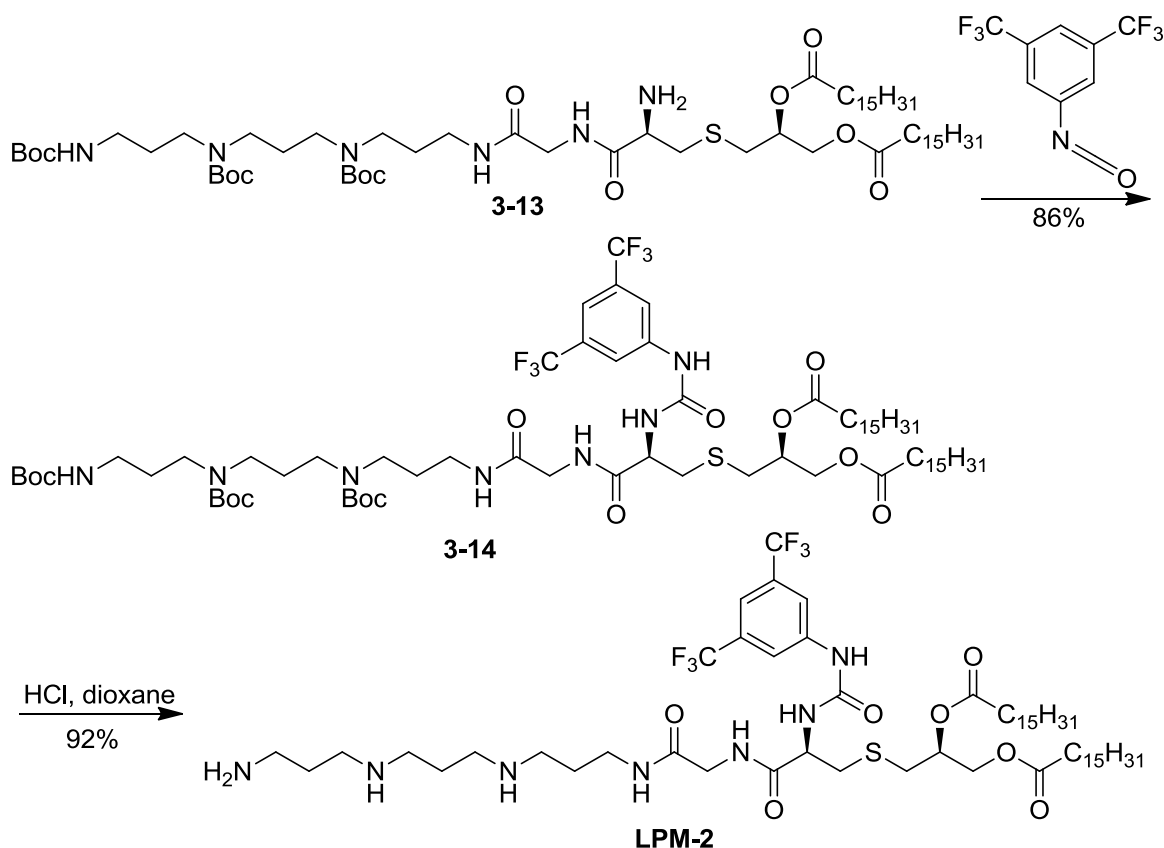
3.2.4 Synthesis of LMP-1 and LMP-2

3-13 was obtained by coupling **3-10** with **3-12**, using EDCI and HOBt. Removing Fmoc protecting group afforded **3-13**. HCl in dioxane was used to do Boc deprotection to accomplish the synthesis of **LMP-1** (Scheme 3-6).

Reacting **3-13** with bistrifluoromethyl phenyl isocyanate, followed by HCl / dioxane deprotection gave **LMP-2** (Scheme 3-7).



Scheme 3-6: Achievement of LPM-1



Scheme 3-7: Achievement of LPM-2

3.2.5 Results and discussion

Mice dendritic cells are used to test TLR responses, which are isolated using the following procedure. The collagenase was diluted to 1:10 in plain RPMI. The spleen was taken out onto a Petri dish containing RPMI (Gibco) from the sacrificed mice. Then, it was hold over the 50ml tube with forceps, and the 1:10 collagenase was injected with the syringe to puff up the spleen. The puffed up spleen was put into the 50ml tube containing about 5ml 1:10 collagenase. The mixture was incubated in an incubator at 37 C for 45 minutes. 1ml HBS was put into 1.5

ependorf tubes for overlay. After 45 minutes incubation, 50mM EDTA (stock is at 500mM, so add 1:10 dilution) was added to quench the reaction. The tubes were cooled on ice for 5 minutes to stop the collagenase reaction. The spleen was transferred into a cell strainer (BD Falcon, 70uM Nylon. REF 352350) in a 50ml, then, meshed with a 1cc syringe plunger. The solution was filtered and the filtration was stored in a 50ml tube. The cells were centrifuged at 1500rpm for 5 minutes, then, washed with 5ml HBS to get rid of teh collagenase.(re-spin at 1500rpm for 5 minutes). The cell pellet was broken up by gently tapping bottom of the tubes and resuspended in 5ml optiprep solution. In a 15 ml tube, 5ml of the cell suspension was mixed well. 1ml of HBS was added slowly using a Pasteur pipette, while tilting the 15ml tube as horizontal as possible. The mixture was centrifuged at 200 rpm for 30 minutes. The cells were taken out from the interface with a Pasteur pipette, then, washed with 4 ml of HBS, and spin at 300g for 5 minutes.

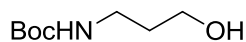
The cells were dispersed into 10^6 / ml in RPMI and stimulated by adding Pam2 (100 ng/mL), Pam3 (100 ng/mL) as controls. LPM1 and LPM2 were added at different concentrations. The plates were incubated at 37 C for 24 hours or 48 hours. ELISA was used to test IL-10 and IL-12p40 levels.

From the result we can see, the ratio of IL-10/IL-12 stimulated by LPM1 is not as high as that by Pam2. However, for TLR2 knocked out mice, both LPM1 and LPM2 didn't stimulate the dendritic cells to secret IL-10, and for TLR6 knocked out mice, not much IL-10 was detected with LPM1 stimulation, but for wild type mice dendritic cells, a substantial jump of IL-10 was observed. That argues that LPM1 is a better TLR6 depended stimulator than Pam2, which

confirmed our previous hypothesis: polyamine will do the same job with peptide chain KKKK in natural Pam2. The results also show that we are on the right direction to develop a TLR6 dependent stimulator.

For LPM2, the TLR6 depended IL-10 release is not as good as LPM1. The only structural difference between them is the bistrifluoromethyl phenyl urea on the cystein amino group. It was designed to fill the third pocket of the TLR2/TLR6 heterodimer to get a more stable binding, but the result is not satisfied. The size of the functional group may be too large. We are preparing other smaller alternatives to fulfill the job.

3.3 Experimental section



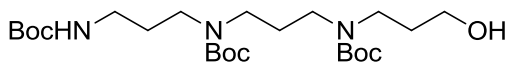
3-1

To a solution of 3-amino-1-propanol (20.64 g, 0.275 mol) in 200 mL of DCM, Boc₂O (60 g, 0.275 mol) was added in portion. The solution was stirred overnight. 45 g of the product was isolated through a column chromatography (SiO₂) in 94% yield. ¹H NMR (CDCl₃, 500 MHz) δ 4.822 (br, 1 H), 3.636-3.668 (m, 2 H), 3.275-3.299 (m, 2 H), 3.097 (br, 1 H), 1.633-1.677 (m, 2 H), 1.439 (s, 9 H); ¹³C NMR (CDCl₃, 125 MHz) δ 158.797, 59.391, 37.055, 33.122, 28.589; HRMS (ESI) calcd for C₈H₁₇NO₃ [M+H]⁺: 176.1208, found: 176.1256.



3-2

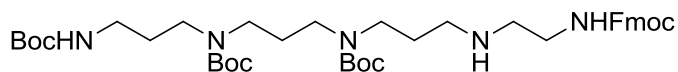
To a solution of 3-boc protected amino-1-propanol (3.2 g, 18.3 mmol) in 20 mL of DCM, MsCl (2.4 g, 21 mmol) and Et₃N (2.12 g, 21 mmol) were added at 0 °C. The temperature was allowed to rise up to room temperature. The solution was stirred for 30 mins. Then, 10 mL of water was used to wash the solution. The aqueous layer was extracted with DCM three times. The combined organic layer was dried over Na₂SO₄. After the solvent was removed, 3-amino-1-propanol (10.32 g, 0.14 mol) was added to dissolve the residue. The solution was stirred at 80 °C for 2 hrs. 3-amino-1-propanol was removed under vacuum. 50 mL of water was used to wash the solution. The aqueous layer was extracted with DCM three times. The combined organic layer was dried over Na₂SO₄. After removing the solvent, the residue was dissolved into 50 mL of DCM. Then, Boc₂O (4 g, 18.3 mmol) was added. The solution was stirred overnight. 4.8 g of the product **3-1** was isolated through a column chromatography (SiO₂) in 79% yield. ¹H NMR (CDCl₃, 500 MHz) δ 3.475-3.054 (m, 8 H), 1.807-1.591 (m, 4 H), 1.413 (s, 9 H), 1.367 (s, 9 H); ¹³C NMR (CDCl₃, 125 MHz) δ 163.851, 158.797, 83.078, 80.677, 79.704, 66.490, 46.368, 44.971, 37.284, 28.445, 28.430, 28.414, 27.772, 27.753, 27.110, 22.257; HRMS (ESI) calcd for C₁₆H₃₂N₂O₅ [M+H]⁺: 333.2311, found: 333.2316.



3-3

To a solution of **3-2** (4.8 g, 14.4 mmol) in 50 mL of DCM, MsCl (2.0 g, 17.5 mmol) and Et₃N (1.8 g, 17.5 mmol) were added at 0 °C. The temperature was allowed to rise up to room temperature. The solution was stirred for 30 mins. Then, 10 mL of water was used to wash the

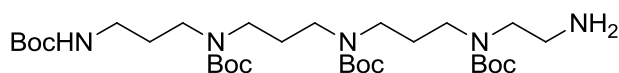
solution. The aqueous layer was extracted with DCM three times. The combined organic layer was dried over Na₂SO₄. After the solvent was removed, 3-amino-1-propanol (10.32 g, 0.14 mol) was added to dissolve the residue. The solution was stirred at 80 °C for 2 hrs. 3-amino-1-propanol was removed under vacuum. 50 mL of water was used to wash the solution. The aqueous layer was extracted with DCM three times. The combined organic layer was dried over Na₂SO₄. After removing the solvent, the residue was dissolved into 50 mL of DCM. Then, Boc₂O (3.2 g, 15 mmol) was added. The solution was stirred overnight. 7.2 g of the product was isolated through a column chromatography (SiO₂) in 99% yield. ¹H NMR (CDCl₃, 500 MHz) δ 4.822 (br, 1 H), 3.754-3.117 (m, 12 H), 3.097 (br, 1 H), 1.696-1.568 (m, 6 H), 1.477 (s, 9 H), 1.437 (s, 9 H); ¹³C NMR (CDCl₃, 125 MHz) δ 156.958, 156.436, 156.422, 80.541, 58.231, 44.158, 42.196, 37.658, 33.065, 31.310, 30.395, 28.827, 28.403, 28.383, 27.647; HRMS (ESI) calcd for C₂₄H₄₇N₃O₇ [M+H]⁺: 490.3414, found: 490.3468.



3-4

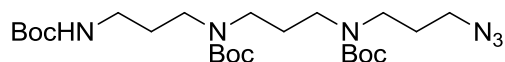
To a solution of **3-3** (3 g, 6 mmol) in 20 mL of DCM, MsCl (0.755 g, 6.6 mmol) and Et₃N (667 mg, 6.6 mmol) were added at 0 °C. The temperature was allowed to rise up to room temperature. The solution was stirred for 30 mins. Then, 20 mL of water was used to wash the solution. The aqueous layer was extracted with DCM three times. The combined organic layer was dried over Na₂SO₄. After the solvent was removed, ethylene diamine (3.6 g, 0.06 mol) was added to dissolve the residue. The solution was stirred at 80 °C for 2 hrs. Then, ethylene

diamine was removed under vacuum. 20 mL of water was used to wash the solution. The aqueous layer was extracted with DCM three times. The combined organic layer was dried over Na₂SO₄. After removing the solvent, the residue was dissolved into 5 mL of DCM. Then, 9-fluorenylmethyl N-succinimidyl carbonate (2 g, 6 mmol) was added. The solution was stirred overnight. 3 g of the product was isolated through a column chromatography (SiO₂) in 53% yield.



3-5

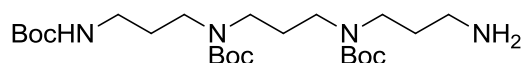
To a solution of **3-4** (3 g, 5.6 mmol) in 5 mL of DCM, Boc₂O (3.2 g, 15 mmol) was added. The solution was stirred overnight. 0.5 mL of Piperidine was then added into the solution. After stirring for 1 hrs, the solvent and the piperidine were removed. 2.4 g of the product was isolated through a column chromatography (SiO₂) in 88% yield.



3-8

To a solution of **3-3** (4.8 g, 14.4 mmol) in 50 mL of DCM, MsCl (2.0 g, 17.5 mmol) and Et₃N (1.8 g, 17.5 mmol) were added at 0 °C. The temperature was allowed to rise up to room temperature. The solution was stirred for 30 mins. Then, 10 mL of water was used to wash the solution. The aqueous layer was extracted with DCM three times. The combined organic layer was dried over Na₂SO₄. After the solvent was removed, 15 mL of DMSO was added to dissolve

the residue. Then, NaN₃ (1.87 g, 28.8 mmol) was added and the mixture was stirred at 80 °C overnight. The temperature was cooled to room temperature then, 50 mL of water and 50 mL of DCM were added. The aqueous layer was extracted with DCM three times and the combined organic phase was dried over Na₂SO₄. After removing the solvent, the product was used in the next step directly. ¹H NMR (CDCl₃, 500 MHz) δ 3.321-3.101 (m, 12 H), 1.809-1.651 (m, 6 H), 1.461 (s, 9 H), 1.453 (s, 9 H), 1.433 (s, 9 H); HRMS (ESI) calcd for C₂₄H₄₆N₆O₆ [M+H]⁺: 515.3479, found: 515.3523.

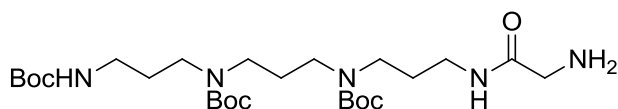


3-9

Route 1: To a solution of **3-7** (3 g, 5.6 mmol) in 5 mL of DCM, Boc₂O (3.2 g, 15 mmol) was added. The solution was stirred overnight. 0.5 mL of Piperidine was then added into the solution. After stirring for 1 hrs, the solvent and the piperidine were removed. 2.4 g of the product was isolated through a column chromatography (SiO₂).

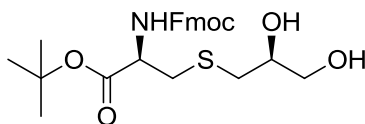
Route 2: To a solution of **3-8**, the residue was dissolved into 10 mL of MeOH. 0.5 g of Pd/C was added and the mixture was hydrogenated overnight under 1 atm. 3.1 g of the product was isolated through a column chromatography (SiO₂) in 44% yield for three steps. ¹H NMR (CDCl₃, 500 MHz) δ 4.681 (br, 1 H), 3.754-3.117 (m, 12 H), 1.696-1.568 (m, 6 H), 1.477 (s, 9 H), 1.437 (s, 9 H); ¹³C NMR (CDCl₃, 125 MHz) δ 156.958, 156.436, 156.422, 80.541, 58.231,

44.158, 42.196, 37.658, 33.065, 31.310, 30.395, 28.827, 28.403, 28.383, 27.647; HRMS (ESI) calcd for C₂₄H₄₈N₄O₆ [M+H]⁺: 489.3574, found: 489.3613.



3-10

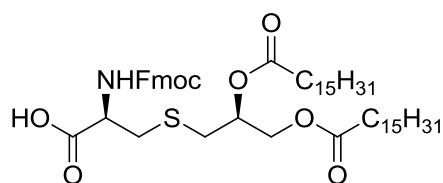
To a solution of Fmoc-glycine (300 mg, 1 mmol) in 5 mL of DCM, EDCI (230 mg, 1.2 mmol) and HOBT (162 mg, 1.2 mmol) were added. The solution was stirred for 30 mins, then, 600 mg of compound **3-9** was added. The solution was stirred overnight at room temperature. Piperidine was then added into the solution. After stirring for 1 hrs, the solvent and the piperidine were removed. 540 mg of the product was isolated through a column chromatography (SiO₂) in 81% yield.



3-11

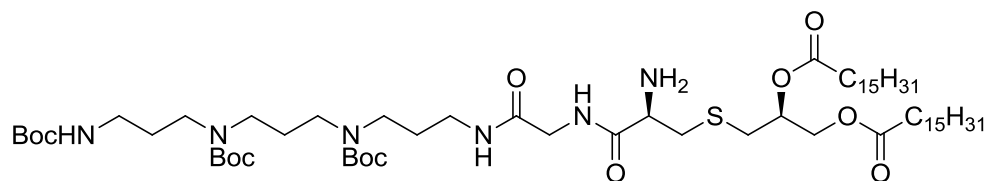
To a solution of (Fmoc-Cys-Ot-Bu)₂ (1.92 g, 2.4 mmol) in 15 mL of DCM, active zinc powder (1.1 g, 16.8 mmol) and a freshly prepared mixture of MeOH, concentrated sulfuric acid and concentrated HCl (100:1:7, 8 mL) were added under vigorous stirring. After 15 min (S)-glycidol (355 mg, 4.8 mmol) was added. The mixture was stirred for 5 hrs. About half of the solvent was evaporated. After filtration, 2 mL of saturated KHSO₄ was added, then, extracted

with DCM three times. The combined organic phase was dried over Na₂SO₄. After removing the solvent, the product was purified through a column chromatography (SiO₂) in 83% yield.



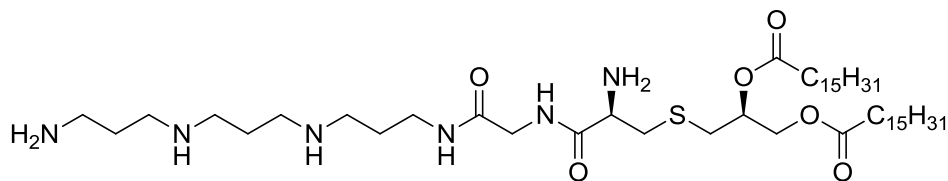
3-12

To a solution of **3-11** (946 mg, 2 mmol) in 10 mL of DCM, palmitoyl chloride (1.21 g, 4.4 mmol) and Et₃N (444 mg, 4.4 mmol) were added at room temperature. The solution was stirred overnight. 10 mL of water was added to wash the solution. The aqueous layer was extracted with DCM three times. The combined organic phase was dried over Na₂SO₄. The solvent was removed and 10 ml of DCM was added to dissolve the residue. 1.5 mL of TFA was added, and the solution was stirred overnight. After removing the solvent and TFA, 1.5 g of the product was isolated through a column chromatography (SiO₂) in 84% yield. ¹H NMR (CDCl₃, 500 MHz) δ 4.681 (br, 1 H), 3.754-3.117 (m, 12 H), 1.696-1.568 (m, 6 H), 1.477 (s, 9 H), 1.437 (s, 9 H); ¹³C NMR (CDCl₃, 125 MHz) δ 173.648, 173.589, 173.542, 172.277, 143.722, 141.288, 129.521, 127.740, 127.095, 126.558, 125.150, 119.986, 110.000, 70.325, 67.357, 63.650, 47.088, 45.895, 35.009, 34.296, 34.109, 32.816, 31.923, 29.703, 29.673, 29.661, 29.646, 29.501, 29.360, 29.288, 29.127, 29.104, 24.894, 24.852, 22.689, 14.115, 8.592; HRMS (ESI) calcd for C₂₄H₄₈N₄O₆ [M+H]⁺: 489.3574, found: 489.3613.



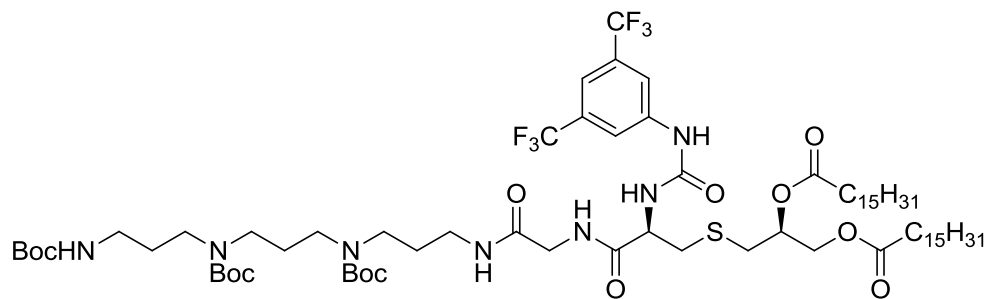
3-13

To a solution of **3-12** (163 mg, 0.18 mmol) in 2 mL of DCM, EDCI (39 mg, 0.2 mmol) and HOBT (28 mg, 0.2 mmol) were added. The solution was stirred for 30 mins, then, 100 mg of compound **3-10** was added. The solution was stirred overnight at room temperature. Piperidine was then added into the solution. After stirring for 1 hrs, the solvent and the piperidine were removed. 140 mg of the product was isolated through a column chromatography (SiO₂) in 65% yield.



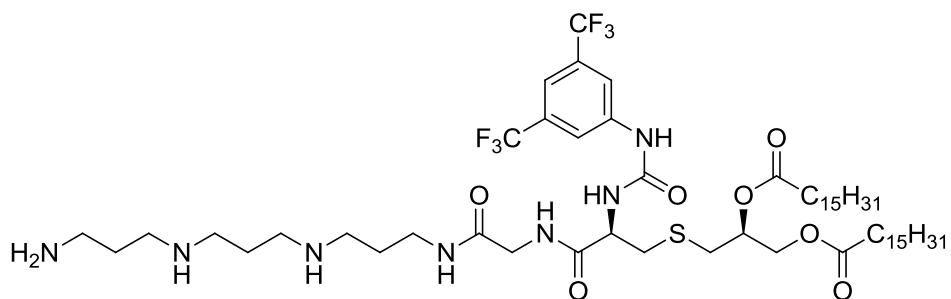
LPM-1

To a solution of 3-13 (50 mg, 0.042 mmol) in 0.1 mL of dioxane, 0.2 mL of 4 N HCl in dioxane was added. The solution was stirred overnight at room temperature, then, the solvent was removed. 31 mg of LPM-1 HCl salt was obtained in 95% yield.



3-14

To a solution of **3-13** (23 mg, 0.016 mmol) in 1 mL of 3, 5-di(trifluoromethyl)phenyl isocyanate (6 mg, 0.024 mmol) were added. The solution was stirred overnight at room temperature, and the solvent was removed. 20 mg of the product was isolated through a column chromatography (SiO₂) in 86% yield.



LPM-2

To a solution of 3-14 (20 mg, 0.017 mmol) in 0.1 mL of dioxane, 0.2 mL of 4 N HCl in dioxane was added. The solution was stirred overnight at room temperature, then, the solvent was removed. 18 mg of LPM-2 HCl salt was obtained in 92% yield.

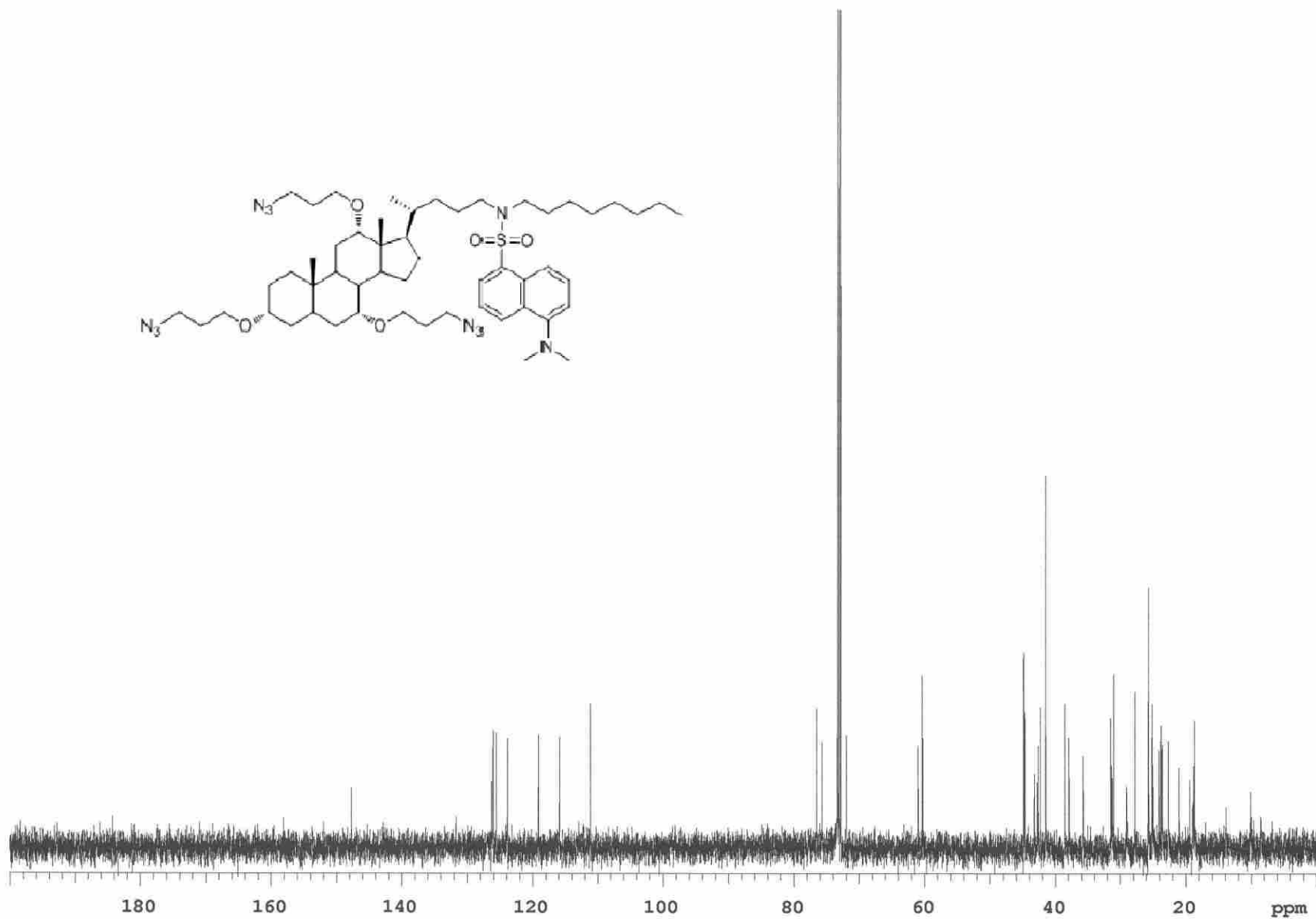
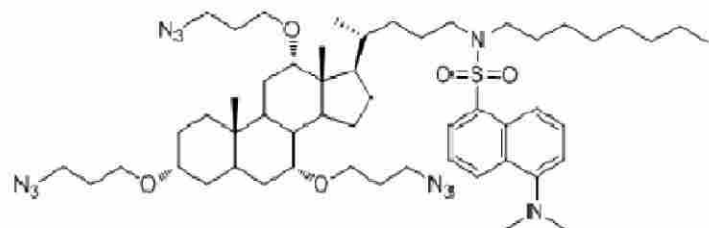
3.4 References

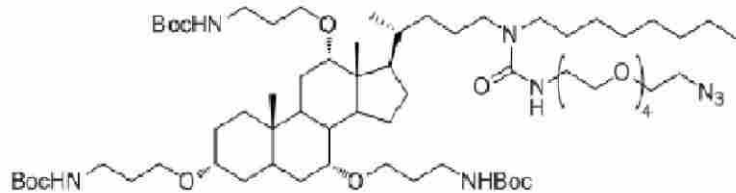
1. Akira, S.; Uematsu, S.; Takeuchi, O. *Cell* **2006**, *124* (4), 783-801.
2. Gerald B. Pier; Jeffrey B. Lyczak, L. M. W., *Immunology, Infection, and Immunity*. 1 ed.; ASM Press: Washington, D. C., 2004; p 6-8.
3. Agrawal, S.; Agrawal, A.; Doughty, B.; Gerwitz, A.; Blenis, J.; Van Dyke, T.; Pulendran, B., Cutting edge: different Toll-like receptor agonists instruct dendritic cells to induce distinct Th responses via differential modulation of extracellular signal-regulated kinase-mitogen-activated protein kinase and c-Fos. *J Immunol* **2003**, *171* (10), 4984-9.
4. Kawai, T.; Akira, S., Pathogen recognition with Toll-like receptors. *Curr Opin Immunol* **2005**, *17* (4), 338-44.
5. Kiura, K.; Kataoka, H.; Nakata, T.; Into, T.; Yasuda, M.; Akira, S.; Inoue, N.; Shibata, K., The synthetic analogue of mycoplasmal lipoprotein FSL-1 induces dendritic cell maturation through Toll-like receptor 2. *FEMS Immunol Med Microbiol* **2006**, *46* (1), 78-84.
6. Jin, M. S.; Lee, J. O., Structures of the toll-like receptor family and its ligand complexes. *Immunity* **2008**, *29* (2), 182-91.
7. Depaolo, R. W.; Tang, F.; Kim, I.; Han, M.; Levin, N.; Ciletti, N.; Lin, A.; Anderson, D.; Schneewind, O.; Jabri, B., Toll-like receptor 6 drives differentiation of tolerogenic dendritic cells and contributes to LcrV-mediated plague pathogenesis. *Cell Host Microbe* **2008**, *4* (4), 350-61.
8. Medzhitov, R.; Janeway, C., Jr., Innate immune recognition: mechanisms and pathways. *Immunol Rev* **2000**, *173*, 89-97.

9. Kruihof, E. K.; Satta, N.; Liu, J. W.; Dunoyer-Geindre, S.; Fish, R. J., Gene conversion limits divergence of mammalian TLR1 and TLR6. *BMC Evol Biol* **2007**, *7*, 148.
10. Netea, M. G.; van de Veerdonk, F.; Verschueren, I.; van der Meer, J. W.; Kullberg, B. J., Role of TLR1 and TLR6 in the host defense against disseminated candidiasis. *FEMS Immunol Med Microbiol* **2008**, *52* (1), 118-23.
11. Sing, A.; Reithmeier-Rost, D.; Granfors, K.; Hill, J.; Roggenkamp, A.; Heesemann, J., A hypervariable N-terminal region of *Yersinia* LcrV determines Toll-like receptor 2-mediated IL-10 induction and mouse virulence. *Proc Natl Acad Sci U S A* **2005**, *102* (44), 16049-54.
12. Sing, A.; Rost, D.; Tvardovskaia, N.; Roggenkamp, A.; Wiedemann, A.; Kirschning, C. J.; Aepfelbacher, M.; Heesemann, J., *Yersinia* V-antigen exploits toll-like receptor 2 and CD14 for interleukin 10-mediated immunosuppression. *J Exp Med* **2002**, *196* (8), 1017-24.
13. (a) Buwitt-Beckmann, U.; Heine, H.; Wiesmuller, K. H.; Jung, G.; Brock, R.; Akira, S.; Ulmer, A. J., Toll-like receptor 6-independent signaling by diacylated lipopeptides. *Eur J Immunol* **2005**, *35* (1), 282-9; (b) Omueti, K. O.; Beyer, J. M.; Johnson, C. M.; Lyle, E. A.; Tapping, R. I., Domain exchange between human toll-like receptors 1 and 6 reveals a region required for lipopeptide discrimination. *J Biol Chem* **2005**, *280* (44), 36616-25; (c) Harris, P. W. R.; Brimble, M. A.; Dunbar, R.; Kent, S. B. H., Synthesis of a C-terminal thioester derivative of the lipopeptide Pam(2)CSKKKKG using Fmoc SPPS. *Synlett* **2007**, (5), 713-716.

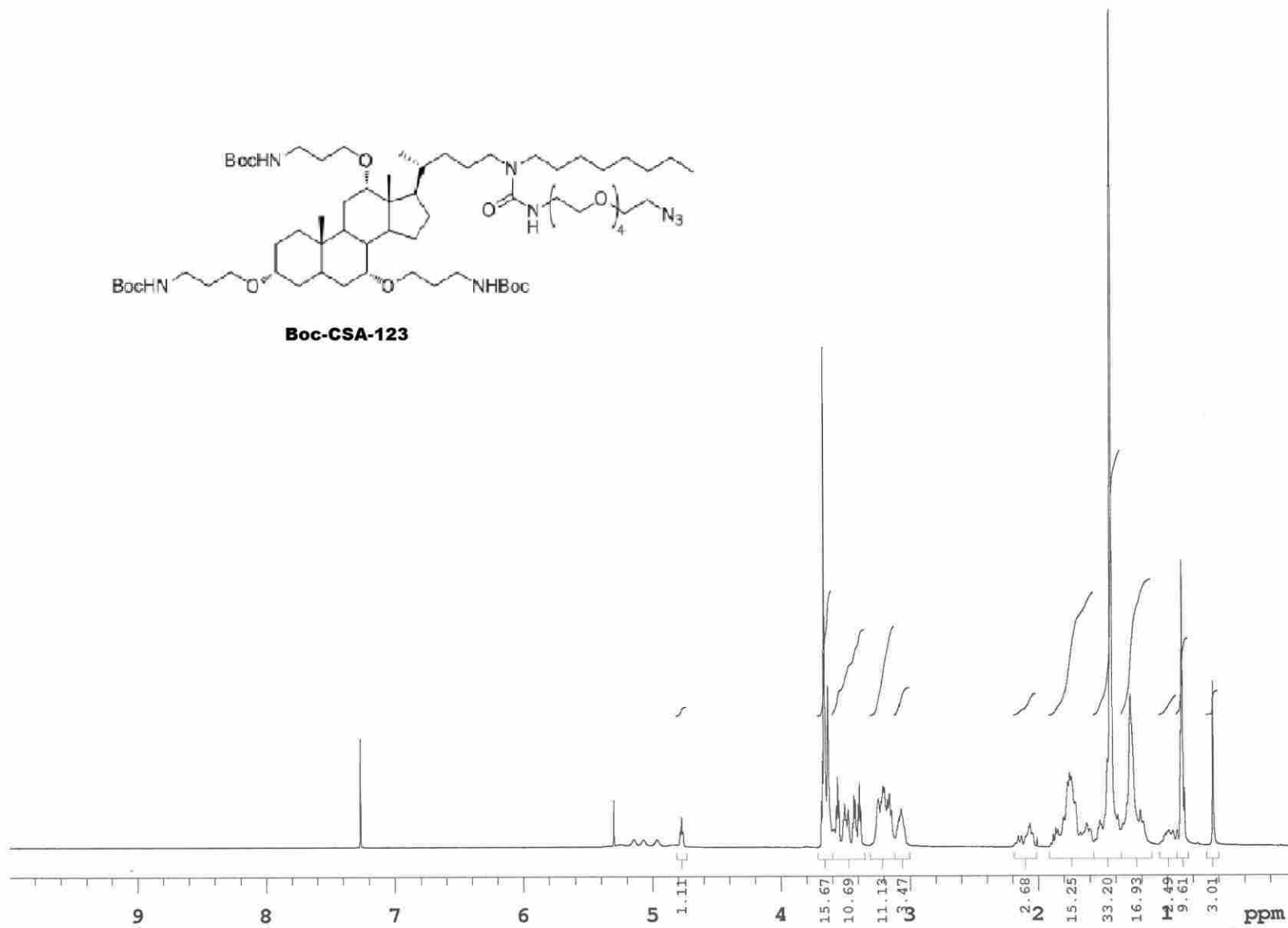
14. Nakao, Y.; Funami, K.; Kikkawa, S.; Taniguchi, M.; Nishiguchi, M.; Fukumori, Y.; Seya, T.; Matsumoto, M., Surface-expressed TLR6 participates in the recognition of diacylated lipopeptide and peptidoglycan in human cells. *J Immunol* **2005**, *174* (3), 1566-73.
15. Jin, M. S.; Kim, S. E.; Heo, J. Y.; Lee, M. E.; Kim, H. M.; Paik, S. G.; Lee, H.; Lee, J. O., Crystal structure of the TLR1-TLR2 heterodimer induced by binding of a tri-acylated lipopeptide. *Cell* **2007**, *130* (6), 1071-82.
16. Metzger, J. W.; Wiesmuller, K. H.; Jung, G., Synthesis of N alpha-Fmoc protected derivatives of S-(2,3-dihydroxypropyl)-cysteine and their application in peptide synthesis. *Int J Pept Protein Res* **1991**, *38* (6), 545-54.
17. Seyberth, T.; Voss, S.; Brock, R.; Wiesmuller, K. H.; Jung, G., Lipolanthionine peptides act as inhibitors of TLR2-mediated IL-8 secretion. Synthesis and structure-activity relationships. *J Med Chem* **2006**, *49* (5), 1754-65.
18. Schromm, A. B.; Howe, J.; Ulmer, A. J.; Wiesmuller, K. H.; Seyberth, T.; Jung, G.; Rossle, M.; Koch, M. H.; Gutschmann, T.; Brandenburg, K., Physicochemical and biological analysis of synthetic bacterial lipopeptides: validity of the concept of endotoxic conformation. *J Biol Chem* **2007**, *282* (15), 11030-7.
19. Lepore, S. D.; Mondal, D.; Li, S. Y.; Bhunia, A. K., Stereoretentive halogenations and azidations with titanium(IV) enabled by chelating leaving groups. *Angew Chem Int Ed Engl* **2008**, *47* (39), 7511-4.
20. Bendelac, A.; Savage, P. B.; Teyton, L., The biology of NKT cells. *Annu Rev Immunol* **2007**, *25*, 297-336.

Appendix: Spectra



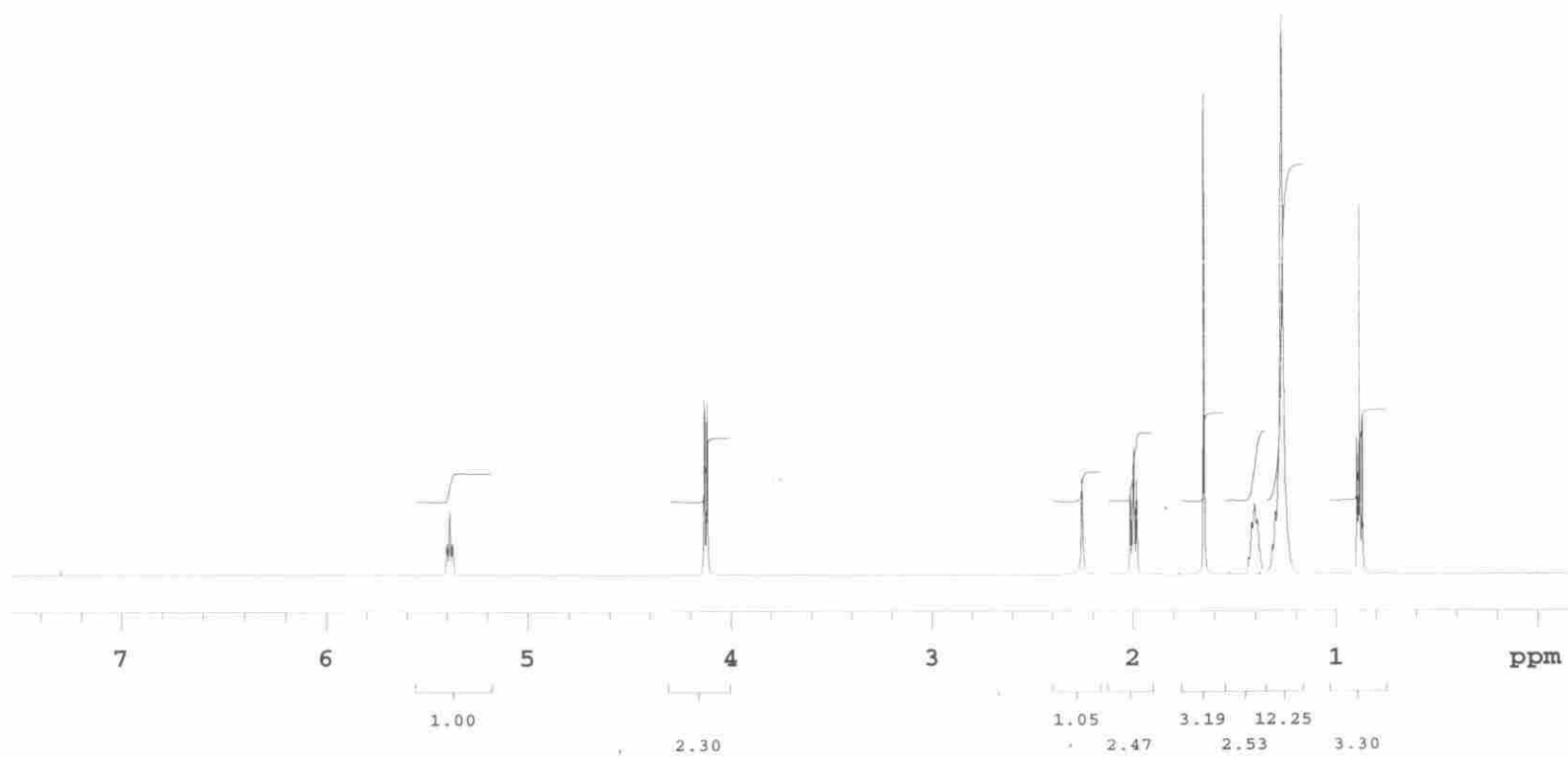


Boc-CSA-123



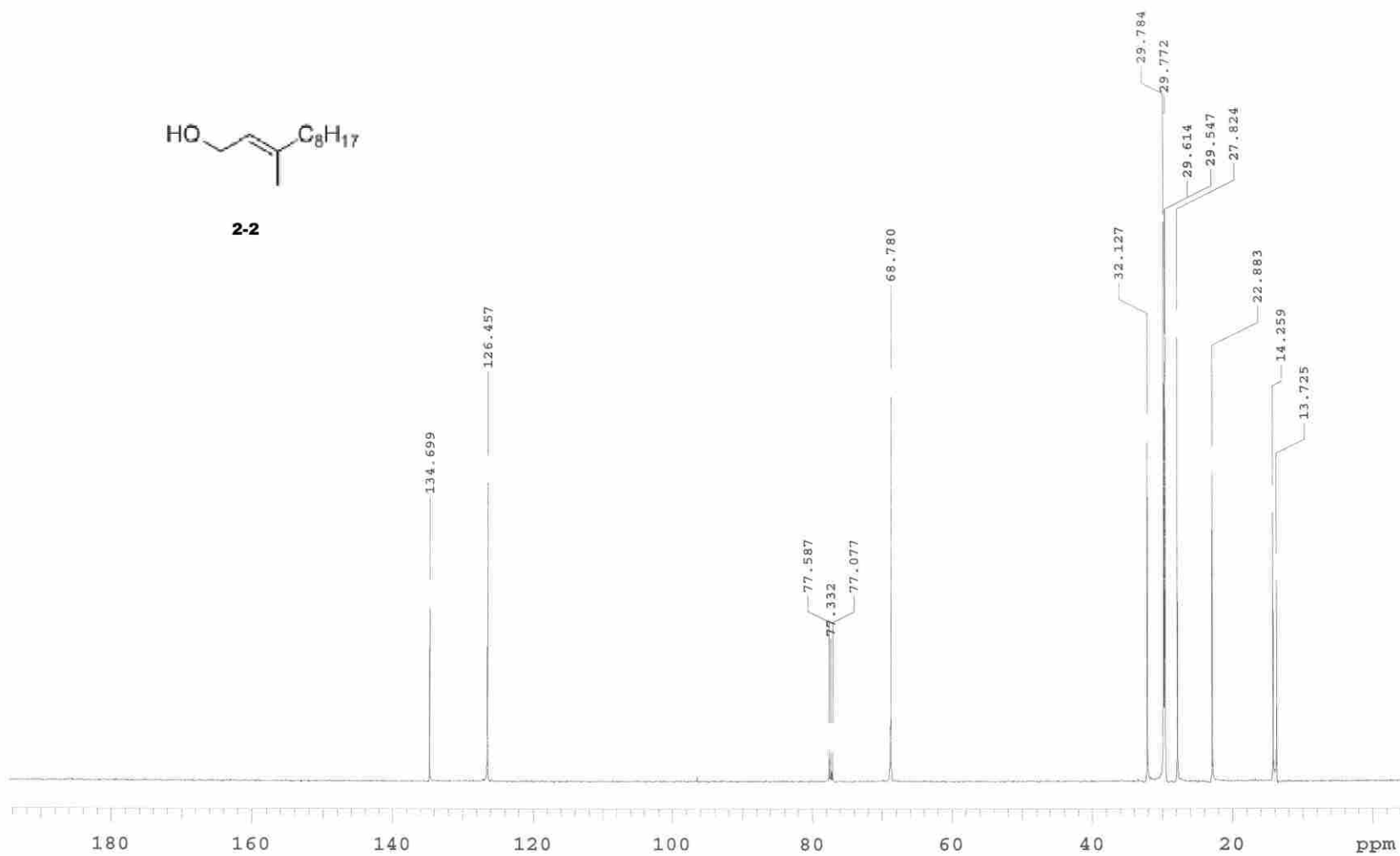


2-2



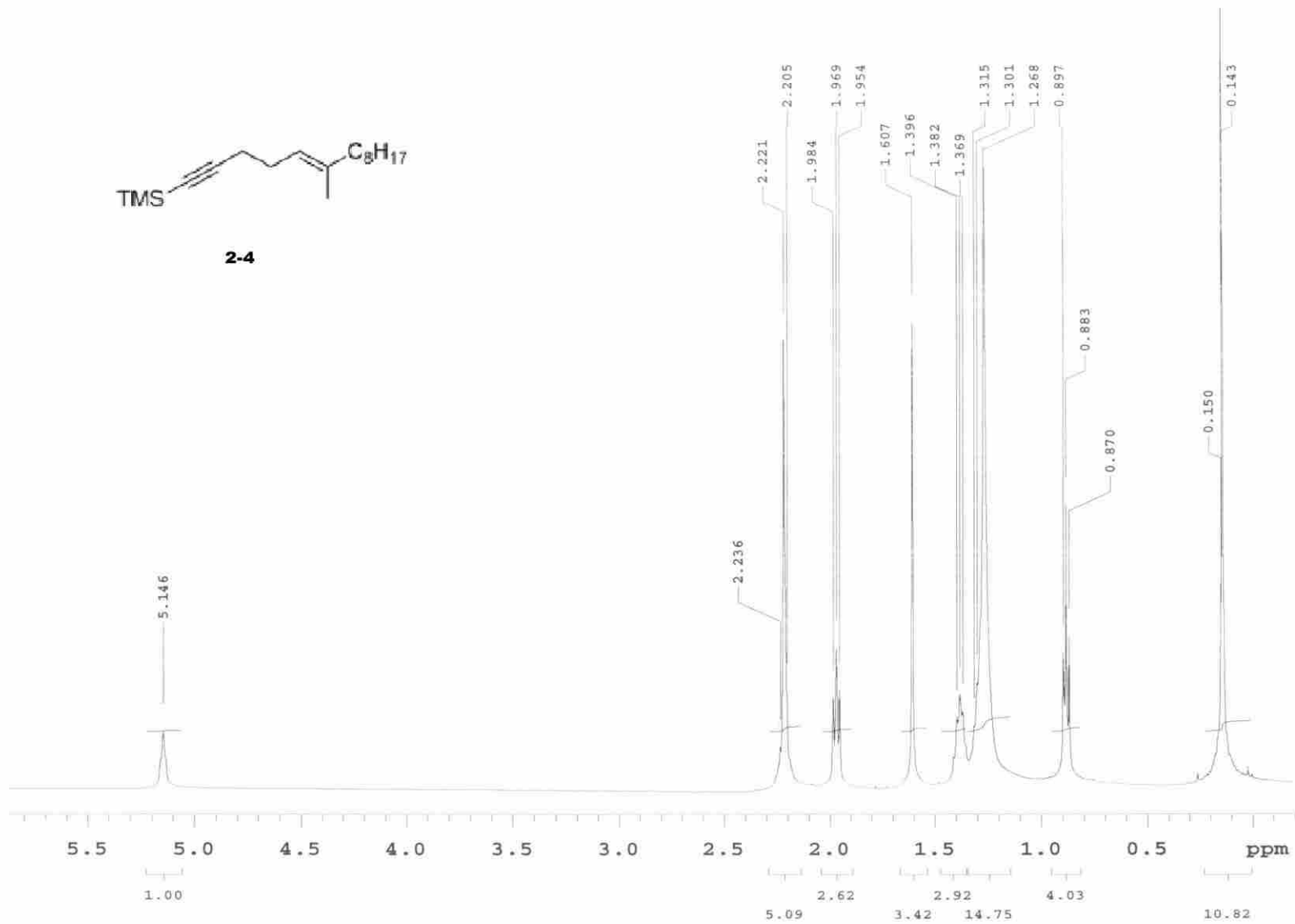


2-2



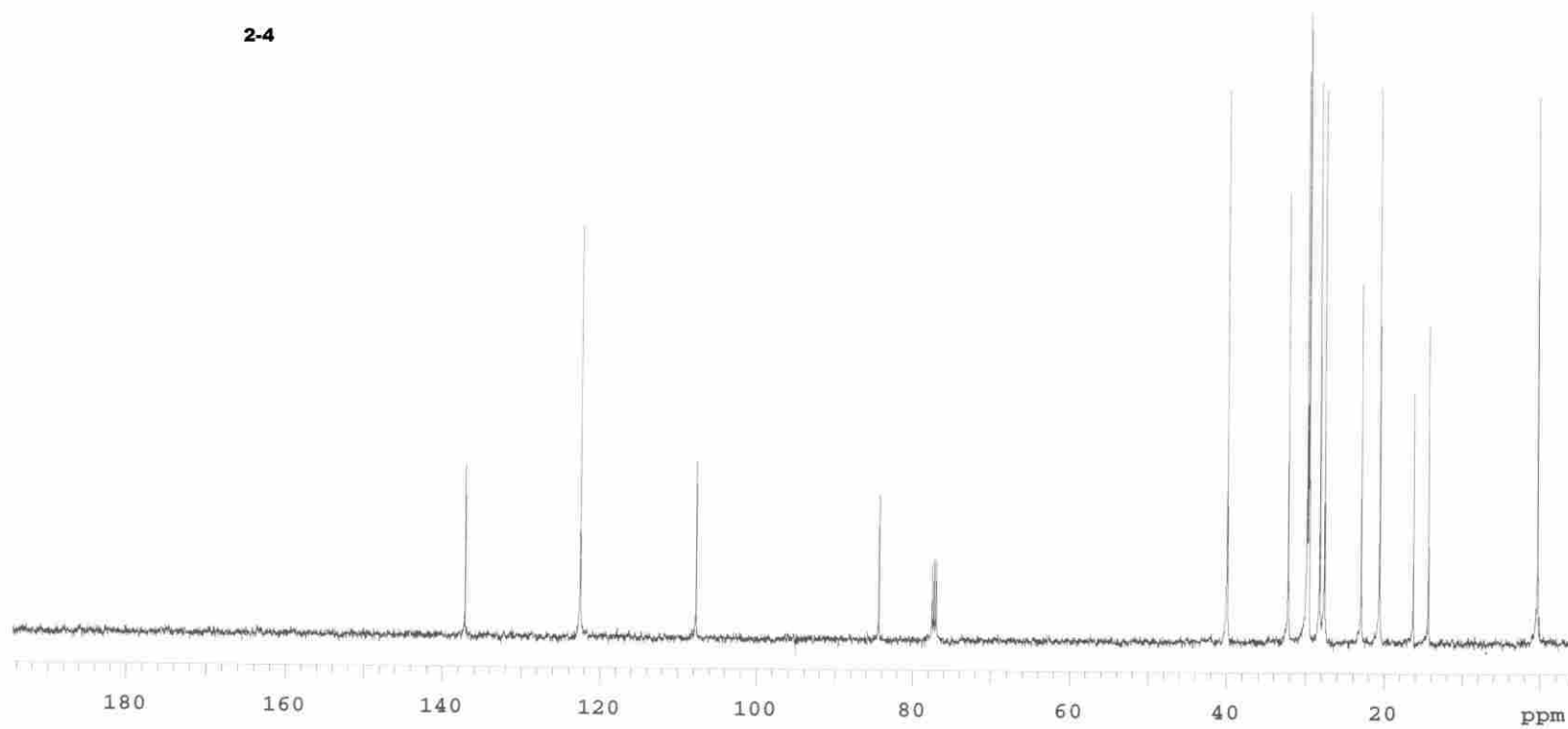


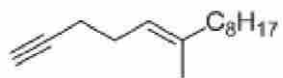
2-4



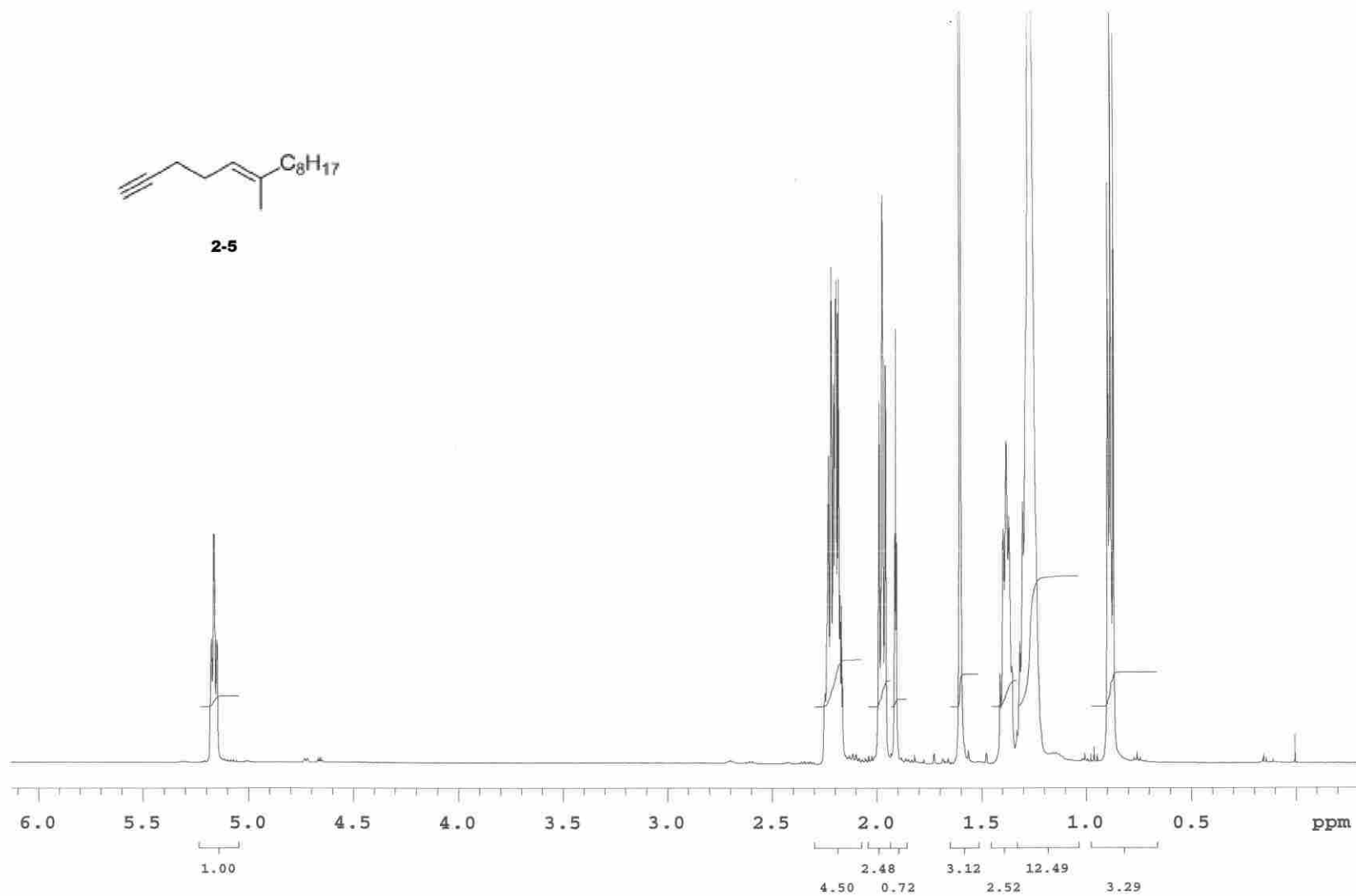


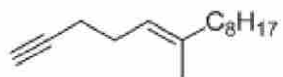
2-4



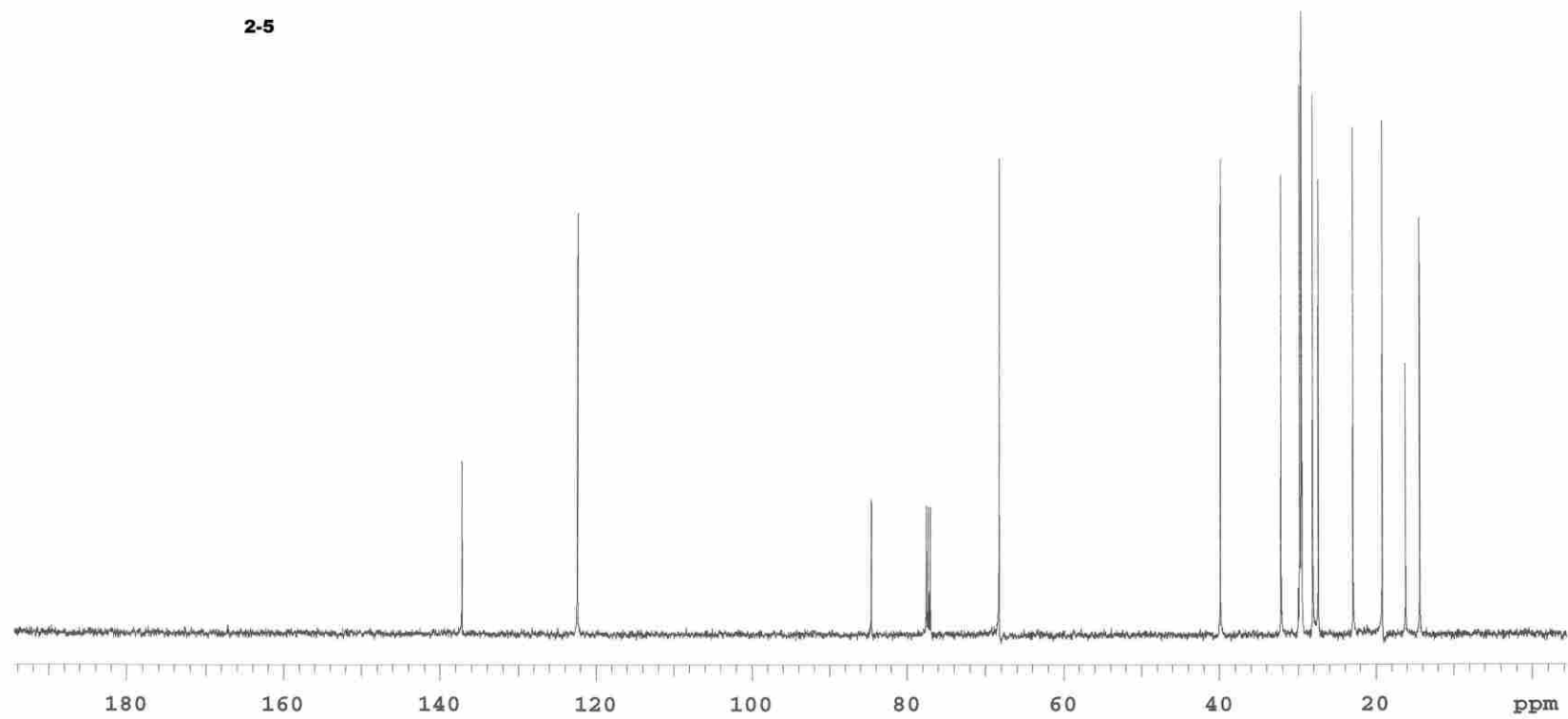


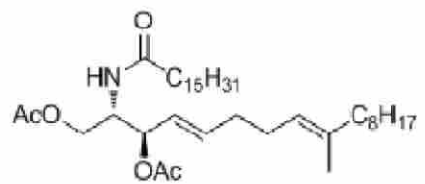
2-5



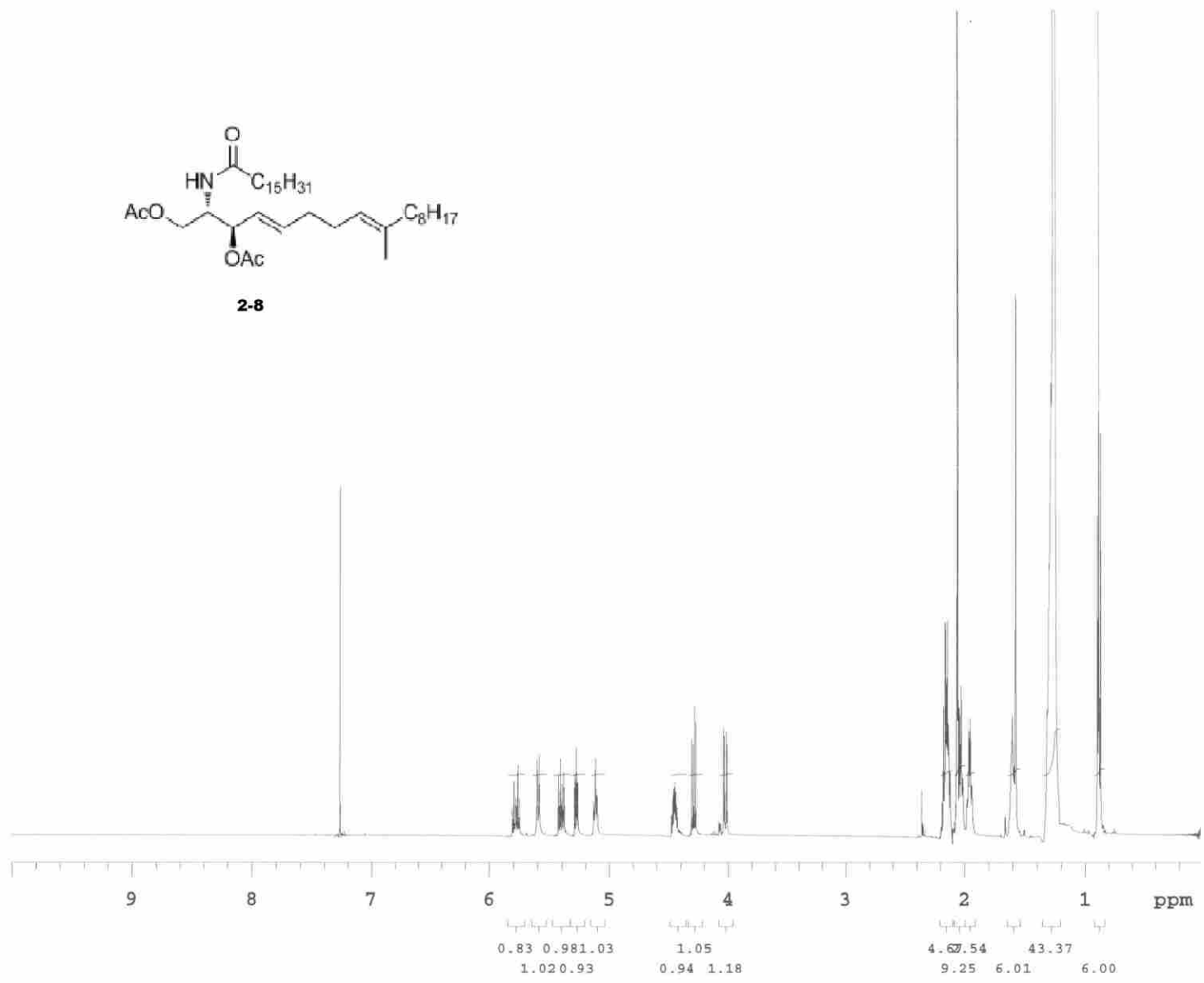


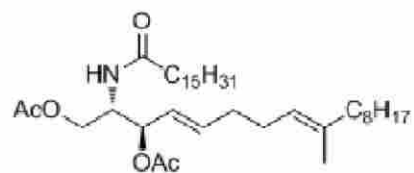
2-5



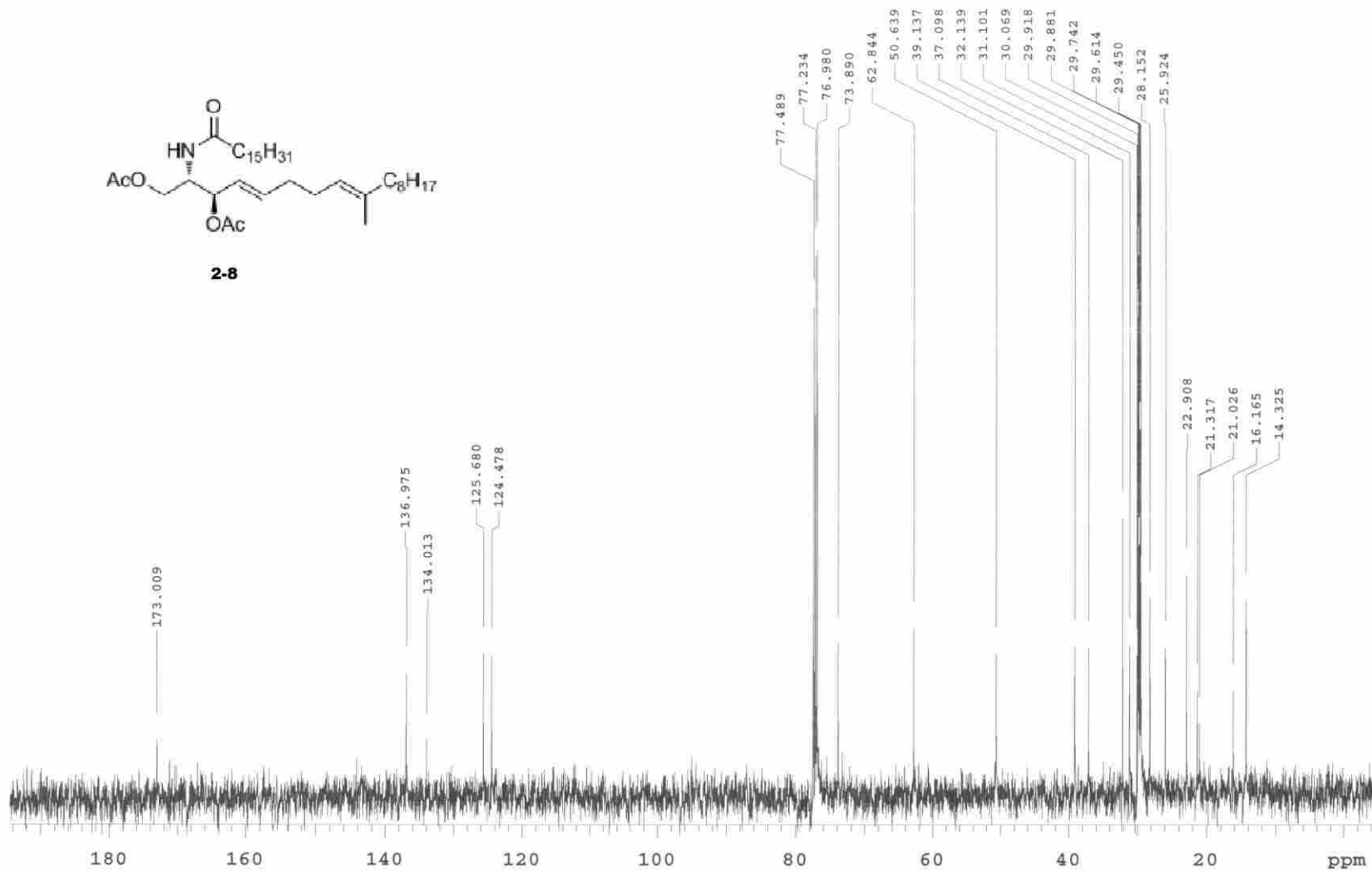


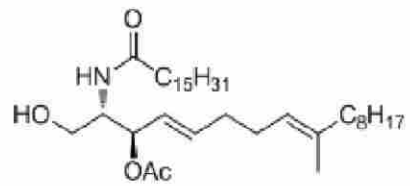
2-8



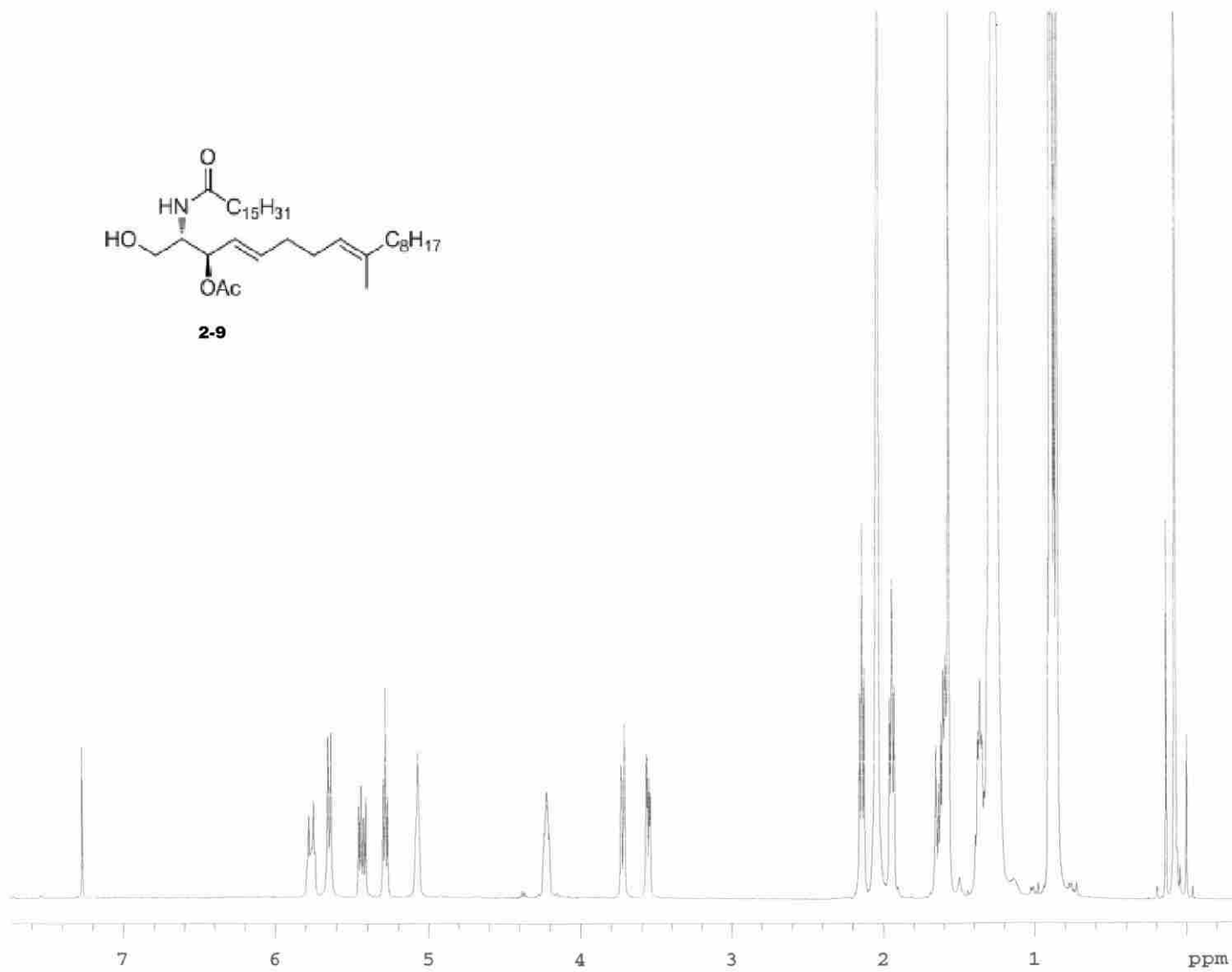


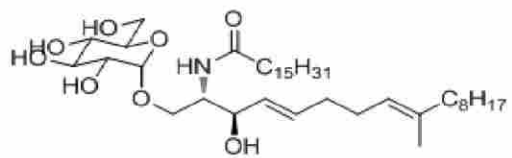
2-8



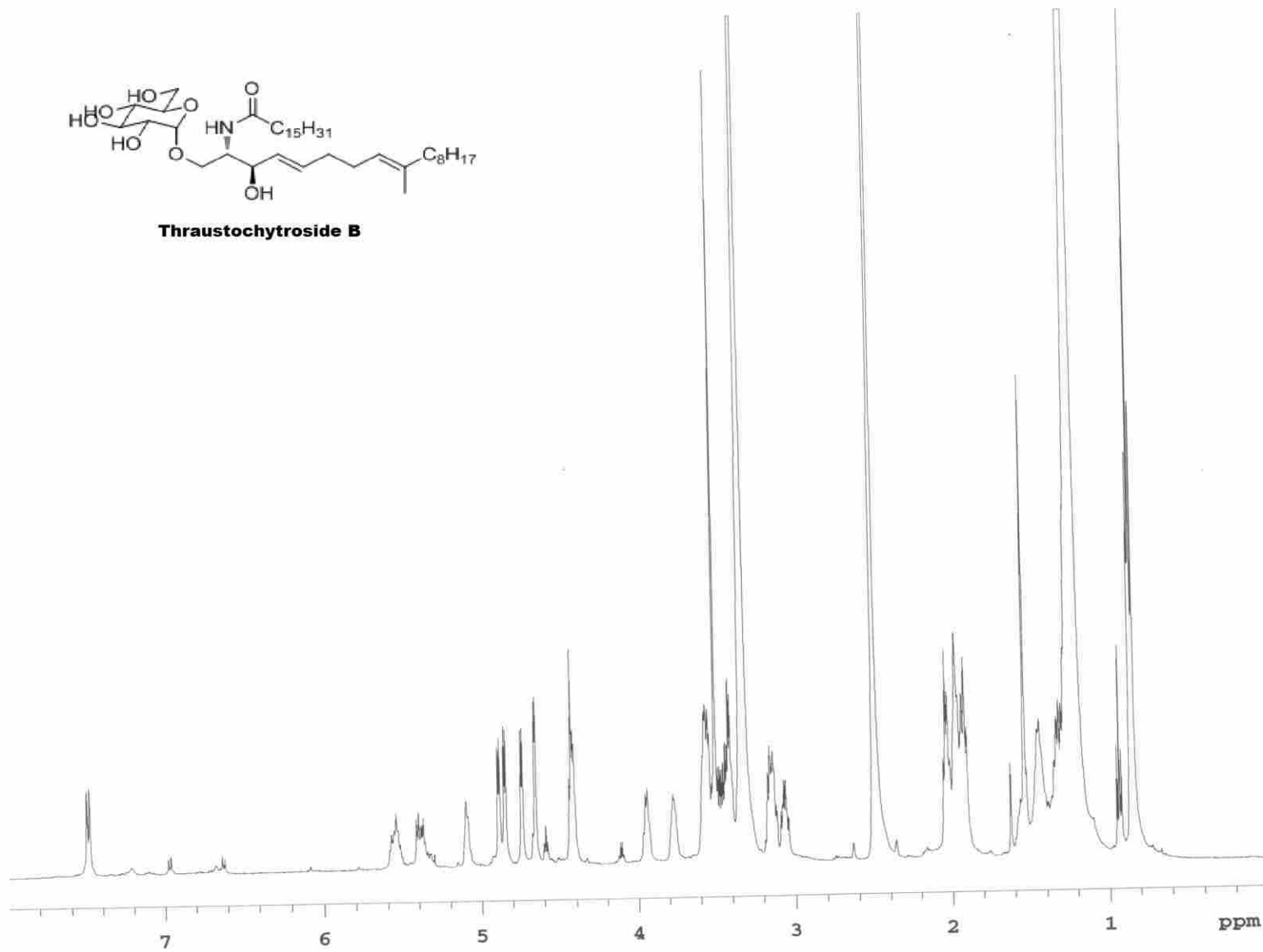


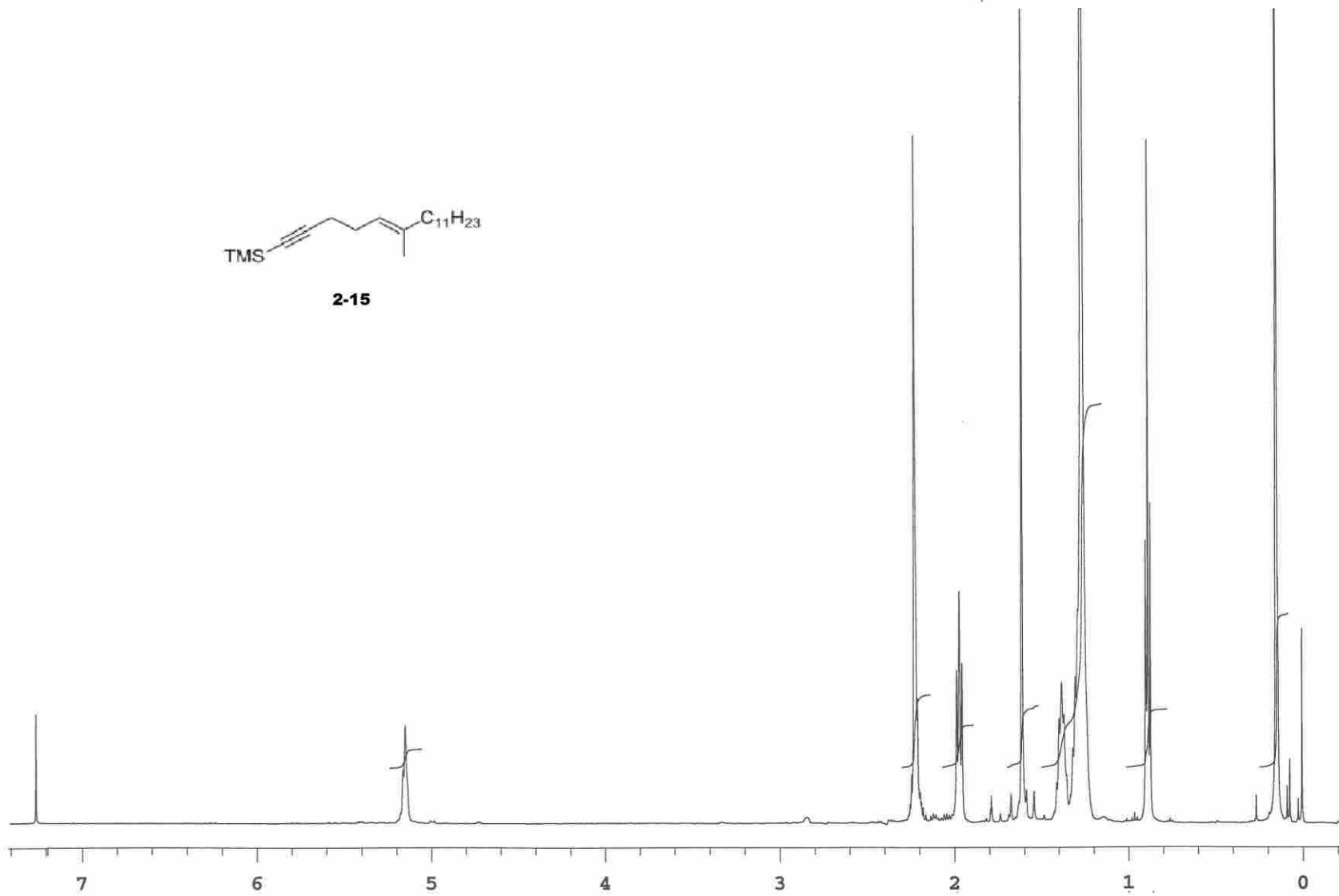
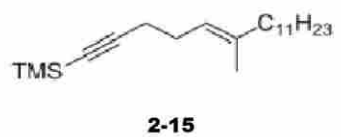
2-9

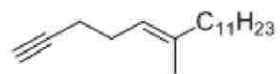




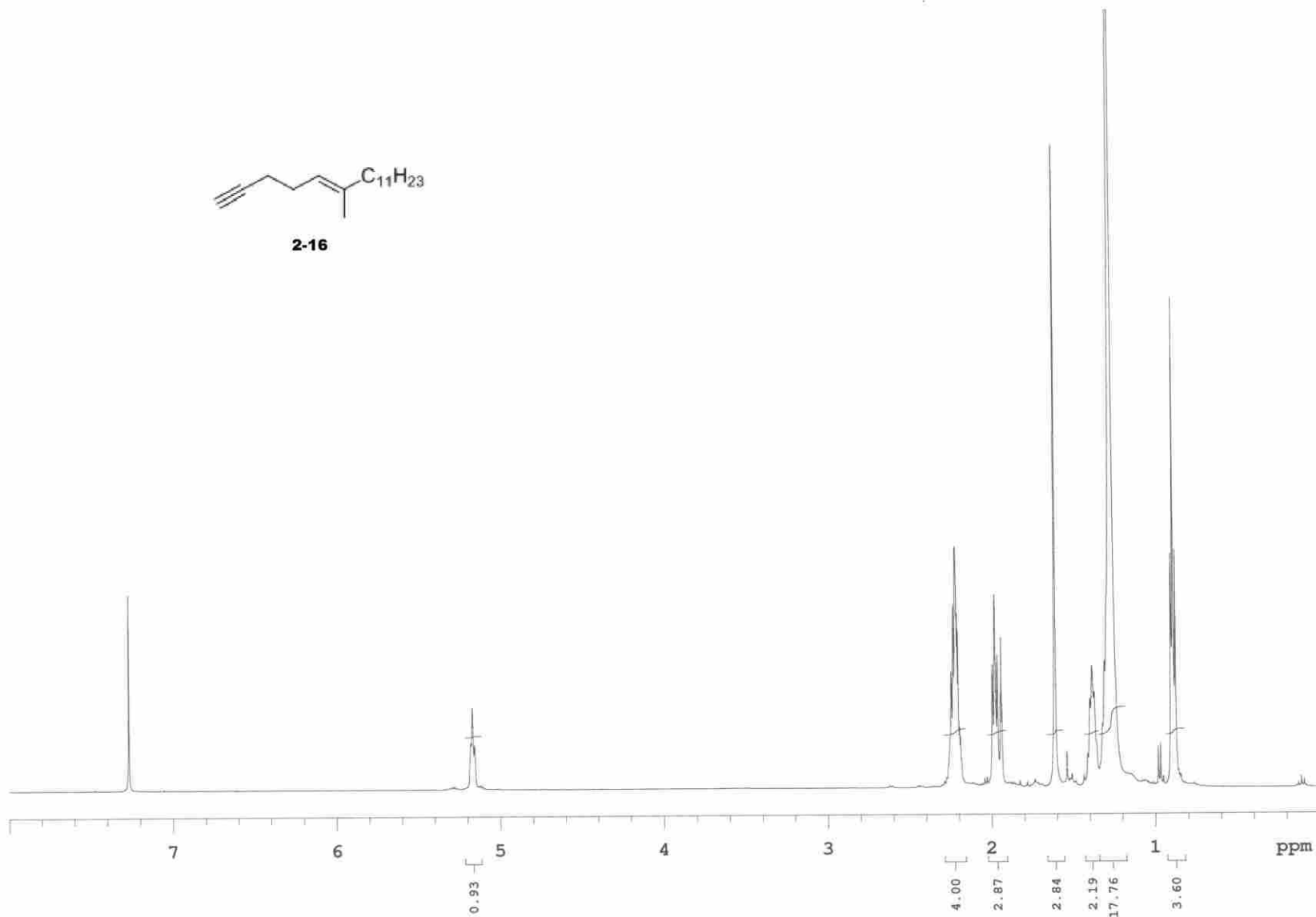
Thraustochytoside B

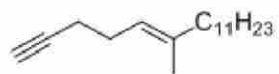




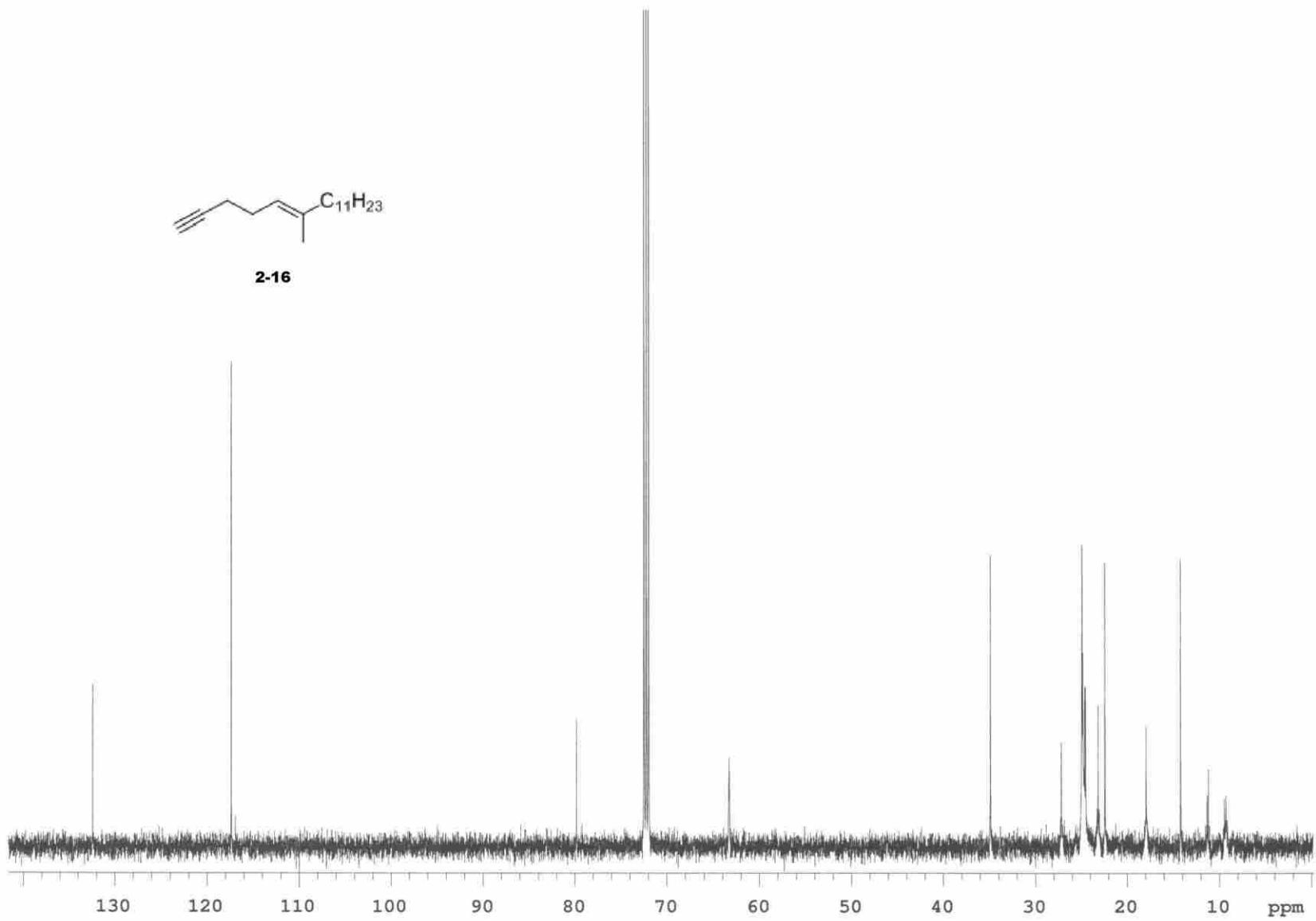


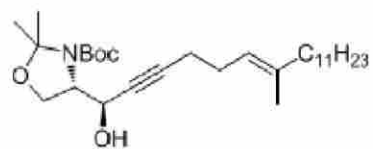
2-16



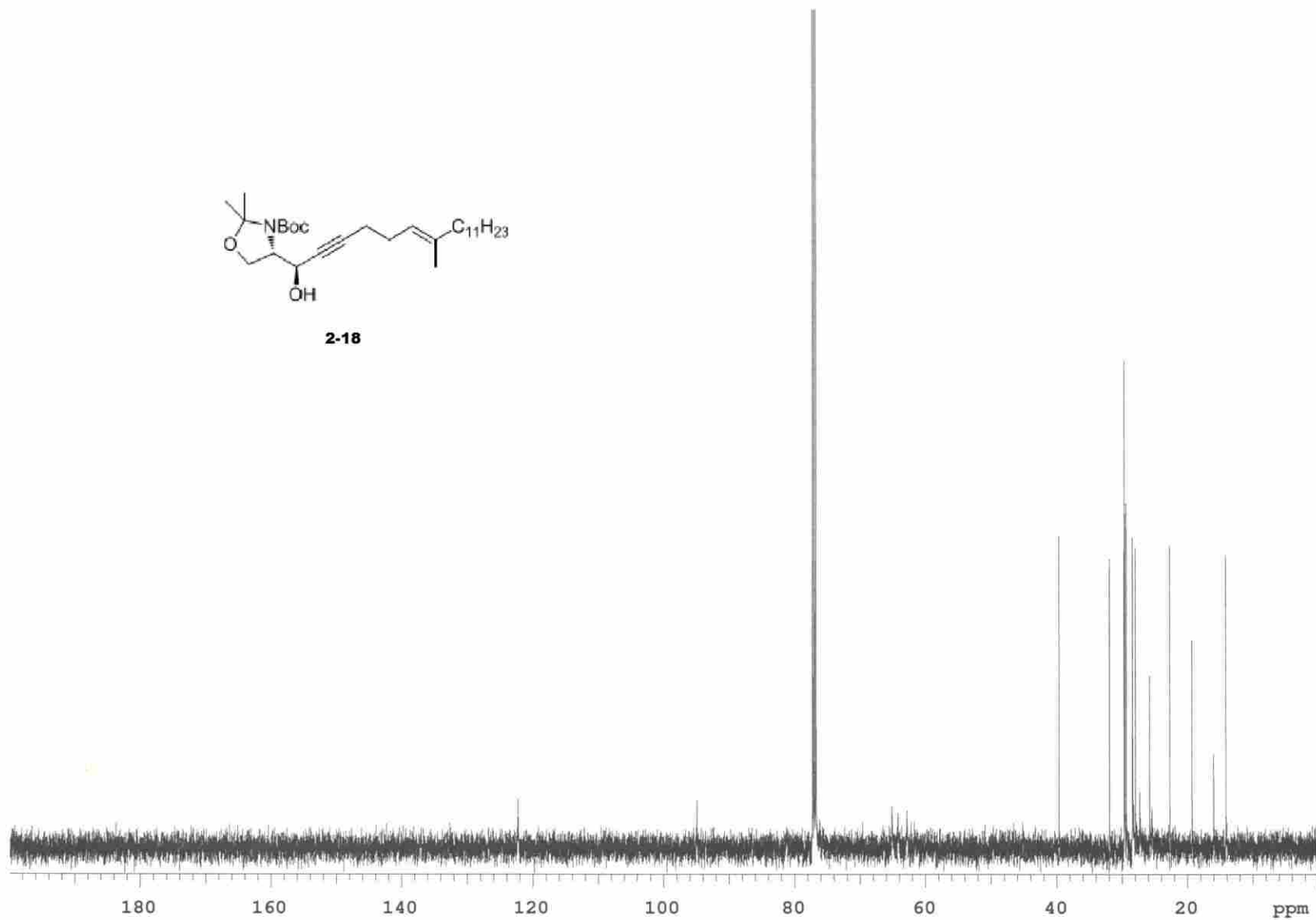


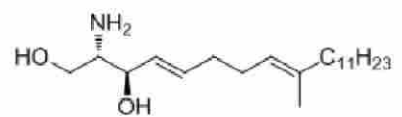
2-16



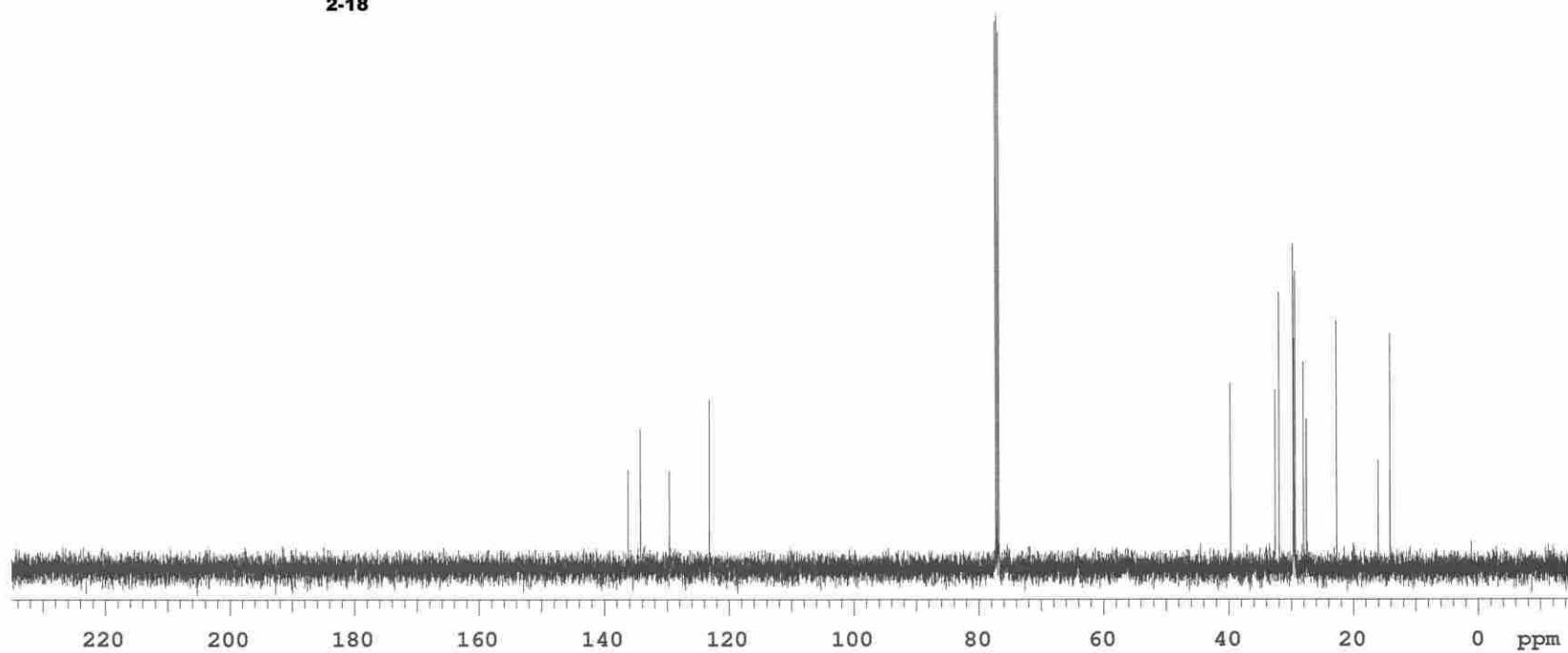


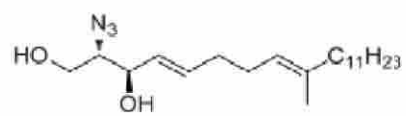
2-18



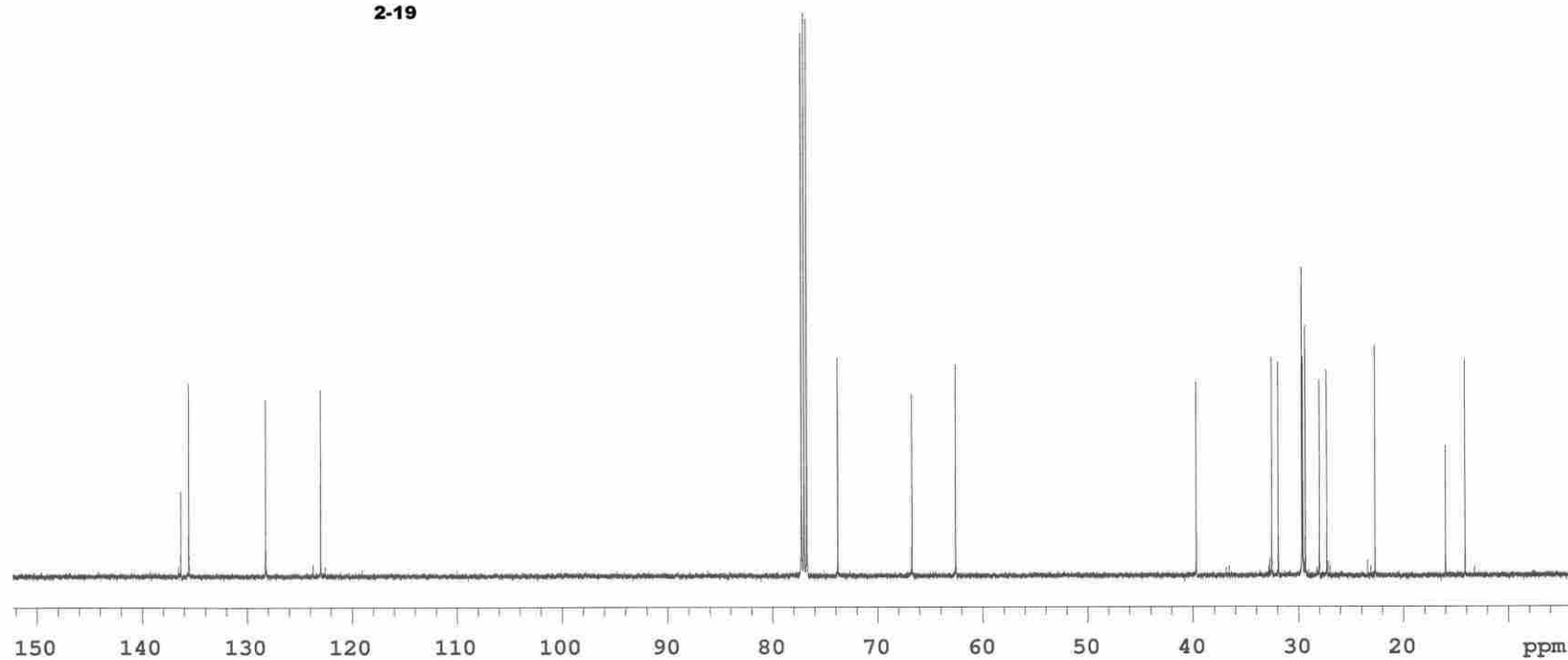


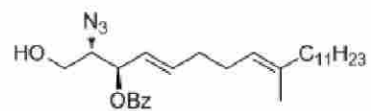
2-18



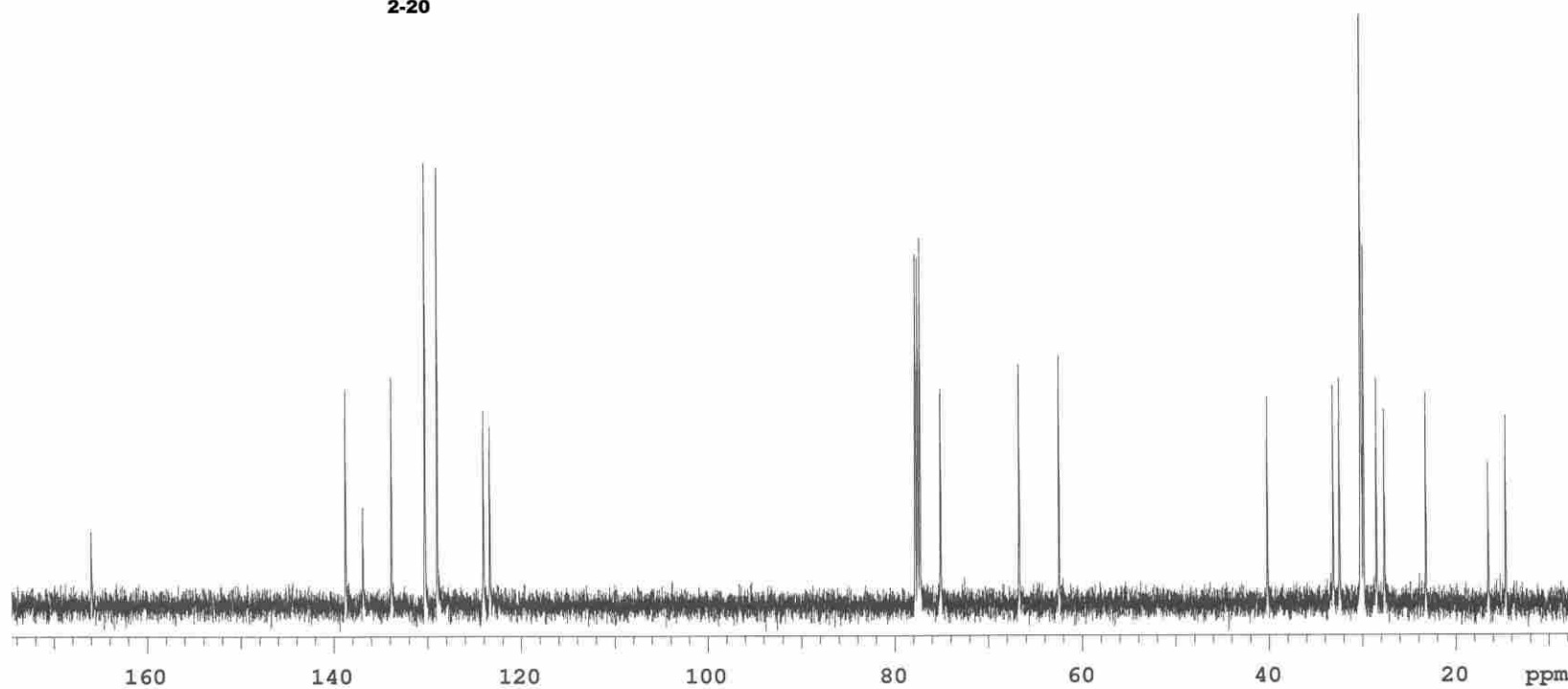


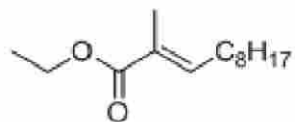
2-19



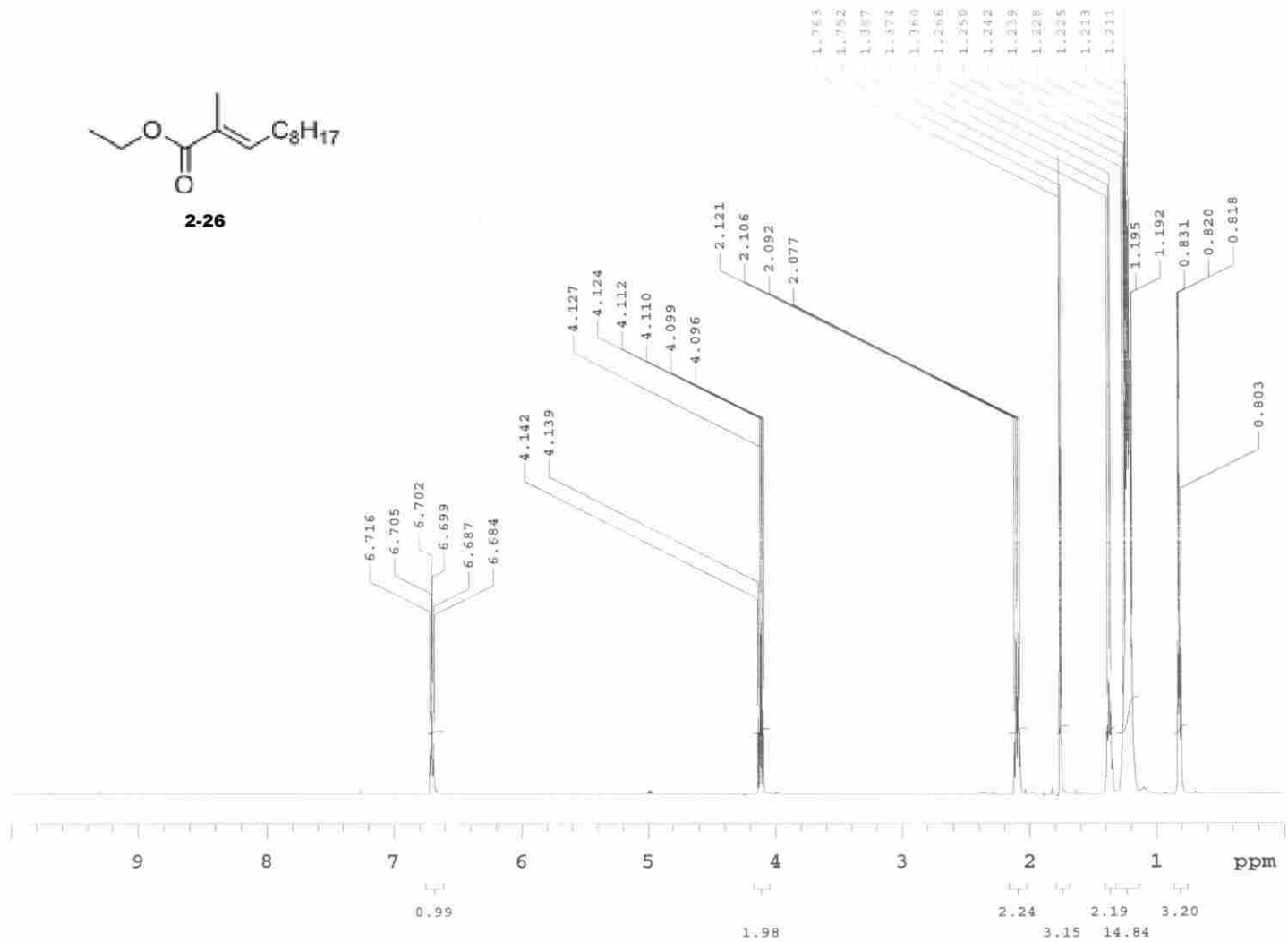


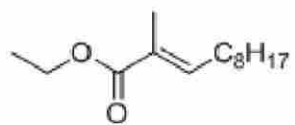
2-20



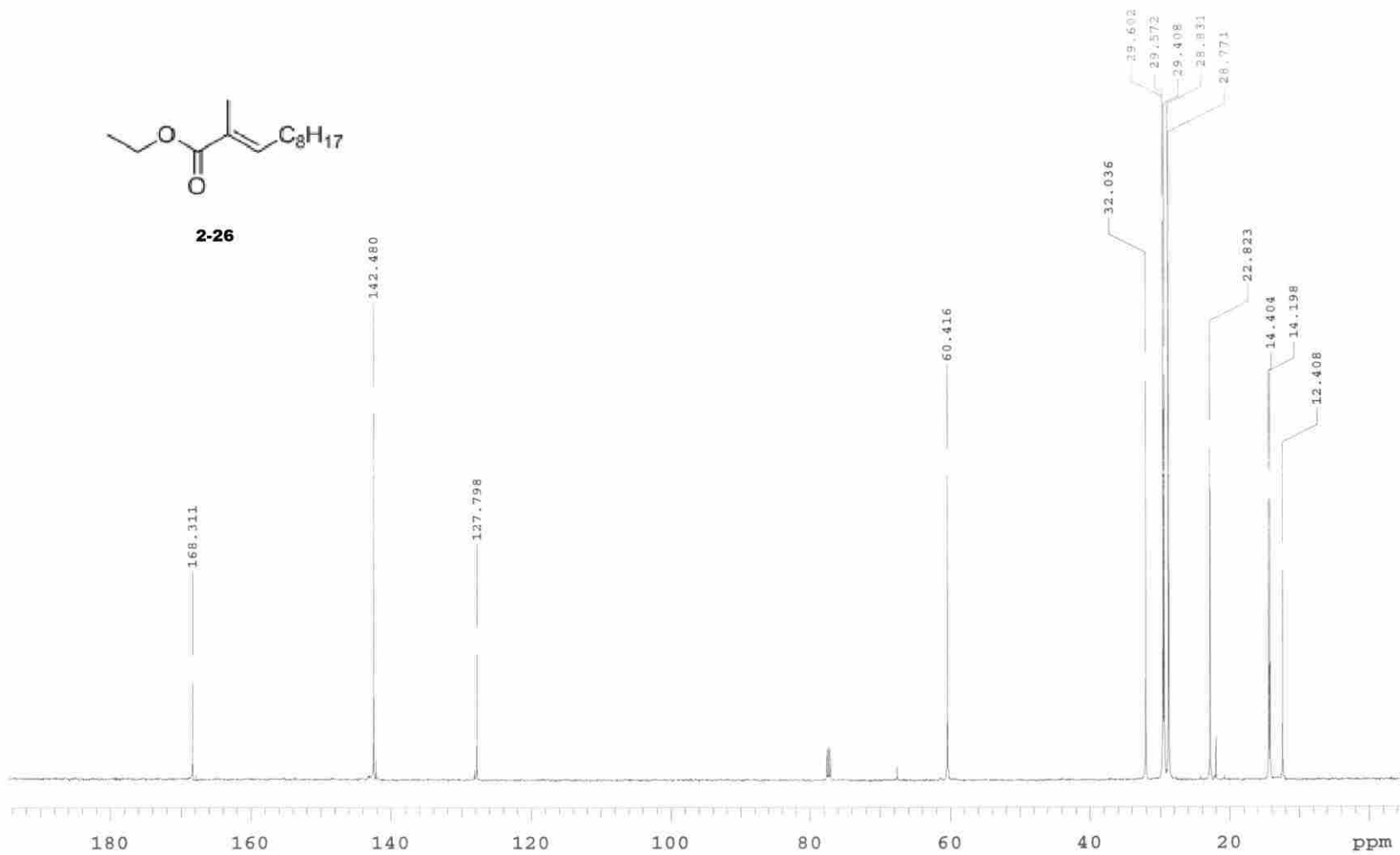


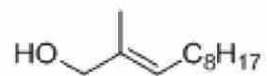
2-26



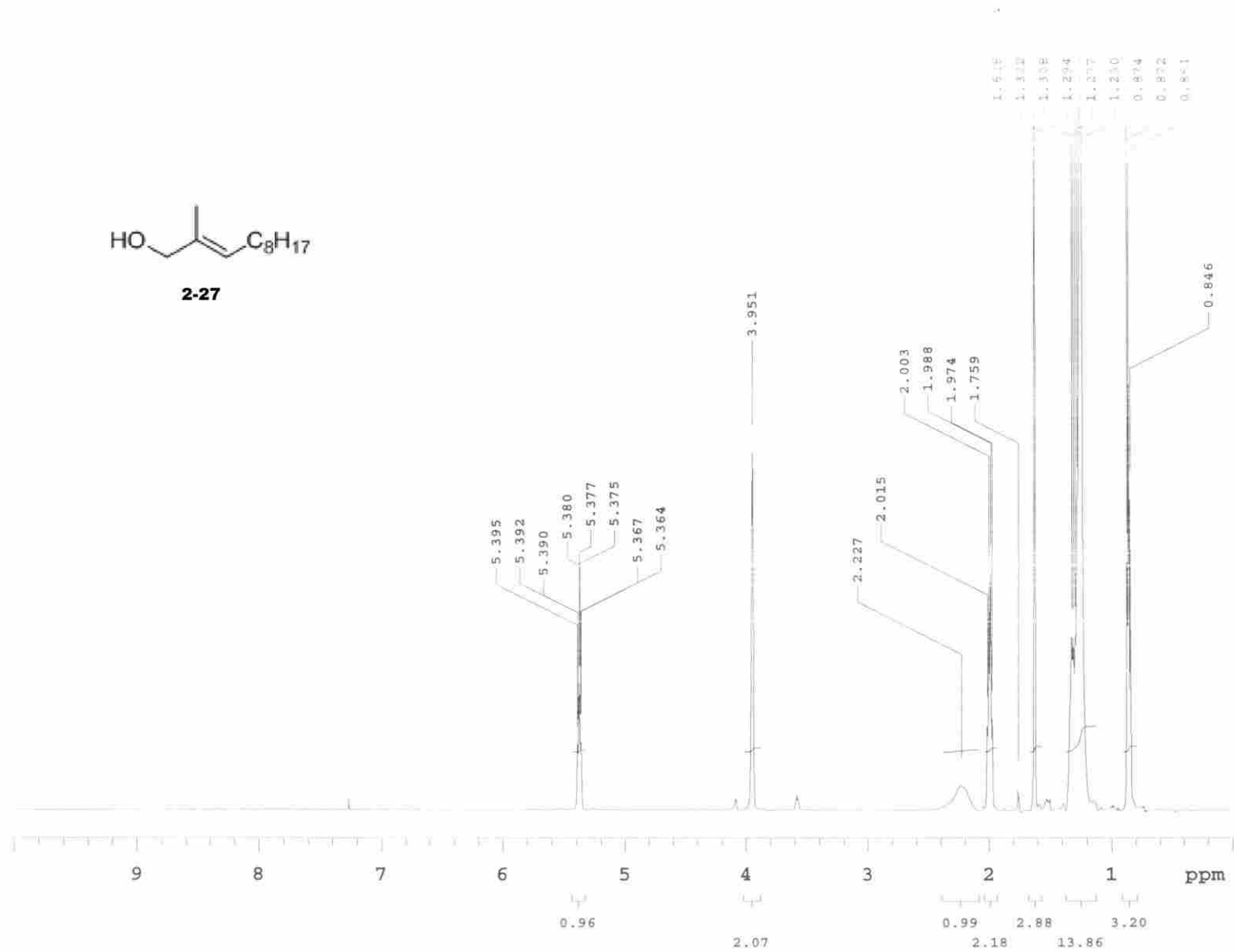


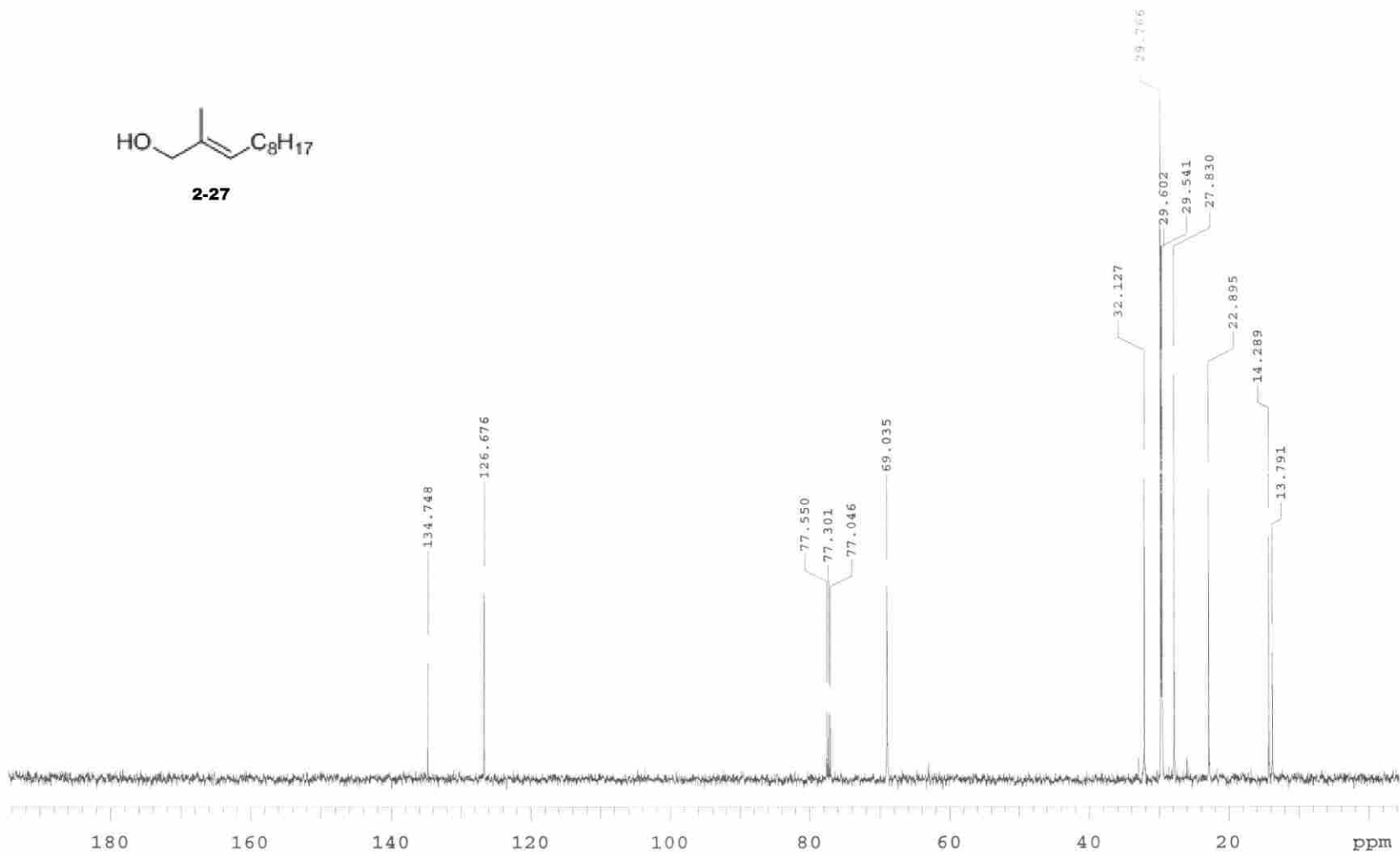
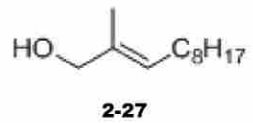
2-26

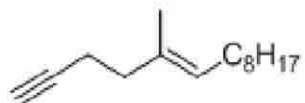




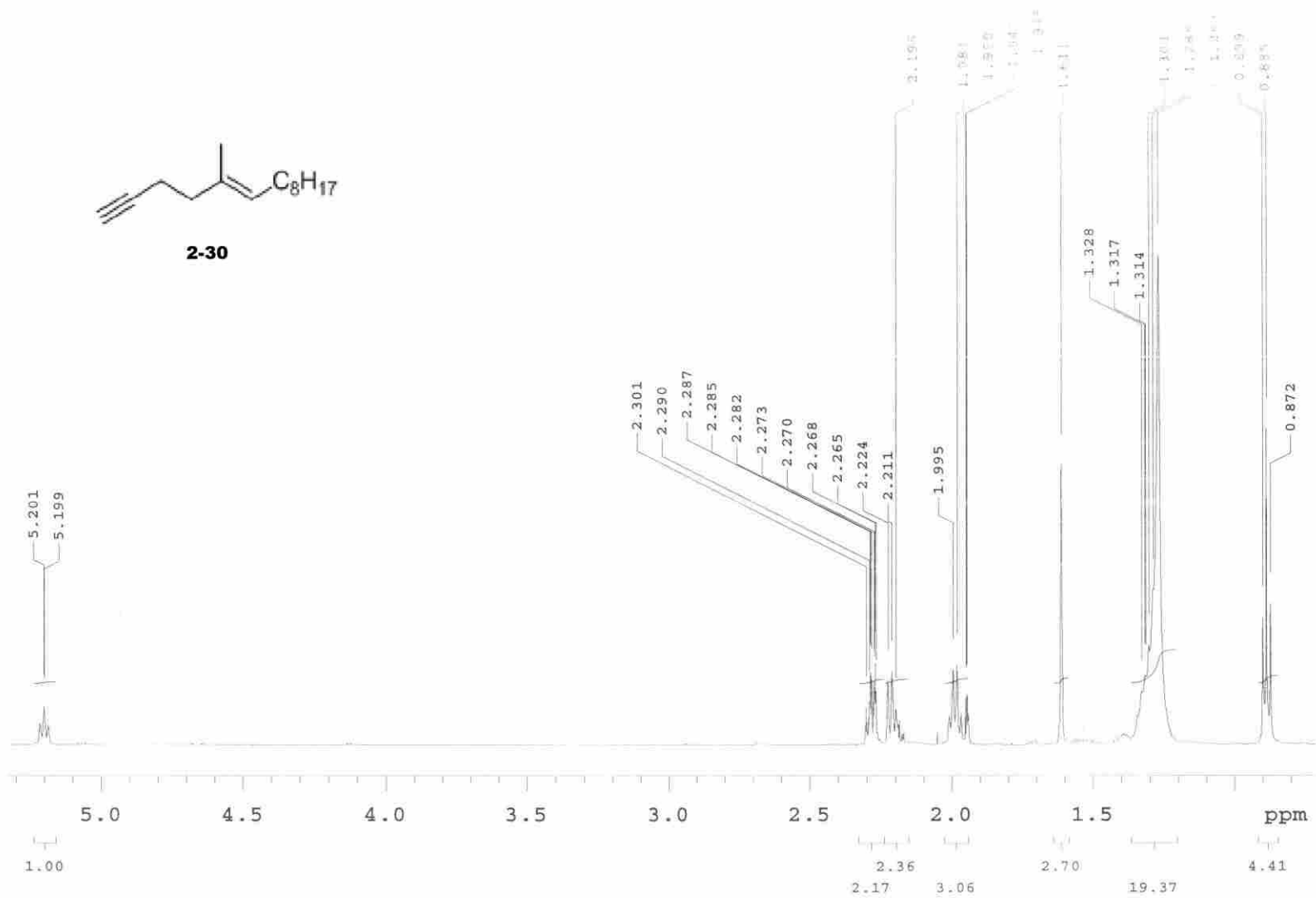
2-27

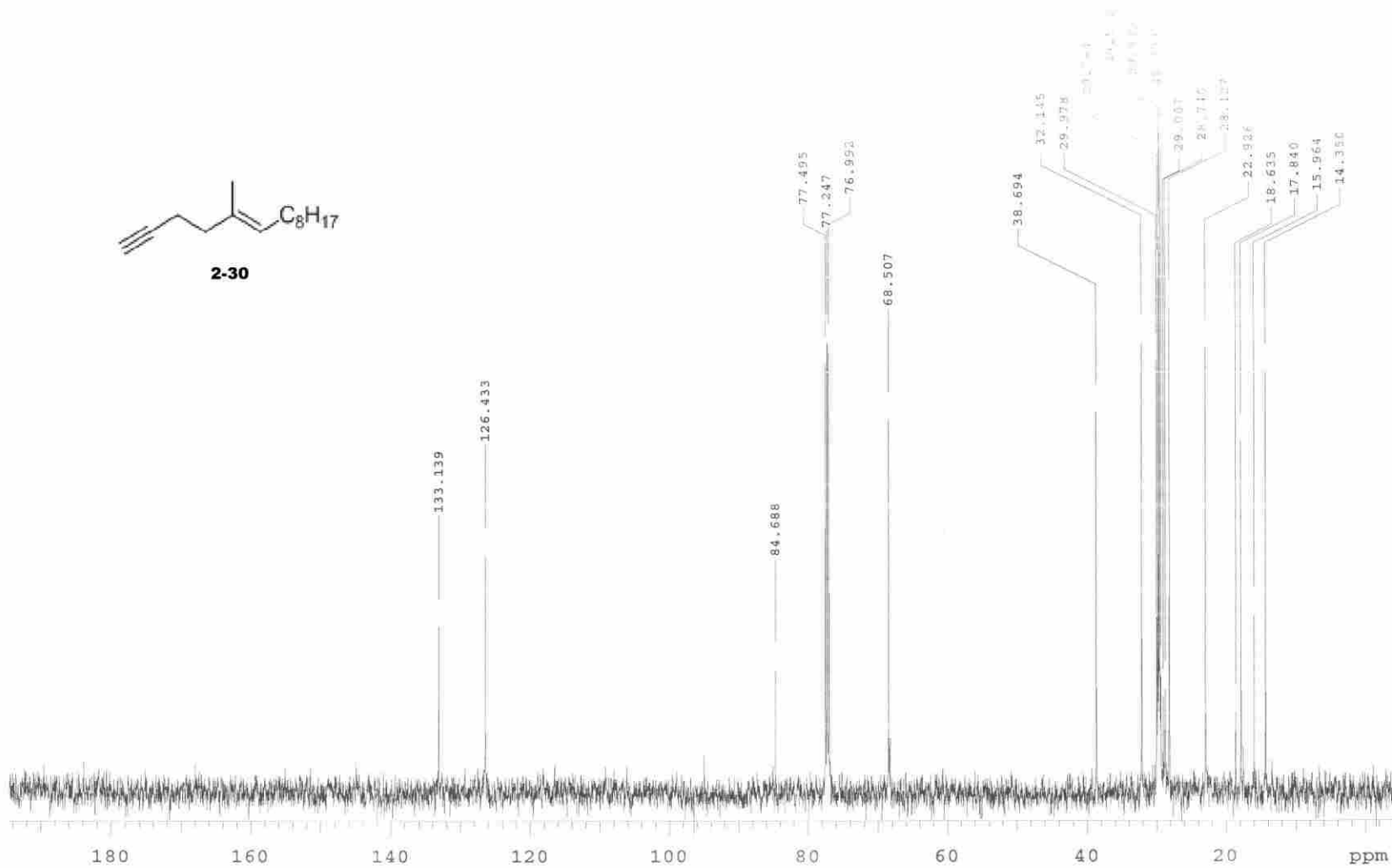
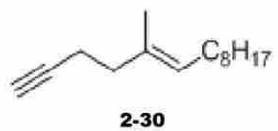


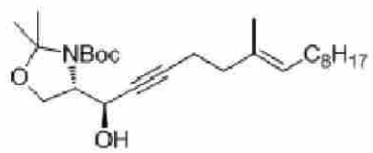




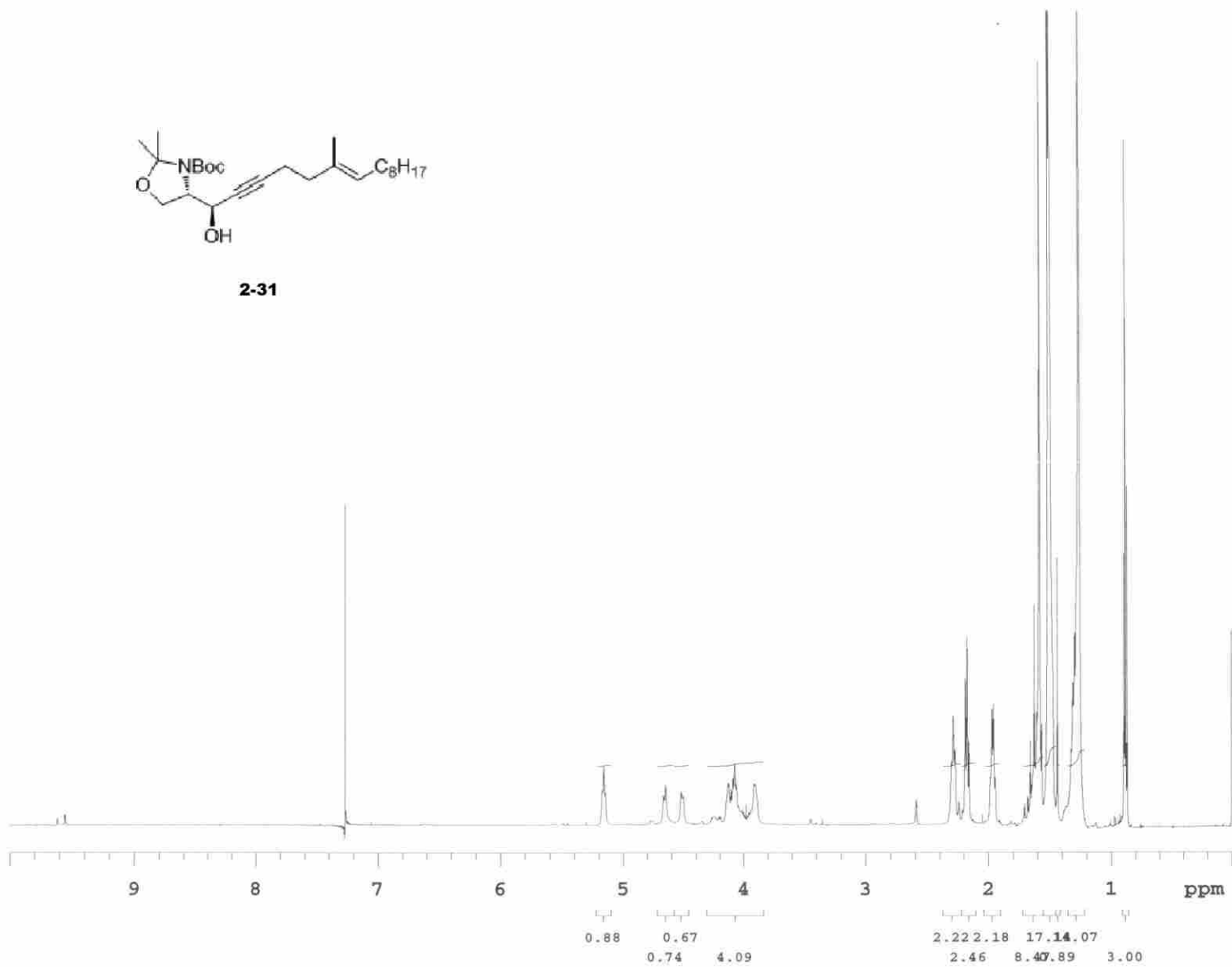
2-30

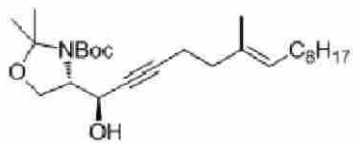




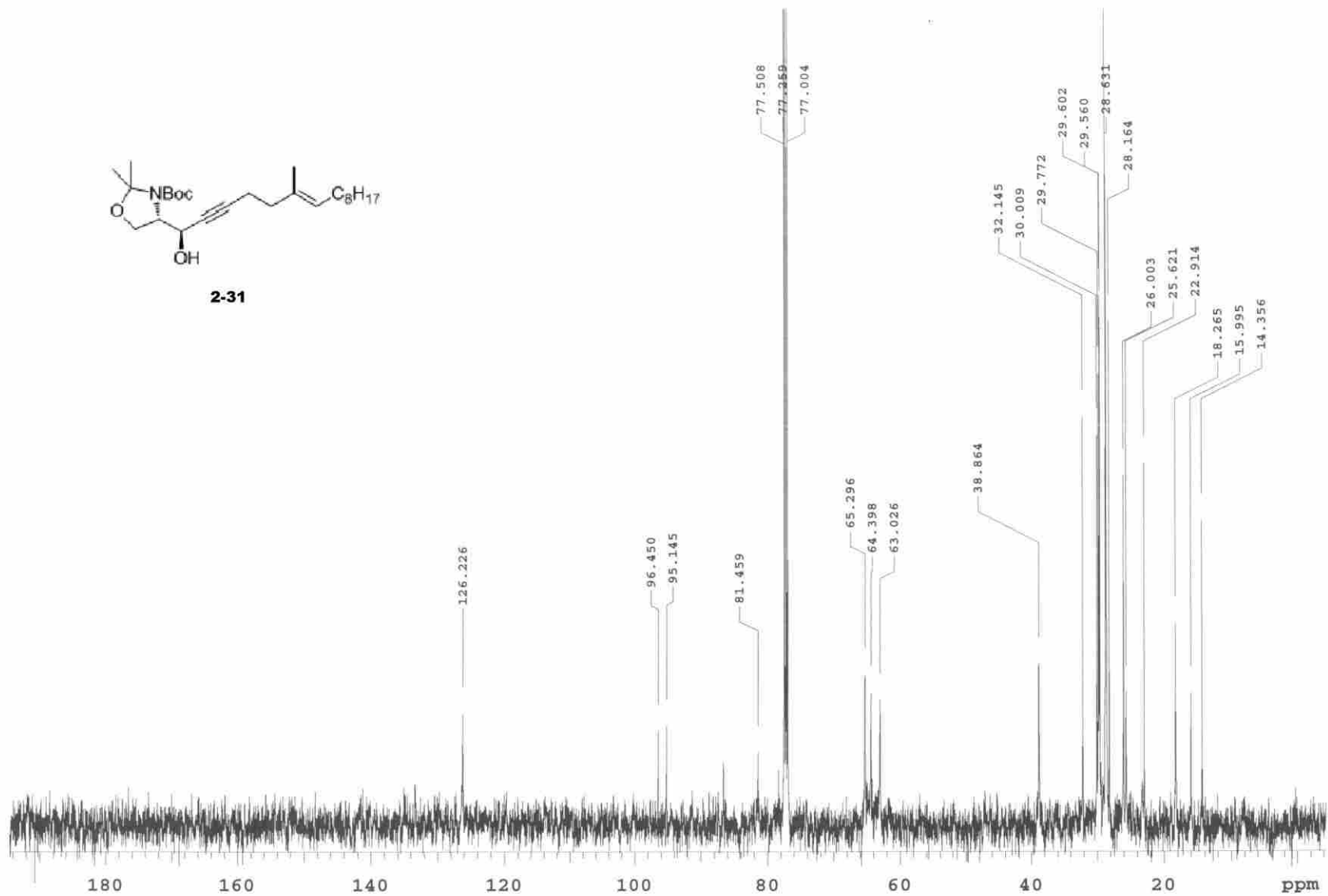


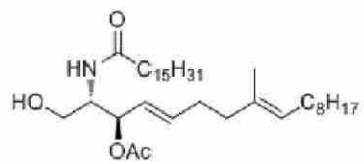
2-31



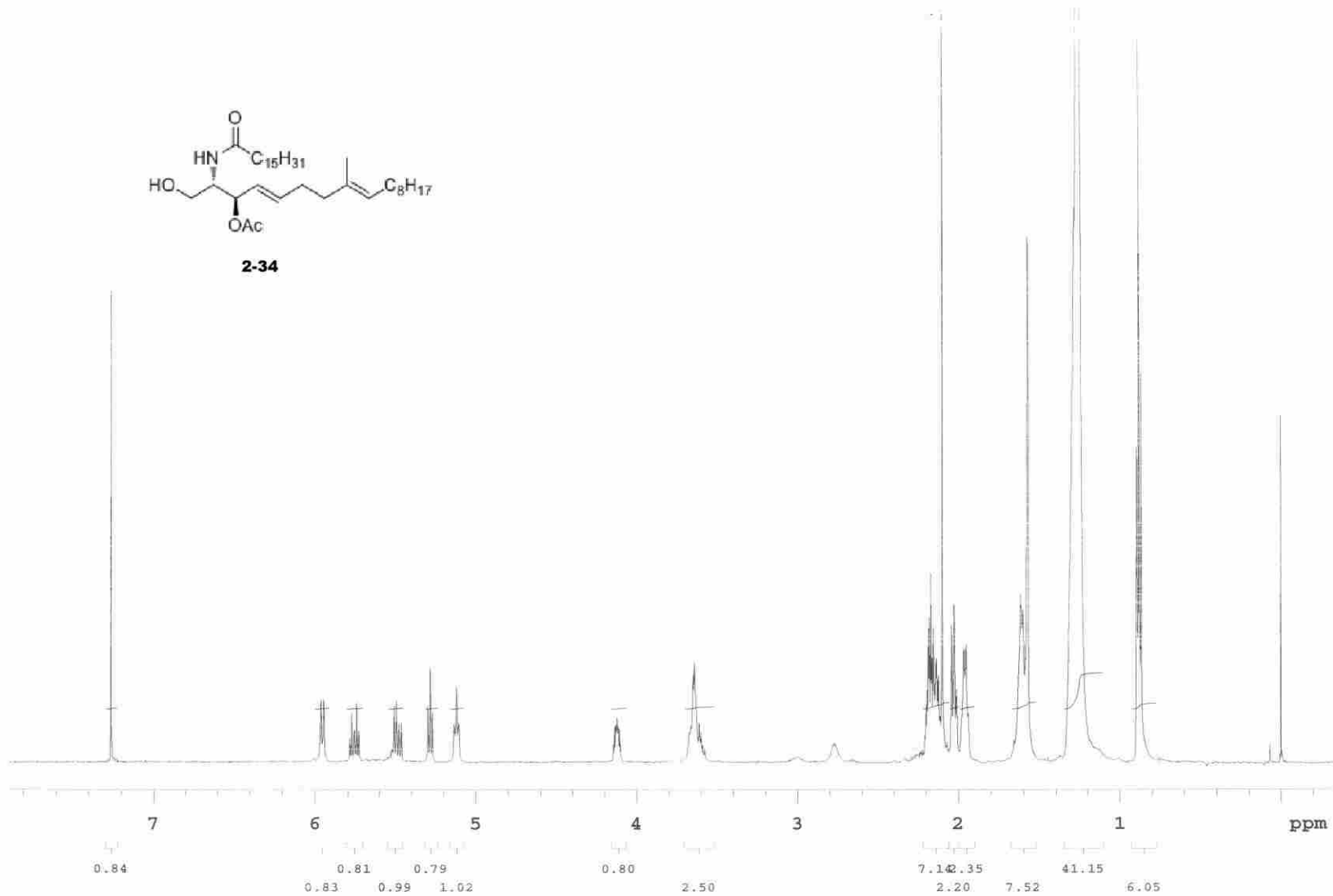


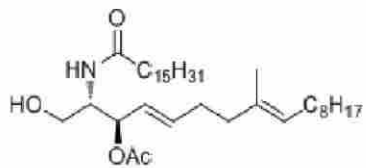
2-31



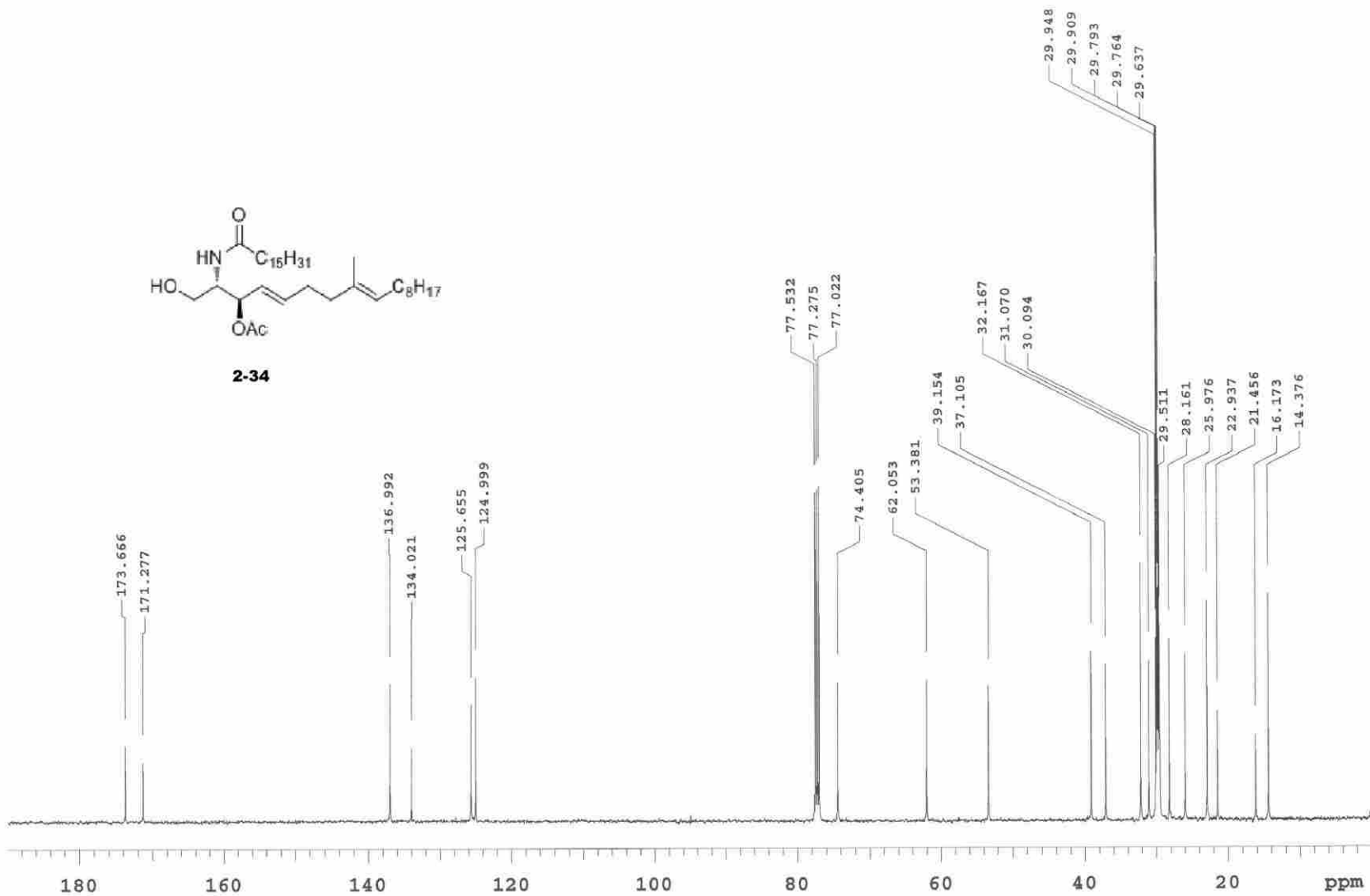


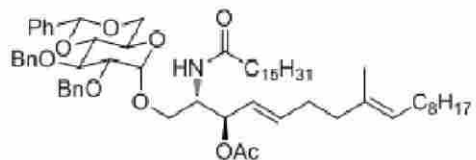
2-34



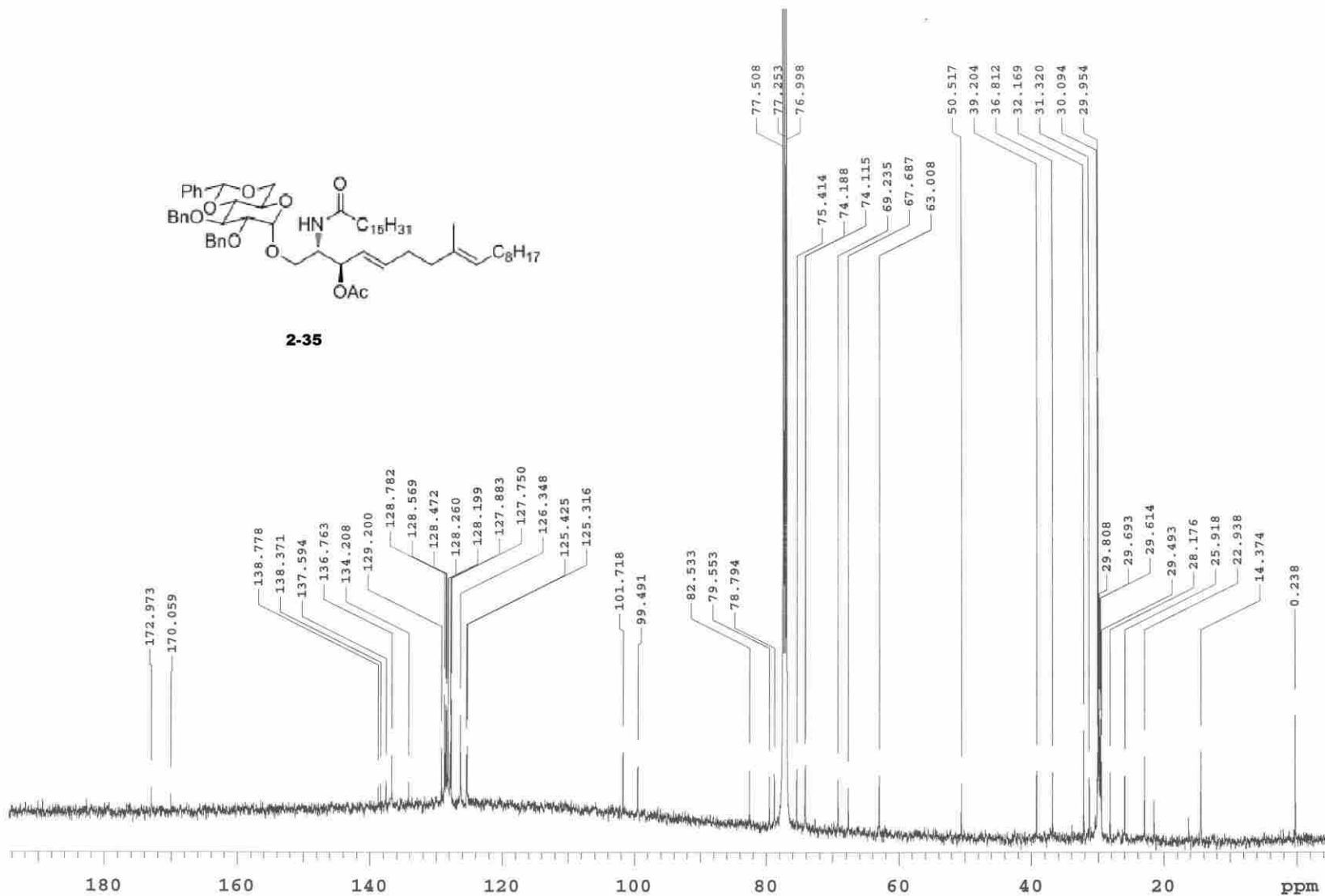


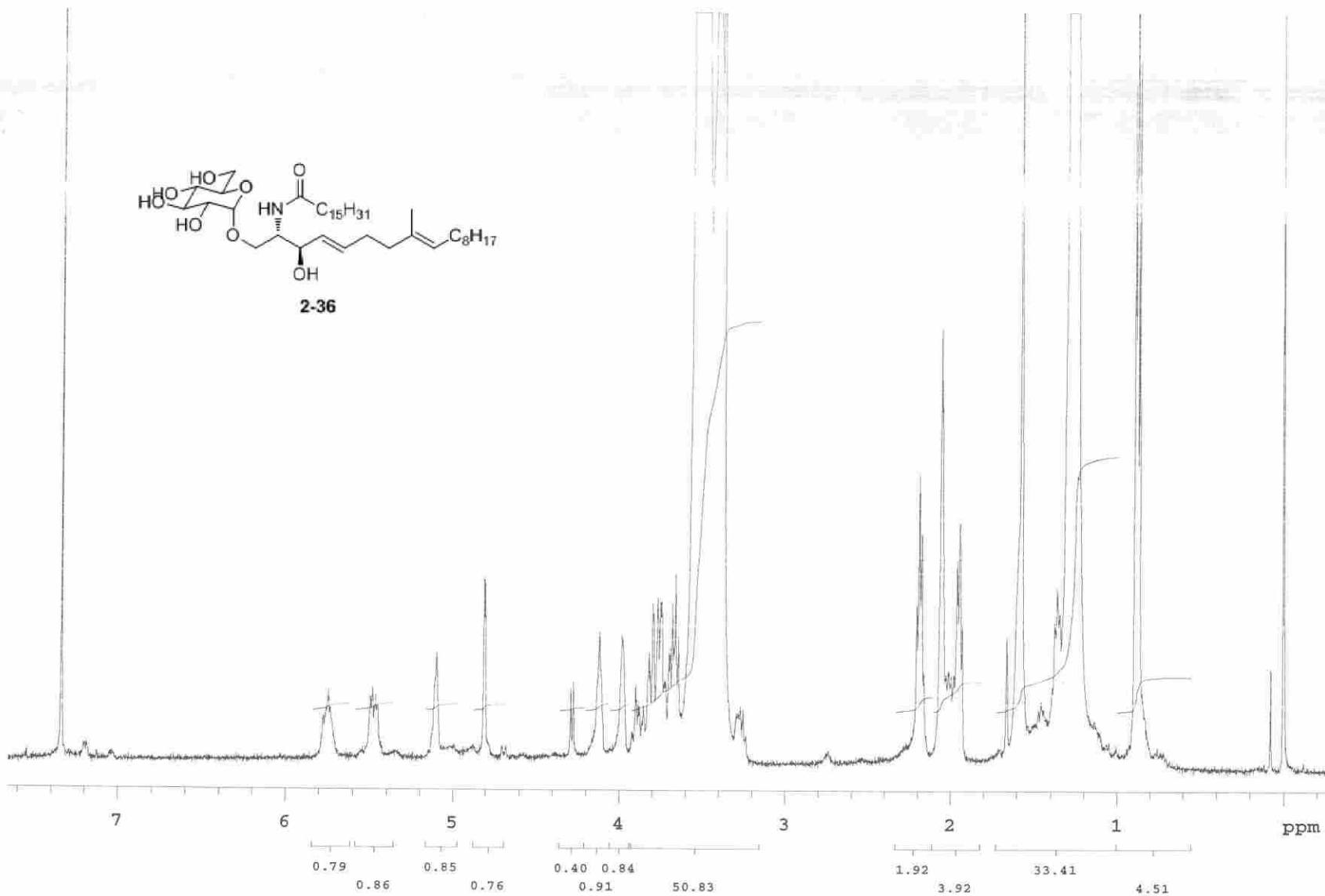
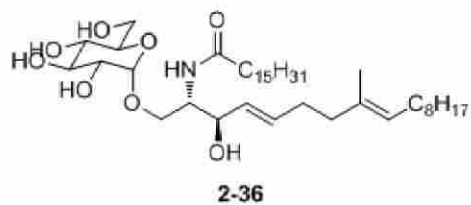
2-34

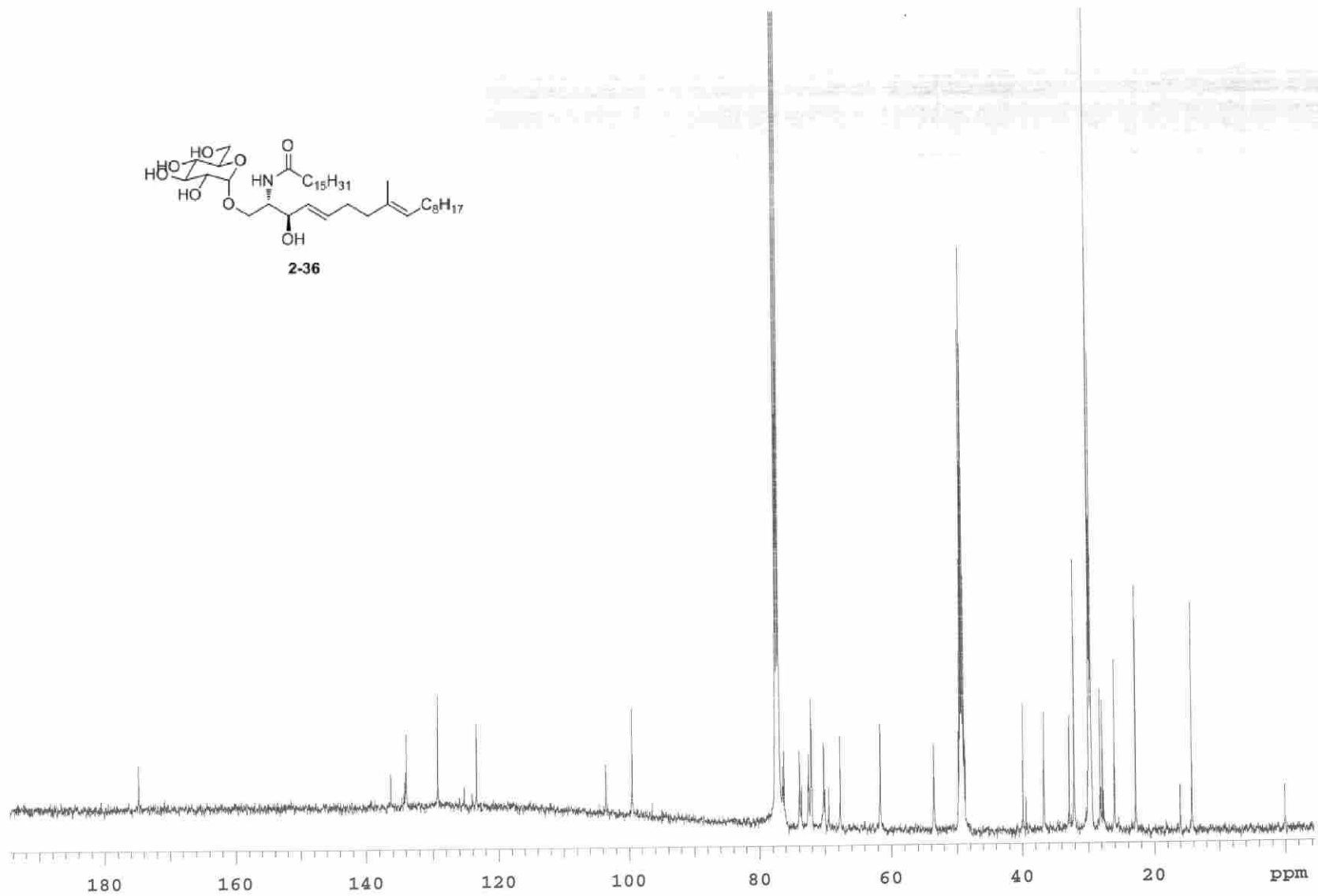
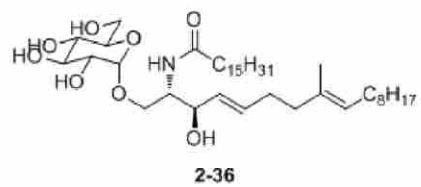


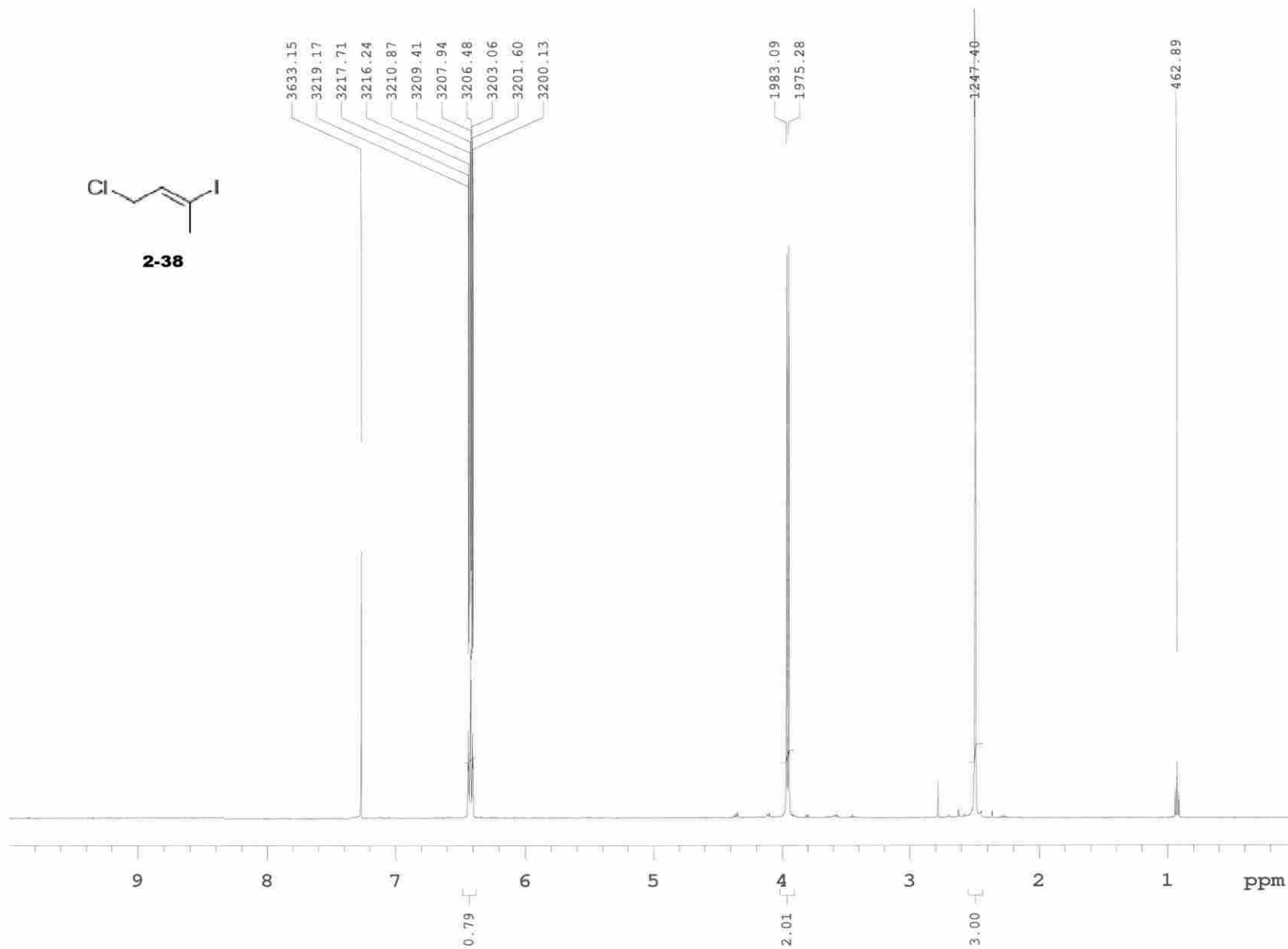
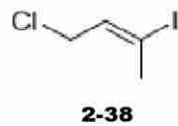


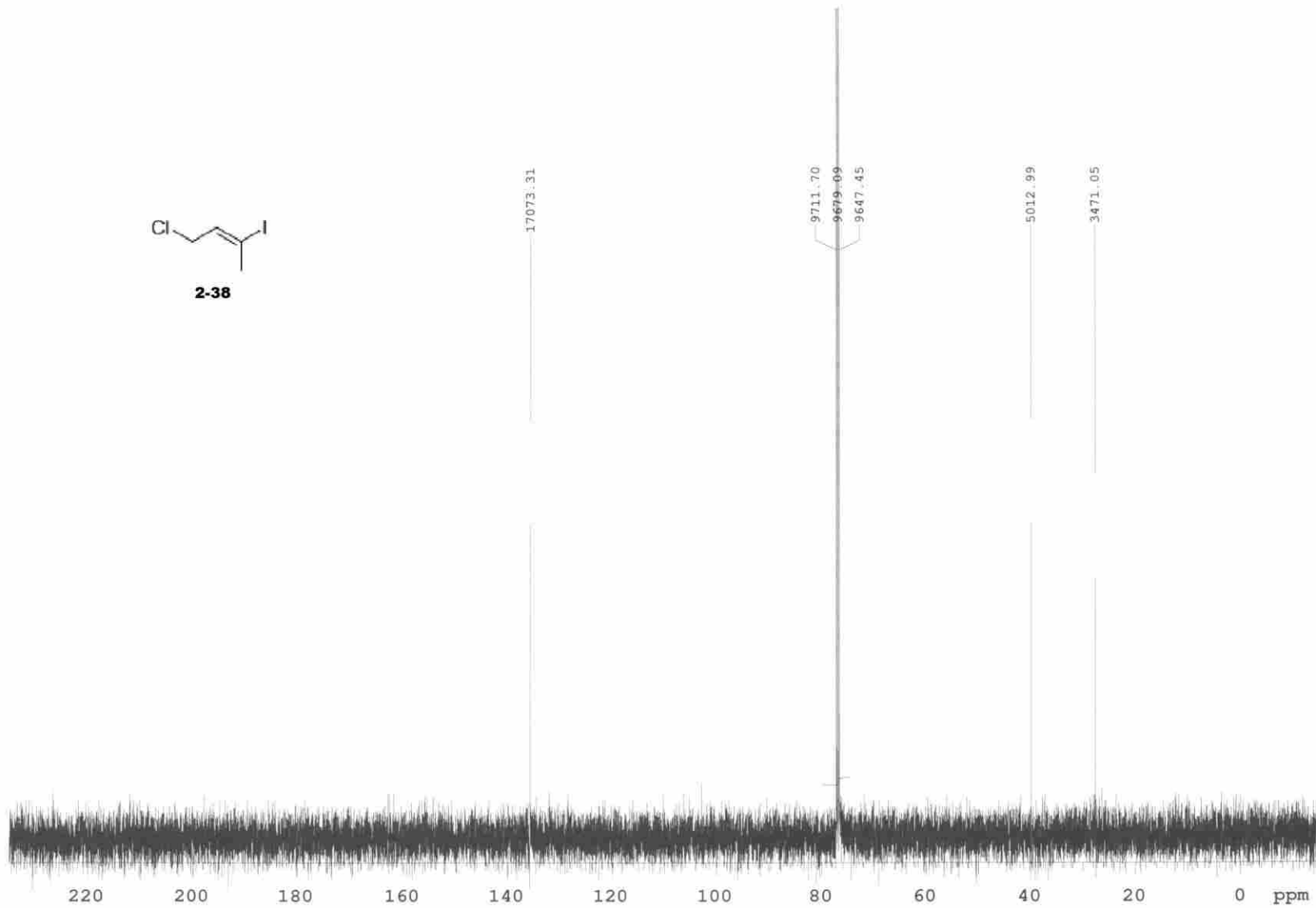
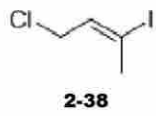
2-35

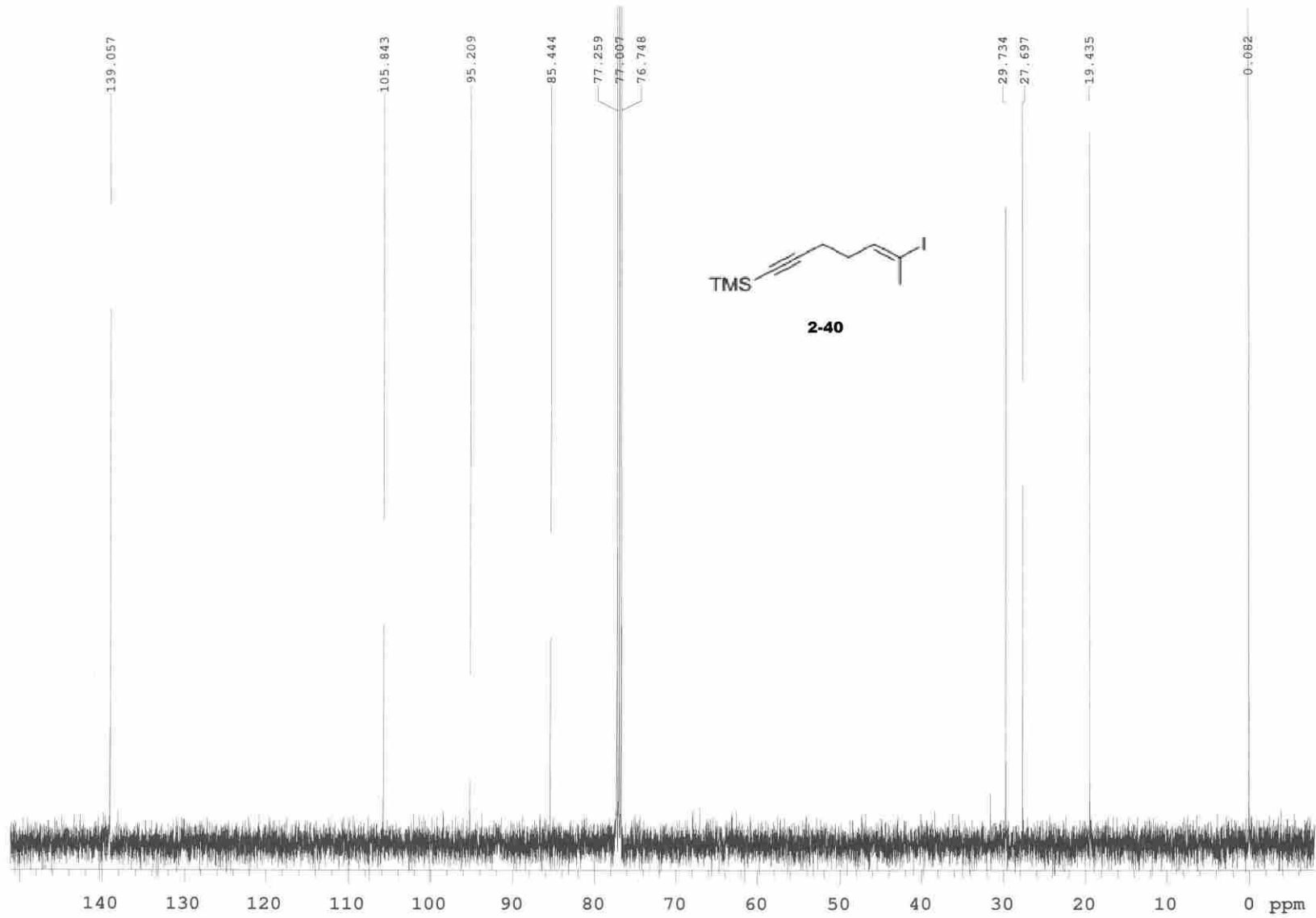


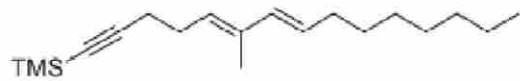




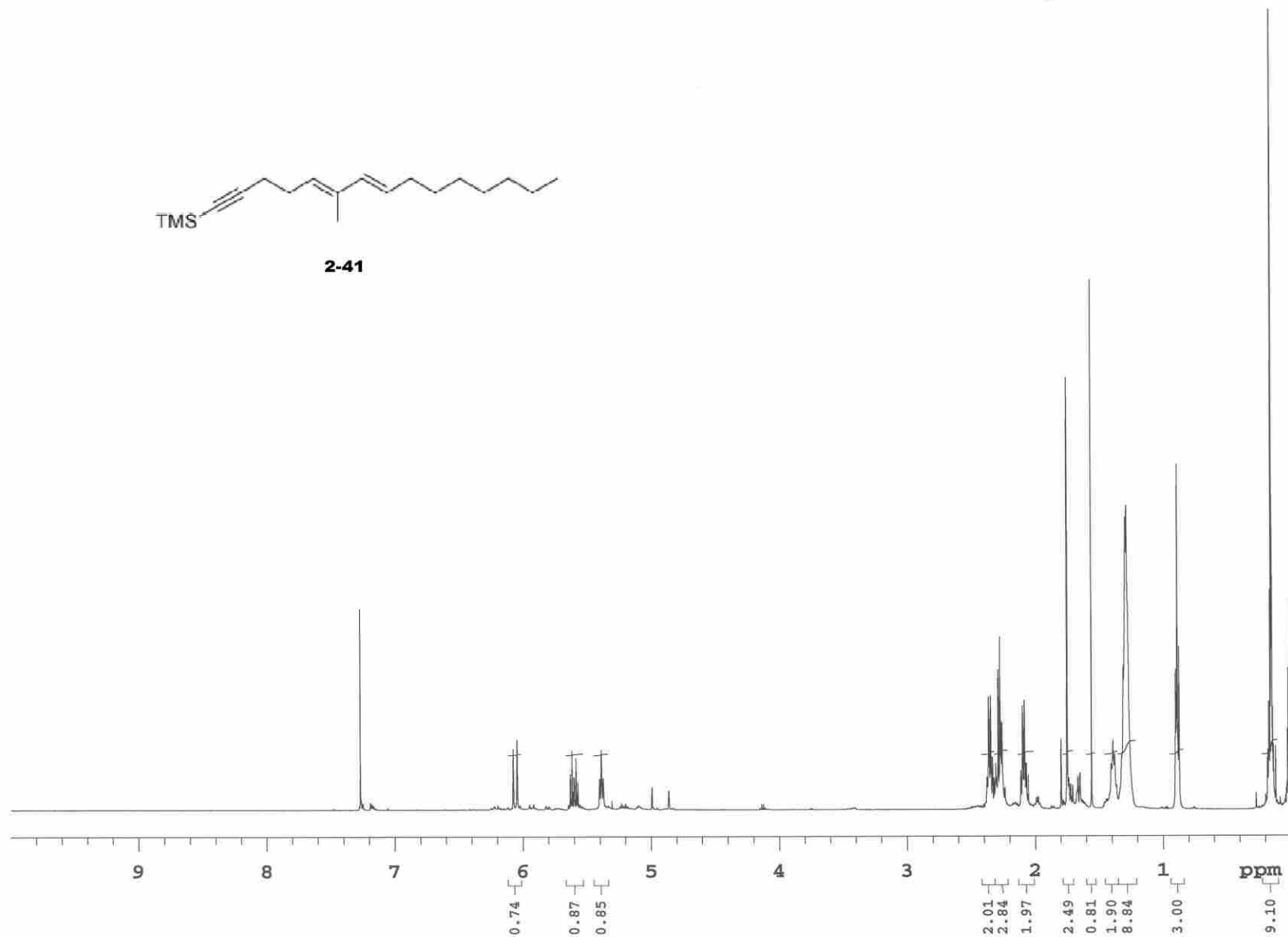






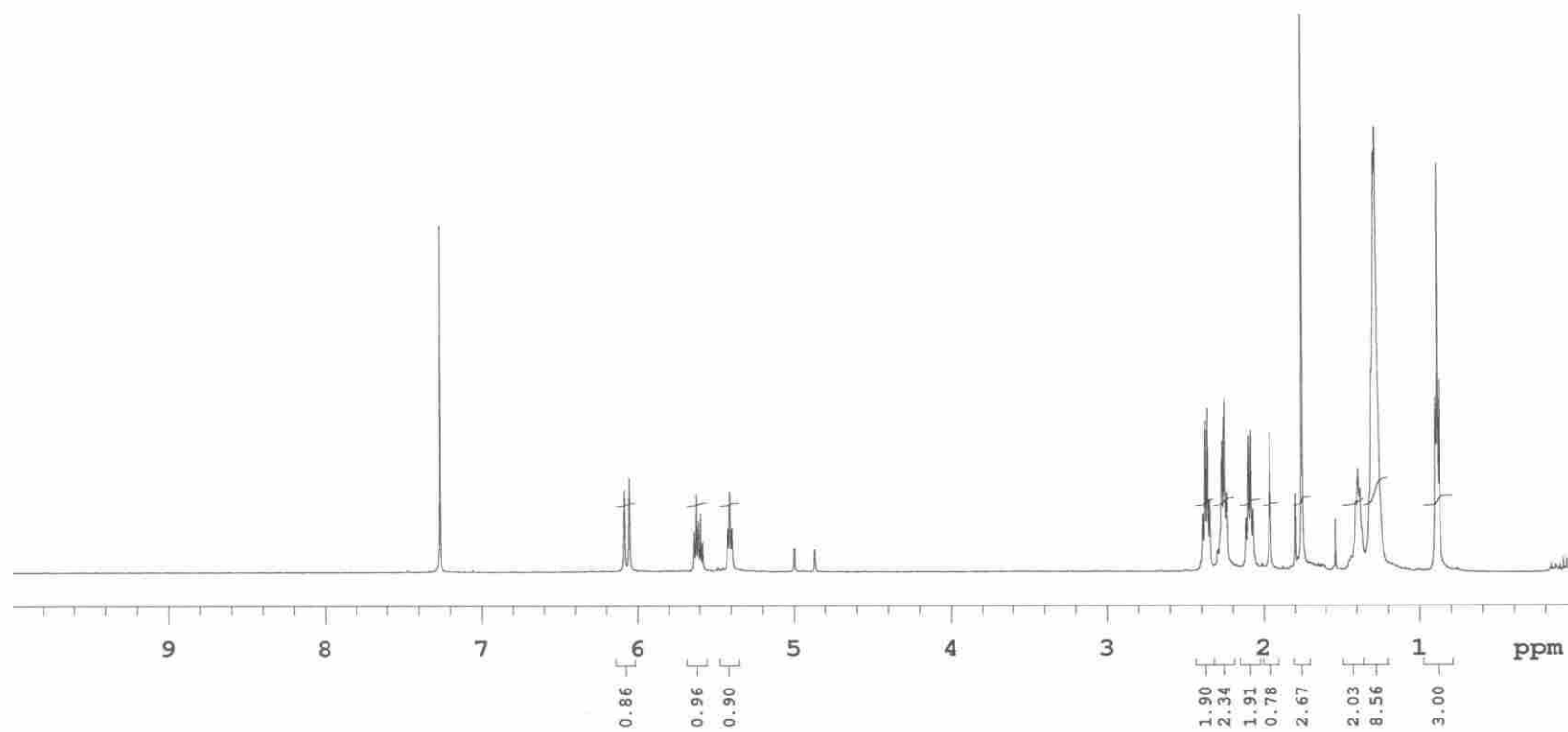


2-41



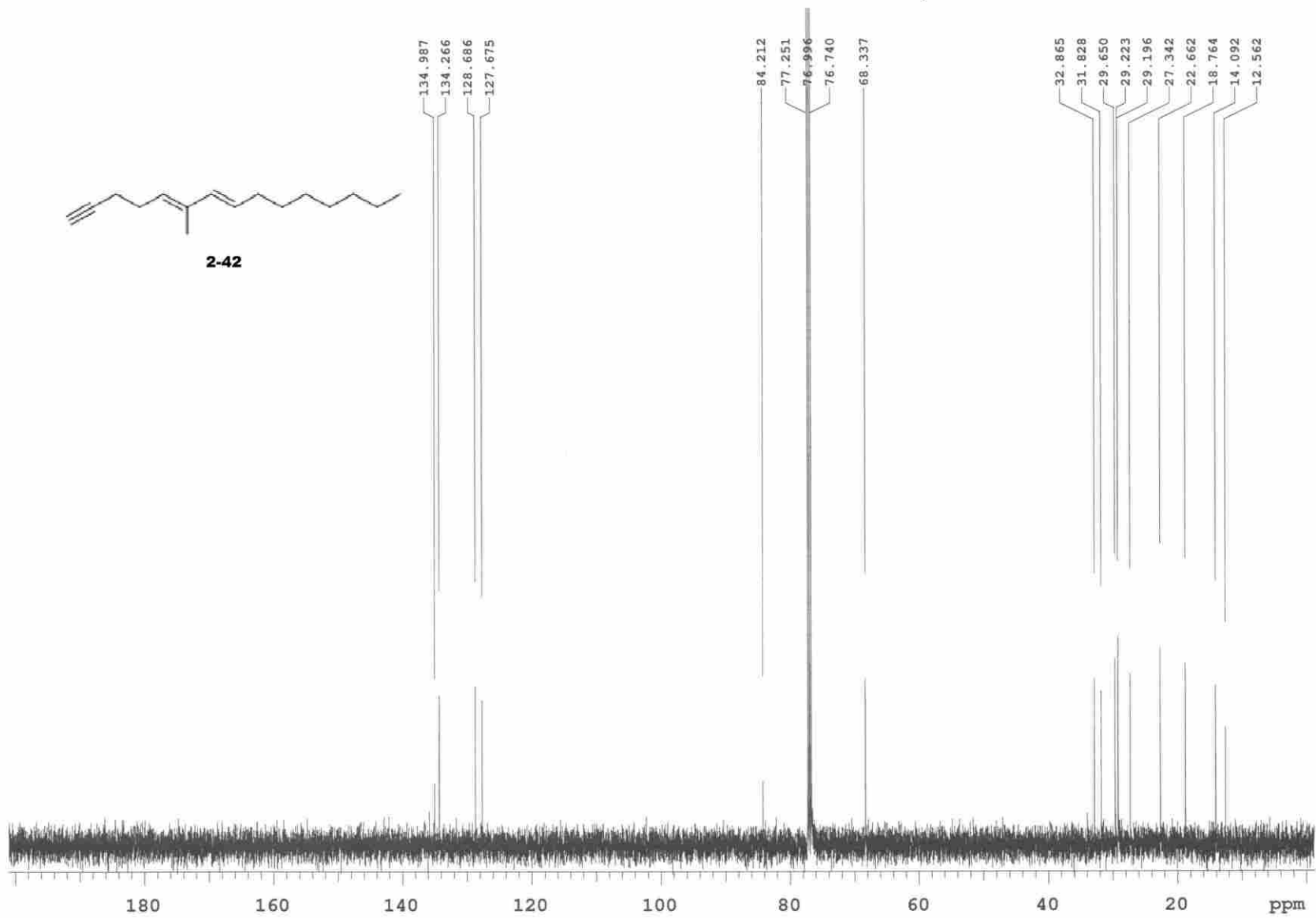


2-42



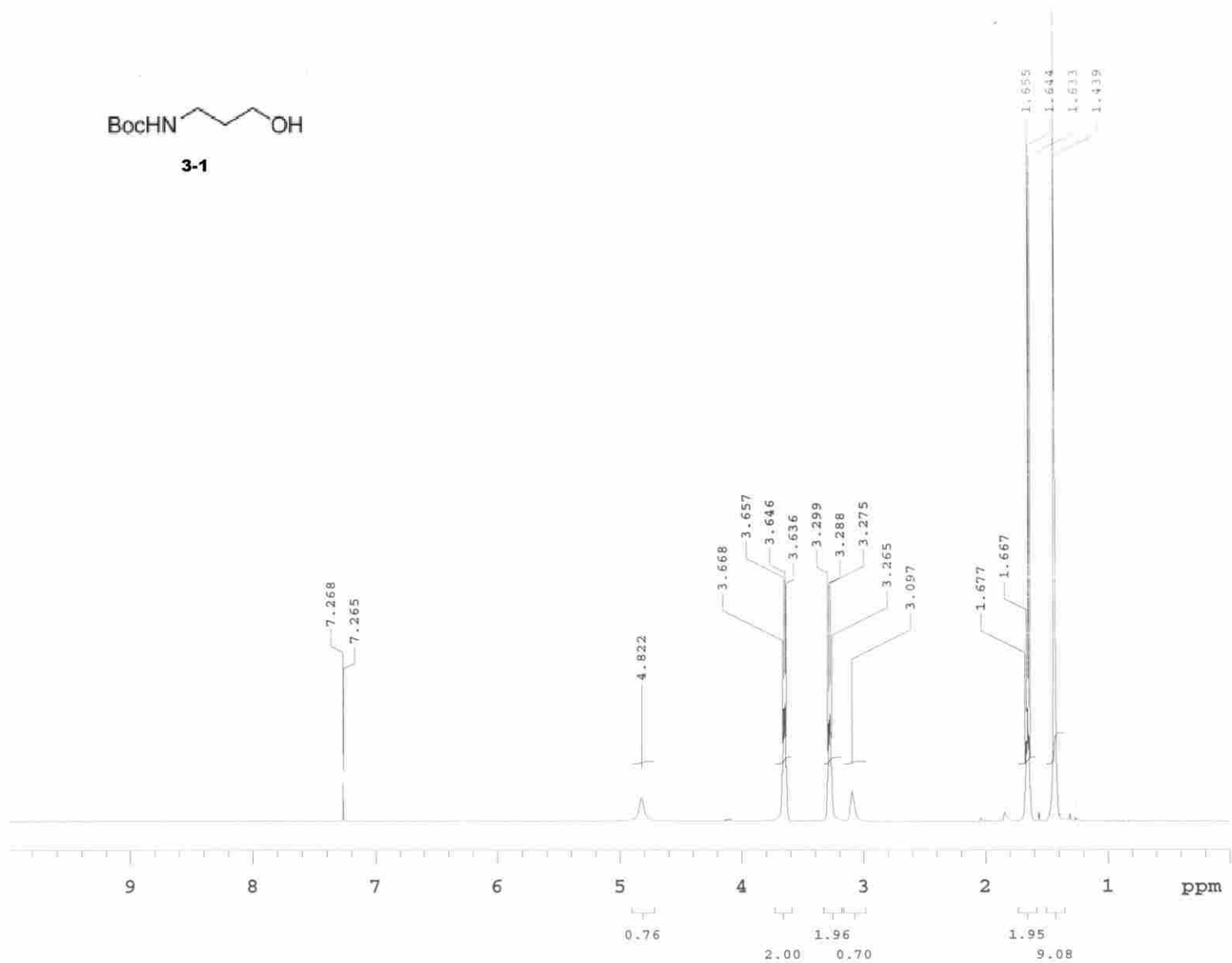


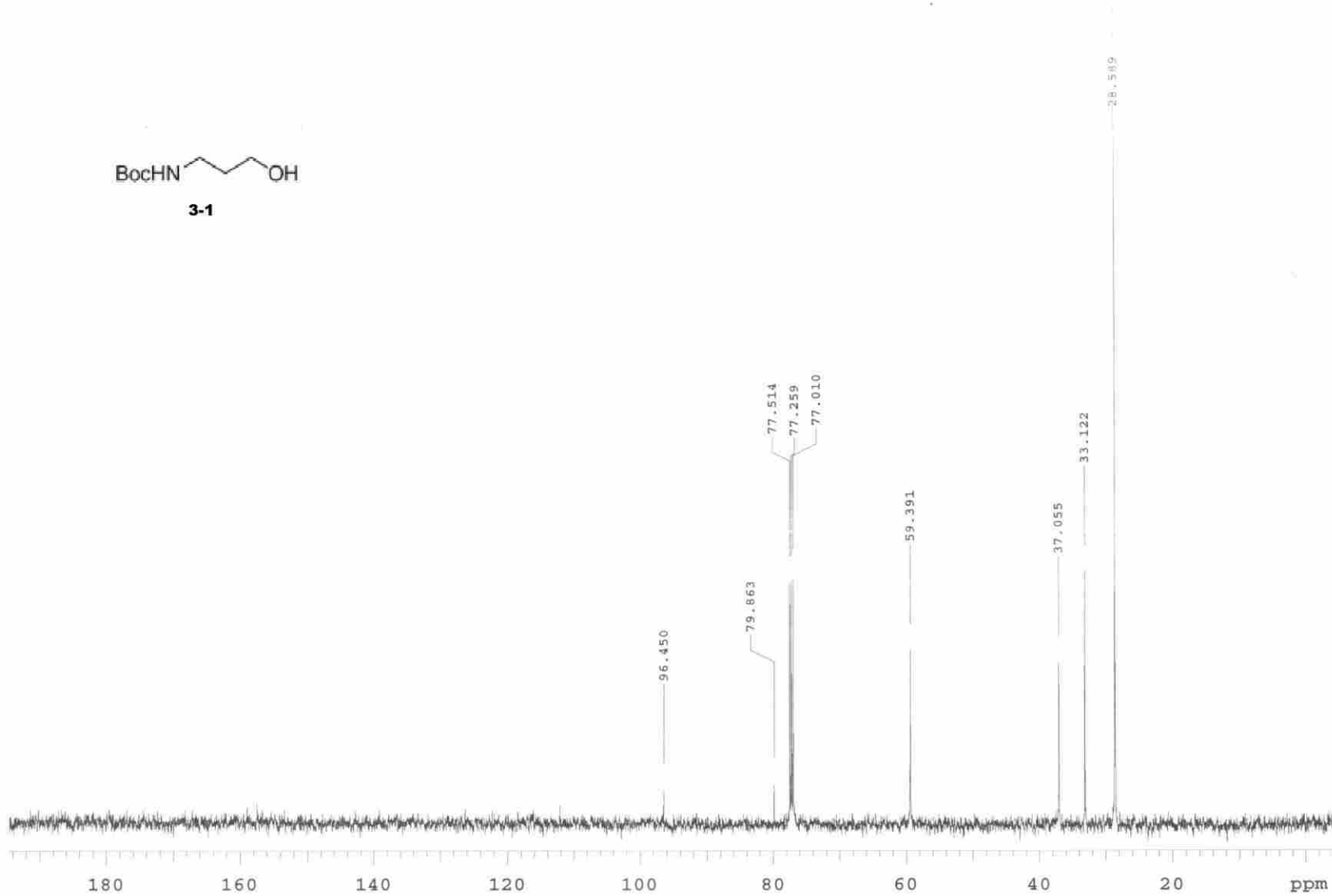
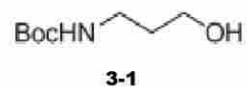
2-42





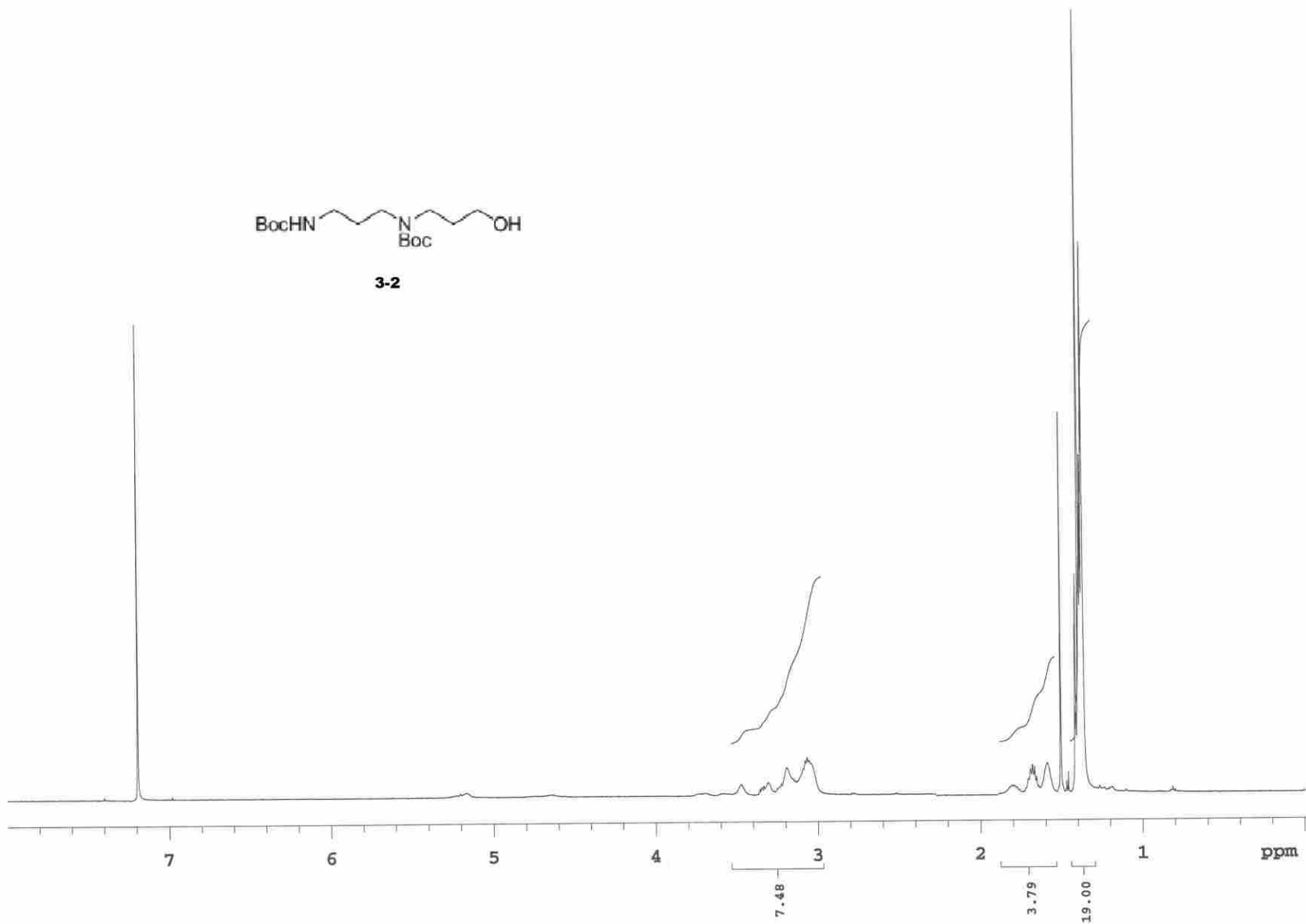
3-1





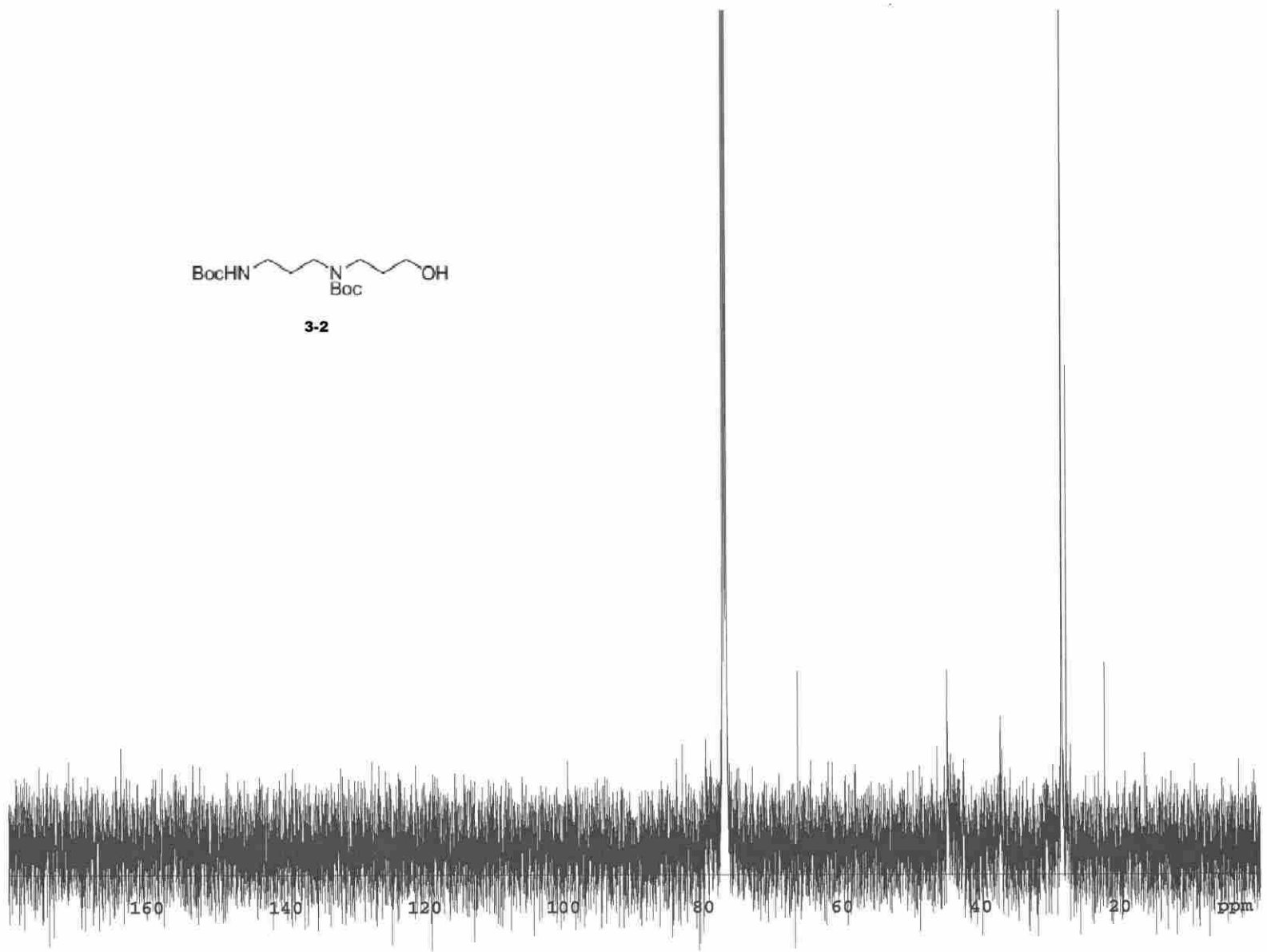


3-2



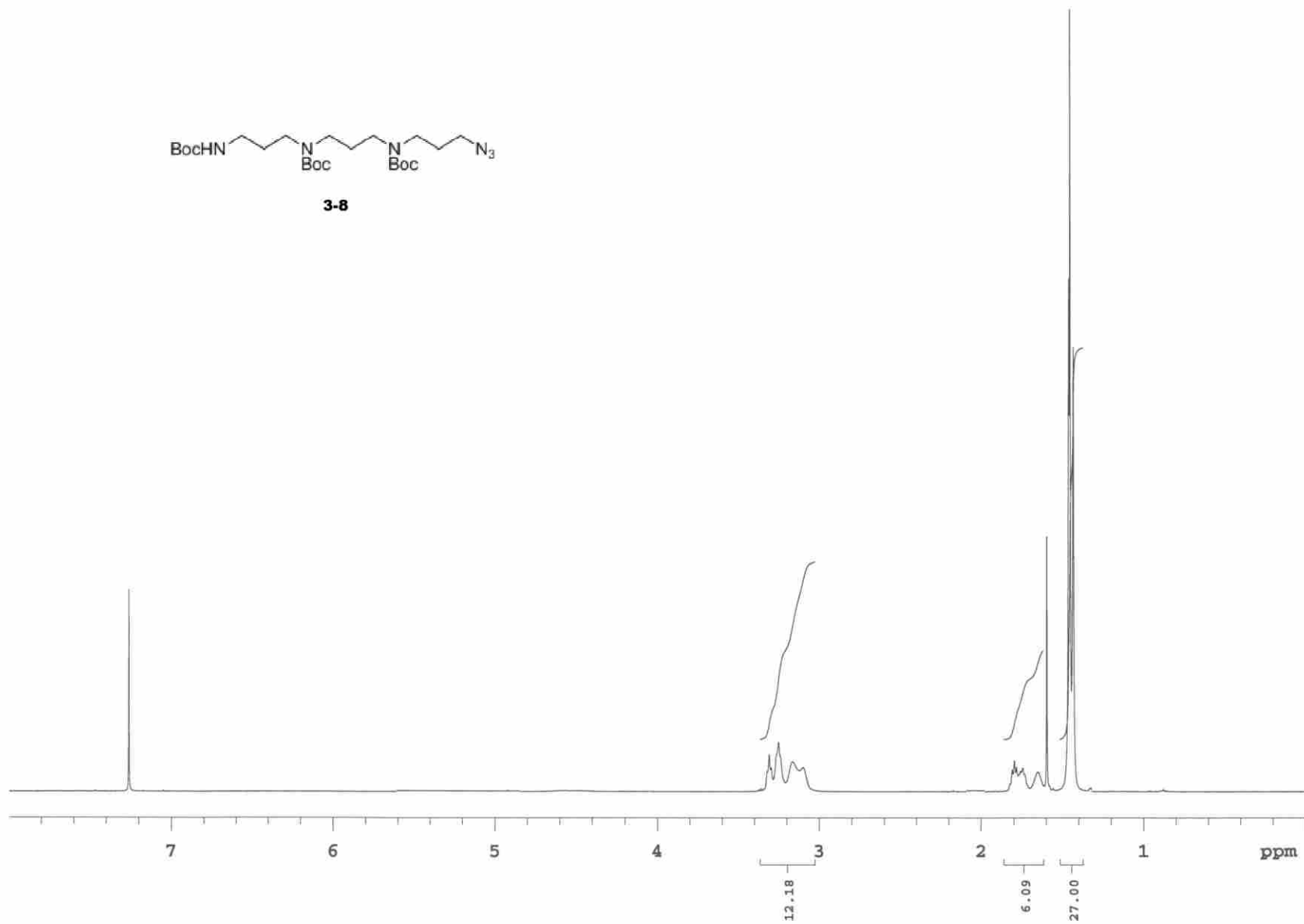


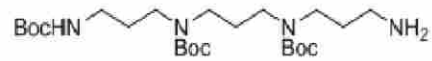
3-2



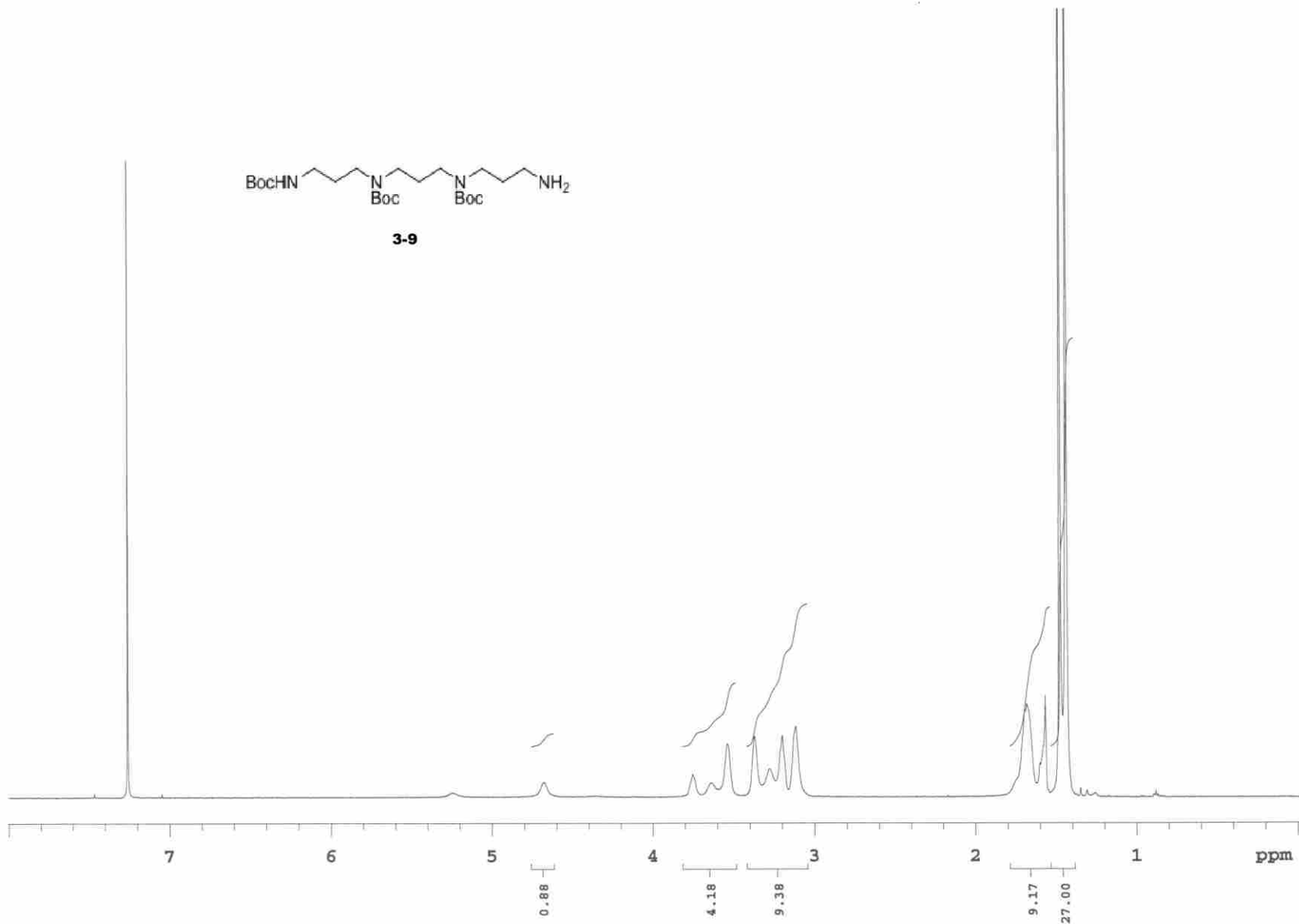


3-8





3-9





3-9

